Final Report for the Design of a VTOL Firefighter Aircraft

Group 13

Bob Beekman	B.B.	4867661
Nino Burgers	N.B.	5532647
Jimmy Chen	J.C.	5580234
Caitlin Cook	C.C.	5101263
Johannes Dinesen	J.D.	5495296
Lauren Jordan	L.J.	5259339
Ishan Kramer	I.K.	5234034
Hanna Niemczyk	H.N.	5517109
Sven Palac	S.P.	5543436
Thijs van Soest	T.S.	5225833

Delft University of Technology

Final Report for the Design of a VTOL Firefighter Aircraft

Group 13

by

Bob Beekman	B.B.	4867661
Nino Burgers	N.B.	5532647
Jimmy Chen	J.C.	5580234
Caitlin Cook	C.C.	5101263
Johannes Dinesen	J.D.	5495296
Lauren Jordan	L.J.	5259339
Ishan Kramer	I.K.	5234034
Hanna Niemczyk	H.N.	5517109
Sven Palac	S.P.	5543436
Thijs van Soest	T.S.	5225833

Project duration:	April 22, 2024 – June 28, 2024
Tutor:	Dr. Calvin Rans
Coaches:	Pieter-Jan Proesmans, Francesco Neri
Group TA:	Marianna Piperigou Grammatika
Institution:	Delft University of Technology
Course :	AE3200 Design Synthesis Exercise
Cover Image:	3DEXPERIENCE Render by Johannes Dinesen

TU Delft

Executive Summary

Contributors: Everyone
Authors: Nino, Johannes, Ishan, Hanna, Sven [1]

The Final Report for the Design of a VTOL (Vertical Take-Off and Landing) Firefighter Aircraft, designated as the FireFly, encapsulates the collaborative efforts of Group 13 from Delft University of Technology. The project was conducted from April 22, 2024, to June 28, 2024, under the supervision of Dr. Calvin Rans and other distinguished coaches. The primary objective of the project was to develop a VTOL aircraft that bridges the performance gap between traditional firefighting helicopters and fixed-wing aircraft. The FireFly is designed to achieve higher speeds, a greater tank capacity and an extended operational range while maintaining the flexibility and versatility required for effective aerial firefighting. This report provides a detailed overview of the sustainability, operational strategies, design process of aircraft configuration, feasibility and risks and economic considerations, reflecting the comprehensive approach adopted by the team.

Sustainability

For this design, not only the sustainability of the aircraft itself should be taken into account, but also the impact this design has on the environment. Controlling fires by extinguishing them to prevent civil areas from burning is the main priority, but it also prevents many emissions. Because of this, sustainability was a core consideration in the FireFly's design, reflecting the urgent need to mitigate the environmental impact of forest fires. Forest fires are significant sources of greenhouse gasses, annually emitting far more than the entire aviation industry. However, forest fires are also necessary for a healthy forest. They remove excessive bushes and waste on the forest ground and create fertile soil for new plants to grow. Only when the bushes become too large, an unhealthy forest fire can arise. In that case, not only the bushes but the whole forest is turned into ashes. Whenever an unhealthy forest fire arises, aerial firefighters are called into action to control the fire, so the fire still removes excessive bushes without reaching civilisation. Next to the environmental impact of a forest fire, society is also socially impacted as areas need to be evacuated and houses could be burned down. As the emissions of the FireFly are small compared to the forest fire emissions, a high-performance firefighting aircraft would be designed for while keeping the design philosophy in mind:

As forest fires are massive emitters, the aircraft should be designed sustainably on the condition that performance is not affected.

With this design philosophy, the FireFly aims to reduce the emissions caused by the forest fire while keeping its own emissions as low as possible. The FireFly's design seeks to address the issues of forest fire consequences by providing rapid and effective responses to forest fires, thereby mitigating their overall impact on the environment and society.

Operations & Logistics

In order to understand the operations and logistics, a mission profile diagram was first created. This allows one to identify crucial mission related aspects and phases, especially about the multi-role capabilities. The biggest takeaway from this part arises from the interactions between the involved parties.

There are two main operators in the world of aerial firefighting. Firstly, the operator who manages the overall firefighting operations is the ground supervisor. They are in charge of managing all firefighters and coordinating between ground firefighting crew and aerial firefighting crew. They are also in charge of dispatching the fleet of aircraft. Therefore, this person has the largest responsibility in AFF operations. Secondly, the Air Attack Group Supervisor's (ATGS) role is to manage and direct all aerial firefighting aircraft. This operator also directs the aircraft to the suitable water refill sources and constantly coordinates with the ground supervisor.

Within operations, many stages can be identified, namely main base, cruise, fire, water pickup, air exchange and ground exchange. Within each of these phases, various operators are involved and interact with each other. The central part to all these phases are the aerial firefighting aircraft.

[1] ChatGPT was used as inspiration for this executive summary.

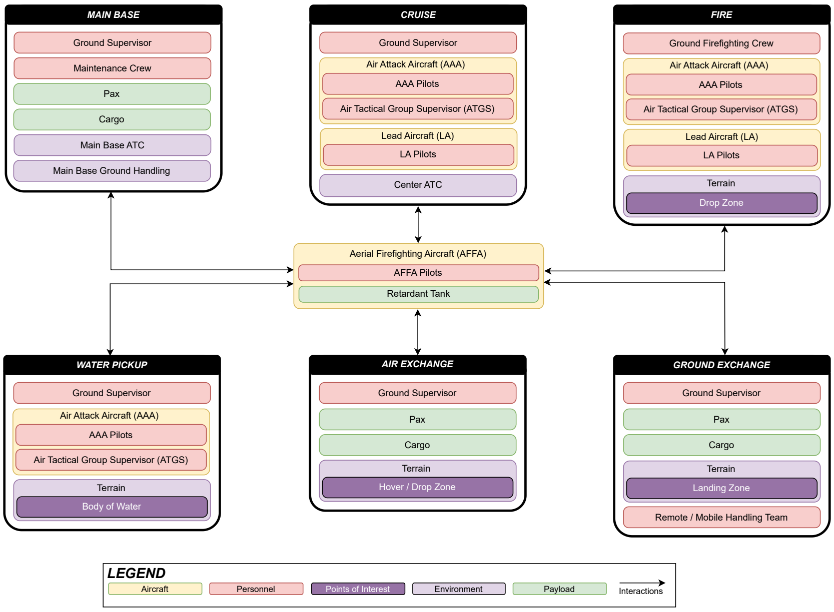

Figure 1: *Overview of all involved parties within the different stages of aerial firefighting.*

Aircraft Characteristics & Configuration

The development of the FireFly was driven by a large set of design requirements. The key ones are the ability to reach a dash speed of at least 400 km/h and having a retardant tank capacity of 10,000 L. To meet these design requirements the FireFly has adopted a quad tiltrotor concept. this aircraft configuration allows for high versatility due to the hover ability as well as substantially higher dash speeds than helicopters due to the ability to tilt the rotors and function like an aircraft. To be a multi-role aircraft able to perform a wide range of missions the aircraft has been equipped with many unique features. This includes large tyres with low inflation pressure to operate on soft uneven surfaces, a big cargo area in the cabin able to be transformed depending on the mission, a cargo ramp large enough to load half pallets onto the aircraft and a 10,000L retardant tank.

the wings have been designed with simplicity in mind and both the front and rear wings are therefore similar and completely rectangular. This allows for easy integration of the driveshaft from the engines through the wings which means that all engines are connected and power can be transferred between the rotors. Because of this an engine failure is not a critical failure and the FireFly is still able to hover with one engine inoperative. To give an idea about the size of the Firefly, an overview of the general external dimensions is given in Table 1 and a render of the FireFly during ground operation can be seen in Figure 2.

Table 1: *General dimension for FireFly*

Parameter	Value	Unit	Parameter	Value	Unit
Maximum take-off weight	35154	kg	Front wing to rear wing	12.3	m
Retardant tank capacity	10000	L	Rotor diameter	6.0	m
Full capacity range	680	km	Wing span	15.3	m
Ferry range	3500	km	Fuselage width	2.1	m
Nose to tail length	20.7	m	Ground to tail height	7.5	m

Risks & Feasibility

Technical risk assessment was conducted to account for possible risks that can occur during the firefighting operations. The main identified risks of the FireFly are related to the malfunctions of the water drop system

Figure 2: *Render of FireFly in Ground Configuration.*

components and stability issues with controlling the aircraft after engine loss. For every risk, a mitigation strategy was found including redundancies in the design, regular maintenance and appropriate crew training. The occurrence of catastrophic risks was reduced by 13 with the use of mitigation strategies.

To assess the feasibility of the FireFly project, first, the compliance with the initial user requirements was analysed. It showed that the FireFly complies with all but two user requirements which take into account the reliability and certification of the FireFly. At this point in the design, an analysis of compliance with those two requirements was not made but it is expected that the aircraft will be able to comply with them once further analysis is made. It is recommended to continue further development of the FireFly since it is expected to make a high impact on an aerial firefighting mission due to its high cruise speed, high water/retardant capacity, VTOL capability and multi-functionality while having no major design flaws that are deemed unsolvable in later design stages. The biggest challenges are expected in terms of stability and control due to an unconventional quad-tilt rotor configuration as well as in aerodynamics due to the same reasons.

Market Analysis & Profit

After an analysis of the AFF market and cost estimations, FireFly is found to be financially viable. A market gap for the FireFly is identified in the mid- to high-capacity aircraft and helicopter range. Within this range the market volume is estimated at 77 units per year and a market share of 19% is found to be achievable for the FireFly. With this market share and a competitive selling price of $60 million, a Return on Investment of 7% can be reached after 10 years and a break-even is reached at a hundred units sold. If the effort is made to collaborate with an established industry firm, the Return on Investment can increase from 7% to 17%. Mainly due to significantly lower RDTE costs and lower risk.

Future Development

Further development of the FireFly would consist of a more detailed design. This would mean CFD analyses to know the effect of the aerodynamics, of the rotors and how the two interact with each other. A more detailed structural analysis and material selection for parts of the aircraft. A simulation where the stability of the FireFly is measured. And finally a better emission analysis. After the detailed design, a production plan needs to be set up and pilots need to be trained, so the FireFly can be tested.

Conclusion

The FireFly represents a significant advancement in aerial firefighting technology, offering enhanced performance, operational flexibility, and sustainability. By addressing the critical needs of modern firefighting efforts and balancing environmental considerations, the FireFly is poised to make a substantial impact on firefighting efficiency and effectiveness globally.

This report encapsulates the meticulous planning, innovative design, and strategic foresight invested in developing the FireFly, demonstrating its potential to redefine aerial firefighting capabilities. The FireFly's design, operational strategy, and economic viability position it as a leading solution in the aerial firefighting market, capable of addressing the growing challenges posed by forest fires and their environmental impact.

Contents

Nomenclature

Abbr.	Description
AAA	Air Attack Aircraft
AC	Alternating Current
ACC	Area Control Centre
ADIRU	Air Data Inertial Reference Unit
AFF	Aerial Fire Fighting
AFFA	Aerial Fire Fighting Aircraft
AoA	Angle of Attack
AP	Auto Pilot
APU	Auxiliary Power Unit
ATC	Air Traffic Control
ATGS	Air Tactical Group Supervisor
CAGR	Compound Annual Growth Rate
CFD	Computational Fluid Dynamics
CFRC	Carbon Fibre Reinforced Carbon
CG	Centre of Gravity
CH	Compound Helicopter
CPDLC	Controller Pilot Data Link Communication
DC	Direct Current
DLR	Deutsches Zentrum für Luft und Raumfahrt
DMC	Display Management Computer
DOT	Design Option Tree
EEC	Electronic Engine Controller
ELT	Emergency Locator Transmitter
FBD	Free Body Diagram
FBS	Functional Breakdown Structure
FFD	Functional Flow Diagram
FDS	Fire Departments stakeholder
FMS	Flight Management System
GD	General Dynamic
GHG	Greenhouse Gas
HVAC	Heat, Ventilation, Air Conditioning
H/W	Hardware
IFR	Instrument Flight Rules
ILS	Instrument Landing System
ITT	Internal Turbine Temperature
LA	Lead Aircraft
LAT	Large Air Tanker
LE	Leading Edge
Abbr.	**Description**
MAI	Manufacturing, Assembly and Integration
MES	Multi Engine Scooper
MFD	Multi-functional Flight Display
MRO	Maintenance, Repair and Overhaul
MS	Margin of Safety
MTOW	Maximum Take-Off Weight
ND	Navigational Display
OEW	Operational Empty Weight
OEI	One Engine Inoperative
PAX	Passengers
PDU	Power Distribution Unit
PFC	Primary Flight Computer
PFD	Primary Flight Display
PIL	Pilot stakeholder
QTR	Quad Tilt Rotor
RAMS	Reliability, Availability, Maintainability and Safety
RDTE	Research, Development, Testing & Evaluation
ROI	Return on Investment
ROC	Rate of Climb
SAF	Sustainable Aviation Fuel
SATCOM	Satellite Communication
SEAT	Single Engine Air Tanker
SES	Single Engine Scooper
SF	Safety Factor
S/W	Software
SWOT	Strengths, Weaknesses, Opportunities & Threats
TCAS	Traffic Collision Avoidance System
TRU	Transformer Rectifier Unit
UHF	Ultra High Frequency
USN	United States Navy
USAF	United States Air Force
VFR	Visual Flight Rules
V&V	Verification & Validation
VHF	Very High Frequency
VLAT	Very Large Air Tanker
VOR	Very High-Frequency Omnidirectional Range
VTOL	Vertical Take-Off and Landing

Symbol	Description	Unit
α	Thermal coefficient	$\mu_{strain}/°K$
ζ	Damping ratio	[-]
η_p	Propulsive efficiency	-
ϕ	Azimuth angle	°
ρ	Density	kg/m^3
σ	Stress	MPa
σ_a	Zero mean stress amplitude	MPa
σ_e	Corrected stress amplitude	MPa
σ_m	Mean stress	MPa
σ_U	Ultimate stress	MPa
σ_y	Normal stress in y	Pa
ω_d	Damped natural frequency	rad/s
ω_n	Natural frequency	rad/s
A	Area	m^2
c	Crack length	mm
c_p	Specific fuel consumption	kgs^{-1}W^{-1}
D	Drag	N
E	Young's modulus	Pa
F	Force	N
$\frac{V_H}{V}$	Tail to wing speed coefficient	-
h	Height	m
h(t - t*)	Impulse response function for t > t*	m/N
I_{xx}	Area moment of inertia about x-axis	m^4
I_{yy}	Area moment of inertia about y-axis	m^4
I_{zz}	Area moment of inertia about z	m^4
I_{xz}	Product moment of inertia	m^4
J	Advance ratio	-
K	Distortion factor	-
ΔK	Fracture toughness	$MPa.m^{1/2}$
L	Lift	N
$\dot{m}$	mass flow	kg/s
$m_{\text{f,total}}$	Total mass fraction	-
M_x	Internal bending moment about x	Nm
M_z	Internal bending moment about z	Nm
m_f	mass fraction	-
m	Constant, Section 6.1	-
m_{MTO}	Maximum take-off mass	kg
N	Number of cycles	-
n_{max}	Max load factor	-
n_{min}	Min load factor	-
P_i	Concentrated force	N
q	distributed load	N/m^2
r	Blade radius	m
R	Radius	m
S	Surface area	m^2
T	Thrust	N
t	Time	s
T_y	Internal torque about y	Nm
ΔT	Change in temperature	K
t_y	Distributed torque about y	N
u(y - y_i)	Heaviside function centred at y_i	–
v	Velocity	m/s
V	Volume	L
$V_{\text{free stream}}$	Free stream velocity	m/s
V_{i}	Induced velocity	m/s
$V_{\text{i hover}}$	Induced velocity in hover	m/s
V_x	Internal shear force in x	N
V_z	Internal shear force in z	N
v	Deflection in z	m
W	Weight	N
W_b	Begin of cruise weight	kg
W_e	End of cruise weight	kg
W/F	Power loading	N/W
W/S	Wing loading	N/m^2
w_z	Distributed force in z	N/m
$\bar{x}$	x distance with respect to the centroid	m
Y	Compressive Young's modulus	GPa
$\bar{z}$	z distance with respect to the centroid	m
z	Distance	m

1 | Introduction

Contributor / Author: Ishan

Wildfires are increasing every year due to global climate change, damaging properties and nature and greatly impacting people's lives. Furthermore, they release thousands of tons of carbon emissions every year, fuelling climate change too. In 2023 only, 2300 tons of carbon emissions were produced by wildfire [1]. Climate change exacerbates hot, dry and arid conditions in certain areas of the world, facilitating the start and spread of these fires. As these fires are spreading over larger areas and becoming increasingly common, an effective method of containing and suppressing wildfires is required. This is where aerial firefighting comes into play. It consists of leveraging the speed, agility and response time of aircraft to drop water or retardant on wildfires.

The current aircraft which conduct aerial firefighting operations are indeed effective. However, they are limited in numerous aspects. These are often existing designs which are modified to carry out aerial firefighting operations. These aircraft are usually extremely capable in a certain field, but certainly lacking in others. Currently, two main categories of aircraft can be identified: aeroplanes and helicopters. Aeroplanes have large cruise speeds and range but are extremely limited in terms of flexibility. On the other hand, helicopters have excellent flexibility but poor endurance and speed. Therefore, the need for an aircraft capable of bridging this gap is indispensable. This report contains a detailed design of a novel aerial firefighting aircraft named FireFly.

This report aims to show the results and process of the design. An important point which is often highlighted in this report is how certain design choices are made and their impact on the aircraft as a whole. The concept of the Firefly is a quad tiltrotor (QTR) meaning it has hover capability as well as cruising at high velocities (more than 400 km/h).

The report is structured as follows. Firstly, Chapter 3 provides an overview of the functional aspects of the aircraft, especially focusing on the basic functions it must fulfil. Secondly, the sustainability approach to and development strategy is presented in Chapter 4. A look at how sustainability is implemented and relevant to the design is described in this chapter. Thirdly, the operations and logistics are described in Chapter 5. First, the mission profile is displayed and next the interactions between all involved parties and users are explained. Fourthly, the aspects of materials and production are presented in Chapter 6. In this chapter, material choices and characteristics are shown, as well as the production plan of the aircraft. Following this chapter, the aircraft characteristics are discussed in Chapter 7. Weight estimations, aerodynamic characteristics, propulsion, stability and control are all analysed and discussed here. Next, the aircraft configuration and its system characteristics are shown in Chapter 8. The subsystems, their interaction and placement are elaborated on in this chapter. After this, a feasibility analysis can be made and is found in Chapter 9. In this analysis, a compliance matrix can be found which shows if requirements have been met or not. Following this, Chapter 10 dives into the verification and validation procedures for the design. As part of this chapter, a RAMS analysis has been conducted. Next, Chapter 12 describes how the proposed design could enter the market and looks into the return on investment (ROI). Lastly, further development analysis is conducted and analysed in Chapter 13. This chapter shows the post-design activities required for successful real-world implementation.

[1] Link [cited on 19-06-2024]

2 | Midterm Summary

Contributor / Author: Caitlin

The FireFly is designed to achieve higher speeds, a higher tank capacity and a longer range than current AFF helicopters whilst being more versatile than fixed-wing AFF aircraft. The main requirements for this design are that the aircraft shall be capable of reaching dash speeds of at least 400 km/hr with a tank capacity of 10000 L and shall be equipped with a snorkel device capable of swiftly refilling the tank in the most inaccessible terrains. From these requirements, the FireFly was born. Moreover, the FireFly's mission is to more efficiently and effectively fight wildfires worldwide.

Prior to this phase, the final, there were three other phases. The Planning Phase was the initial phase in which planning was set up for the entire duration of this project. The planning included setting up a workflow diagram, a work breakdown structure and a Gantt chart. Additionally, a literature study was done in order to familiarise the team with the topic of aerial firefighters and to be in a position to ask pointed questions to experts in the field. This proved to be very useful as the team has spoken to multiple firefighting experts around the world and gained valuable insights into aerial firefighting operations.

Moreover, the second phase also known as the Baseline, consisted primarily of determining the user and system requirements. These proved to be essential for developing the concept designs and the phases afterwards. It was then possible to set up design options trees (DOT) for individual subsystems of the aircraft. This was done to prepare for the trade-off in the Midterm Phase. Additionally, a functional flow diagram and functional breakdown structure were created to visualise what operations would be done during a mission.

Furthermore, in the Midterm Phase, an extensive trade-off was done to determine which aircraft concepts would be feasible for the Detailed Design stage. Initially, seven feasible concepts were created out of the various subsystem configurations. It was decided to choose two concepts out of these seven which would be designed in further detail. The two designs were a QTR and a Compound Helicopter (CH). Both designs complimented each other in terms of mission success and both performed well in manoeuvrability. A summary of the criteria and weights is found in Table 2.1. The criteria were graded from -2 to 2 with -2 performing the worst.

Table 2.1: *Concept trade-off matrix with the criteria and their respective weights as the width of the columns and placed in between brackets.*

Criteria → Concepts ↓	Initial Response Time(5)	Sustainability(1)	Cost(2)	Full Capacity Range(4)	Manoeuvrability(4)	Technology Readiness Level(3)	Complexity(3)	Risk(2)	**Tot.**
CH	0	2	0	0	2	1	2	0	**19**
QTR	2	0	-1	2	2	-1	-1	1	**15**

The team decided to split into two separate teams to develop each concept further. Following this, the Detailed Design phase will be described in this report. It was decided that this team would be designing the FireFly aircraft in the next phase of the report.

The aircraft was named the FireFly and has four tilt rotors located at the ends of the main wing and the horizontal stabiliser (the rear wing). The aircraft has a water tank and pump system of 10 000 L. Additionally, the design of the fuselage was decided to not be circular due to the cabin not being pressurised. There is a retractable ramp at the rear of the aircraft through which additional payload can be taken in or out. The water tank is located at the bottom of the fuselage and leaves sufficient room to transport six passengers if desired. The wings on the aircraft are identical in shape and size and have a constant chord throughout. The engines chosen for the tiltrotor are the AE1107F turboshaft engines manufactured by Rolls Royce and each has a rotor with a 12 m diameter. The aircraft is able to fly in hover or in horizontal flight and can switch between these flight modes at will.

3 | Functional Overview

3.1. Functional Flow Diagram

Contributors: Ishan, Jimmy. Authors: Caitlin, Jimmy

The aircraft will need to perform certain functions during every mission. In order to have an overview of the logical order in which functions are to be performed, a functional flow diagram (FFD) was created. Additionally, an overview of the entire lifecycle, from production to retirement, was created.

Some characteristics of the concept have changed since the Baseline report. The most apparent change is the removal of the scooping function in the water refilling branch of the operational FFD. During the conceptual trade-off, scooping had been eliminated, so the FireFly will only refill in hover mode. In addition to that, the payload exchange functional flow has been refined to better reflect the sequence of functions in a ground exchange and in an air exchange. Finally, the logic of the FFD has been improved. For one, decisions that also require communications with other involved parties like ATC or ground crew, have been better represented in the functional flow. Besides that, the decision to start a mission has been moved before the decision to reload the payload. The FFD can be found in Appendix A

3.2. Functional Breakdown Structure

Contributors: Hanna. Authors: Caitlin

The Functional Breakdown Structure (FBS) is essentially an AND tree that displays which functions the product is supposed to perform. A preliminary version was made in the baseline report, but now that a concrete selection has been made, an iteration is required. The main changes are the same as the ones in the FFD such as removing the scooping function. Additionally, some functions have been rephrased and the final diagram can be found in Appendix A.

4 | Sustainability Development Strategy

Contributor / Author: Nino

Sustainability needs to be considered in the design, as it is important to prevent unnecessary emissions. A sustainable design can be achieved with sustainable development. According to Brundtland [1], sustainable development has the following definition; "Sustainable development is the development that meets the needs of the present without compromising the ability of future generations to meet their own needs.". The current need would be the overall objective of this project, which is; "Develop a multi-role VTOL aerial firefighter that can bridge the capability cap of traditional firefighting helicopters and fixed-wing aircraft." This statement needs to be achieved while emitting as little emissions as possible to not compromise future generations.
The following sections explain how sustainability is taken into account for the design of the FireFly, compare the impact of forest fires and firefighting fleets and explain why better aircraft performance is more sustainable for the overall mission than better aircraft sustainability.

4.1. Impact of Forest Fires

Before sustainability can be implemented in the design itself, it is important to understand the threat a forest fire poses to the environment and humanity. In this case, that would be areas with forest fires. Forest fires have major impacts on the environment, but also impact social and economic aspects of a society.

4.1.1. Environmental Impact

Forest fires cause a lot of emissions. When a wildfire ignites, vegetation and organic matter will be burned and release greenhouse gasses (GHG), harmful mixtures of air pollutants, smoke and particulate matter into the atmosphere.

The main greenhouse gasses released by fire are carbon dioxide (CO_2), methane (CH_4), and nitrous oxide (N_2O).[1] N_2O is a product of combustion, CH_4 is emitted due to incomplete combustion of biomass and CO_2 is mainly released due to the complete combustion of biomass. CO_2 is released when trees and plants are burned, as these store CO_2 from the atmosphere. The amount of emissions produced by wildfires will be discussed in Section 4.2.

The smoke from wood, but also structural fires, such as residential or industrial fires, can contain toxic particulate material including metals, CO and toxic organic compounds. These particles build up in all living bodies and could cause numerous problems to their health. Some immediate effects would be burning eyes, runny nose, scratchy throat, irritated sinuses, irritated coughs and shortness of breath. Some health effects due to exposure to small particles of 2,5 microns are an increase in severity of asthma, COPD, inflammation or infections, including bronchitis and pneumonia. Long-term exposure to these particles could cause memory loss, learning disorders and reduced lung function. [2] Because of this, it is important to prioritise forest fires close to urban areas.

When a forest fire occurs, much damage is done to flora and fauna. However, according to Natural-Resources Canada, apart from the destruction forest fires cause, fires are advantageous to the forest: "Forest fires release valuable nutrients stored in the litter on the forest floor. They open the forest canopy to sunlight, which stimulates new growth. They allow some tree species, like lodgepole and jack pine, to reproduce, opening their cones and freeing their seeds."[3] The current problem with forest fires is that the fires become too big, because of the heavily crowded trees and bushed areas. Healthy forest fires only burn the excess bushes on the ground. Unhealthy forest fires burn down the whole forest. Causing the trees to not grow back anymore after a fire. The main job of an aerial firefighter is then to control the fire and not necessarily to extinguish it. The control of the fire is important, as the fire can not spread too much and come too close to civil or industrial areas. If it does, plastics and other non-natural and natural materials will burn up and release toxic

[1] Link [cited on 12-06-2024]
[2] Link [cited on 12-06-2024]
[3] Link [cited on 12-06-2024]

materials into the atmosphere.

4.1.2. Social Impact

Forest fires also create a large social impact on a community. Water and electricity can be cut off, roads are blocked, cities need to be evacuated and houses can burn down. These impacts can be noticed weeks after a fire and it can take a long time to rebuild the damage done by the fire.

4.1.3. Economic Impact

The economy of a community is also heavily affected by a forest fire. The main economic impact is created due to the high cost of repairing the damage and destruction of infrastructure and buildings caused by wildfires. This is another reason to prioritise forest fires close to urban areas. The first and most important objective is to save citizens. In addition, the economic impact can be reduced by preventing the destruction of properties. The economic impact can also be noticed in the business sector. Areas close to the wildfires will be evacuated and businesses will be temporarily closed. This means no revenue will be made, while there are a lot of damage costs. This is the case for the forest industry in Canada. More than 200.000 people work in this industry in rural and remote areas, which need to be evacuated in case of a forest fire. In 2017 up to 40% of the forestry companies in British Columbia had to shut down due to forest fires. This decreased lumber production by 20% and increased the prices of wood, affecting many more sectors. [2]

The tourism sector will also be affected by forest fires, as it is less attractive to go on vacation near a forest fire. This results in fewer people going to that area to spend their money, making it even harder for local businesses to recover from the economic forest fire damage. If the VTOL firefighting aircraft is efficient in extinguishing and controlling forest fires, urban areas will be protected and the economic impact on businesses in the area of the wildfire will be minimised.

4.2. Emissions of Forest Fires and Firefighting Fleets

The environmental impact also has an impact on the emissions caused by forest fires. Forest fires are massive emitters and every year they cause gigatonnes of carbon emission[4]. In Figure 4.1 a graph is shown of the yearly carbon emissions caused by forest fires. In that image, it can be seen that in 2023 about 2200 megatonnes (Mt) of carbon have been emitted by forest fires worldwide. To put this into comparison, the whole aviation industry, including all commercial and cargo flights, has emitted 800 Mt of carbon in 2021 [3]. Worldwide emission due to forest fires in 2021, was about 1800 Mt of carbon. This means forest fires produced more than double the emissions of the aviation industry.

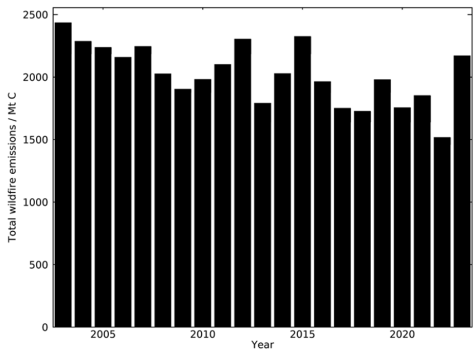

Figure 4.1: *Yearly worldwide carbon emissions caused by forest fires[4].*

However, the only part of the aviation sector that directly affects forest fires, is the firefighting aircraft. If you want to take into account the impact of firefighting aircraft on forest fires, the emissions of the two should also be compared to each other.

S. Alvarez used a compound method to determine the emissions of a Spanish firefighting fleet. The Spanish firefighting fleet, consisting of 20 helitankers, would have emitted a total of 5497 tonnes of carbon [4] in 2012. To have a fair comparison, this number should be compared to the forest fire emissions of the region where these helitankers have operated, Spain. March 2012 was the peak of the forest fire season in Spain with a

[4] Link [cited on 17-06-2024]

total of 0,38 Mt of carbon emitted [5]. Meaning forest fires already emitted 69 times more carbon than the firefighting fleet when taking into account only one month of the year. When assuming the firefighting fleet of 20 helitankers only operates in a smaller region, the province of Asturias in Spain, forest fires still emit a lot more carbon than the firefighting fleet. In March 2012 a total of 0,08 Mt of carbon was emitted in Asturias [5]. Meaning the forest fires still emit 14 times more carbon than the firefighting fleet. As said in Subsection 4.1.1 forest fires are natural, so not all of these emissions can be prevented by aerial firefighters. However, it still is important to control the fires to prevent unnecessary spreading or burning of civilised areas. This way the emissions can still be minimised.
On top of this, multiple studies have found that climate change does have an impact on wildfire season length, wildfire frequency and total burned area [5]. With this change, more firefighting aircraft are necessary to fight wildfires. However, operationally it is difficult and expensive to increase the firefighting fleet as more pilots, storage space and maintenance are needed. That is why a new type of firefighting aircraft is needed to more efficiently control the wildfires.

4.3. Sustainability Development Strategy

From Section 4.2 it can be concluded that forest fires emit a lot more carbon than firefighting fleets. This means that when firefighting fleets are effective in extinguishing forest fires, a lot of emissions can be prevented. However, this also means that low-performing firefighting aircraft indirectly cause a lot of emissions by not extinguishing fires effectively. In order to have the most sustainable design, a balance should be found between a high-performing aircraft, which prevents forest fire emissions, and a sustainable aircraft, which prevents aircraft emissions. With a good balance, the overall sustainability and the impact it makes on the environment is as low as possible. As the forest fires produce significantly more emissions than the aircraft itself, the decision is made to make a performance-focused aircraft. This will prevent the most emissions that an aerial firefighter has an impact on. The forest fire emissions are significantly more than the emissions of an aerial firefighter, thus it is important to prioritise these emissions for a sustainable design. Meaning that a high-performance aircraft can prevent more emissions than a high-sustainable aircraft. However, it is important to prevent emissions from the aircraft itself as much as possible by making sustainable choices for parts that do not have a large effect on performance, such as material choice. Based on these reasons a design philosophy has been set up:

As forest fires are massive emitters, the aircraft should be designed sustainably on the condition that performance is not affected.

This design philosophy should be adhered to but is not a strict requirement. Exceptions can be made if there is good reasoning for it. To create a sustainable, but high-performance design, one is required to look at multiple parameters. These parameters should be assessed and it should be determined how much they affect the performance of the design. If performance is highly affected, that parameter should be designed for high performance. However, it is acceptable if small sacrifices should be made on performance for a very sustainable aircraft. For example, choosing a battery-powered aircraft over a propulsive-powered aircraft, is probably a big loss for performance, as batteries are very heavy and it is difficult to design long-range battery-powered aircraft with the current technology. However, when choosing propulsive aircraft, a sustainable aviation fuel (SAF) could be used to prevent emissions, but still have high performance. Based on the design philosophy, a policy has been created. When using this policy, the following questions should be answered in order to make a sustainable design choice:

- How does this design choice impact performance?
- How does this design choice impact sustainability?
- Does performance significantly decrease with a more sustainable design choice?

When the first two questions are answered, the impact of that design choice on the environment and performance is known. With the knowledge of the first two questions, the final question can be answered. If the answer to this question is 'yes', then performance should be prioritised for that specific design choice. If the answer is 'no', the most sustainable design choice should be made. Parameters to take into account for the impact on performance are first response times and turnaround times. Sustainability parameters to be taken into account are manufactural & operational emissions and recyclability. By answering these questions during the design process, sustainability will be taken into account by finding a balance between aircraft per-

[5] Link [cited on 24-06-2024]

formance and aircraft sustainability. This way the aircraft will have a positive impact on the environment as it prevents emissions from forest fires. Application of this strategy will be done in the next section and in Section 6.1and 7.6.

4.4. Impact of the FireFly

Contributor / Author: Nino, Caitlin
Next to the impact of wildfires, it is also important to look at the impact FireFly has on its environment. The effect on manufacturing, engine selection and operational efficiency will be further explained.

4.4.1. Manufacturing

The manufacturing method of the aircraft should reflect the sustainability desired for the mission. The manufacturing method should employ 'lean manufacturing'. This would minimise waste during production and manufacturing, in return also reducing emissions.

Lean manufacturing is taken into account in the design choices. For example in the aerodynamics of the aircraft. As will be explained in Section 7.6, the FireFly has identical wings with no taper, sweep or dihedral. This simplifies the manufacturing process, as fewer different types of parts need to be produced. Resulting in a faster manufacturing process and reduced emissions.
Compared to the air tractor AT-802F, the FireFly has more than twice the payload capacity[6]. Having one FireFly aircraft would replace the need for approximately three air tractors. The material used by the air tractors emits approximately 7.3 kg of CO_2 per kilogram of material produced for the aircraft (using material AL2024 T3), whereas the FireFly produces 8.78 kg of CO_2 per kilogram of AL2195 T8. Since the firefly uses a lighter material and has approximately the dimensions of two air tractors, producing one firefly would approximately equal the same amount of CO_2 as two air tractors. In conclusion, producing one FireFly instead of three air tractors would save approximately one-third of the CO_2 needed in order to maintain the same fire retardant capacity.
The material chosen for the FireFly takes recycling into account. A large part of the aircraft is made of AL2195, which has a recycling possibility. Composites were largely avoided in the material choice, such that the carbon footprint in production would be minimised, and additionally, composites are often not reusable. The recyclability of the aircraft indicates that at the end of life, most material resources can be repurposed and used for other projects.

4.4.2. Engine Selection

Three types of engines are considered for the FireFly. Namely, battery-powered, hydrogen-powered and SAF-powered engines. This subsection will go more into detail about how the choice of a propulsive engine is made concerning sustainability.

Turnaround at Base
Firefighting aircraft also need to refuel at some point. For the engine selection, this is important to take into account. Fires can spread up to 23 kph, meaning a quick turnaround time is essential[7]. With regards to the refuelling/recharging time, batteries are unfeasible. The reason is that batteries need a lot of time to charge up. During this recharging time, the wildfire will spread further. The longer recharging takes, the more difficult it will become to control the fire. In the case of hydrogen and SAF, these are still applicable as the turnaround time would be approximately the same and the aircraft can be refuelled a lot quicker.

Another aspect to look into with refuelling/recharging, is the infrastructure of the fuel type. For SAF engines, there are a lot of refuelling stations around the world. However, for hydrogen- and battery-powered aircraft, the infrastructure is almost non-existent. Let alone having these types of refilling stations in the deep forests where wildfires could occur and FireFly could be stored. It will be difficult and would cause a lot of emissions if these need to be acquired especially for the FireFly. It will also be more difficult to quickly deploy an aircraft in areas without the infrastructure for hydrogen or battery infrastructure. Whereas a SAF-powered aircraft can be refuelled at almost any airport in the world.

Specific Energy and Energy Density
The mass of the individual propulsion systems varies immensely. Even though hydrogen is very energy dense

[6] Link [cited on 24-06-2024]
[7] Link [cited on 25-06-2024]

(33.333 Wh/kg) [8], it requires more in terms of volume when compared to SAF. When using hydrogen, the fuel tanks would have to be increased in volume by approximately four times as much to contain the hydrogen required. In the case of batteries, it is the least energy-dense method considered with only 110 Wh/kg [9]. Therefore a battery with a large capacity is required, which consequently will have a lot of mass. It was determined that 1 080 000 kg of battery would be required to make the aircraft function. In conclusion, the more sustainable options for the propulsion system are simply not feasible for the mission of this project. The difference in fuel volume and wet fuel system mass of the propulsion systems are shown in Figure 4.2.

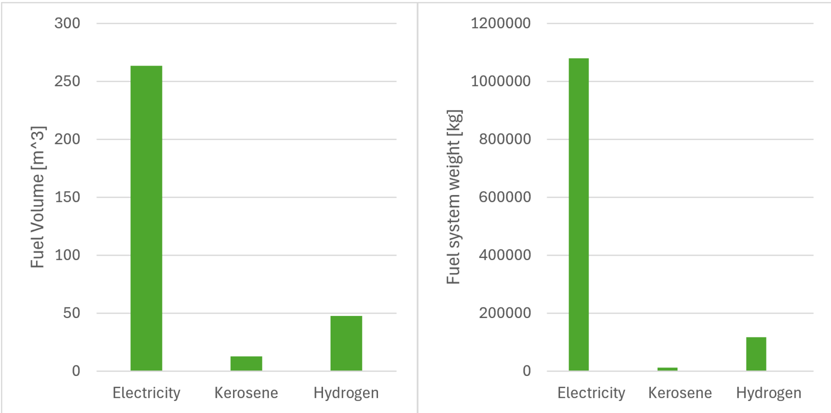

Figure 4.2: *Fuel volume and wet fuel system mass comparison*

Reliability
The reliability of the different systems differs. The SAF systems have been tested and used since the 1930s with kerosene and have been continuously developed and iterated since then. Systems such as hydrogen and electrical power are still in extensive testing phases and are not widely used in the aviation industry.

Moreover, hydrogen fuel is extremely reactive and the mission of the FireFly is to extinguish fires. Normal aircraft which use hydrogen fly at high altitude where temperatures are low. FireFly will fly at low altitude with very high temperatures caused by the fire. If the tank warms up too much or there is a tank failure at any point during a mission, a large explosive reaction could take place, consequently increasing the severity of the wildfire. If such failure occurs, this could be catastrophic for the aircraft, the people and the environment.

In conclusion, the SAF system is most applicable to the firefighting mission in terms of turnaround time, mass, volume and reliability.

4.4.3. Operational Efficiency

To get a better grasp on the impact of the FireFly, it is also important to compare the operational efficiency of the aircraft. The FireFly has versatile payload configurations. Meaning it can carry a variety of configurations of water, medical equipment, firefighting crew or equipment for something unrelated to firefighting. Because of this, the FireFly is not only a firefighting aircraft but is a multi-role aircraft. FireFly can next to firefighting, also be deployed for roles such as search & rescue, supply drops and humanitarian aid. The multi-role function results in airbases needing a smaller fleet of aircraft. No separate aircraft are needed for rescuing humans and dropping retardant, as the FireFly could first drop retardant and afterwards pick up humans from the ground at any location. This will also reduce the number of pilots or increase the operational efficiency significantly if multiple FireFlys are used.

[8] Link [cited on 25-06-2024]
[9] Link [cited on 25-06-2024]

5 | Operations & Logistics

To analyse the tasks that the aircraft has to perform for a successful mission, the operations and logistics aspects are explored in this chapter. First, the mission profile is created to analyse the capabilities that the aircraft has to successfully accomplish concerning the multi-role design of the FireFly aircraft. Furthermore, the operational and logistic concept is established to determine the relations between all parties involved in the operations of the FireFly aircraft.

5.1. Mission Profile

Contributor / Author: Ishan

The purpose of creating a mission profile diagram is to understand certain characteristics which the aircraft must be capable of and implement these in the design stage. The particularity of FireFly is its multi-role capability. This aircraft is capable of fulfilling a wide range of missions. Figure 5.1 aims at showing the standard flight profile, but also the mission specific profiles.

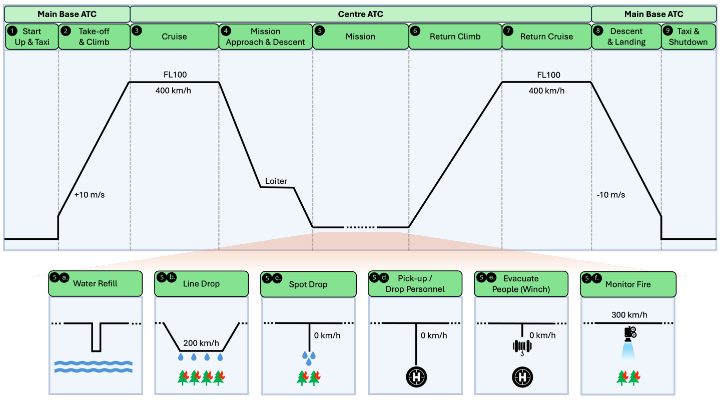

Figure 5.1: *Mission profile for multi-role firefighting operations.*

Some important conclusions can be made from such a profile, concerning the design considerations of the aircraft. Firstly, the aircraft must be able to fulfil certain performance requirements. It must be able to climb comfortably, either by hovering, tilting the rotors or in conventional flight mode. Additionally, it must also be able to drop the water/retardant at low speeds in and around 110-150 knots [1]. These performance requirements are further elaborated on in Section 7.7. Secondly, another massive takeaway is the fact that the aircraft flies at very low altitudes for extended periods of time: during water refilling, drops, evacuation and fire monitoring. This means it is important to provide situational awareness to the pilot through different means: high cockpit visibility, large cockpit displays, night vision capability or air traffic alerting systems. These design choices are later discussed in Chapter 8. Lastly, the aircraft must be capable of off-airport operations. This means considerations with landing gear must be taken. The wheels must sustain the static load of the aircraft while not sinking on soft ground. This is elaborated on in Table 8.1.

5.2. Operational & Logistic Concept Description

Contributors/Authors: Ishan, Thijs

During firefighting operations, no standard mission profile can be set up. Different agencies, governments and companies all operate under different conditions and procedures. By looking at a certain case, a good general impression can be given of how the design might function within an aerial firefighting operation in any region. For this analysis, a look is taken at aerial firefighting operations in the US [6][7][8]. The hierarchical structure in US operations is well-documented and thorough thus providing good insight into the possible operations and logistics of the design.

[1] Link [cited on 25-06-2024]

5.2.1. Operation Parties

As previously mentioned, during a firefighting operation, there is no standard mission profile, as each fire is different and involves different strategies and tactics to fight it. Nevertheless, each operation usually has the same involved parties, each having a specific role and contributing to the mission's success. A complete list of these roles and their descriptions are shown below [6].

- **Command**
  - **Ground Supervisor**
    The ground supervisor manages the overall firefighting operation by supervising both aerial and ground-based firefighters. They also keep an overview of the fire and weather situation at all times.
  - **Air Tactical Group Supervisor**
    The ATGS manages the complete aerial firefighting operation from the air in cooperation with the ground supervisor. They are in the Air Attack Aircraft (AAA) and have a complete overview of the aerial tactical situation and directly update the ground supervisor frequently.
- **Ground logistics & operations**
  - **Main Base Ground Handling**
    This team works on the main base and handles all firefighting aircraft by marshalling them, providing fuel & retardant, performing pre-flight checks and transporting & loading any payload. They communicate with the pilots of the aircraft, the ground supervisor and the Air Traffic Control (ATC).
  - **Maintenance crew**
    This crew maintains the systems and airframe of the aerial firefighting aircraft on the main base between missions.
  - **Remote / Mobile Handling**
    These teams can be deployed close to the mission area, where they are able to refuel and refill the aircraft, as well as aid in loading/unloading.
- **Air Traffic Control**
  - **Main Base Air Traffic Control (MATC)**
    MATC consists of air traffic controllers who manage the airspace surrounding- and including the main base. They are the contact point for the AFF pilots for ground operations, take-off and landing.
  - **Centre Air Traffic Control (CATC)**
    CATC consists of air traffic controllers who manage area control centres (ACC), which include the mission area.
- **Firefighting in mission area**
  - **AAA Pilot**
    The AAA pilot is the person who flies the AAA with the ATGS in it. They fly a circular pattern over the mission area and keep in contact with ATC.
  - **AFFA pilots**
    - ◇ **(Very) Large Air Tanker ((V)LAT) pilots**
      These pilots fly (V)LATs and drop their load in (usually) long lines to create a firebreak at the instruction of the ATGS and ground commander. They also remain in close contact with ATC since after a drop they must return to base.
    - ◇ **Scooper aircraft pilots**
      These pilots fly rotorcraft or scooper planes. These aircraft are capable of refilling using bodies of water and thus remain in the mission area for longer. They are in close contact with the ATGS and the ground commander as well as ATC.
    - ◇ **FireFly pilots**
      These pilots fly the quad tiltrotor and are able to remain in the mission area for longer much like the aforementioned scooper pilots. They are also able to land on unpaved landing areas to be refuelled by the remote handling unit. They are in contact with the ATGS and ground command to decide on the drop areas.
    - ◇ **Lead Aircraft (LA) pilots**
      The LA pilots guide (V)LAT pilots to the drop zone as instructed by the ATGS. They lead the larger aircraft around the terrain and indicate the drop zone. They remain in contact with the (V)LAT pilots, the ATGS and ATC to keep a safe mission area.
  - **Ground crew** This group of people fight the fire from the ground. They keep in contact with the

ATGS and ground commander providing vital information for the AFF operation.

- **Passengers (PAX)**
  The passengers board the aircraft on base or in the mission area. They can be in the form of regular passengers, smokejumpers, evacuees or regular ground personnel.

5.2.2. Definition of Operational Phases

In terms of logistics and operations, it was decided to split an aerial firefighting operation into 6 phases: main base, cruise, fire, water pickup, air exchange and ground exchange. Within each stage, each of the involved parties plays a role and interacts with each other. It is important to note that some parties may play a role in multiple stages. Figure 5.2 shows the implication of users in all the phases.

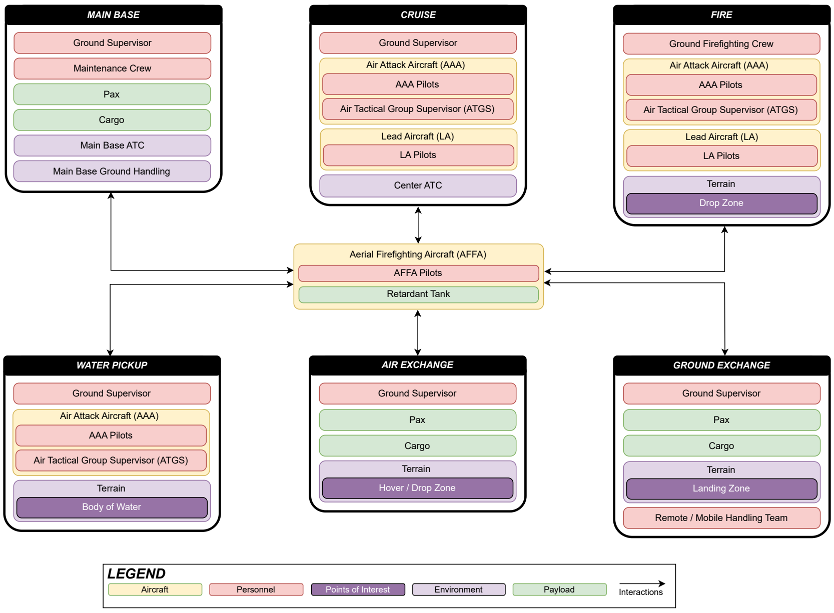

Figure 5.2: *Overview of all involved parties within the different stages of aerial firefighting.*

A description of each stage and its main role is described below. Additionally, precise interactions between the users can be identified for each phase, shown in Figure 5.4. It is important to define what the interactions mean. The arrows represent one-way or two-way communication.

- **Main Base**
  The main base is the base from which the aircraft operates while fighting a fire. The main operator in Figure 5.4a is the ground supervisor. They interact directly with the AFFA as they are the ones who scramble aircraft and coordinate the aerial mission once a fire is declared. The maintenance crew directly report to the ground supervisor to let them know what aircraft are available or grounded. The cargo and PAX are also managed by the ground supervisor based on the needs arising from fighting the fire. The main base ground handling also reports to the ground supervisor to update them on the progress of aircraft readiness on the ground. Lastly, main base ground handling is also in direct contact with local ATC which itself is in direct contact with the AFFA.
- **Cruise**
  The cruise phase is where the main purpose of the aircraft is to transition from the main base to the mission site. This also includes loitering between a water pickup and a drop or the other way around. During the cruise phase, as can be seen from Figure 5.4b the ground supervisor is mainly in contact with the ATGS. The ground supervisor is in one-way contact with AFFA too. The ATGS manages the LA which itself manages the AFFA. The centre ATC constantly oversees the civilian airspace by communicating with the AAA, LA and AFFA.
- **Fire**
  The fire phase is the phase where the retardant drop is prepared and executed, including a short ap-

proach to the drop zone and the drop itself. During the fire phase shown in Figure 5.4c, the main involved party managing the operation is the ATGS. They are constantly aware of the location of all AFFA, and communicate this to the LA. The LA also leads the AFFA onto the drop zone. Lastly, the LA and AFFA communicate and coordinate the status of the drops with the ground firefighting crew.

- **Water Pickup**
  The water pickup phase consists of loading the tanks with water, using the snorkel. In the water pickup phase, all involved parties interact with the body of water, as seen on Figure 5.4d. The AFFA interacts with it, as it picks up the water. The ground supervisor decides which bodies of water are adequate for pickup, and thus which bodies of water will be used to collect water. The ATGS is informed by the ground supervisor on which bodies of water can be used. They can then decide which AFFA collects water from what source, and direct the AFFA to that body of water.
- **Air Exchange**
  The air exchange is simply an exchange of cargo or people while staying in the air and not touching down. For example, smoke jumpers can be dropped on a specific zone, a rescue team can be hoisted down, evacuees can be hoisted up or supplies to ground firefighting crew can be dropped. In the air exchange phase, everything is centred around the payload; this payload consists of passengers, cargo or both, displayed on Figure 5.4e. The payload can both be loaded in the AFFA (with a winch) and unloaded from the AFFA (either with a winch or parachutes). The loading happens in the hover/drop zone, which is a zone assigned by the ground supervisor in agreement with the ground firefighting crew. The ground supervisor also decides what payload needs to be transported, and communicates this to the AFFA, which then flies to the hover/drop zone.
- **Ground Exchange**
  The ground exchange phase is the phase where the aircraft lands outside the base and for a different purpose than picking up water. This can happen if fire crews have to be relocated, if civilians need to be evacuated or if some equipment is needed near the fire. During a ground exchange, the aircraft can also be refuelled or refilled with retardant (additives). In the ground exchange, many interactions are the same as in the air exchange, with some adjustments, as shown in Figure 5.4f. These include the change from the hover/drop zone to the landing zone, which then also removes the need for a winch or parachute. An additional element is introduced as well, the remote/mobile handling teams. They can help with loading the cargo, but can also refuel the aircraft and refill it with retardant (additive).

To help visualise all of these phases and involved parties, a map can be generated with the location and role of each individual involved in aerial firefighting operations which is shown in Figure 5.3.

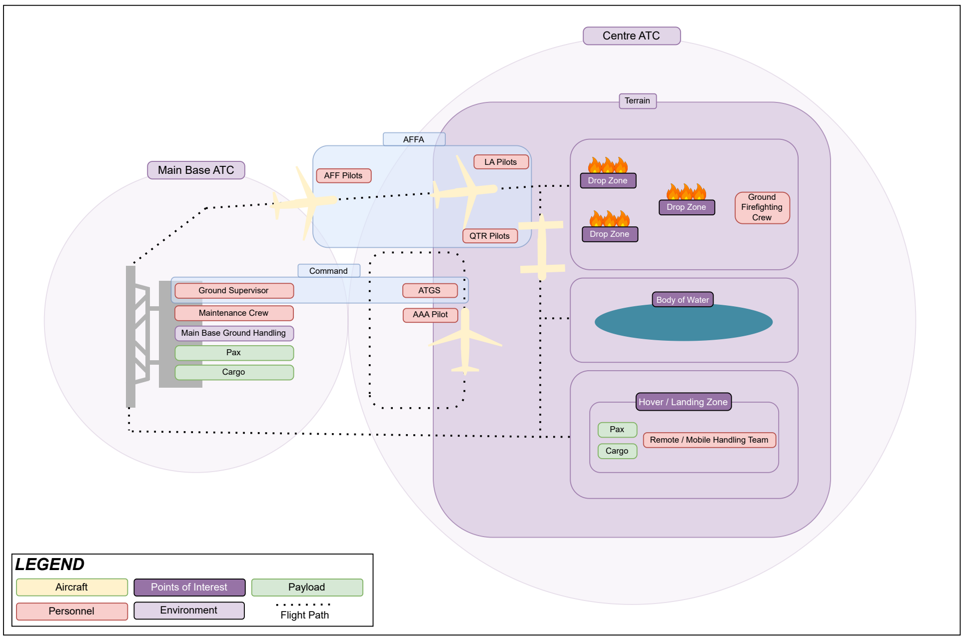

Figure 5.3: *Map depicting all phases, involved parties and their roles.*

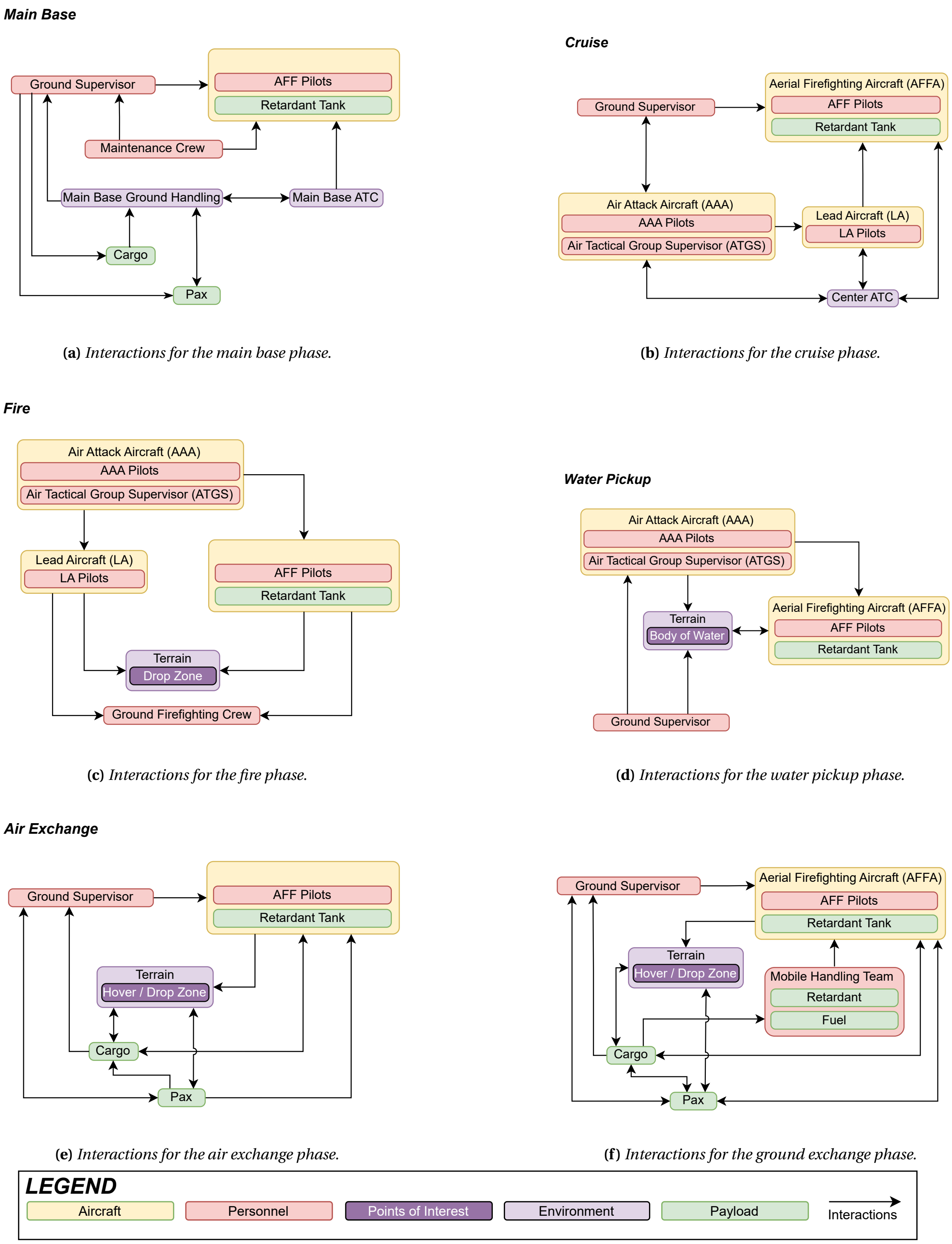

(a) *Interactions for the main base phase.*

(b) *Interactions for the cruise phase.*

(c) *Interactions for the fire phase.*

(d) *Interactions for the water pickup phase.*

(e) *Interactions for the air exchange phase.*

(f) *Interactions for the ground exchange phase.*

(g) *Legend for the interactions.*

Figure 5.4: *Breakdown of interactions between involved parties for all phases.*

Maintenance

In between these different operational phases, maintenance will need to be performed on the aircraft. More information on the expected maintenance schedule for the FireFly can be found in Section 11.2.

6 | Materials & Production

The material selection is conducted for certain subsystems where multiple factors such as yield stress, ultimate stress, sustainability, thermal service temperature and more are explored. The chapter ends with the manufacturing, assembly and integration plan. Where this plan walks through the production steps that will be taken for significant parts and subsystems that are necessary for the development of the FireFly.

6.1. Material Characteristics

Contributors / Authors: Caitlin, Lauren, Jimmy

The material choices for the aircraft are carefully chosen to comply with the requirements and to ensure that the aircraft can withstand the loads applied during missions. Additionally, the material should be affordable and durable. There is a strong preference for material that can be recycled and has low carbon emissions during the lifetime of the material. In the midterm report, three components' materials have already been chosen for the aircraft. The fuselage and the water tank were decided to be made out of Aluminium 2195. The propeller blades were decided to be S-grade fibreglass composite. [9]

Since the fuel tank is decided to be a bladder tank, a corrosion-resistant and flexible material must be chosen. The material chlorosulfonated polyethylene, otherwise known as CSPE, is chosen as a suitable option. The material includes chlorine which makes it such that it is self-extinguishing in case of fire. Additionally, this material has been used more often in the lining of tanks due to its corrosion resistance against moisture [1].

To help the rotor blades maintain their shape and geometry, a honeycomb structure material is placed inside it. The honeycomb structure in the rotor blades was decided to be Aluminium 5052 honeycomb (0.016), W direction. It was important for the structure to be light and heat resistant, and this material has a low density (15.7-16.3 kg/m^3) and a melting temperature of 323-386°C.

The material for the wing box was determined using an optimisation algorithm. Nine material options have been considered as shown below, and the algorithm loops through all of them.

- Aluminium Al2024T851
- Aluminium Al2195T8
- Aluminium Al7068T6511
- Stainless Steel AISI304L
- Titanium Ti6Al4V
- Titanium Ti-60%Be
- Carbon Fibre Reinforced Carbon CFRC
- Phenolic/E-glass fibre
- Epoxy/S-glass fibre

Unlike the actual wing model for structural design, the wing structure for material selection is modelled as a rectangular thin-walled, constant-thickness beam both to save time and because the relative performance of the materials is more important. The external loads are treated as fixed in the optimisation. The only variables which vary are the material choice and the thickness of the structure. The algorithm loops over these two variables and calculates the required thickness to satisfy the stiffness and strength constraints. The geometry which leads to the lowest structural mass is then saved in a csv-file. The specifics behind calculating the deflections and the stresses are explained in Section 7.3.

The structural mass and cost for each material are calculated using the algorithm described. The alloys Al7068 and Al2195 perform the best in terms of mass out of the metals. The three composite materials tend to yield a lower structural mass, but across the board, they are less sustainable and generally more expensive. As stated before, there is a strong preference for materials that can be recycled, so only Al7068 and Al2195 shall be considered in the wing box design process while the other materials are discarded. Al2024 will also be considered as a baseline because this aluminium alloy is the most prevalent in the aerospace industry[2]. These three materials have been summarised in Table 6.1.

[1] Link [cited on 15-06-2024]
[2] Link [cited on 18-06-2024]

Table 6.1: *The materials which are used in the wing box design.*

Material	**Structural mass** [Mg]	**Structural cost [k€]**	**Costs [€/kg]**	**Density** [Mg/m^3]	**Thermal shock resistance** [°C]	**Yield strength** [MPa]	**Maximum Service Temperature** [°C]
Aluminium alloy 2024	0.84	3.0	3.01-4.03	2.75-2.78	217-245	386-427	170-200
Aluminium alloy 2195	0.66	13.6	19.1-22.1	2.71	221-265	538-560	145-255
Aluminium alloy 7068	0.52	3.4	5.64-7.6	2.85	378-444	648-756	80-100

From the data in Table 6.1 alone, there are merits in using either Al2195 or Al7068. The former has a much higher maximum service temperature, but the latter is much cheaper and slightly lighter. To come to a selection, one would have to investigate other material properties. Especially relevant to the mission are the fatigue properties of the materials, so the next step in material selection is investigating the fatigue performance of the three materials.

Fatigue Analysis

Contributor / Author: Lauren

The fatigue analysis was considered for AL 2195-T8, AL 7086-T6511 and AL 2024-T851 to determine how fatigue affects the performance of the material after N cycles. The resulting stress amplitude for N cycles for a desired loading case was then taken to size for the thickness of the wing box.

Firstly, a desired number of cycles was established. The expected amount of drops per year was taken as a metric to determine this number of cycles. As the FireFly is expected to be in operation for a maximum of 200 hrs a year performing approximately 10 drops/hour, it is expected that the FireFly will experience 2000 cycles. Therefore, the aircraft was designed for 10 years of operation without the need for maintenance.

The stress amplitude was determined by looking at the expected extreme loading cases during a drop. A conservative estimate of 3.25 g and −1 g was taken as a maximum and minimum loading on the aircraft. As the fatigue analysis is a function of this stress amplitude, it is an iterative process. The relationship between stress at a zero mean stress and load cycles is described using Basquin's equation as seen in Equation 6.1.

To establish the relationship between stress and fatigue cycles, the zero mean stress at zero cycles and the zero mean endurance stress at 10^7 cycles had to be known. For the first iteration, the yield stress of the material was taken to be the stress experienced at 3.25g for the design component such as the wing or the fuselage. The minimum thickness was then calculated for the part and the stress at −1 g was determined. Using Goodman's Rule to correct for the mean stress, the stress amplitude for 20 000 cycles could be determined[3]. The Goodman method postulates that positive mean stress furthers fatigue degradation, which is why the allowable stress amplitude must be corrected for this non-zero mean stress. Iterating until convergence, the design stress amplitude could be determined to size for the minimum thickness of the wing box.

$$\sigma_a^k \cdot N = C \tag{6.1}$$

$$\sigma_e = \frac{\sigma_a}{1 - \frac{\sigma_m}{\sigma_U}} \tag{6.2}$$

Where S_a is the zero-mean stress amplitude in MPa, k is the constant exponent, N is the fatigue life in cycles and C is a constant. where S_e is the corrected stress amplitude in MPa, S_m is the mean stress in MPa, S_U is the ultimate stress in MPa.

[3] Link [cited on 19-06-2024]

The resulting relationships can be plotted as a straight line on a log-log graph to determine the desired stress amplitude for 20000 drop cycles. The results of this analysis for the wing box will be discussed in Section 7.3.

Crack Propagation

Contributor / Author: Caitlin

From the fatigue analysis, the crack propagation properties and the effect of cyclical loading on the remaining useful life can be investigated.

The crack propagation properties can be analysed with the help of the Paris Law [10]. The Paris Law shows what the crack propagation is per cyclic loading. The slope of the curve can be calculated using Equation 6.3.

$$\frac{dc}{dN} = A\Delta K^m \tag{6.3}$$

Where $\frac{dc}{dN}$ is the slope of the curve, A and m are constants that are experimentally determined and ΔK is the difference in fracture toughness. Since the constant m could not be determined for the specific aircraft being designed, approximate values were used. Since the constant m is often between 2-4, it was taken to be equal to 3. For the constant A, this value changed for every material and was determined with Equation 6.4.

$$A = \frac{1}{N_f}\left(\frac{c_0}{(\Delta K_{\text{eff},0})^m} - \frac{c_{cr}}{(\Delta K_{\text{eff,cr}})^m}\right) \tag{6.4}$$

Where N_f is the number of cycles until the critical crack length is reached in the material, c_0 is the initial crack length and c_{cr} is the critical crack length. Term $\Delta K_{\text{eff},0}$ is the fracture toughness corresponding to the initial crack length c_0, and likewise, $\Delta K_{\text{eff,cr}}$ corresponds to the fracture toughness of the critical crack length. All values were determined using the material properties as found in Granta[4]. The initial crack length was set to 1 mm as this crack can be detected with the naked eye. The number of cycles desired was determined to be 20 000 as mentioned in the fatigue analysis. The crack length c_i was calculated using Equation 6.5.

$$\Delta K = \Delta\sigma\sqrt{\pi c_i} \tag{6.5}$$

In this equation, $\Delta\sigma$ is determined from the stress analysis in Section 7.3, and ΔK was taken from the material properties of each respective material. The results of this analysis are discussed in Section 7.3.

Recyclability

Contributors: Caitlin, Lauren, Jimmy, Nino
Author: Nino

Recyclability also needs to be taken into account with respect to the sustainable development strategy. Preferably most of the used material in the FireFly would be recyclable. However, it needs to be looked at if recyclability affects the performance of the aircraft. To do so, different parts of the aircraft need to be analysed. The fuselage, water tank, wing box and other structural components can be made of an aluminium alloy. This would still provide enough strength and stiffness, thus not compromising on performance, while being a sustainable product. Parts that will be more difficult to recycle are the fuel bladder tank and the outer layer of the rotor blade. These parts are exposed to corrosive materials or need to endure high stresses. If these parts were made of recyclable materials, the fuel tank and rotors could fail or decrease in performance. This is not wanted. However, the parts that will be made of aluminium are a big part of the aircraft. This means that most parts of the aircraft will be recyclable.

Chosen Material Characteristics

Contributor / Author: Caitlin

To provide an easily accessible overview of all materials used in the aircraft, all relevant material properties are presented in Table 6.2

[4] Link [cited on 12-06-2024]

Table 6.2: *The materials used in the aircraft design.*

Material	**Location of material**	**Costs** [€/kg]	**Density** [kg/m^3]	**Ultimate strength** [MPa]	**Yield strength** [MPa]	**Maximum Service Temperature** [°C]	Fracture Toughness [MPa m$^{0.5}$]	Recyclable?
Aluminium alloy 2195	Fuselage, water tank, wing box	19.1-22.1	2710	221-265	538-560	145-255	30-37.5	Yes
Aluminium 5052 honeycomb	Rotor blade inner structure	15.7-26.2	15.7-16.3	$2.55\cdot10^{-3}$-$2.42\cdot10^{-3}$	$2.19\cdot10^{-3}$-$1.47\cdot10^{-3}$	130-200	-	Yes
EP/S-glass	Rotor blade outer layer	18.2-29	1840-1970	1700-1760	1700-1760	140-220	77.6-94.9	No
CSPE	Fuel bladder tank	4.37-4.4	1070-1270	20.3-31.8	20.3-31.8	140-150	0.167-0.401	No

This table was used in other analyses such as the crack propagation and minimum skin thickness determination. It includes the location of where the material is used, the cost per kg, the density, the ultimate and yield strength, the maximum service temperature, the fracture toughness, and last but not least the recycling capability.

6.2. Manufacturing, Assembly and Integration Plan

Contributor / Author: Sven

The Manufacturing, Assembly and Integration (MAI) Plan presents a step-by-step FireFly firefighting aircraft production roadmap from small parts and subsystems to the fully finished FireFly. The plan includes all significant parts of the aircraft which form sub-assemblies and systems. These are later integrated and installed to produce the final FireFly aircraft product. The full MAI plan diagram is found in fig. 6.1. The arrows in the diagram show the sequence of full aircraft production.

The production process starts with the assembly of the three fuselage sections followed by the integration of four wings and the vertical tail with the elevons and rudder respectively. The nose and main landing gear are integrated into their respective fuselage section during this part of the assembly to allow the aircraft to stand freely without additional support. Once the main aircraft structural assembly is done, the integration of the propulsion system can start. This is done by mounting four engines and nacelles at the tip of each wing followed by the installation of rotors. The integration of all smaller parts of the rotor assembly can be started at the same time as the assembly of wings and fuselage sections to ensure it is ready on time for rotor installation. Simultaneously, the integration of subsystems such as avionics, electronics and hydraulics. Furthermore, all internal and external equipment such as cockpit seats, winch for lifting and snorkel are installed at this stage. After all production activities are completed, the aircraft is ready for delivery to the customer.

Several aircraft features ensure time-efficient and cost-minimisation production. The most important one is the fact that both front and rear aft wings are identical eliminating the need to produce different parts for each wing which reduces the number of part-specific tools and crew training needed. Furthermore, two time-consuming production stages are performed simultaneously, namely the integration of the propulsion system and the integration of the interior and different subsystems saving production time when compared to the sequential method. Many parts and subsystems of the FireFly are off-the-shelf products, such as avionics, snorkel pump and engines, which reduces the time and money needed to produce completely new parts and train the manufacturing crew in doing so. The assembly of the aircraft is expected to last one month, comparable to other commercial aircraft. Since the expected production rate is 12 aircraft per year, the assembly facility is expected to be organised in a fixed-position assembly method. Once the aircraft is produced, due to the large ferry range it can be directly flown to the customer. Temporary fuel tanks can be installed in the cabin to extend the delivery range or the flight can be done with one or more refuelling stopovers.

Considering the ongoing dynamic geopolitical and economic situation that the world is facing and which is expected to continue into the coming years, the production of the FireFly will as much as possible make use of materials and parts originating from Western world countries such as the United States, Australia or the European Union. This was already implemented with the choice of subsystems as parts such as engines and avionics, both coming from the United States. In the later stage of the design and production planning it would be beneficial to consider backup options for externally sourced parts and materials to prevent long-term production suspension of the FireFly in case of unexpected events such as major supply chain issues or bankruptcy concerning the primary suppliers.

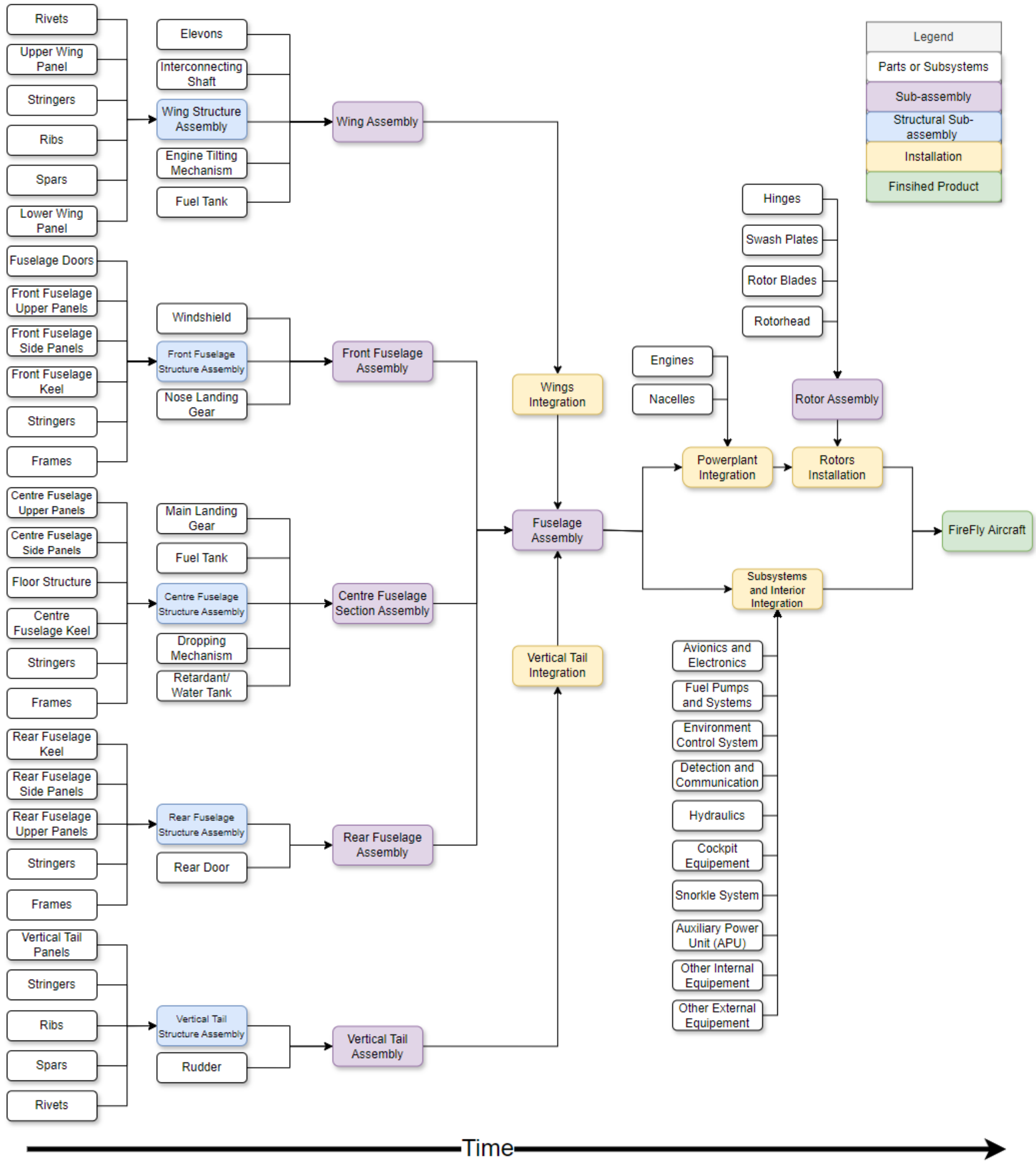

Figure 6.1: *Manufacturing, assembly and integration plan diagram.*

7 | Aircraft Characteristics

This chapter goes through the detailed design of the FireFly. The mass of the aircraft is updated by means of a Class II weight estimation. Additionally, the aerodynamics, propulsion, structures, stability & controls and performance are optimised to meet all relevant subsystem requirements to ensure mission success.

7.1. Initial Weight Budget

Contributors: Lauren, Bob, Johannes, Nino. Authors: Lauren

The initial weight estimation was performed using the weight estimation method proposed by Roskam [11]. This method made use of an initial estimation for the MTOW and payload weight. From this initial guess and a design range, the fuel weight could be determined by making use of the Breguet range equation. Additional statistical relations were then used to iterate the masses until convergence. The resulting mass estimations are shown in Table 7.1 [12].

Table 7.1: *Class I weight estimations.*

Parameter	Mass [kg]
MTOW	30000
Empty weight	15300
Fuel weight	9700
Payload weight	14000

7.2. Class II Weight Estimation

Contributor / Author: Lauren

The Class II weight estimation was conducted using the Roskam method [13]. Similarly as in Section 7.1, the FireFly was chosen to be in the military patrol, bombers & transport category due to its fluctuation in load cases during its mission. The Class II weight estimation was done using a combination of United States Air Force (USAF), United States Navy (USN), General Dynamic (GD) and Torenbeek standard Class II weight estimation methods. When the FireFly could be categorised under more than one of these standard methods, the average was taken between them as it would produce a more accurate result [13][pg. 29].

To begin the weight estimation, the weight estimate from the Class I weight estimation was used. This was 30 000 kg. Other weight estimates which were used but were not iterated upon were the payload mass 14 000 kg and the fuel mass of 9700 kg.

Furthermore, the weight estimation can be split up into four categories, namely: the fuel, engine, wing and fuselage groups. Each subsystem contains multiple subsystems and certain assumptions have been made for each. The combination of these groups plus the payload gives an initial estimate of the MTOW. Iterating the MTOW until a convergence of 0.5% occurs results in a new, more refined estimate for the MTOW. The convergence of 0.5% is standard practice [13][pg. 30]. Moreover, a more accurate estimation of the OEW can also be estimated by summing all the aircraft's components bar its fuel and payload.

Fuel System (FUE)

For the fuel system weight estimation, the mass of the fuel was used to size the fuel tank system. However, the aircraft is assumed to carry full payload and thus the mass of the fuel is not incorporated into the fuel system weight estimate. Section 7.7 describes the breakdown of relative mass between fuel and payload mass. For the tank system, it was assumed that the aircraft would have a sealant bladder bag to protect the tank from wear and tear. In terms of the fuel, it was assumed that the wing could accommodate the fuel and that kerosene would be used. The resulting weight estimation for the fuel system can be seen in Table 7.2.

Engine System (ENG)

The engine system weight estimation consists of the following components: nacelle, propeller, engine controls, engine starting system, propeller controls and the oil system & cooler. As mentioned in Section 7.4, an AE1107F turbo-shaft engine is chosen as the engine of choice for the FireFly. However, for the Class II weight estimation (using the Roskam method), it was assumed that a turboprop engine would be used as the only options available for the weight estimation were piston and turboprop engines. Furthermore, it was assumed that the propulsion system has beta controls in order to have more controllability and the water injection system sizing was neglected as the AE1107F does not make use of it.

An important factor to take into account is that the engine system was sized according to the maximum power needed at take-off. However, the statistical relationships derived from Roskam are for conventional take-off only [13]. The FireFly has a relationship between the surface area of the wings and the lift generation of the power plant for take-off as the wings will generate drag. Thus, the lack of lift generation from the wings during take-off has not been taken into account for the engine system weight estimation and thus the resulting mass may not be accurate. It is expected that larger props will be needed to account for this and consequently will result in a larger engine system mass.

Moreover, the resulting engine system mass estimation including all the aforementioned subsystems can be seen in Table 7.2.

Wing System (WIN)

The wing system consists of the front and rear wings only. However, one significant assumption is that the rear wing's mass was estimated by stating that the rear wing acts as a wing and not as a horizontal tail. Using the initial sizing of the wing as mentioned in Subsection 7.6.1, the mass of the main and rear wings could be estimated.

This weight includes the weight of normal high lift devices, the effect of having two wing-mounted engines and the landing gear will not be stored in the wings. The added mass due to the presence of speed brakes, spoilers and Fowler flaps were neglected for now. This weight estimation will be revisited if these systems are incorporated into the design. Moreover, the mass estimated for the main and rear wings are seen in Table 7.2

Fuselage System (FUS)

The fuselage system consists of multiple subsystems, namely: the fuselage structure, landing gear, flight control system, avionics, electrical systems, air conditioning & deicing, oxygen, APU, furnishing, auxiliary power, paint, pneumatic system and the total payload of 14 000 kg. The APU and paint weights were taken as the average weight for military transporters as an initial estimate and for the hydraulics system, a conservative estimate was taken to take into account the complexity of the systems onboard. Contingency was set at 20% due to the preliminary stage of the design and also according to the contingency set for the preliminary design in the [14].

Table 7.2: *System weight estimations.*

System group	**Subsystem**	**Mass** [kg]	**Contingency**
FUE	Fuel tank	1428	20%
ENG	Engines	6262	20%
WIN	Front wing	1006	20%
	Rear wing	1006	20%
FUS	Fuselage	11412	20%
OEW	Sum	21164	20%

Operational Empty Weight & Maximum Take-off Weight

From the previous system weight estimations, the operational empty weight (OEW) and the maximum take-off weight (MTOW) can be estimated. The OEW was calculated by summing all four previously aforementioned subsystem weights and subtracting the payload mass of 14 000 kg. The MTOW includes the total payload with no fuel. The final results of the Class II weight estimation and the comparison with the Class I estimation values can be found in Table 7.3.

Table 7.3: *MTOW & OEW weight estimation.*

Class II		Class I		
Subsystem	Mass [kg]	Subsystem	Mass [kg]	Difference
MTOW	35160	MTOW	30000	+17.2%
OEW	21164	OEW	15300	+38.3%
Payload	14000	Payload	14000	-
Fuel	9700	Fuel	9700	-

The MTOW and OEW have increased considerably. This increase is mainly due to the more accurate estimation of the empty airframe. In the class I estimation, reference tilt rotors were used. Most of these tilt rotors however, only feature two rotors which allow for a much smaller fuselage. This likely resulted in an underestimation of the empty weight. This new estimate for the OEW and MTOW was used to get a more accurate estimate for the aerodynamic, propulsive, stability & control and structural analyses.

7.3. Structural Characteristics

Contributors / Authors: Lauren, Caitlin, Jimmy

To ensure that the aircraft structure adheres to the requirements set by the client and the team, the relevant requirements are listed in Table 7.4.

Table 7.4: *Structural subsystem requirements.*

Identifier	Parent	Subsystem Requirements
QTR-STR-01	FTF-SYS-FDS-05.15 / FTF-SYS-REG-02.8 / FTF-SYS-REG-02.9	The airframe should be designed to withstand loads of -1 to +3.25 g.
QTR-STR-02	FTF-SYS-REG-01.9	The fuselage shall be equipped with emergency exit doors on both sides of the fuselage.
QTR-STR-03	FTF-SYS-FDS-07.1	The windshield shall include an anti-icing system.
QTR-STR-04	FTF-SYS-FDS-07.2	All structural components shall be made from salt water corrosion-resistant materials.
QTR-STR-05	FTF-SYS-FDS-07.2	All exposed metallic surfaces shall have applied protective coating from corrosion.
QTR-STR-06	FTF-SYS-REG-01.13 / FTF-SYS-REG-02.8 / FTF-SYS-REG-02.9	The structure shall withstand limit loads without permanent deformation.
QTR-STR-07	FTF-SYS-REG-01.13 / FTF-SYS-REG-02.8 / FTF-SYS-REG-02.9	The structure shall be able to support ultimate loads without failure for at least 3 seconds.
QTR-STR-08	FTF-SYS-REG-02.2	All material shall be able to withstand 30 sec of flight in 180 degrees.
QTR-STR-09	FTF-SYS-REG-01.7	The cockpit windows shall allow an unobstructed primary field of view to both pilots in accordance with CS25 requirements.
QTR-STR-11	FTF-SYS-PIL-04.2	The aircraft shall be equipped with an emergency exit accessible from the cockpit.
QTR-STR-12	FTF-SYS-PIL-04.2	The aircraft shall be equipped with an emergency exit accessible from the cargo hold.
QTR-STR-13	FTF-SYS-REG-01.7	The cockpit shall have windows that provide visibility in adherence to CS 29.773.
QTR-STR-14	FTF-SYS-PIL-01.1	Seats in the aircraft shall fit a person with a height of 188 cm.

Continued on next page

Table 7.4 – continued from previous page

Identifier	Parent	Subsystem Requirements
QTR-STR-16	FTF-SYS-SUP-01.1	The aircraft shall be fully operational during flight in cruise in weather conditions between −36 degrees Celsius and 50 degrees Celsius.

The structural design aims to ensure that the structure can withstand all extreme load cases throughout all phases of the mission. The structural analysis ensures that all aforementioned requirements have been met. Three cases will be investigated. These are the thermal loads, the wing loading and the response of the structure to dropping payload in hover.

Thermal Analysis

Contributors / Authors: Lauren, Caitlin

Firstly, the thermal loads acting on the structure were analysed to see the affect of the external environment on the structure during a mission in extreme cases. The bottom of the fuselage was identified as having the highest risk of long-term heat exposure when fighting the fire. Therefore, it is important to understand if exposure to high temperatures will cause yield in the material. The underside of the fuselage was assumed to be a thin plate made of AL2195 that is constrained at all four sides. To analyse the thermal stress due to expansion, Equation 7.1 was used[15].

$$\frac{F}{A} = Y\alpha\Delta T \tag{7.1}$$

In this equation, Y denotes the compressive Young's modulus [GPa], α is the thermal coefficient [μstrain/°C] and ΔT is the change in temperature [°C]. Additionally, A is the affected area [m^2], and F is the force due to thermal stresses [N].

The yield stress of AL2195 is 538 MPa [1]. Using Equation 7.1 the temperature difference that would cause yielding would have to be 332 °C. It is expected that 180 °C will be the highest temperature experienced above a fire at an altitude of above 40 m during a mission [16][pg. 4]. According to QTR-PYL-09, the cargo bay shall be heated to 20 °C or below. Therefore, the temperature difference between the ambient air and the skin of the panel is not expected to exceed this temperature difference.

Furthermore, the thermal shock of AL2195 is between 221 −265 °C[1]. Investigating the sudden change in temperature near a fire at 40 m altitude shows that the temperature difference will not be higher than the damaging thermal shock temperatures of AL2195-T8.

Additionally, extending this analysis by investigating the heat propagation through a thin plate with the minimum thickness obtained in the structural analysis is recommended. This should be done to analyse how quickly the temperature increases through the plate to determine if a heat sink is necessary. This ties into technical risk **QTRR29** which is assessed in Section 11.1.

Fuselage Thickness & Stiffness

Contributors / Authors: Caitlin, Lauren

To analyse the fuselage, some assumptions were necessary to simplify calculations. The assumptions were made as follows:

- The cross-section of the fuselage is symmetric in the yz and xz plane: the fuselage is designed to be symmetric.
- As seen in Figure 7.1 top and bottom of the fuselage are approximated to a semi-circle whilst the middle section is considered a rectangle: in reality the cross section is a rectangle with rounded corners, so the approximation is less conservative and some margin will likely have to be considered as a result.
- The walls are thin (t«h): the thickness of the fuselage is much smaller than the height or width of the panels. Therefore higher order terms of thickness ('t') were neglected. This results in a slightly lower result but the difference is considered negligible.

[1] Link [cited on 05-06-2024].

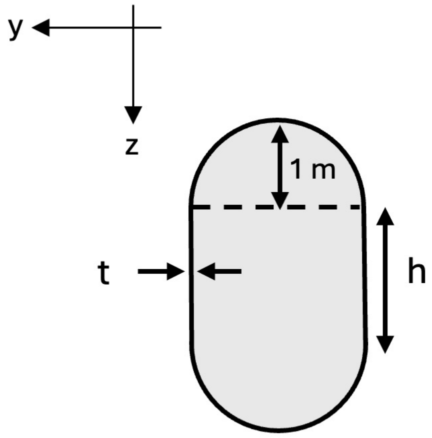

Figure 7.1: *Fuselage cross section.*

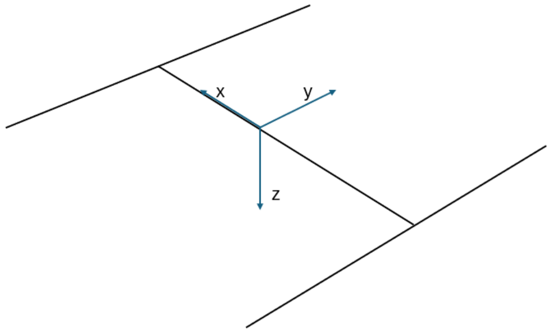

Figure 7.2: *Aircraft approximated as simplified beams with the associated axis system.*

The thickness was calculated by analysing the maximum stress caused by either bending or shear. The aircraft was analysed in various situations. Firstly, hover mode was considered as a static case (n=1) with full payload on board. Secondly, a drop case was considered where the aircraft is analysed just after a drop. The same was done for a dive manoeuvre where the maximum load factor of 3.25 g was taken into account as this proved to be the most limiting case.

The coordinate system corresponds to the usual convention of aircraft axis systems, meaning that the x-axis goes through the nose of the aircraft, the y-axis is positive through the starboard side of the aircraft and the z-axis points downwards.

The moment around the c.g. was calculated by means of simplifying the fuselage to be a simply supported beam representing the connection to the wings. The weight of the wings and engines were forces applied at the end of the fuselage beam and the weight acting at the centre of gravity consisted of the remaining weight of the aircraft. This was done to analyse the stresses experienced in the fuselage and wing for the two expected extreme loading cases, namely hovering with full payload and a full spot drop in hover. The loads of the fuselage were modelled as point loads, as this is a more conservative approximation.

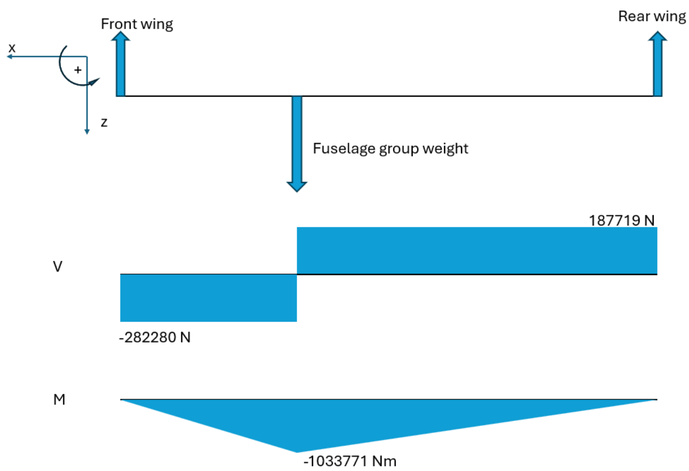

Figure 7.3: *The shear and moment diagram of the fuselage.*

In Figure 7.3, the 'Front wing' force includes the weight of the wing, the fuel in the wing and the engine group attached. Additionally, the thrust generated by the propellers in hover mode is taken into account in this force. The same was done for the 'Rear wing' force. The fuselage group weight consists of the weight of the fuselage, the fuel and maximum payload.

The bending stress was then calculated using Equation 7.2, where σ is the bending stress in MPa, M is the moment around the centre of gravity around the y-axis, and z is the maximum distance to the fuselage from the centre of the cross-section.

$$\sigma_x = \frac{Mz}{I_{yy}} \tag{7.2}$$

From the material selection as described in Chapter 6, AL2195-T8, AL7068 and AL2024 were the most desirable materials moving forward. Therefore, investigating the internal shear and bending moments of the fuselage for both cases, the minimum thickness of the fuselage was determined.

After the analysis for both cases, it was found that the internal moments when performing a dive with full payload were most limiting for the thickness. The minimum thickness for each material can be seen in Table 7.5 below:

Table 7.5: *Minimum thickness of the fuselage for the chosen materials.*

Material	Yield Stress [MPa]	Minimum thickness [mm]
AL2024 T851	386	1.63
AL2195 T8	538	1.20
AL7068 T6511	648	0.97

Design of the Wing Structure

Contributors / Authors: Jimmy, Lauren

The wing structure is designed following a systematic framework of designing to requirements.

The wing structure has its own set of requirements, which must be met. The strength requirement of the wing box flows from **QTR-STR-01**, **QTR-STR-06** and **QTR-STR-07**. The maximum magnitude stress under the most critical loading condition may not exceed the yield strength of the wing box material. Unique to the wing structure, there is also a stiffness requirement when it is subjected to the hover load. In hover, the engines must provide all the lift. Due to the deflection of the wing, the engines are no longer aligned with the vertical axis which results in a loss of lift. This means that the deflection slope at the tip of the wing, where the engine is mounted, may not exceed 0.55 rad. This is the angle at which the engines at maximum thrust can still generate enough lifting force.

In this early stage of the design, it is customary to make assumptions which simplify the analysis. This is in the interest of time because an optimal wing geometry must be synthesised via iterations, so a simpler model makes the design process faster. This allows for a quicker progression towards detailed design, which is when the model is refined. The main assumptions have been listed below.

- WA1: The wing is modelled as an Euler-Bernoulli beam.
- WA2: The wing structure is thin-walled (t « h).
- WA3: The shear centre coincides with the centroid.

WA1 is a valid assumption as long as the wing is slender. The wing, however, has a low aspect ratio, which means that the wing is not very slender. This means the effects of shear become less negligible, meaning the Euler-Bernoulli beam model is not accurate. However, at this stage of the design, the emphasis lies on identifying feasible structural geometries, so using an Euler-Bernoulli beam model still leads to useful results. In a further design step, one would have to use a more refined beam model like a Timoshenko beam. WA2 is the most justifiable assumption, because aerospace structures, especially wing structures, are thin-walled stiffened shell structures. It is only when the required structural wall thickness becomes too large that WA2 is invalid. However, it should never come to this because stiffeners can be used to reduce the required thickness. WA3 is made to simplify the analysis of shear, but in general, the shear centre does not coincide with the centroid. Because the wing box is not symmetric in x and z, the shear centre will not coincide with the centroid. That said, the wing box section is not too far from being a rectangle, so it stands to reason that the shear centre is close to the centroid. In that case, the difference in torque caused by assuming the internal shear forces act through the centroid may be negligible. A future design step would be to calculate the positions of the shear centre and analyse its effect on the design.

The last influence on the design process is the modelling choices. These do not follow directly from the structural requirements or the assumptions. Instead, they follow from practical considerations or from other subsystems. The design choices have been summarised below.

- MC1: The wing is modelled by the wing box alone.
- MC2: The wing section is constant.
- MC3: The wing box is made from one material.
- MC4: Stiffeners are not modelled.

Modelling the wing by only the wing box vastly speeds up the analysis of the wing structure, and for the same thicknesses, it is more conservative because the wing box encloses a smaller area than the aerofoil. MC1 allows for modelling the wing section as a single-cell beam, which is significantly easier to analyse because no displacement compatibility equations are necessary. In further design, the wing section will be modelled so that the whole shape is captured. MC2 follows from the supposition that a constant wing section makes manufacturing easier. Next to that, there are aerodynamic motivations for keeping the section constant, as will be apparent from Subsection 7.6.1. MC3 also makes the design and analysis of the wing structure easier. If the wing section is made from multiple materials, it would require the use of compatibility equations, even if the wing section is modelled by a single-cell wing box. MC4 is made because the design of stringers is supposed to be the subject of detailed design. By assuming that the skin and spars only carry the loads, the required thicknesses are overestimated. However, in a more detailed design phase, the area concentrated in the skin can be reduced by considering stringers. The anticipated effect of this is that the overall structural mass will decrease because stiffened skin panels are more efficient than thick skin panels.

Methodology
The analysis of the wing consists of static and dynamic analysis. The emphasis is placed on analysing the wing structure subjected to quasi-static loads. The wing box is also sized based on that. The dynamic analysis is performed on the wing structure to investigate the effect on the fatigue performance of the structure. Buckling and aeroelastic analysis are considered to be outside of the scope of the DSE because of the required level of detailed design to analyse the structural response. Therefore, the analysis of buckling and aeroelasticity is left to a more detailed design phase. However, it is recognised that there are risks associated with disregarding these failure modes. The impact of which usually results in an increase in structural mass. These risks have been identified as **QTRR27** and **QTRR28** and will be assessed in Section 11.1.

An overview of the design process of the wing box can be seen in Figure 7.4.

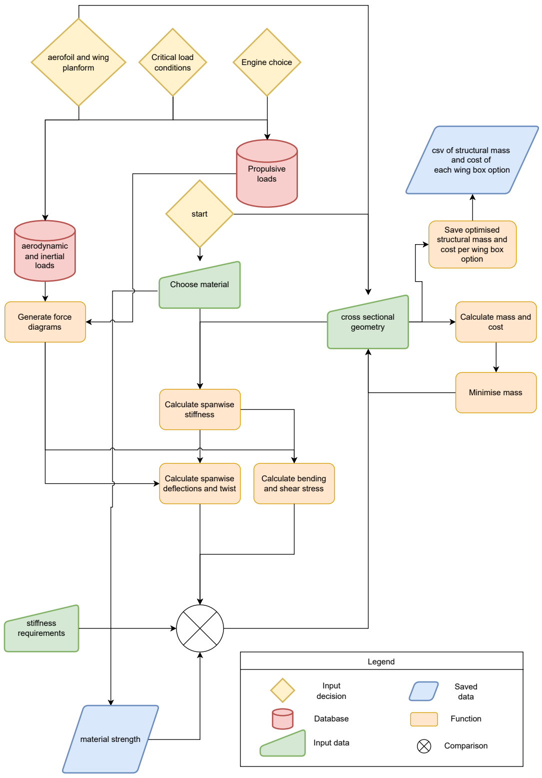

Figure 7.4: *The flowchart of the structural optimisation algorithm.*

Figure 7.4 is similar to the one for materials selection because the algorithm is effectively the materials optimisation algorithm repurposed for the design of a trapezoidal wing box. The biggest differences now are that the algorithm does not loop through the materials; the user must specify the material, and part of the strength requirement is also the allowable stress amplitude which comes from the fatigue analysis.

Based on the most critical static loading condition, the deflections and stresses in the wing structure are calculated. The algorithm optimises the different skin and spar thicknesses for 20 000 cycles to minimise the structural mass while still satisfying the strength and stiffness requirements.

The critical loading condition is identified to be hover. In hover, the entire lift force caused by the engine is concentrated at the wing tip, which causes a larger internal bending moment compared to a distributed lifting force encountered in the cruise. A free body diagram of this load case is shown in Figure 7.5.

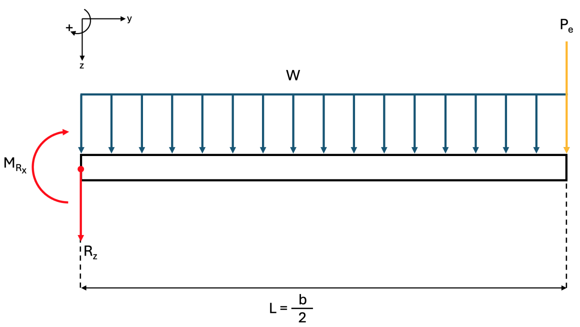

Figure 7.5: *The free body diagram of the starboard wing in hover.*

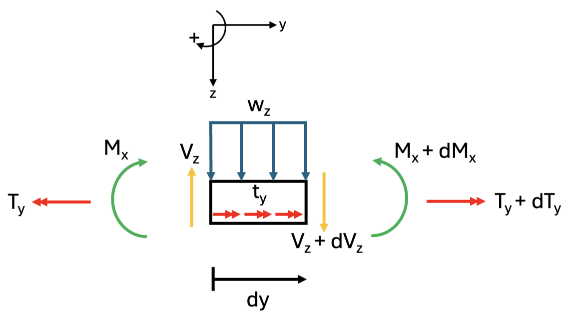

Figure 7.6: *The sign conventions of the internal loads in the starboard wing.*

Figure 7.5 is a free body diagram of the starboard wing when the aircraft is hovering. This means the structure is subjected to a distributed load w, signifying the distributed weight of the wing structure, and a point load P_e, signifying the force caused by the engine. All loads are assumed positive in the directions they have been shown in.

Figure 7.6 shows a structural element with exposed internal loads. All loads are shown in their positive directions.

From the free body diagram of Figure 7.5, the internal loading diagrams for shear, bending moment and torque can be generated using the sign convention defined in Figure 7.6. The methodology of generating these diagrams is taken directly from Aircraft Structures for Engineering Students [17]. The plots of the span-wise internal shear force distribution, the span-wise internal bending moment distribution and the span-wise internal torque distribution are included as Figure 7.11, Figure 7.10 and Figure 7.12 respectively.

With the span-wise internal load variations known, the beam bending equation can be used to calculate the deflection of the wing box. The flexural equation is taken from Aircraft Structures for Engineering Structures [17] and is shown as Equation 7.3.

$$v''(y) = -\frac{M_x(y)I_{zz}(y) - M_z(y)I_{xz}(y)}{E\left(I_{xx}(y)I_{zz}(y) - I_{xz}^2(y)\right)} \tag{7.3}$$

v'' is the curvature of the deflection field along the wing span rad/m in the z-axis. I_{xx} and I_{zz} are the area moments of inertia about the x-axis and z-axis respectively in m^4. I_{xz} is the product moment of inertia in m^4, which in general is not zero if the cross-section has no symmetry planes. E is Young's modulus of the material in Pa. M_x and M_z are the internal bending moments about the x-axis and z-axis respectively in [Nm].

Equation 7.3 relates the curvature to the span-wise variation of the bending moment and the span-wise variation of the geometrical stiffness. The area moment of inertia and the product moment of inertia are calculated using the geometry of a section. A wing box section is shown in Figure 7.7.

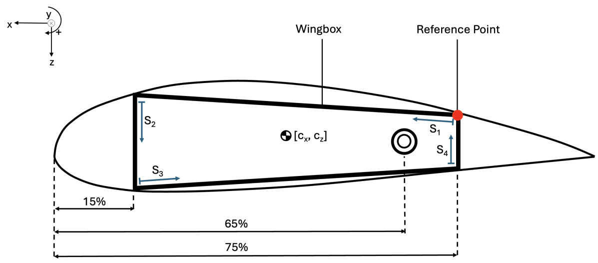

Figure 7.7: *Schematic drawing of the wing box of the starboard wing, looking from the root.*

Figure 7.7 shows the geometry of the wing box, with only the thickness of the four segments being variables. This way, I_{xx}, I_{zz} and I_{xz} can be calculated as a function of the four thicknesses. It also shows the centroidal coordinates, C_x and C_z, which are also the coordinates of the shear centre, as well as the position of the driveshaft at 60 percent chord length from the leading edge.

When the span-wise variation of the bending stiffness and the internal bending moment is known, Equation 7.3 can be integrated once to find the deflection slope and twice to find the deflection itself.

The normal stresses and shear stresses in the section can be calculated using the span-wise variation of the internal loads and the geometric stiffness using the methods described in Aircraft Structures for Engineering Students [17]. Specifically, for bending stress, Equation 7.4 is used.

$$\sigma_y = \frac{\bar{x}\left(M_z I_{xx} - M_x I_{xz}\right)}{I_{xx}I_{zz} - I_{xz}^2} + \frac{\bar{z}\left(M_x I_{zz} - M_z I_{xz}\right)}{I_{xx}I_{zz} - I_{xz}^2} \tag{7.4}$$

σ_y is the bending stress at a section in Pa. $\bar{x}$ is the x-position with respect to the centroid in m. $\bar{z}$ is the z-position with respect to the centroid in m.

The maximum normal stress and shear stress in each section can now be plotted along the span of the wing. Aside from those, a combined maximum stress state can be found using a stress transformation, as is described in Mechanics of Materials [18]. Using a failure criterion like the Tresca yield criterion, one can calculate the margin of safety of one section. The equation for which is given by Equation 7.5 [2].

$$MS = \frac{\sigma_{\text{failure}}}{SF\,\sigma_{\text{applied}}} - 1 \tag{7.5}$$

σ_{failure} is the failure stress of the material and σ_{applied} is the applied stress on the material in Pa. SF is a safety factor, which is taken as equal to the design safety factor.

When the margin of safety is plotted along the wing span, it gives an idea of how efficient the design of the structure is. MS should be as close to zero as possible without decreasing below zero. This information can then be used in a later design stage to further optimise the structure.

The implementation of the methodology involves discretising the wing as an assembly of wing elements. This means the wing assembly is split into a number of elements. The size of such an element, that is to say, the step size, impacts both the computational time and the accuracy of the model. One must strike a balance between minimising computational time and maximising accuracy. To this end, a sensitivity analysis was performed on the effect of the step size on the stress calculations. The specimen is a trapezoidal wing box made from Al7068T6511. This analysis aims to find out at which step size the output, in this case, the normal stress at the root, begins converging to one value. This step size is the optimal step size. The result has been plotted in Figure 7.8.

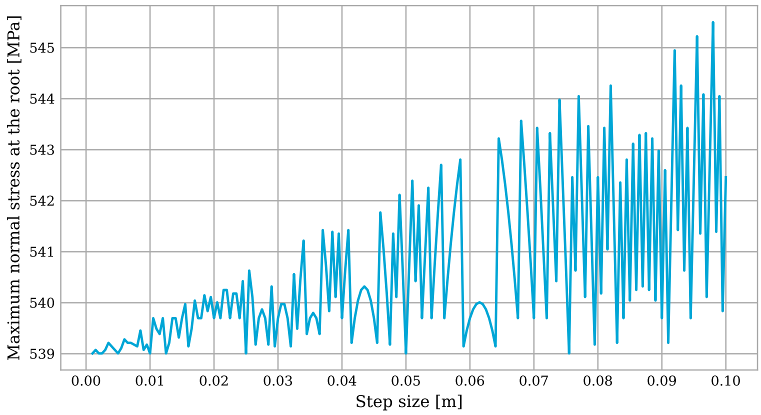

Figure 7.8: *The sensitivity of maximum normal stress to step size.*

Looking at Figure 7.8, there is a very distinct oscillation in the results. Although there is a general sense of convergence towards one value as the step size approaches infinitesimally small, the intense oscillations are a major peculiarity. One possible explanation is the fact that the quadrature rule used for the numerical integration of Equation 7.3 is a trapezoidal rule, which is a two-point Newton-Cotes method. This works well for small step sizes, but when the elements become larger, a two-point quadrature rule will not be able to accurately approximate the actual integral. This notwithstanding, there is still a step size below which the results start to converge and the oscillations decrease, this is a step size of 0.01 m. As such, this step size will be used in all structural calculations of the wing.

Results

Running the optimisation algorithm while following the fatigue procedure for 20000 cycles as described in Table 6.1 yields the data shown in Table 7.6.

Table 7.6: *Optimised wing box options for Al2024T851 and Al2195T8.*

Wing box	Material	Mass [kg]	Cost [€]	$t_{\text{upper skin}}$ [m]	$t_{\text{front spar}}$ [m]	$t_{\text{lower skin}}$ [m]	$t_{\text{rear spar}}$ [m]
Baseline3	Al2024T851	1282	4514	0.02	0.01	0.015	0.01
WB2A3	Al2195T8	913	18817	0.015	0.01	0.01	0.005

[2] Link [cited on 25-06-2024]

Although the optimisation algorithm is constrained by fatigue stress besides yield strength, the static stress caused by hover drives the design. This will be apparent from Figure 7.14. The margin of safety in hover comes the closest to zero, which implies that the static stress in hover drives the wing structural design.

As the fatigue life of a material is dependent on the stress resistant properties of the material, it is natural that Al2195 T8 would perform better in fatigue. Therefore, in order to make an informed decision about the material choice for the wing box, a crack propagation analysis had to be performed. Following the procedure for crack propagation as per Equation 6.1, it can be seen in Figure 7.9 that AL2024 performs better than AL2195T8. However, from Table 7.6, it is observed that WB2A3 is significantly lighter than Baseline3. This is as expected because in Table 6.1, the Al2195 structure was also lighter than the Al2024 structure. Therefore, it was a trade off between mass and crack propagation.

As the FireFly will endure frequent high loads, Al2195T8 was chosen as it performs better under high stresses and saves weight. Since its crack propagation is worse than the AL2024T851, more frequent maintenance will be put in place to catch any sort of damage in its early stages. It was found however, that more than $1000 \cdot 10^3$ cycles can be done before critical crack length is reached.

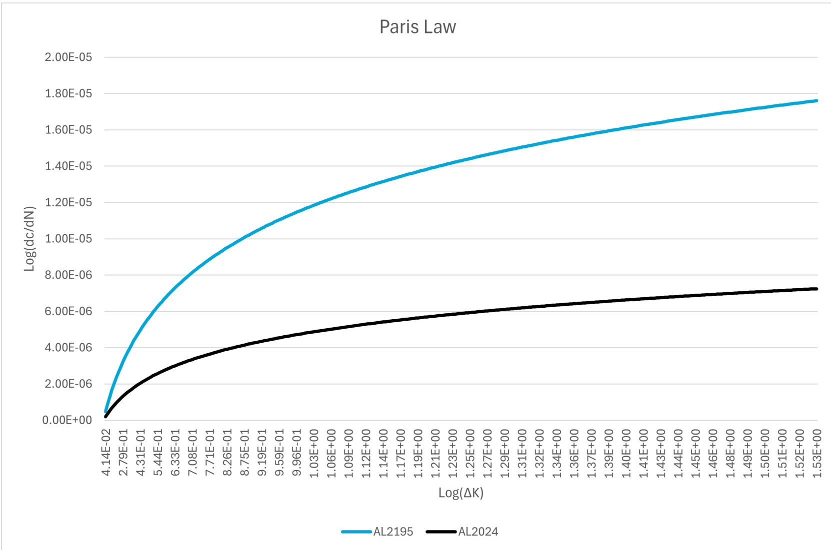

Figure 7.9: *The different aluminium alloys with the Paris Law applied.*

Moreover, it should be noted that the skin thicknesses are very high. Skin thicknesses are usually in the order of a millimetre, but because the wing model assumes no stiffeners, the skin thicknesses have increased to cope with the stress.

The data for WB2A3 are used as inputs for the generation of the static analysis plots and the dynamic analysis plots.

Static Analysis Plots

Using the free body diagram signified by Figure 7.5, the internal loading diagrams have been generated as Figure 7.10, Figure 7.11 and Figure 7.12. With Figure 7.10 and the data for WB2A3 from Table 7.6, the span-wise maximum normal stress distribution and the span-wise factor of safety in hover can be plotted as shown in Figure 7.13 and Figure 7.14 respectively.

Figure 7.10 shows a decreasing approximately linear relation and is positive. This is as expected because the point load by the engine causes positive bending, but the tip is not subjected to any point moments, so the internal bending moment must be zero there. In reality, there should be a quadratic relation due to the constant distributed force w_z, but because P_e is much larger, this effect is less visible. Figure 7.11 shows a decreasing linear relation and is negative. Following the sign conventions and the internal load relations from Aircraft Structures for Engineering Students [17], this makes sense. The engine load causes a negative shear because P_e drawn in Figure 7.5 is actually negative.

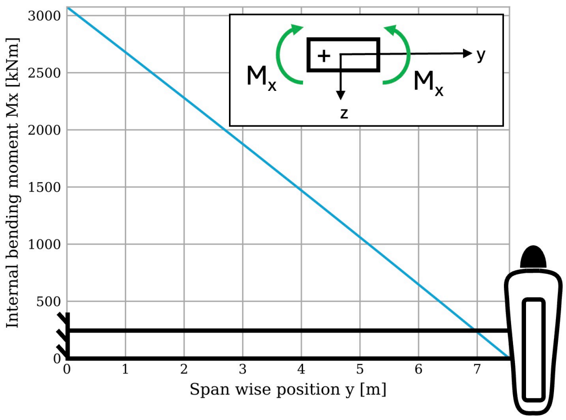

Figure 7.10: *Span-wise internal bending moment diagram in hover.*

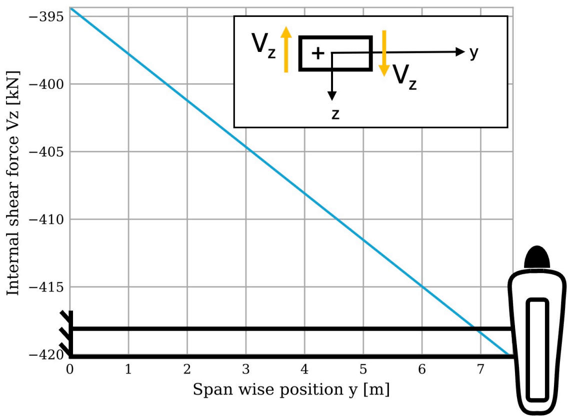

Figure 7.11: *Span-wise internal shear force diagram in hover.*

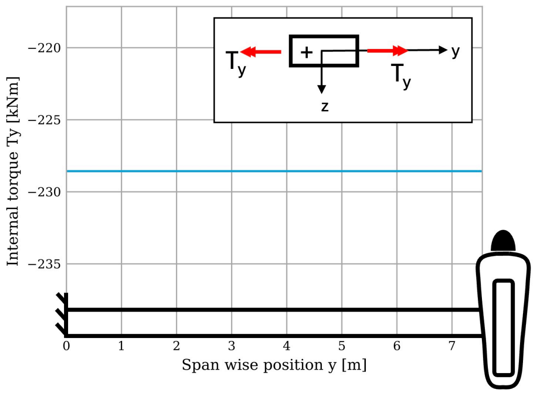

Figure 7.12: *Span-wise internal torque diagram in hover.*

Figure 7.12 signifies a constant and negative internal torque distribution. The internal torque is negative because of the torque caused by the engine load. The engine load is applied at the driveshaft, the position of which was shown in Figure 7.7. Because the driveshaft is not coincident with the sectional shear centre, this load causes an internal torque. By the sign convention of the internal torque, the engine load causes a negative internal torque.

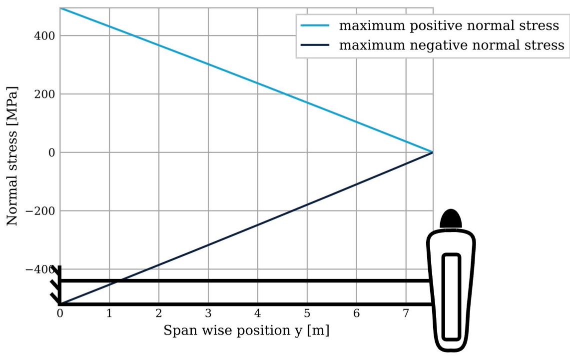

Figure 7.13: *Span-wise normal stress distribution of WB2A3 in hover.*

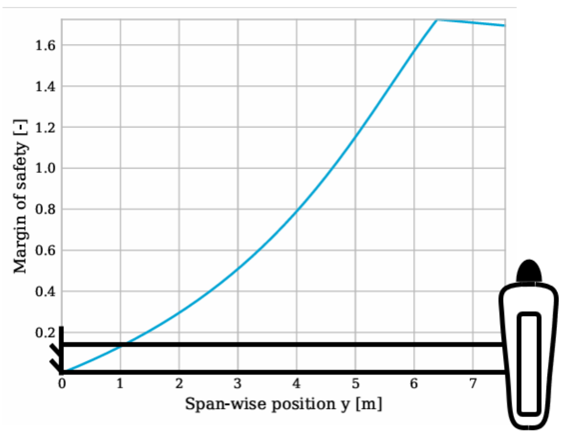

Figure 7.14: *Span-wise factor of safety of WB2A3 in hover.*

Figure 7.13 is a plot of the maximum positive and negative normal stress at each section along the wing span.

By Figure 7.5, this stress is caused by the internal bending moment and it reduces to zero towards the tip because the internal bending moment goes to zero towards the tip. Figure 7.14 gives an idea of the structural efficiency of the wing box. The closer the margin of safety is to zero, the more efficient the structure is. As can be seen, the margin of safety steadily rises to 1.75 near the tip, evidently because the normal stresses go to zero at the tip, but the cross-section is kept constant. This means the structural mass near the tip is effectively underutilised. A more efficient structure would taper the thicknesses towards the tip so that the margin of safety is closer to zero. However, this would sacrifice the manufacturing benefits of a constant cross-section. This trade-off would have to be further investigated in a more detailed design phase. The margin of safety also gives an idea of how much a loading case drives the design. Figure 7.14 shows that the margin of safety comes very close to zero towards the root of the wing. This reinforces the fact that hover drives the design of the wing structure.

Dynamic Analysis

A general dynamic analysis of the structure is outside of the scope of the DSE, however, a vibrational analysis and its effect on fatigue is a worthwhile endeavour because of the implications on the mission.

The specific load case that is investigated would be the case of dropping the full payload of 10 000 kg in one go. It is of interest to investigate the vibrational response of this sudden drop on the wing. This is because the aircraft may conduct many such drops during operations, so analysing the effect of this vibrational response on the fatigue of the wing structure allows for making design choices which can lower the severity of the fatigue life impact of the vibration. This in turn leads to more load cycles without the need for maintenance and repair, which means less downtime.

The effect of dropping all the payload is that the aircraft fuselage accelerates up due to a loss of mass. This can effectively be modelled as an impulse load $P_0\delta(t)$ where P_0 is equal to the payload weight and $\delta(t)$ is the Dirac pulse. The fuselage transfers this impulse load onto the wings, which will cause a vibration.

The vibrational model used is shown in Figure 7.15.

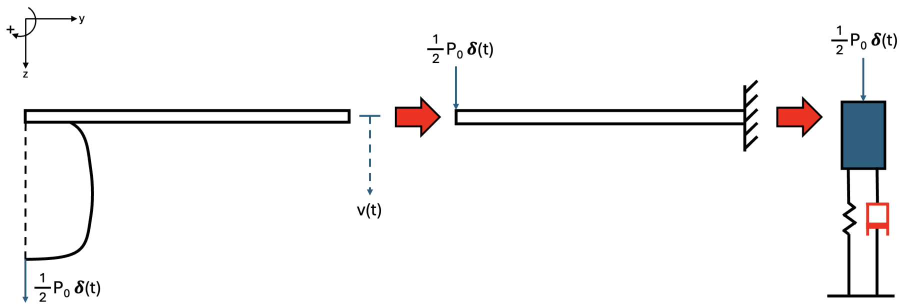

Figure 7.15: *The vibration of the aircraft is modelled as the tip vibration of a cantilevered beam which can be modelled as a mass-spring-damper system.*

As seen in Figure 7.15, to simplify the analysis, only one wing half is taken, which means that $\frac{1}{2}P_0\delta(t)$ acts on the wing. One further simplification is to model the wing as a cantilevered beam where the tip is the built-in end and the root is the 'free' end. This allows for following the methodology described in Engineering Vibration [19] to model the tip deflection of a cantilevered beam as the deflection of an equivalent stiffness mass-spring-damper system. The impulse response function of this system assuming the system is under-damped and starts from rest can be found to be Equation 7.6.

$$h(t-t^*) = \frac{1}{m\omega_d} e^{-\zeta\omega_n(t-t^*)} \sin(\omega_d(t-t^*)) \tag{7.6}$$

Equation 7.6 holds for $t > t^*$. m is the mass in kg, ζ is the damping ratio, ω_n is the natural frequency in rad/s and ω_d is the damped natural frequency in rad/s. When subjected to an impulse load $P_0\delta(t-t^*)$, the time response of the deflection is found by Equation 7.7.

$$x(t) = P_0 h(t-t^*) \tag{7.7}$$

Equation 7.7 also holds only for $t > t^*$; for $t < t^*$, it is equal to zero. Using Equation 7.7, the time response of the deflection at the wing root can be found. This also allows for finding the time response of the bending moment at the root, which can be directly translated into the time response of the maximum tensile stress at the root. The sign convention for positive deflection and positive external force is as shown in Figure 7.15.

One big hurdle is that the damping ratio of the wing structure is not known at this point. This means that it is not possible to know for certain what the stress amplitude caused by the impulse load will be. Instead, the vibrational analysis has been carried out for different damping ratios and the results have been plotted in Figure 7.16 and Figure 7.17 utilising the data of WB2A3 from Table 7.6.

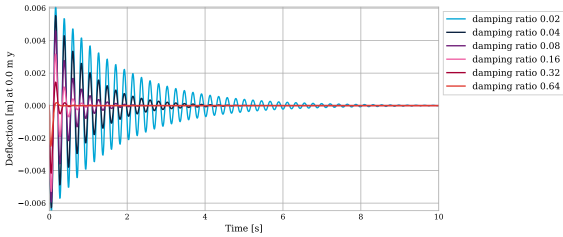

Figure 7.16: *The time response of the deflection at the root due to an impulse load for different damping ratios.*

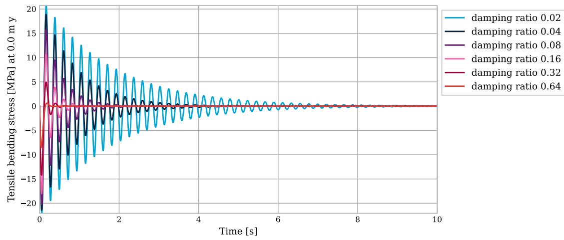

Figure 7.17: *The time response of the maximum bending stress in the lower wing skin at the root due to an impulse load for different damping ratios.*

As seen from Figure 7.17, depending on how well the structure is damped, the stress variation can either quickly dampen out or persist for several cycles. This stress variation can be superimposed onto the quasi-static stress, resulting in a total stress which may not exceed the yield strength of the structure. Because the wing box geometry is optimised so that the factor of safety at the root is closest to one, this will likely mean that the dynamic stress causes the total maximum normal stress to exceed the material yield strength, necessitating a stronger structure.

With the vibrational analysis, a framework has been set up for designing structural dynamics should it turn out further down the line that the damping ratio of the structure is low enough that the stress amplitude significantly affects the fatigue life of the structure. At that point, a trade-off can be made to strengthen the structure by decreasing the stress amplitude or to use materials which are more resistant to fatigue like fibre metal laminates.

7.4. Propulsion Analysis

Contributor / Author: Bob

To select the propulsion system, a power required estimation was conducted and the subsystem requirements were taken into account. It is determined that the Rolls-Royce AE1107F engine is the best option for the FireFly[3].

Requirements

For the propulsion system, the following subsystem requirements are considered:

Table 7.7: *Propulsion subsystem requirements.*

Identifier	Parent	Subsystem Requirements
QTR-PRP-01	FTF-SYS-FDS-03.1 and QTR-FUL-01	The engines shall have a total average fuel mass flow rate of less than 0.36 kg/s during ferry flight.
QTR-PRP-02	FTF-SYS-FDS-03.2 and QTR-FUL-01	The engines shall have a total average fuel mass flow rate of less than 0.9 kg/s during the refilling and dropping phases of aerial firefighting.
QTR-PRP-03	FTF-SYS-FDS-03.3 and QTR-FUL-01	The engines shall have a total fuel mass flow rate of less than 0.82kg/s while operating with a full retardant tank at a minimum dash speed of 400km/h.

Continued on next page

[3] Link [cited on 25-06-2024]

Table 7.7 – continued from previous page

Identifier	Parent	Subsystem Requirements
QTR-PRP-04	FTF-SYS-FDS-05.1	The engine shall be connected to a tilting mechanism to rotate the thrust vector.
QTR-PRP-05	FTF-SYS-FDS-05.1	The tilting mechanism shall allow each engine's thrust vector to rotate 135° from its horizontal flight mode position.
QTR-PRP-06	FTF-SYS-FDS-05.1	Each engine's tilting mechanism shall be able to be rotated independently.
QTR-PRP-07	FTF-SYS-FDS-04.1	The engines shall be able to provide a minimum of 35kN thrust in horizontal flight at sea level in ISA conditions.
QTR-PRP-08	FTF-SYS-FDS-05.2	The propulsion system shall provide dynamic thrust changes during water refilling to compensate for increasing weight.
QTR-PRP-09	FTF-SYS-FDS-05.15	Rotors shall be able to sustain loads of -1 to 3,5 g without deformation that influences performance.
QTR-PRP-10	FTF-SYS-FDS-05.16	The propulsion system shall be able to produce a minimum of 27kN in horizontal flight at 3000 meters in ISA conditions.
QTR-PRP-11	FTF-SYS-FDS-07.1	Then engine inlet shall be equipped with an anti-icing system.
QTR-PRP-12	FTF-SYS-FDS-07.1	The individual propeller blades shall be equipped with an anti-icing system.
QTR-PRP-13	FTF-SYS-REG-01.10	The powerplant shall be accessible for necessary inspections and maintenance.
QTR-PRP-14	FTF-SYS-FDS-07.2	The individual propeller blades shall have salt water corrosion protective coatings.
QTR-PRP-15	FTF-SYS-REG-01.11	One engine failure shall not prevent normal operations of all other engines.
QTR-PRP-16	FTF-SYS-REG-01.11	There shall be means of stopping each engine individually.
QTR-PRP-17	FTF-SYS-REG-01.11	There shall be means of restarting each engine in-flight.
QTR-PRP-18	FTF-SYS-REG-01.3	Power ratings shall be established for all engines.
QTR-PRP-19	FTF-SYS-REG-01.5	The engines shall be certified according to CS-E regulations.
QTR-PRP-20	FTF-SYS-FDS-06.4	The engines shall be easily accessible by maintenance crew.
QTR-PRP-21	FTF-SYS-FDS-06.4	The engines shall use industry-standard parts.
QTR-PRP-22	FTF-SYS-REG-01.6	The propellers shall be tested on impact resistance.
QTR-PRP-23	FTF-SYS-SUP-01.2	The engines shall be able to use at least one of the following fuels: Jet A-1 and Jet B.

Table 7.8: *List of engine models considered.*

Manufacturer	**Model**	**Power** [hp]	**BSFC** [lb/h · hp]	**Application** [20]
Rolls-Royce	AE 1107C	6000	0.426	V-22 Osprey
Rolls-Royce	AE 1107F	7000	0.426	V-280 Valor
General Electric	T408	7500	≈ 0.4	CH-53K
Rolls-Royce Turbomeca	RTM 322	2270	0.42	Eurocopter X^3
General Electric	T700-GE-701D	1940	0.462	Sikorsky S-70

In Figure 7.18 power required for cruise and hover combined is plotted against velocity. When not enough lift is generated by the wings the rotors will rotate and generate thrust. It shows that the limiting case is One Engine Inoperative(OEI). This stems from CS-E regulations requiring the ability to maintain a rate of climb of 2/3 m/s when one engine cuts out. As can be seen in Figure 7.18, the AE1107F engines provide enough power for this. This does take into account that all engines will be connected through gearboxes and driveshafts so that all four rotors can be turned by the three remaining engines in the OEI scenario. In case a total engine efficiency(output power/shaft power available) of 0.83 is assumed, Figure 7.18 also shows that there is enough power to overcome drag at high cruise speeds and accelerate to high dash speeds of over 500 kph.[4]

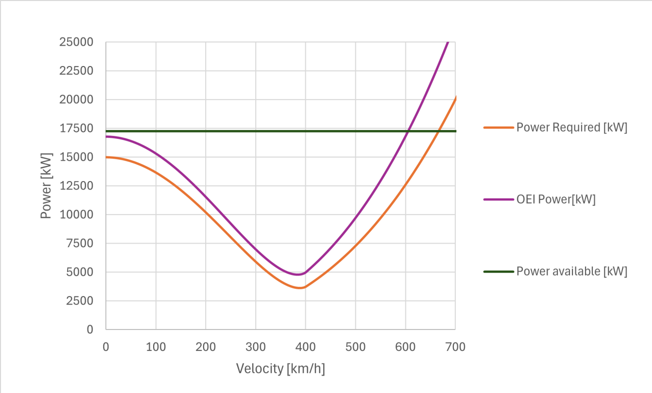

Figure 7.18: *Power required.*

Besides providing enough power, the AE1107F engines are specifically designed for use on tilt rotors as they are to be installed on the new V-280 Valor aircraft. Being an improved iteration of the AE1107C engines installed on the V-22 Osprey and with the V-280 entering service in 2031, the AE1107F will have been thoroughly tested by the time FireFly enters its prototype phase. Being designed for combat situations, the AE1107 engines proved to be reliable and robust with over 70 million flight hours on the record. Along with established supply chains and part commonality with other AE series engines ensuring good maintainability, this engine will provide FireFly with a reliable power output during its lifetime[5].

7.4.1. Fuel Type

Contributors / Authors: Nino, Bob

Regarding sustainability, it has not been tested whether the AE1107 engines can run on SAF. However, multiple Rolls-Royce engines have been proven to be able to run on 100% SAF which is promising and shows that Rolls-Royce is capable of adapting their engines to run on SAF.[6] SAF has many benefits compared to general fossil jet fuel. SAF is the more sustainable option for jet fuel. SAF is made from waste oils, which reduces the total CO_2 emission of the aircraft by 80%. This is a large portion of the total operational carbon emission. On top of this SAF also has an improved fuel efficiency compared to kerosine of 1-3%. [7] The cost of SAF is eight times more expensive than kerosine and demand is high compared to the supply. On top of this, SAF is a drop-in fuel. Meaning no special equipment or adjustments is needed to use the SAF fuel. It can just be mixed in with general fossil jet fuel. So if SAF is available at a refilling station, it should be used.

7.5. Noise Analysis

Contributor / Author: Nino

The main social impact the FireFly will have has to do with noise caused by the four prop-rotors. According to the ICAO, there is no maximum noise level for tilt-rotor aircraft in aeroplane mode. [21] This means that the noise only needs to be analysed during hover at a take-off, approach or drop procedure. For this, only the people outside the aircraft are taken into account, as it is assumed that the pilots will have sufficient protective gear against the rotor noise. This estimation is done to get a ballpark guess of the noise created by the proprotors, so it is known if the ICAO requirements are met. On top of this it is assumed that in the forest fires and near airports of firefighting bases, no one will complain when an aerial firefighting aircraft is called into action. However, the noise safety requirements of the ICAO, still need to be met for the times when the FireFly does need to fly near civil areas for transportation or maintenance of the aircraft. According to the ICAO regulations, the measurements need to be done from 150 meters from the aircraft. The maximum allowable decibels are based on the MTOW of the aircraft and shown in Table 7.9. [21]

[4] Link [cited on 19-06-2024]
[5] Link [cited on 19-06-2024]
[6] Link [cited on 19-06-2024]
[7] Link [cited on 14-06-2024]

Table 7.9: *Noise regulations according to ICAO and noise caused by the FireFly in decibels (dB) [21] [22].*

Parameter	Take-off	Drop	Approach	Unit
Allowed Noise	105.6	104.6	106.6	dB
Noise	92.9	92.2	91.3	dB

The estimations in Table 7.9 have been calculated with a generalized rotor noise estimation. Most noise calculations require tedious computer operations. However NASA has created a simplified noise analysis, which can be performed by hand calculations. Further explanation of the calculations can be found in the paper of NASA [22]. With uniform incoming flow, the accuracy is +- 2dB when compared to the computational operations. The noise limits are not exceeded according to the noise analysis from NASA, even when 2dB are added. Thus noise will not have a large implication on the design.

7.6. Aerodynamic Characteristics

To ensure good aerodynamic characteristics, the aircraft adheres to the aerodynamic requirements set by the Fire Departments (FDS) and Pilot (PIL) stakeholders. The applicable requirement for aerodynamics is shown in Table 7.10. This section will explain how the aerodynamic requirement is met.

Table 7.10: *Lift subsystem requirements.*

Identifier	Parent	Subsystem Requirement
QTR-LFT-04	FTF-SYS-FDS-05.16	The wings shall be able to sustain lift at 3000m in ISA conditions.

Lift Required

Contributor/Author: Nino

In hover, the lift is created by the proprotors, which need to provide as much lift or thrust as the weight. In cruise, the lift is provided by the wings and is designed to be equal to the FireFly's MTOW of 35154 kg. This is a conservative factor of safety for lower stall speed than calculated. The total lift force needed during cruise would then be about 344.9 kN.

Airfoil Selection

Contributor / Author: Nino

In the midterm report the same airfoil as the V-22 Osprey, the Bell A821201, was selected for both the front and rear wing [9]. However, the decision is made to switch to a NACA airfoil with a similar geometry. The main reason for the decision is that little data is available on the Bell airfoil. NACA airfoils have a sufficient amount of data available on the airfoils. This speeds up the design process, as no Computational Fluid Dynamics (CFD) programs need to be run to find the airfoil characteristics. The airfoil chosen is the NACA 4421 airfoil, as the geometry and thickness over chord ratio is similar to the Bell airfoil. The geometry of the NACA 4421 airfoil is shown in Figure 7.19a. The lift coefficient (C_l; [-]) over angle of attack (AoA; α; [deg]) is shown in Figure 7.19b [8].

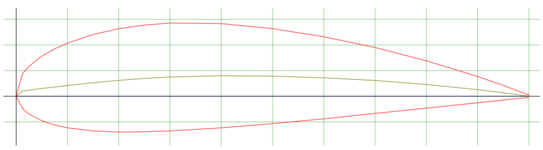

(a) *NACA 4421 airfoil layout.*

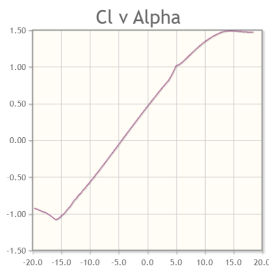

(b) *C_l/α curve of the NACA 4421 airfoil where AoA is in degrees.*

Figure 7.19: *NACA 4421 airfoil geometry and Cl over α curve.*

[8] Link [cited on 11-06-2024]

7.6.1. Wing Sizing

Contributors: Nino, Bob. Author: Nino

The wing sizing is a complicated system with many dependencies. A lot of variables need to be taken into account and a lot of parameters need to be determined, like span and chord, but also sweep, taper and rotor rotation.

Surface Area Determination

The total lift surface area required is determined with the lift equation in Equation 7.8. Where S is surface area in m^2, L is the total lift generated in N, C_L is the dimensionless lift coefficient, ρ is the air density in kg/m^3 and V is the cruise velocity in m/s. With a C_L of 0.8 at about 4 deg AoA, a cruise altitude of 10,000 feet with a density of 0.905 kg/m^3 and a cruise velocity of 400 km/h, the total surface area needed is 77.16 m^2. This would meet the requirement, as 10000 ft is at a higher altitude than 3000 m.
For this phase of the design, it is assumed that the lift coefficient for the airfoil (C_l) and the lift coefficient for the wing (C_L) are the same. This will be explained in further detail later in this section when proprotor rotation is discussed.

$$S = L/(C_L \cdot 0,5 \cdot \rho \cdot V^2) \tag{7.8}$$

Span Determination

With the total surface area known, it should be decided how the area is divided among the front and rear wings of the aircraft. With a difference in wing sizing, the oncoming wake on the rear wing also changes. In Figure 7.20 a sketch is shown of three possible options. The first green option is when the rear wing has a larger span than the front wing, the second blue option is when the wings are equal in size and with the third orange option, the span of the front wing is larger than the rear wing span.

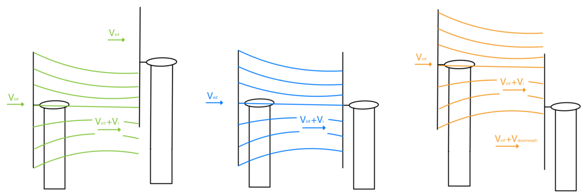

Figure 7.20: *Incoming flow on rotors with wake of three possible span options. This sketch is not to scale.*

The rear proprotor of the first option is half in the slipstream of the front rotor and half in the freestream velocity. Thus there is a differential in slipstream between the inner and outer part of the incoming flow on the rear proprotor. This means that when the rear proprotor is rotating, the blades will endure a constant change between a turbulent flow and a laminar flow creating a fatigue cycle by the unequal forces on the left and right sides of the rotor. This fatigue cycle would cause an extra risk of failure, resulting in more maintenance time for the aircraft, as the proprotors need more time for sufficient inspections and replacements. The same can be said for the third option where the front wing has a larger span.
The second option has wings of the same size and only has an incoming flow from the proprotor. The load from the incoming flow will be the same when the proprotor is rotating. Thus it will not have a fatigue cycle like options one and three.
One disadvantage of option two compared to option one is that option one has clean air on half the proprotor and option two does not. Option three has the wake of the wing and would be less efficient than option one. This means the rear proprotor of the second option is in the full wake or jet from the front proprotor, increasing drag.

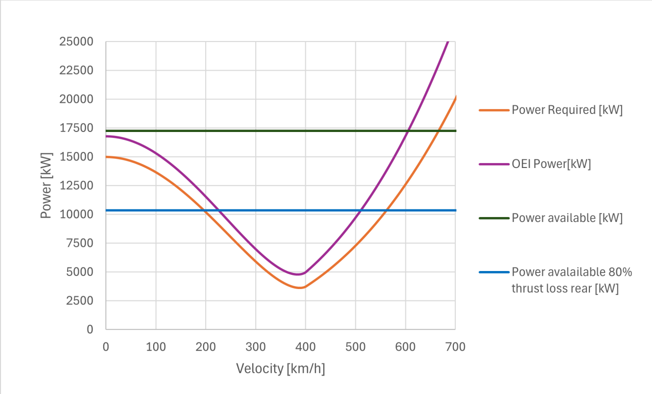

Figure 7.21: *Power required for cruise velocity with 20% thrust at the rear wings.*

However, a power calculation has been done and is shown in Figure 7.21. The rear engines only produce 20% of the available power. With this, a minimum velocity of around 195 km/h and a maximum velocity of 550 km/h can still be achieved. Operating at 20% rear power comes with a lower drag and fatigue cycle, as the air deflection is decreased and thus is a more sustainable flight mode. If lower velocities are required, the pilot can let the rear proprotors rotate faster to generate a sufficient amount of thrust for lower velocities. The fact that the cruise velocity can still easily be reached with only 20% thrust from the rear proprotors, is a confirmation to choose equal spans for both wings. This reduces maintenance time and increases the availability of the aircraft to extinguish wildfires more effectively.

For better manoeuvrability and weight reduction, it was decided to make the span as small as possible. With a proprotor radius of 6 meters, a fuselage width of 2 meters, and a clearance of 55 cm on each side of the fuselage, the span of the aircraft is 15.1 meters. The V-22 Osprey has a clearance of 30 centimetres [23]. This was extended with an additional 25 centimetres, as the FireFly RPM of the rotors is higher than the V-22. The rotor radius is about the same and thus the RPM will be higher [23].

For production simplicity and cost reduction, the wings will have the exact same sizing and surface area. When the wings are the same size, only one type of wing needs to be manufactured. The same parts can be used for both wings. This speeds up the process of manufacturing as only one production line is needed for both wings. As manufacturing time is shorter and a smaller variety of parts needs to be produced, the cost is also reduced. This results in a chord of 2.56 meters and a surface area of 38.6 m^2 per wing.

Sweep Determination

The sweep on the wing is chosen to be zero degrees. Sweep is mainly applied for aircraft that reach high speed to increase the critical Mach number. The FireFly will at most reach a Mach number of 0.6 making the use of sweep redundant.

On top of this, a rearward sweep would cause the proprotors to collide with the wings in conventional flight mode, as can be seen on the left side of Figure 7.22. Rotating the proprotors is considered, but is deemed as no feasible option. Rotating the proprotors would increase the fuel consumption, as a force to the side is introduced which cannot be used for forward flight which is shown on the right side of Figure 7.22. This means some of the power is lost, efficiency decreases and a less sustainable design, as more thrust is necessary to reach cruise velocity. On top of this, extra stress is introduced in the wing resulting in more wing weight. Forward sweep would cause divergence when bending is introduced on the wing. When a forward-swept wing bends upwards, the angle of attack increases, introducing more bending loads, making the angle of attack even higher. This will eventually break the wing unless the wing needs to be designed for high stiffness, which will significantly increase the weight of the wing. Because both forward and rearward sweep are deemed unfeasible for the design of the FireFly, no sweep is applied to the wings.

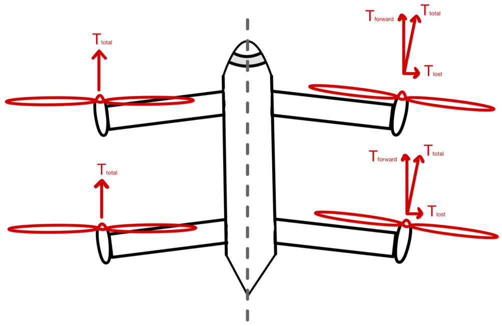

Figure 7.22: *A sketch of the FireFly with rearward sweep is shown. On the left side, it can be seen that the proprotors collide with the wings when a rearward sweep is applied. On the right side, the proprotors are rotated with the sweep so they do not collide with the wings. However, a force to the side is introduced. This force cannot be used in conventional flight and is a loss in useful thrust.*

Dihedral Determination

The dihedral of the wings is chosen to be zero. The main reason is to simplify the driveshaft of the proprotors. The driveshafts are placed in the wings as a backup option in case one engine fails and will only connect the two engines on the same wing. Without any dihedral one big driveshaft can connect the two engines, without having any gears in between. This simplifies the driveshaft, which decreases weight and increases the reliability of this safety feature.

Proprotor Rotation

A proprotor can be rotated in two ways. One where the inward part of the rotor closest to the fuselage rotates upward, the other where the inward part rotates downward. Propellers leave behind a swirling flow that washes over the wings. This phenomenon is called slipstream and has an impact on the local lift and drag over the wing. It was decided to let all proprotors rotate inward upwards, as this is the most beneficial and sustainable way to use the proprotors. The arguments of this decision will be further explained in this section by looking at the induced velocity.

The induced velocity in cruise influences the lift distribution of the wing. When the rotor rotates inward downward, a downwash is created and the local angle of attack decreases, which also decreases the lift of the wing as shown in Figure 7.23c. The proprotor downwash is added with the downwash created by the wing. The change in final vertical flow velocity will be significantly large. When the rotor rotates inward upward, an upwash is created and the local angle of attack is increased, which results in an increased lift of the wing shown in Figure 7.23a. The wing causes a downwash and the proprotor causes an upwash, resulting in the cancellation of some of the change in velocity, making the final change in flow velocity smaller. This way the incoming flow will be less disturbed and more similar to the freestream flow than the inward downward rotating proprotors. As the proprotor covers a large part of the wing, this is an important aspect to take into account. This phenomenon is shown in Figure 7.23b, where both inward upward and downward options are shown. On the bottom a rough estimation of the lift distribution is shown based on the Master Thesis of Robert Nederlof [24].

For this stage of the design, it is assumed that this downwash caused by the wings and proprotor will cancel each other to simplify calculations and design choices. With this lower downwash or upwash, it is also assumed that the lift coefficient of the airfoil and the coefficient of the wing are the same. The vortices created by the rotors and wings are shown in Figure 7.23b for clarity.

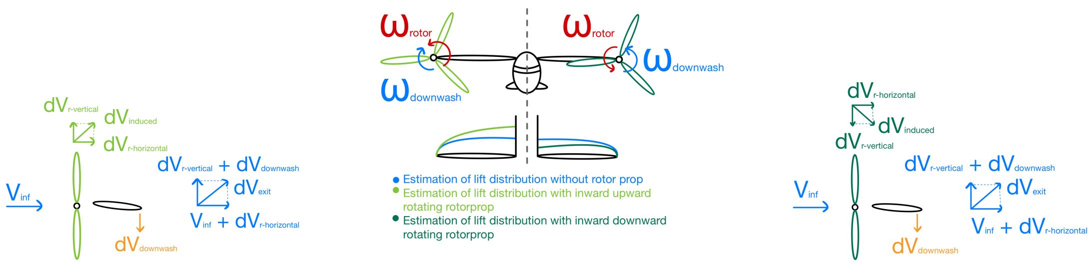

(a) *An upward rotating proprotor and wing are displayed in configuration and changes in velocity due to these objects are observed.*

(b) *Shows vorticity implications of proprotor rotations direction viewed from the front of the aircraft with a rough estimation of the lift distribution shown at the bottom of the figure.*

(c) *A downward rotating proprotor and wing are displayed in configuration and changes in velocity due to these objects are observed.*

Figure 7.23: *The top figures show the change in direction of velocity vectors with an upward and downward rotating proprotor. The bottom figure shows the tip vorticity at the wings.*

Next to cruise, it is also important to look at the rotation of the proprotors in hover and transition. For low-speed flight, the proprotors need to be in the transition phase where both hover and thrust are provided. On the left side of Figure 7.24, two inward upward rotating proprotors are shown. In the transition mode of hover to cruise, this means the airflow would go downward and backward. For the right side, with one inward downward rotating proprotor, this would mean the airflow would go downward and would escape on the side of the aircraft.

The two inward upward proprotors would be beneficial, as the airflow over the rear wing would be the highest, creating a lower pressure area and producing the highest amount of lift. When looking at the right side of the figure, it can be seen that some air over the wing would be accelerated forward. This would lead to a decrease in lift generated, resulting in a more hover-like configuration and lower flight speed. Four inward upward rotating proprotors are chosen, as this has benefits for generating lift in cruise and transition at high and low-speed flights, leading to less fuel consumption and a more sustainable design.

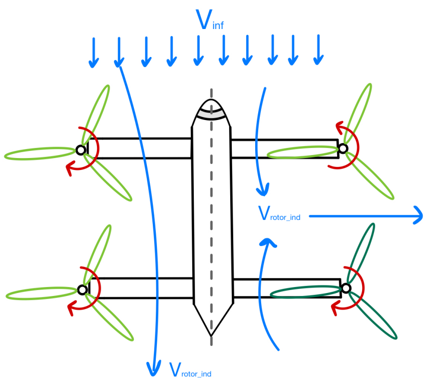

Figure 7.24: *Airflow over the rotation of proprotors in transition configuration at low-speed flight. The left side has two inward upward rotating proprotors, the right side has one inward upward rotating proprotor on the front wing and one inward downward rotating proprotor on the rear wing.*

Taper Determination

Taper is mainly used to control your lift distribution over the wing. This lets one control which part of the wing stalls first. This will cause the wing to vibrate, which lets the pilot know they are approaching stall conditions. Preferably, the root stalls first to use the control surfaces near the tip of the wing.

In the design of the FireFly where four inward upward rotating proprotors are present, this phenomenon of letting the root of the wing stall first is already present. The part of the proprotor blade near the tip has a lower absolute velocity when rotating than the part of the blade near the root. This way, the air near the root is accelerated more than the air near the tip. This means the part of the wing near its root has a higher upwash, creating a higher local angle of attack, resulting in an earlier stall near the root than the tip. Because of this, wing taper becomes unnecessary and the taper ratio will be 1. A taper ratio of 1 also has many advantages to the manufacturing of the wing. With this taper ratio, manufacturing will be easier and cheaper as the same parts are needed multiple times to assemble the wing.

7.6.2. Proprotor Geometry

Contributor / Author: Bob

For the FireFly to have efficient thrust generation rotor geometry has to be designed so that it has high efficiency in both hover and cruise configurations. For this reason, a proprotor has properties of both propellers and rotors, hence the name. In the Midterm report [9], initial rotor sizing was conducted. These values were iterated on resulting in a disc radius of 6 m, a disc loading of 77.7 kg/m^2 and an average chord of 0.66 m.

Advanced wind tunnel testing and CFD analysis necessary to optimise proprotor geometry for both hover and cruise are beyond the scope of this project. It is decided to adapt the rotor geometry of the V-22 Osprey and size it to the characteristics determined for FireFly.

The Osprey rotor has four airfoils with a decreasing thickness from the XN-series, these airfoils are XN28, XN18, XN12 and XN09. The numbers represent the maximum thickness-to-chord ratios in percentage [%]. They are respectively located at the 0.2, 0.5, 0.75 and 1 radial stations(r/R) and interpolated in between. To ensure an optimal angle of attack for every section of the blade, the blade is twisted. Along with the chord distribution in Figure 7.25, the twist distribution is shown in Figure 7.26 and is a compromise between hover and cruise optimized for maximum lift. [25]

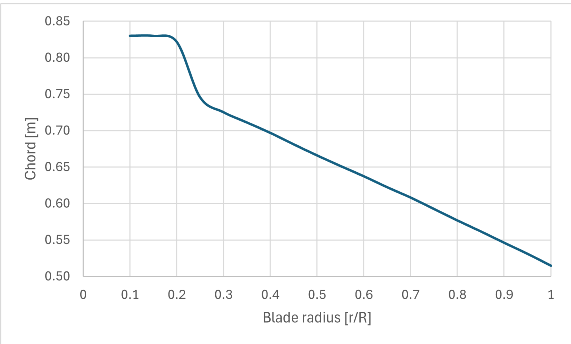

Figure 7.25: *Chord distribution*

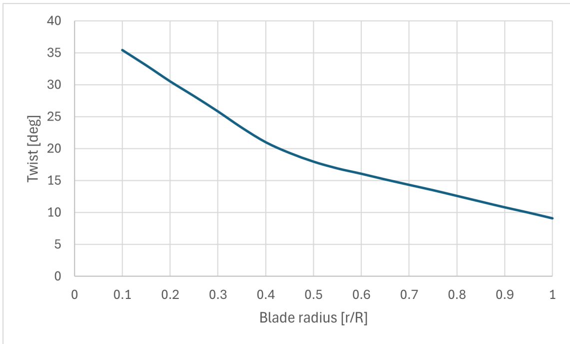

Figure 7.26: *Twist distribution.*

Rotor Performance

Contributor / Author: Bob

The rotor performance characteristics shown in figures 7.27, 7.28 and 7.29 are found from (McVeigh et al. 1986)[25]. In the latter two graphs the efficiency is plotted for various values of J, this is the advance ratio. The advance ratio is the forward velocity divided by the rotor tip velocity. The range of advance ratio that FireFly is designed for is between 0.5 and 0.7 resulting in the optimal RPM for cruise being about 350 RPM. These graphs show rotor efficiencies of over 70% in hover and 80% in cruise at various thrust settings. As the initial estimate for the figure of merit was 0.6, rotors provide higher hover efficiency than initially estimated. Meaning that these rotors will provide the desired performance in both hover and cruise configurations.

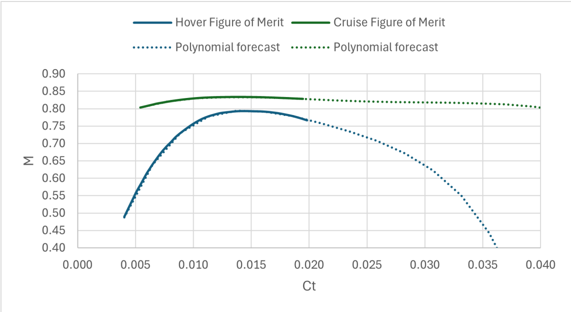

Figure 7.27: *Figure of merit in cruise and hover.*

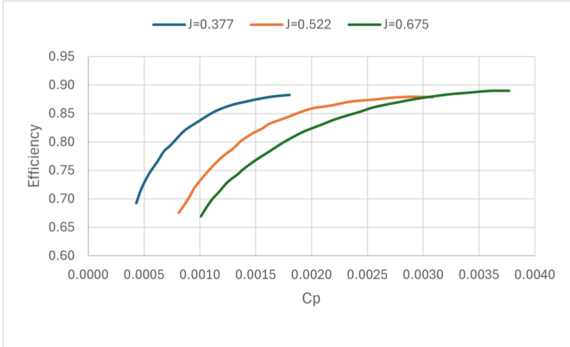

Figure 7.28: *Efficiency versus power coefficient.*

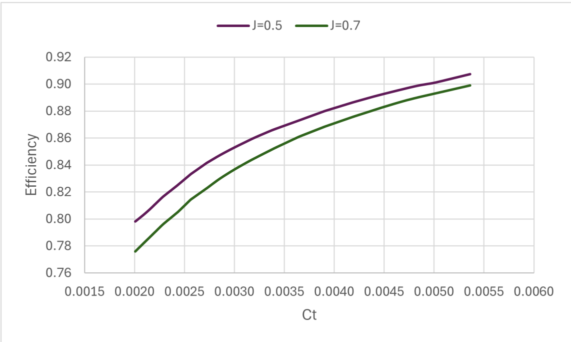

Figure 7.29: *Efficiency versus thrust coefficient.*

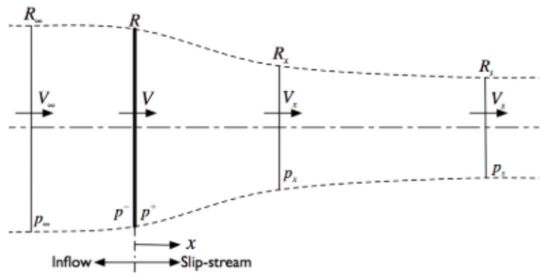

Figure 7.30: *Propeller momentum theory. [26]*

Propeller Performance

Contributor / Author: Lauren

To analyse if the rotors that have been selected can reach 400 km/hr or higher as specified in **FF-US-05**, A blade element momentum analysis was performed, assuming that the blades are propellers. The procedure that was taken to determine the thrust and torque of the propellers at different speeds at cruise altitude can be found in section 2.3 in the proceedings of the 27th International Congress of the Aeronautical Sciences 2010 by M. K. Rwigema [26]. In this analysis, the tip correction was applied only.

Before discussing the results, the following assumptions must be discussed; Firstly, optimal twist was assumed irrespective of the twist mentioned in the previous subsection. An optimal angle of attack of 3 ° was taken across the blade to determine the optimal twist at different rotational speeds. Furthermore, a non-tapered chord was assumed and was manually varied to determine the best performance. Moreover, the XN18 airfoil was taken as the primary airfoil rather than the distribution mentioned in the previous subsection due to time constraints.

To determine if the rotors can reach the required cruise speed of 400 km/hr, the definition of the power required had to be determined. It was taken as the power required to turn the rotor and to overcome the drag of the blades of all four rotors [9]. The power required at different rotational speeds can be seen in Figure 7.31.

From this graph, it can be seen that for rotational speeds slightly above 400 RPM, the FireFly cannot reach 400 km/hr dash speeds. However, as mentioned in the previous section, the FireFly is being designed for an advance ratio between 0.5-0.7. Looking at the power required for 333 RPM, the maximum cruise speed that could be obtained is 522 km/hr. This results in an advance ratio of 0.69, which falls within the operational range of the FireFly. This means that the FireFly can reach much higher than the required dash speed, increasing response time and mission effectiveness.

In terms of the rotor geometry, the optimal twist was determined to be 39 ° and the chord line length of 0.5 m was chosen. It is recommended for further analysis to perform a sensitivity analysis on the optimal twist and chord length distribution. Furthermore, it is also recommended to analyse the rotor using the four airfoils

[9] Link.[Cited on 25-06-2024]

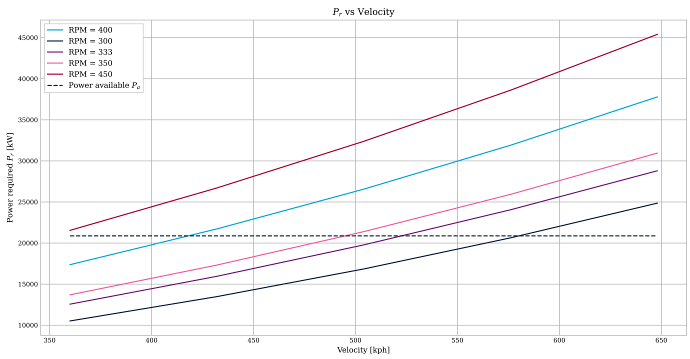

Figure 7.31: *Power Required vs Velocity*

previously mentioned to determine the performance with this combination. Moreover, using rotor blade element momentum theory when in hover or in tilted configuration will determine the amount of thrust the rotors can produce at different tilt rotor angles for different speeds and thus will also size the optimal twist and chord line distribution.

It is important to note that since the RPM is high, it is expected that the rotor will have large tip vortices due to the large tangential speed of the rotor. As this flow will be directly going over the main wing, it may hinder its performance. Similar can be said about the rear wing. As mentioned in Section 7.6, the rotors in forward flight will rotate inwards out from the fuselage. Thus, it is possible that the induced angle of attack of the wing due to this up wash will cause the main or rear wing to stall. Therefore, due to the complex nature of the flow behind the wing, the effect on the performance of the rear rotor and rear wing was not analysed numerically and is recommended to be investigated further.

7.6.3. Improvements for the Next Design Phase

Contributors: Nino, Lauren, Bob. Authors: Nino, Lauren

As this design of the FireFly is still preliminary, there is still more investigation to be done in terms of aerodynamics. Some aspects of the wing sizing still need to be looked at in more detail in the following design phases. The first improvement that needs to be investigated is at which angle the rear wing is in the complete wake of the front wing and how this affects the controllability of the aircraft. To check the feasibility of the rear wing and rotor placement, it is recommended to computationally analyse the flow behind the front wing. The distance between the front and rear wing is one parameter to change for this. If necessary, a height difference between the front and rear wing can also be taken into account. If this option is chosen, maintenance time would go up due to the introduced fatigue cycles during high-speed flight. It is expected that a possible solution to preventing stall of the rear wing is that its incidence angle can be adjusted to combat the effects of the incoming flow if the upwash/turbulent behaviour is present downstream.

However, this type of stalling due to the high angle of attacks during cruise is very unlikely to happen. High angle of attacks will only be present during manoeuvres for dropping and picking up water, which will happen at low speed when the proprotors are in hover or transition mode. When the aircraft does stall at a high angle of attack during manoeuvres, the proprotors are able to generate extra thrust and rotate to go into hover mode. Although this does work out in theory, further analysis needs to be performed to determine the exact effects.

Another implication which needs to be investigated is the effect of the proprotors on the lift and drag of all wings. As already explained, the proprotors have an effect on the lift and drag in multiple ways. The lift distribution of the wing is heavily affected by the proprotors. The change in lift distribution due to the varying velocity flow of the front rotors also has an effect on the stall process of the wing. These implications need to be looked at in further detail in order to optimise the wing configuration. This could be done by analysing the lift distribution of the wing at different velocities. The lift distribution could be optimised by changing the taper ratio of the wings.

To conclude this subsection about wing sizing, an overview of all main wing parameters is shown in Table 7.11.

Table 7.11: *Aircraft wing sizing values.*

Parameter	Value	Unit	Parameter	Value	Unit
Total surface area	77.16	m^2	Taper ratio	1	-
Span	15.1	m	Sweep	0	degrees
Chord	2.56	m	Dihedral	0	degrees
Aspect ratio	5.91				

7.6.4. Drag Estimation

Contributor / Author: Nino

With the wing sizing known, a class II drag estimation from Roskam Part VI is used to determine the drag of the aircraft [27]. This class II estimation determines the zero-lift drag en drag due to lift separately from each other for each group of aircraft. In the case of the FireFly, the four groups are fuselage, front wing, rear wing and the sponses. The results of the drag estimation are shown in Table 7.12. Due to the preliminary stage of the analysis, the drag contingency is set as 20%, as also mentioned in the baseline report[14].

Table 7.12: *Class II drag budget estimation results.*

Parameter	Symbol	Value	Parameter	Symbol	Value
Zero-lift front wing drag	$C_{D0_{fw}}$	0.0044	Front wing drag due to lift	$C_{DL_{fw}}$	0.0420
Zero-lift fuselage drag	$C_{D0_{fl}}$	0.0073	Fuselage drag due to lift	$C_{DL_{fl}}$	0.000139
Zero-lift rear wing drag	$C_{D0_{rw}}$	0.0047	Rear wing drag due to lift	$C_{DL_{rw}}$	0.0157
Zero-lift sponses drag	$C_{D0_{sp}}$	0.0035	Total drag coefficient	C_D	0.078
Sponses drag due to lift	$C_{DL_{sp}}$	0.00013	**Drag [kN]**	**D**	**33.63**
Total drag due to lift	C_{DL}	0.058	**Lift over Drag**	**L/D**	**10.25**

The total C_D is calculated by summing up all C_{D0} and C_{DL} values of all aircraft groups. The drag is determined with the drag equation which uses dynamic pressure and surface area. The calculations of the separate coefficients for the front wing, fuselage and rear wing are well-explained in [27]. For the drag calculation, some assumptions are made which are not mentioned in the book.

- Box assumption: assumed that the fuselage is a rectangular box of size 2.00x19.75x3.60 m^3.
- Tail assumption: the rear wing is assumed to be a large horizontal tail, where downwash is only taken into account at the drag due to lift.
- Induced rotor velocity: The incoming velocity of the rear wing is assumed to be zero. This assumption is taken to be conservative with the lift generation of the rear wing.
- Sponses drag: The sponses are assumed to be a second fuselage. This is done to be conservative with the drag estimation, as the Roskam calculation does not take sponses into account. With this assumption, the wetted area of the sponse is divided by the area of the side of the fuselage as this area affects the drag of the sponses.

Because of these assumptions, the actual drag of the aircraft will be different and probably larger than it is now. However, this will not be a problem, as the engines have a lot of excess thrust in cruise, as explained in Section 7.4.

Next to the cruise, there is also drag in hover. This drag is caused by the proprotors blowing wind on the part of the wing that is underneath the proprotor in hover. This causes a loss in thrust and is called download. The ratio download over thrust is determined using the method in [28] utilising the formula shown in Equation 7.9.

$$\frac{D_v}{T} = \frac{S_s}{S_w} \cdot C_{Dv} \cdot \frac{w}{w_w} \tag{7.9}$$

Where $\frac{S_s}{S_w}$ is the fraction of wing area in the slipstream of the rotor and total wing area, C_{Dv} is the vertical drag coefficient of the wing and $\frac{w}{w_w}$ is the fraction of disc loading over wing loading. With the download determination two assumptions have been made which are not mentioned in the book.

- Flat plate assumption: The airfoil is assumed to be a flat plate for the vertical drag calculation where $C_{Dv} = 1.28$.
- Wing rectangle assumption: the area in the slipstream of the proprotor is an area of chord length times proprotor radius.

These calculations give a download-over-thrust ratio of 17.4%. Resulting in a 17.4% increase of thrust in order to counteract the download and produce enough thrust for hover. The download-to-thrust ratio of download is high when comparing it to other VTOL aircraft. This is could be attributed to the conservative assumptions and the high wing area covered by the propeller during hover.

7.6.5. Aerodynamic Centre

The aerodynamic centre of the aircraft is also determined with the Roskam Part VI [27]. The calculation of the aerodynamic centre of the NACA 4421 airfoil is located at 0.242 x/c [27]. The assumption made during this calculation is that the rear wing is assumed to be a large horizontal tail. As a result, the aerodynamic centre will be located at 9,43 meters from the nose of the aircraft.

7.7. Performance Analysis

The performance analysed the feasible ranges that the FireFly can reach with different carried payloads and fuel. Following from the payload-range analysis, the performance of the FireFly was investigated to determine its feasibility in drop configuration, cruise and climb. This analysis results in the limitations of the design with respects to mission success and possible solutions for further analysis are presented.

Payload-Range Diagram

Contributor / Author: Thijs

With a better idea of the aircraft properties, an updated payload-range diagram can be set up. The Breguet range equation is used to determine the cruise range of the aircraft as shown in Equation 7.10. Here, the specific fuel consumption (C_p) can be gathered from the engine data[10], the lift-to-drag ratio (L/D) has been determined in Subsection 7.6.4 and the cruise mass fraction (W_b/W_e) can be determined more accurately from the class II mass estimation in Section 7.2. The total propulsive efficiency (η_p) must still be estimated from a statistical value [11]. The constant values used are tabulated in Table 7.13

Table 7.13: *Constants used to determine the aircraft range.*

Parameter	Value
c_p [$\text{kgs}^{-1}\text{W}^{-1}$]	7.198e-8
η_p [-]	0.83
L/D [-]	10.25

$$R = \frac{\eta_p}{g c_p} \frac{L}{D} ln \frac{W_b}{W_e} \tag{7.10}$$

In order to determine the range, the cruise weight fractions can be determined for each aircraft configuration; first, the aircraft is taken at a full (effective) payload mass of 11000 kg[11] and OEW. Fuel is then added until the MTOW is reached. The payload is then decreased as more fuel is added so as not to exceed MTOW. Once the maximum fuel capacity is reached, the payload mass is decreased further until the ferry range is determined (no payload).

The total mass fraction of the aircraft can be determined using Equation 7.11, from which the cruise mass fraction is found by dividing $m_{\text{f,total}}$ by the product of the mass fractions from all other phases. These fractions are taken from statistical data as tabulated in Table 7.14 [11] [12]. The resulting payload-range diagram is shown in Figure 7.32 where the left axis shows the gross weight as a percentage of the MTOW and the left axis displays the total fuel- and payload mass. From this analysis, the mission range (payload mass of 10.000 kg) is 680 km. This number is lower than the initial value of 900 km which is due to the increased OEW. Adversely, the maximum ferry range has increased considerably.

[10] Link [Cited on 18-06-2024]

[11] Note that in the class II weight estimation, the maximum payload is taken as 14000 kg without any fuel. The effective maximum payload capacity is taken at 11000 kg to allow for fuel at maximum payload.

[12] From the estimated mass fractions during all operations outside cruise, a minimum of 2000 kg of fuel is needed for these phases.

$$m_{\text{f,total}} = \frac{m_{\text{OEW}} + m_{\text{Payload}}}{m_{\text{OEW}} + m_{\text{Payload}} + m_{\text{Fuel}}} \tag{7.11}$$

Table 7.14: *Mass fractions for different flight phases.*

Phase	Startup	Taxi	Take-off	Climb	Descend	Landing + Shutdown
Mass fraction	0.99	0.99	0.995	0.983	0.99	0.991

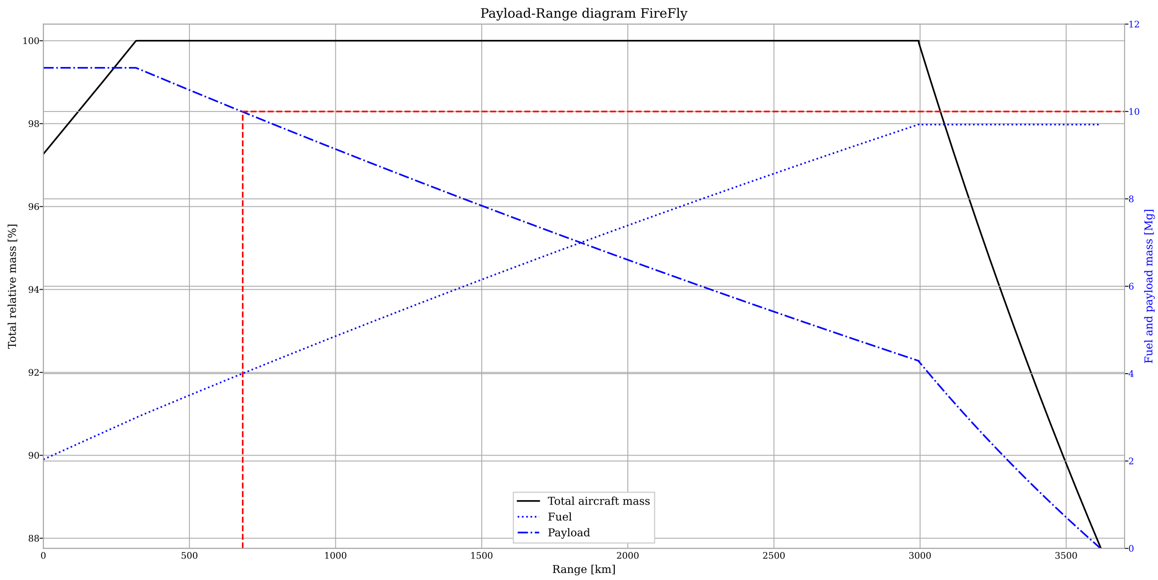

Figure 7.32: *Payload-range diagram of FireFly*

7.7.1. Inverse Power Loading vs Wing Loading

Contributor / Author: Lauren

Typically, inverse power loading vs wing loading diagrams are used to validate the design of an aircraft. However, this diagram was used to see how the design can be optimised in terms of performance by seeing what performance characteristics limit its feasibility when in a line drop in forward flight configuration. A line drop was taken to be the most constraining case as it is where the performance of the aircraft is most crucial. The inverse power loading W/P was plotted against the wing loading W/S to determine its performance in regards to the cruise speed, stall speed for line drop manoeuvres, climb rate and climb performance at drop speeds.

Sizing for Cruise Performance

Sizing for cruise performance is essential in order to understand how much power and wing area would be required in order to meet requirement FF-US-05 regarding the minimum dash speed of 400 km/hr. Adhering to requirement FTF-SYS-FDS-05.16, the minimum cruise altitude will be 3 km and thus was used in this analysis.

To size for the cruise performance, Equation 7.17 was used to get the relationship between the inverse power loading and the wing loading. To determine this equation, the following steps were taken:

Firstly, it was stated that the power available P_a is equal to product of the propulsive efficiency η_p and the brake power P_{br}. The power loading in terms of the power available was written as seen in Equation 7.12 [29][pg. 64].

$\frac{P_a}{W}$ is the power loading in terms of the power available, η_p is the propulsive efficiency and P_{br} is the brake power.

In cruise, assuming that the power required P_r is equal to the product of the drag D times the cruise velocity V, the power loading can be derived as seen in Equation 7.13, taking drag as $C_D \frac{1}{2}\rho V^2 S$ [29][pg. 64].

$$\frac{P_a}{W} = \frac{\eta_p \cdot P_{br}}{W} \quad (7.12) \qquad \frac{P_r}{W} = \frac{C_D \cdot 0.5\rho V^3}{(W/S)} \quad (7.13)$$

where $\frac{P_r}{W}$ is the power loading in terms of the power required, C_D is the drag coefficient, ρ is the density, V is the velocity and $\frac{W}{S}$ is the wing loading.

For the maximum speed of a propeller aircraft, the power available P_a is equal to the power required P_r [29][pg. 64]. Therefore, equalling Equation 7.12 to Equation 7.13, the power loading relationship can thus be rewritten as Equation 7.14.

$$\frac{P_a}{W} = \frac{P_r}{W} = \frac{\eta_p \cdot P_{br}}{W} = \frac{C_D \frac{1}{2}\rho V^3}{(W/S)} = \frac{C_{D_0} \frac{1}{2}\rho V^3}{(W/S)} + \left(\frac{W}{S}\right)\frac{1}{\pi A e \frac{1}{2}\rho V} \quad (7.14)$$

This derivation was done by splitting up the drag coefficient C_D in terms of the zero-lift drag C_{D_0} and the induced drag $\frac{C_L^2}{\pi Ae}$.

Looking at the induced drag, the lift coefficient C_L can be rewritten in the following way; In cruise, lift L is equal to weight W thus the lift coefficient C_L can be rewritten as seen below.

$$C_L = \frac{L}{\frac{1}{2}\rho S V^2} = \frac{W}{\frac{1}{2}\rho V^2 S} = \left(\frac{W}{S}\right)\frac{1}{\frac{1}{2}\rho V^2} \quad (7.15)$$

where C_L is the lift coefficient, L is the lift generated by the aircraft, W is the weight of the aircraft and S is the surface area of the wing , ρ is the density.

Furthermore, in order to get the inverse power loading at sea level conditions, or in other words, at take-off conditions, the effect of altitude needs to be incorporated. In order to take altitude into account, the following relation was used to describe the relationship between power and atmospheric density [29][pg. 65]. As the brake power P_{br} is equal to the power at take-off P_{TO}, substituting P_{TO} into Equation 7.14, the resulting relationship for the inverse power loading can be seen in Equation 7.17.

$$P_{TO} = P\left(\frac{\rho_0}{\rho}\right)^{3/4} \quad (7.16)$$

$$\frac{W}{P_{TO}} = \eta_p \left(\frac{\rho}{\rho_0}\right)^{\frac{3}{4}} \left[\frac{C_{D_0}\frac{1}{2}\rho V^3}{\frac{W}{S}} + \left(\frac{W}{S}\right)\frac{1}{\pi A e \frac{1}{2}\rho V}\right]^{-1} \quad (7.17)$$

where P_{TO} is the power at take-off, P is the power, $\frac{W}{P_{TO}}$ is the inverse power loading at take-off, η_p is the dimensionless propulsive efficiency, C_{D_0} is the zero-lift coefficient, A is the aspect ratio and e is the Oswald coefficient.

To find the relationship between the inverse wing loading and the wing loading, the zero-lift drag C_{D_0}, the aspect ratio A, the Oswald coefficient e, and the propulsive efficiency η_p are needed. These characteristics for the FireFly were determined from the previous aerodynamic analysis in Section 7.6 and the propulsion analysis in Section 7.4.

Using the Equation 7.17, the inverse power loading for a range of wing loading values was calculated to capture the cruise speed limitations. It is important to note that the FireFly has a tandem wing configuration. The two wings were taken as one to get an initial order of magnitude for the surface area as a whole.

Sizing for Stall Speed

Sizing for stall speed is important in order to depict the maximum wing loading required in order to not stall at speeds higher than the stall speed in forward-flight configuration without rotor tilt. Sizing for slow speeds is important to ensure that the aircraft is controllable in pitch, roll and yaw and thus was sized to not need rotor tilt.

To calculate the wing loading $\frac{W}{S}$, the formula below was used. This formula makes use of the appropriate maximum lift coefficient during landing $C_{L_{max}}$, stall speed during landing V_{stall} and the density ρ.

$$\frac{W}{S} = \frac{1}{2}\rho V_{\text{stall}}^2 C_{L_{max}} \tag{7.18}$$

where V_{stall} is the stall speed and $C_{L_{max}}$ is the maximum lift coefficient.

The maximum lift coefficient of the wing is 1.52 at 15 ° angle of attack. Therefore, rotor tilt is therefore the only way to increase the lift if more than 1.52, if high lift devices are not implemented. This increase in lift can be calculated using the following relation:

$$\Delta L = \frac{1}{2}\rho V^2 \Delta C_L S \tag{7.19}$$

where ΔL is the required extra lift and ΔC_L is the change in lift coefficient.

As the centre of gravity is located closer to the front of the aircraft, the main wing will require more lift than the rear wing. Therefore, in order to keep the same rotor tilt angle of the rear motors, the main rotors will have to have additional blade pitch to produce the required lift. Therefore, to determine the rotor tilt, the thrust of the rear rotors were investigated.

From Figure 7.33, it can be seen that to calculate the tilt angle, assuming thrust equals drag, Equation 7.20 was used:

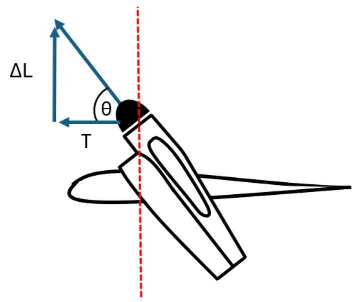

Figure 7.33: *Rotor tilt.*

$$\theta = \arctan\left(\frac{\Delta L}{T}\right) \tag{7.20}$$

Furthermore, it is important to mention that the stall speed in clean configuration was not investigated as it is not applicable to this design application. The aircraft will likely never be in a situation where it will be travelling at stall speed in clean configuration without utilising the tilt-rotor functionality. Thus, it was neglected assuming that the tilt-rotor functionality can provide any additional lift that would be needed in this configuration.

Sizing for Climb Rate Performance

Sizing for the rate of climb is crucial for analysing the aircraft's mission capabilities. The aim is to maximise the rate of climb in order to have quicker operations. For example, if a line drop is performed in an enclosed area, it is important to get out of that area as quickly as possible to avoid obstacles. Thus, knowing the rate of climb is crucial to analyse the mission effectively.

To size for the climb rate, an FBD was made as seen in Figure 7.34 depicting the aircraft entering a climb. The FBD is drawn in the trajectory frame. Assuming that the acceleration in the x- and y-directions are zero and the thrust vector is aligned with the flight path vector, the set of equations seen in Equation 7.21 and Equation 7.22 were derived.

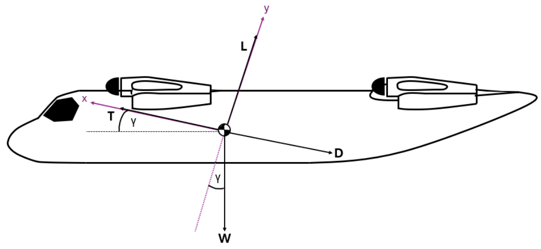

Figure 7.34: *FBD of the aircraft.*

$$\sum F_x = T - D = W\sin(\gamma) \quad (7.21)$$

$$\sum F_y = L = W \quad (7.22)$$

where T is the thrust, D is the drag, γ is the flight path angle, $\sum F_x$ is the sum of forces in the x direction and $\sum F_y$ is the sum of forces in the y direction.

To derive the Rate of Climb (ROC), denoted by C in formulas, Equation 7.21 is multiplied across by the velocity V and rearranging for $V\sin(\gamma)$ gives the expression for the ROC. This can be seen in Equation 7.23.

$$C = \frac{P_a - P_r}{W} \quad (7.23)$$

As of now, the ROC is a function of the excess power and the weight. In order to investigate the sizing of the climb rate performance, Equation 7.23 needs to be rewritten in terms of the inverse power loading $\frac{W}{P}$ and the wing loading $\frac{W}{S}$. This is done by rewriting P_r as $DV = C_D \frac{1}{2}\rho V^3 S$. Using the relation established in Equation 7.22 and dividing this expression for the power required P_r by the weight W, the following equation can be written for the power loading with respects to P_r:

$$\frac{P_r}{W} = \frac{C_D \frac{1}{2}\rho V^3 S}{C_L \frac{1}{2}\rho V^3 S} = \frac{\sqrt{\frac{W}{S}} \cdot \sqrt{2}}{\frac{C_L^{3/2}}{C_D} \cdot \sqrt{\rho}} \quad (7.24)$$

As mentioned earlier, for a propeller aircraft, the power available P_a can be written as $\eta_p \cdot P_{br}$, where η_p is the propulsive efficiency and P_{br} is the brake power in W. From this, Equation 7.25 was established.

$$C = \frac{\eta_p \cdot P_{br}}{W} - \frac{\sqrt{\frac{W}{S}} \cdot \sqrt{2}}{\frac{C_L^{3/2}}{C_D} \cdot \sqrt{\rho}} \quad (7.25)$$

From the above equation, rewriting $\frac{W}{P}$ as y and $\frac{W}{S}$ as x, Equation 7.26 was derived. Additionally, similar to the cruise performance analysis, the brake power P_{br} is equal to the take-off power P_{TO} [29][pg. 64].

$$y = \frac{\eta_p}{C + \frac{\sqrt{x} \cdot \sqrt{\frac{2}{\rho}}}{\frac{C_L^{3/2}}{C_D}}} \quad (7.26)$$

The parameters that were needed in order to establish the relationship between the inverse power loading and wing loading were $\frac{C_L^{\left(\frac{3}{2}\right)}}{C_D}$ and the ROC. Firstly, as can be shown by maximising the ROC with respect to the lift coefficient C_L, the maximum ROC is obtained when $\frac{C_L^{\left(\frac{3}{2}\right)}}{C_D}$ is maximised [29][pg. 76]. Therefore, Equation 7.27 and Equation 7.28 were used to obtain the optimal lift coefficient C_L and the drag coefficient C_D for propeller aircraft in order to maximise $\frac{C_L^{(\frac{3}{2})}}{C_D}$ [29][pg. 76].

$$C_L = \sqrt{3C_{D_0}\pi Ae} \qquad (7.27) \qquad\qquad C_D = 4C_{D_0} \qquad (7.28)$$

Using these relations for C_L and C_D, $\frac{C_L^{(\frac{3}{2})}}{C_D}_{max}$ was determined by substituting in these expressions for C_L and C_D. The equation below shows the simplified form of this parameter. Using the values specified in **??**, this parameter was determined and was substituted into Equation 7.26.

$$\frac{C_L^{(\frac{3}{2})}}{C_D}_{max} = 1.345\frac{(Ae)^{\frac{3}{4}}}{C_{D_0}^{1/4}} \tag{7.29}$$

Furthermore, as the ROC in horizontal flight was not a concrete requirement, the FireFly's largest competitor, the CL-415's climb rates was analysed. The climb rate of the CL-415 was chosen to try design for an equivalent performing aircraft in horizontal flight. This climb rates is 6.6 m/s [30] [31][p. 13].

With $\frac{C_L^{(\frac{3}{2})}}{C_D}$ and the ROC determined, the relationship between the inverse power loading $\frac{W}{P}$ and wing loading $\frac{W}{S}$ could be analysed.

Sizing for Climb Gradient Performance

The climb gradient is an important performance parameter as it tells us how much horizontal distance is needed for a certain altitude gain. For example, this parameter becomes significant when the aircraft is performing line drop manoeuvres in an enclosed area. It is crucial to understand how much horizontal distance is needed in order to avoid any obstacles. Thus, the climb gradient will be analysed for the aircraft in horizontal configuration only.

From performance theory, the climb gradient is defined as the ROC C over the velocity V [29][pg. 90]. This relationship can be seen in Equation 7.35. It is derived from Equation 7.23 in the following way in order to analyse the relationship between the inverse power loading and the wing loading:

Firstly, Equation 7.23 was divided across by the velocity V in order to determine the climb gradient. Furthermore, the power available P_a was rewritten as the product of the brake power P_{br} and the propulsive efficiency η_p, and the power required P_r was rewritten as drag D times velocity V.

From Equation 7.22, the lift L is equal to the weight W. Thus, the drag over weight $\frac{D}{W}$ could be rewritten as $\frac{C_D}{C_L}$. This derivation can be seen below.

$$\frac{D}{W} = \frac{D}{L} = \frac{\frac{1}{2}\rho V^2 C_D S}{\frac{1}{2}\rho V^2 C_L S} = \frac{C_D}{C_L} \tag{7.30}$$

From Equation 7.23, implementing these changes results in a relation for the climb gradient as seen in Equation 7.31.

$$\frac{C}{V} = \frac{P_a - P_r}{W\cdot V} = \frac{\eta_p \cdot P_{br}}{W\cdot V} - \frac{D\cdot V}{W\cdot V} = \frac{\eta_p \cdot P_{br}}{W\cdot V} - \frac{C_D}{C_L} \tag{7.31}$$

However, Equation 7.31 does not depend on the power loading and the wing loading. Therefore, rewriting the velocity as seen in Equation 7.32, $\frac{\eta_p P_{br}}{W\cdot V}$ can be rewritten as shown in Equation 7.33. Substituting this relationship into Equation 7.31, a relationship between the climb gradient with power loading and wing loading can be obtained, as seen in Equation 7.34.

$$V = \frac{1}{\sqrt{\frac{W}{S}\frac{2}{\rho}\frac{1}{C_L}}} \tag{7.32}$$

$$\frac{c}{V} = \eta_p \cdot \frac{P_{br}}{W} \cdot \frac{1}{\sqrt{\frac{W}{S}\frac{2}{\rho}\frac{1}{C_L}}} - \frac{C_D}{C_L} \tag{7.34}$$

$$\frac{\eta_p P_{br}}{W \cdot V} = \frac{\eta_p P_{br}}{W} \cdot \frac{1}{\sqrt{\frac{W}{S}\frac{2}{\rho}\frac{1}{C_L}}} \tag{7.33}$$

In order to establish the relationship between the inverse power loading and wing loading in terms of climb gradient performance, Equation 7.31 was rewritten similarly to climb rate performance where the inverse power loading $\frac{W}{P}$ was rewritten as y and the wing loading $\frac{W}{S}$ as x. The resulting equation for the climb gradient can be seen in Equation 7.35.

$$y = \frac{\eta_p}{\sqrt{x}\left(\frac{c}{V} + \frac{C_D}{C_L}\right)\sqrt{\frac{2}{\rho}\frac{1}{C_L}}} \tag{7.35}$$

As previously mentioned, the climb gradient is an essential parameter when it comes to performing a line drop in an enclosed area. Thus, the speed used is the drop speed to analyse the most critical case. Furthermore, as the maximum climb gradient is desired, the lift coefficient C_L and drag coefficient C_D determined using Equation 7.27 and Equation 7.28 were used in order to minimise $\frac{C_D}{C_L}$. From this, the relationship between power loading and wing loading for the climb gradient performance was analysed.

Results

In Figure 7.35, the final inverse power loading vs wing loading diagram can be seen. The green region in the graph is an acceptable region of the inverse power loading and wing loading combinations. The red dot in the graph represented the FireFly design. It can be seen that the performance is limited by the climb gradient and the drop speed.

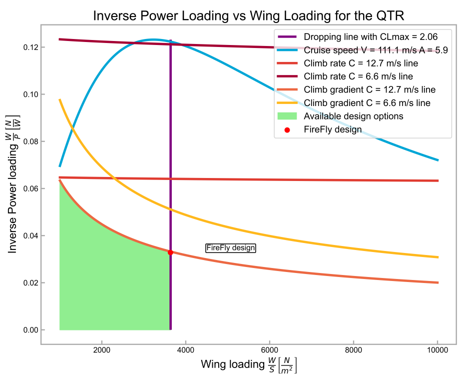

Figure 7.35: *W/P vs W/S.*

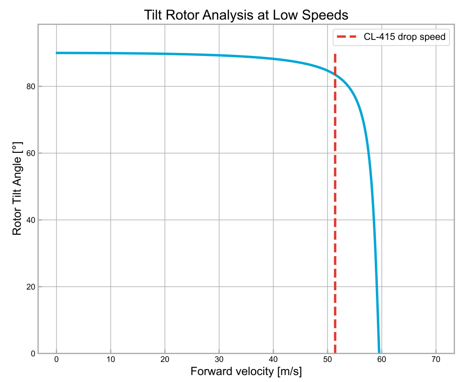

Figure 7.36: *Rotor tilt angle vs velocity at sea level.*

For the dropping speed, it was concluded that approximately 59 m/s could be achieved before rotor tilt was necessary if high lift devices were added. This almost meets the performance of the CL-415, as can be seen by the dashed red line in Figure 7.36. An increase in lift coefficient of 1.26 was obtained by sizing for single-slotted flaps. The flap sizing is further discussed in **??**.

Furthermore, analysing the climb gradient at this drop speed, it was concluded that a climb rate of 12.7 m/s could be achieved in horizontal flight with an angle of attack of approximately 5°. It is important to note that this analysis was done assuming that the FireFly has one wing. It is also worth mentioning that this analysis was done to improve the controllability of the FireFly at low speeds. However, slower speeds and higher climb rates can be achieved by tilting the rotors, assuming the engines can produce enough thrust.

It is recommended to do a blade element momentum analysis on the rotors to determine the performance metrics in different flight modes.

7.8. Stability & Control Characteristics

Owing to the special mission of the FireFly, flying at low altitudes and dropping water loads over wildfires, it is critical to ensure that the aircraft will remain stable within the operations. Performing accurate drops and precise manoeuvres make controllability a desired characteristic of the FireFly. Longitudinal stability is analysed to prove that the aircraft will remain stable during the horizontal flight while reaching high speeds to ensure prompt fire response. Control surfaces will be designed to ensure lateral stability and the tilting manoeuvre will also be analysed.

7.8.1. Subsystem Requirements

Contributor / Author: Sven

The subsystem requirements of the stability and control system were derived from the system requirements concerning the Fire Departments and Pilot stakeholders. The five stakeholder requirements that will be addressed in this section can be found in Table 7.15. The stability and control system includes everything needed to control and stabilise the aircraft such as control surfaces, engine tilting mechanism and engine thrust control.

Table 7.15: *Stability and Control subsystem requirement.*

Identifier	Parent	Subsystem Requirements
QTR-STA-01	FTF-SYS-FDS-01.2	The control system shall compensate for changes in c.g. location during flight.
QTR-STA-02	FTF-SYS-FDS-01.3	The control system shall include predictive algorithms for effects on stability due to retardant drop.
QTR-STA-03	FTF-SYS-FDS-07.2	All control surfaces shall have salt water protective coatings.
QTR-STA-04	FTF-SYS-PIL-02.1	The fly-by-wire system shall imitate the stick forces of an S-70.
QTR-STA-05	FTF-SYS-PIL-03.1	The empennage shall allow for directional stability.

7.8.2. Operating Empty Weight Centre of Gravity Determination

Contributors: Caitlin, Sven, Hanna. Authors: Caitlin, Sven

The centre of gravity (CG) range for OEW was first estimated in the baseline report[14]. Now that the design has progressed, it is necessary to iterate the OEW c.g. range. The initial estimate was based on historical data from existing aircraft. The OEW c.g. range is calculated to gain insight into the behaviour of the c.g. under different loading of the aircraft. Since the design progressed after the midterm report instead of an OEW c.g. range, one location of OEW c.g. was calculated which has to be iterated with any future design change. Furthermore, the calculation has to be expanded with a more detailed layout of the components in the aircraft later on.

To calculate the OEW c.g., the aircraft is divided into three component groups, namely the fuselage group, front wing group and rear wing group. The wing groups include two engines with rotors. The fuselage group includes the vertical tail and the landing gear. Going by the methods as specified in "Airplane Design part II" by Dr Roskam, the c.g. of the fuselage and both wing groups can be determined [32].

Since the wings have no sweep, their c.g. locations are defined to be between 0.38-0.42 of the chord length from the leading edge (LE) of the wings. The wings' c.g. was estimated to be 0.40 of the chord length due to the presence of the driveshaft in the aft section of the wingbox. Additionally, it was assumed that the powerplant c.g. coincides with the longitudinal c.g. of the wings due to its central placement when compared to the chord of the wing. This length will be added up with the distance from the nose to the leading edge to determine the c.g. of the wings. The same process was done for the fuselage where the c.g. location is defined to be at 0.38-0.45 of the fuselage length. It was estimated to be towards the end of this range at 0.43 times the fuselage length due to the presence of the vertical tail aft of the aircraft and structural elements of the rear wing.

To calculate the total OEW CG location, the distance of the CG from the nose of each group was multiplied by the respective weight of the group. Then these values were summed up and divided by the total OEW. The table summarising the c.g. locations with respect to the nose and weight of each group as well as OEW can be found in Table 7.16. The OEW c.g. was calculated to be located at 9.76 m from the nose of the aircraft which is 49.42 %.

Table 7.16: *Centre of gravity with respect to the nose & weight of OEW and its components.*

Component	**c.g.** [m]	**Weight** [kg]
Front wing group	5.22	4659
Rear wing group	17.52	4659
Fuselage group	8.49	11836
Total OEW	9.76	21156

7.8.3. Centre of Gravity Range Determination

Contributor / Author: Sven

The OEW c.g. is calculated but the c.g. of the complete and loaded aircraft will change depending on how the aircraft is loaded. The aircraft c.g. range is crucial for the determination of stability and controllability characteristics both inflight and on the ground. The FireFly aircraft has four main variable MTOW components namely front wing fuel, rear wing fuel, fuselage fuel and payload. The c.g. locations of the fuel components were contained by the layout of the aircraft while the payload c.g. is more flexible. Since the water/retardant is the heaviest and most common payload of the FireFly aircraft it was decided to centre the water/retardant tank at the OEW c.g. location to avoid large c.g. deviations during water refilling and dropping.

To determine the aircraft c.g. range, loading diagrams were created for two different extreme cases. The first case is with the fuel tanks at maximum capacity of 9700 kg of fuel and as much payload as possible while staying below the MTOW. The loading diagram of the first case can be found in Figure 7.37a. The second case is with the maximum capacity of the water tank and firefighting foam tank which is equal to 10 050 kg while the fuel tanks are filled with the maximum possible fuel while staying below the MTOW. Figure 7.37b presents the loading diagram of the second case.

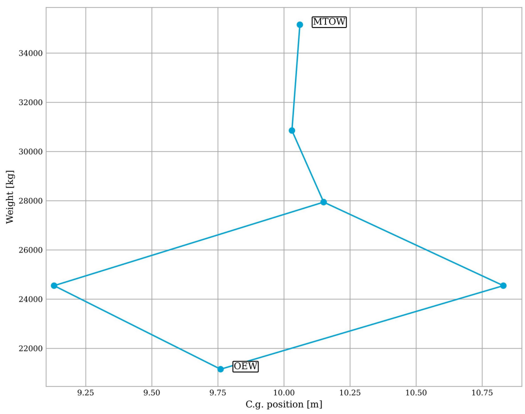

(a) *Full fuel loading diagram.*

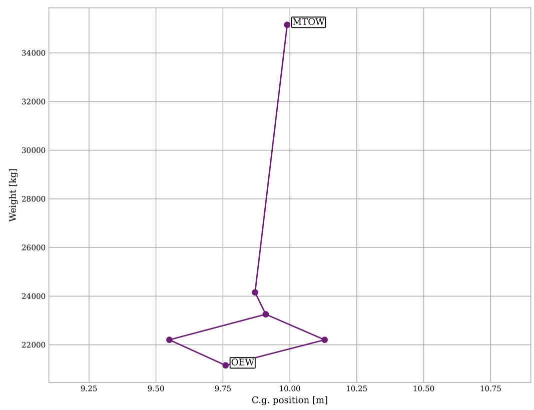

(b) *Full water and foam loading diagram.*

Figure 7.37: *Extreme cases loading diagrams.*

The loading diagrams show that the case where the fuel is filled to the maximum capacity is the one that produces the largest c.g. range. This is expected because there is a relatively large variable weight of the fuel in each wing with a long moment arm around the OEW c.g. The loading of the payload caused a small change in the c.g. because it was decided to place the water tank at the OEW c.g. This ensures the feasibility of the placement choice. Due to this, the system is also expected to comply with subsystem requirement QTR-STA-02 from Table 7.15 since the change in c.g. due to the water drop is not large. Nevertheless, a dynamic analysis of the c.g. change during the drop manoeuvre must be further analysed since this manoeuvre is expected to be critical for stability and controllability of the aircraft.

From the full fuel loading diagrams Figure 7.37, it can be seen that the most forward c.g. is located at 9.13 m from the nose of the fuselage while the most aft c.g. is located at 10.83 m from the nose. It is important to note that the cases involving the loading of payloads other than water or retardant were not explicitly analysed at this stage of the design. Nevertheless, these are not expected to cause a larger c.g. range in most cases because the payload would still be located close to the OEW c.g. and have lower mass than the full water tank. This is the case in missions such as search and rescue where the weight of evacuees will be much lower than the 10 000 kg of the full water tank.

7.8.4. Hover Mode

Contributor / Author: Sven

The aircraft will be in hover mode when the engines are in a fully vertical position. This will, for instance, happen in the take-off and landing segments of the flight. To analyse the hover mode a Free Body Diagram (FBD) was made identifying all the forces and moments acting on the aircraft. It can be found in Figure 7.38. There are three types of forces present in the FBD. Firstly, the weight of the aircraft W which is assumed to act at the c.g. of the aircraft. Secondly, the thrust of the rotors T acts upwards and pulls the aircraft up. Lastly, the force DL called download is present due to the fact that rotor-wash from the engine propellers is hitting the top surface of the wing. This creates a downward force, sometimes also referred to as vertical drag.

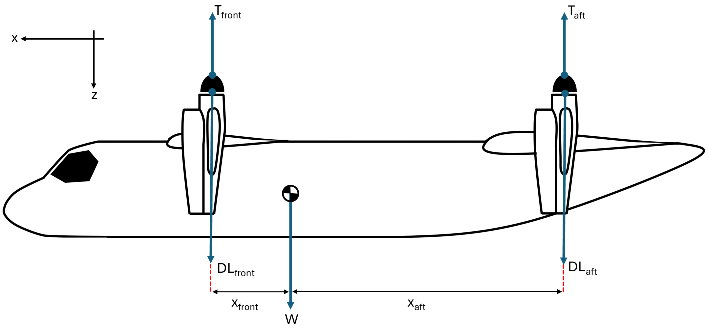

Figure 7.38: *FBD of the aircraft in hover mode.*

To keep the aircraft stable in hover, the forces will have to adhere to the equilibrium equations Equation 7.36 and Equation 7.37. It is clear that the front and aft rotors will have to produce different amounts of thrust to keep the aircraft in equilibrium due to the c.g. placement. It is advised to develop and use an automated control system to achieve this stability because it would be very difficult for the pilot to manually keep the aircraft level in hover. This system has to be a closed-loop control system which will measure the pitch of the aircraft and adjust the engine settings to achieve the pitch angle of zero degrees also ensuring compensation for changes in c.g. during the flight, for instance, this shift can be caused by refilling or dropping the water. This compiles with subsystem requirement **QTR-STA-01** from Table 7.15.

$$Z : T_{\text{front}} + T_{\text{aft}} - DL_{\text{front}} - DL_{\text{aft}} - W = 0 \tag{7.36}$$

$$M_{cg} : T_{\text{front}} \cdot x_{\text{front}} + DL_{\text{aft}} \cdot x_{\text{aft}} - T_{\text{aft}} \cdot x_{\text{aft}} - DL_{\text{front}} \cdot x_{\text{front}} = 0 \tag{7.37}$$

In the hover mode, the aircraft also has to be controllable. This will be achieved with the following mechanics for the three principal axes of the aircraft:

- **Pitch:** The pitch control will be achieved by changing the difference between the lift provided by the front and the aft wing rotors. This can also be done by the same closed-loop control system briefly explained earlier by inputting the desired pitch angle. Increasing lift will be achieved by increasing the blade pitch angle. This allows for more precise and more flexible rotor lift control when compared to increasing the lift by only increasing the rotor speed.
- **Roll:** The control in roll is achieved by the variation in lift provided by the rotors on the right and on the left side of the wings.
- **Yaw:** Slightly tilting the rotors on each side of the wing in different directions will achieve the yaw control of the aircraft. This will produce a small horizontal force of the same magnitude but opposite direction on each side of the wings which in turn creates a yaw moment about the z-axis.

Previously mentioned closed-loop automatic control systems can be further expanded upon for aircraft stability and control in hover mode in all three described axes. The system would measure the three control angles and adjust engine thrust and lift accordingly. Similarly, it can be used to control the translational movements of the aircraft. It is recommended to develop this control system in future stages of design.

7.8.5. Horizontal Flight Mode

Contributor / Author: Hanna

In the horizontal flight, the aircraft behaves closely to a conventional aircraft. The difference between the FireFly and the latter is that there is no conventional horizontal tail arrangement but rather a double-wing configuration. To ensure an efficient operation and prompt firefighting response, fulfilling the dash speed capabilities, it is critical to analyse the stability in horizontal flight mode. For the purpose of the stability and control analysis, it was decided to treat the rear wing as a horizontal tail to apply the techniques used for the conventional aircraft as the tandem wing analysis would go beyond the scope of the project. The Figure 7.39 contains the simplified FBD of the aircraft, along with important values indicated. Later on in the analysis, these locations will prove useful in establishing the stability and control characteristics of the design. A list of assumptions was compiled for further analysis.

Assumptions [29]

- Gliding flight assumption: possible vertical thrust is not included in the analysis.
  - This assumption could impact the analysis in case the tilt angle would have to be introduced for some of the conventionally horizontal flight operations. To achieve the most effective high dash speed, the tilt is assumed to be 0, making this assumption relevant.
- Contribution of the horizontal thrust is neglected, as it does not introduce a significant moment into the analysis relative to other components.
- The aerodynamic centre contribution is assumed to be located only in the front wing as the airfoil of the rear wing is the same as the front wing. Additionally for the analysis, the main contribution to the aerodynamic reference centre for the whole aircraft the contribution will be dominated by the fuselage.

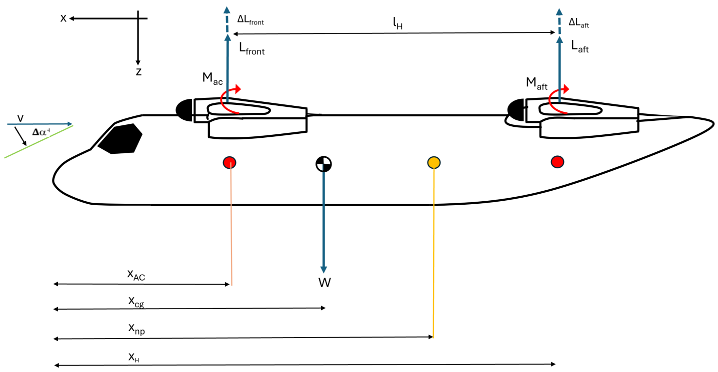

Figure 7.39: *FBD of tilt rotors in forward flight.*

Based on the FBD the simplified equations of motion for our aircraft could be derived.

$$Z : L_{\text{front}} + L_{\text{aft}} - W = 0 \tag{7.38}$$

$$M_{cg} : M_{\text{aft ac}} + M_{\text{front ac}} + L_{\text{front}} \cdot (x_{\text{cg}} - x_{\text{ac}}) - L_{\text{aft}} \cdot (x_{\text{cg}} - x_{\text{H}}) = 0 \tag{7.39}$$

Making the moment equation dimensionless, would result in the following:

$$C_m = C_{m_{\text{aft ac}}} + C_{m_{\text{front ac}}} + C_{L_{\text{front}}} \frac{x_{cg} - x_{ac}}{\bar{c}} + C_{L_{\text{aft}}} \left(\frac{V_h}{V}\right)^2 \frac{S_h}{S} \frac{x_{cg} - x_H}{\bar{c}} = 0 \tag{7.40}$$

Based on that equation, further analysis will be performed.

7.8.6. Lateral Control and Directional Stability

Contributor / Author: Sven

To improve aircraft directional stability and yaw control, a vertical tail with a rudder was added at the aft position of the aircraft. Adding a vertical tail will increase the weight of the aircraft, which has not been taken into account in the Class II weight estimation as initially it was assumed that the yaw control could be solely done using the rotor tilt. Adding the vertical tail is not expected to increase the weight of the aircraft substantially.

This design choice will ensure compliance with subsystem requirement **QTR-STA-05** from Table 7.15. Preliminary sizing of the vertical tail and the rudder was performed based on the Class I method for empennage sizing by Roskam [33]. For this method, the FireFly aircraft was classified as patrol, bomb and transport aircraft where a similar total wing area was used as reference. After the moment arm of the vertical tail was estimated to be located 8 m from the OEW c.g., the vertical tail area was calculated to 13.27 m^2. Furthermore, the tail geometry was determined by still using methods by Roskam[34] with all important parameters summarised in Table 7.17. It was decided to use the symmetrical NACA0015 airfoil for the root and symmetrical NACA0010 for the tip, identical to the V-22 Osprey aircraft since it is a comparable aircraft and symmetrical airfoils are generally used for vertical tails.

Table 7.17: *Vertical tail geometry parameters.*

Area [m^2]	**Root chord** [m]	**Tip chord** [m]	**Height** [m]	**c/4 sweep** [deg]	**Aspect ratio** [−]
13.27	3.5	2.3	4	26.7	1.21

Similarly to the vertical tail, the control surface sizing was performed according to the method by Roskam[34] using aircraft with similar total wing surfaces. The rudder was determined to use 42% of the root vertical tail chord and 50% of the tip chord. On the other hand, the chord length of ailerons and elevons was constrained by the location of the wingbox to 23% of the wing chord. This chord was then used to determine the ratio of ailerons and elevons span with respect to the wingspan resulting in 45% of each wing span being occupied by the ailerons in the case of front wings and elevons in the case of rear wings. To generate the highest rolling moment around the centre line of the aircraft, ailerons and elevons were positioned to the most outboard position on the wings. To comply with the subsystem requirement **QTR-STA-03** from Table 7.15 the control forces will have to be coated with anti-corrosive material. The exact coating was not determined at this stage of the design but it is not expected to have any major influence on the design. The vertical tail with the rudder (not to scale) is presented in Figure 7.40.

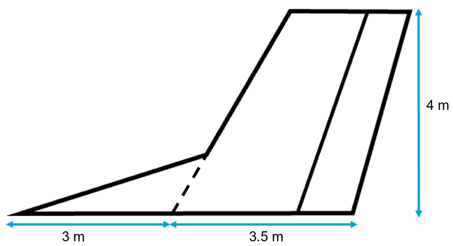

Figure 7.40: *Vertical tail with general dimensions.*

7.8.7. High Lift Devices sizing

Contributor / Author: Hanna

The High Lift Devices need to be sized to ensure controllability during the line drop maneuver as dictated by the tilt rotor analysis. As the ailerons and elevons have been sized already, the positioning of the flaps n_i and n_o was limited. Additionally, owing to the wingbox placement, the flap chord c_f was fixed as well. The following values were used in sizing. For the fixed size of the flap, it was identified using estimation suggested in [33] that the necessary increase in lift can be produced by choosing single slotted flaps and deflecting them by σ_{flap} 35 deg. For the analysis, the aircraft was assumed to be long coupled, owing to the ratio between the fuselage length l_f and the mean chord $\bar{c}$, which enforces an additional factor of 1.05 on the required lift. The following final values were obtained for the flap dimensions as presented in Table 7.18.

Table 7.18: *Values obtained for the flap sizing.*

c_f [m]	n_i [% of span]	n_o [% of span]	$C_{L_{\text{drop}}}$ [-]	$C_{L_{\max}}$ [-]	σ_{flap} [deg]	$C_{L_{\alpha_{\text{flap}}}}$
0.6	0.01	0.53	3.2	1.5	35	6.45

It was found that using these flaps, it is possible for the FireFly to perform the line drop maneuver with a speed of 59 m/s. The schematic drawing of the wing with relevant dimensions can be seen in Figure 7.41. The flaps will be placed on both wings.

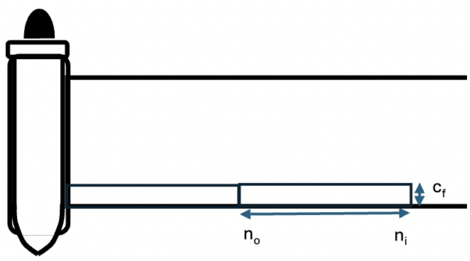

Figure 7.41: *Dimensions of the single slotted flaps*

7.8.8. Scissor Plot

Contributor / Author: Hanna

To analyse whether, with the current horizontal tail size, the aircraft can remain stable and controllable, it was decided to use a scissor plot, which provides an x_{cg} margin per horizontal tail size. Usually, this type of plot is used for sizing the horizontal tail, however, in the case of FireFly, the rear wing becomes a horizontal tail which has already been sized. The scissor plot will be used to show how the chosen rear wing size is affecting the stability and controllability of the aircraft.

The following assumptions were made during the calculations; firstly, the aircraft is only reaching subsonic speeds (order of 0.4 Mach), the horizontal flight mode is assumed, the effects of propulsive forces are neglected and the analysis is stick-fixed.

Stability

The following equation will be used for sizing the stability curve [29].:

$$\bar{x}_{c.g.} = \bar{x}_{AC} + \frac{C_{L\alpha_H}}{C_{L\alpha_{A-H}}}\left(1 - \frac{d\varepsilon}{d\alpha}\right)\frac{S_H l_H}{S\bar{c}}\left(\frac{V_H}{V}\right)^2 - SM \tag{7.41}$$

To use this equation, some of the coefficients needed to be estimated. All of the coefficients will be computed at cruise speed of 380 km/h. The term at the end of the equation includes a stability margin SM which enforces a safety margin in operation of the aircraft and ensures appropriate controllability characteristics. To estimate the aerodynamic centre of the aircraft less tail $\bar{x}_{ac}$, the following equation was used [35]:

$$\bar{x}_{ac} = \left[\left(\bar{x}_{ac}\right)_w + \left(\bar{x}_{ac}\right)_{f_1} + \left(\bar{x}_{ac}\right)_{f_2}\right] + \left(\bar{x}_{ac}\right)_n + \left(\bar{x}_{ac}\right)_{fair}$$

The contributions accounted for the destabilising effects of the nose $\left(\bar{x}_{ac}\right)_{f_1}$ and the front nacelles $\left(\bar{x}_{ac}\right)_n$, as well as the stabilising effect of the wing-fuselage intersection $\left(\bar{x}_{ac}\right)_{f_2}$, rear nacelles $\left(\bar{x}_{ac}\right)_n$ and fairings $\left(\bar{x}_{ac}\right)_{fair}$. To simplify the estimate of the landing gear storing fairings' contribution to the aerodynamic centre, they were modelled as an instance of fuselage-mounted nacelles and subsequently incorporated into the equation.

To estimate the tail-to-wing speed ratio $\frac{V_H}{V}$, a non-standard method was used that was dictated by our configuration. The ratio was assumed to be a non-standard value, because of the rotor configuration as mentioned and explained in Figure 7.6.2. The flow behind the wing is increased because of the main rotor and therefore the speed over the rear wing is increased relative to the main wing. This causes the tail-to-wing speed ratio to be increased, as opposed to a typical aircraft configuration.

The lift rate coefficient of the tail $C_{L\alpha_H}$ was known, as the wing was sized before constructing the scissor plot. The fuselage contribution to the lift rate coefficient $C_{L\alpha_{A-H}}$ was estimated assuming a conventional plane configuration.

The downwash effect is assumed to be 0, as the downwash is expected to be negligible during the cruise. This assumption is conservative as in fact there could be upwash effects present on the rear wing/tail, which are beneficial for stability, as it is discussed and explained further in Figure 7.6.2. In Table 7.19 the final computed values are summarised.

Table 7.19: *Values used to compute the stability part of the scissor plot.*

$\overline{x}_{AC}$ [% of MAC]	$C_{L\alpha_H}$ [-]	$C_{L\alpha_{A-H}}$ [-]	$\frac{d\varepsilon}{d\alpha}$ [-]	l_H [m]	$\overline{c}$ [m]	$\left(\frac{V_{aft}}{V_{front}}\right)^2$ [-]	SM [-]
3.42	0.103	0.278	0	15.55	2.56	1.5	0.05

Controllability

To plot the controllability part of the curve the following equation was used [29]:

$$\overline{x}_{c.g.} = \overline{x}_{ac} - \frac{C_{m_{ac}}}{C_{L_{A-h}}} + \frac{C_{L_h}}{C_{L_{A-h}}} \frac{S_h l_h}{S\overline{c}} \left(\frac{V_h}{V}\right)^2 \tag{7.42}$$

To use the equation some of the coefficients needed to be estimated. The aerodynamic centre of the aircraft along with l_H, $\overline{c}$ and the tail-to-wing speed ratio were already computed for the stability curve.

To estimate the C_{L_h}, the tail was assumed to be fixed. To estimate the $C_{m_{ac}}$ the contribution from the wing along with the fuselage contribution was taken into account. It was found that the contribution of the fuselage adds a very negative pitching moment contribution.

The controllability was computed with HLDs deployed, as this is the limiting condition in the case of line dropping with the FireFly. The exact values used to compute the controllability curve are presented below in Table 7.20.

Table 7.20: *Values used to compute the controllability part of the scissor plot.*

$\overline{x}_{AC}$ [% of MAC]	$C_{m_{ac}}$ [-]	$C_{L_{A-h}}$ [-]	C_{L_h} [-]	l_H [m]	$\overline{c}$ [m]	$\frac{V_H}{V}$ [-]
0.43	-0.58	2.5	-0.63	15.55	2.56	1.5

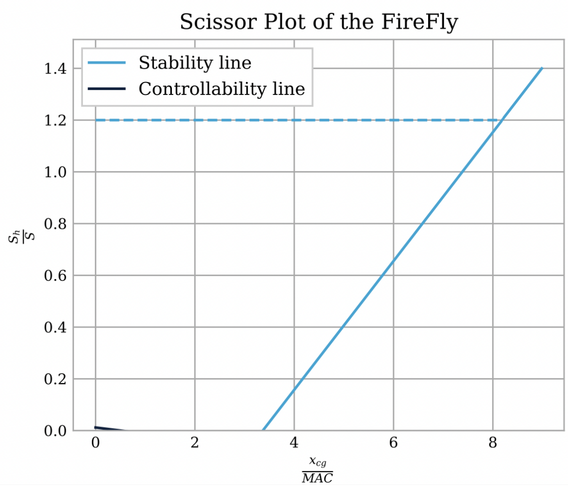

Figure 7.42: *Scissor plot.*

The final scissor plot is presented in Figure 7.42. Based on the scissor plot alone, the following c.g. range was obtained.

Table 7.21: *C.G range resulting from the scissor plot.*

Forward c.g $[x_{cg}/MAC]$	**Aft c.g.**$[x_{cg}/MAC]$
0	6.019

As can be noticed, this range is within the range estimated using the loading diagrams which also means that the system can compensate for the changes in aircraft c.g. inflight as stated in requirement **QTR-STA-01** from Table 7.15. Additionally, as the fuselage ends at 6 MAC, the value for the aft c.g, 7.384 MAC, that was obtained from the plot was discarded, as it was extending beyond the fuselage.

7.8.9. Neutral Point Calculations

Contributor / Author: Sven

As an additional requirement for the aircraft to remain stable for stick fixed condition, the c.g. has to be located in front of the neutral point. The neutral point is the longitudinal location of the aircraft around which the sum of moments caused by the change in lift ΔL due to perturbations in the angle of attack is zero. This means that these moments must be equal. [35] Looking at the FBD in Figure 7.39, simple moment equilibrium equation can be made Equation 7.43. This is further expanded to Equation 7.44. Finally, the neutral point x_{np} can be calculated from Equation 7.45. As the wings are the same, lift coefficient C_{L_α}, density ρ and surface area S can be removed from both sides of the Equation 7.44.

$$\Delta L_{front} \cdot (x_{np} - x_{AC}) = \Delta L_{aft} \cdot (x_H - x_{AC}) \tag{7.43}$$

$$C_{L_{\alpha_{front}}} \cdot \Delta\alpha \cdot \frac{1}{2} \cdot \rho \cdot V_{front}^2 \cdot S_{front} \cdot (x_{np} - x_{AC}) = C_{L_{\alpha_{aft}}} \cdot \Delta\alpha \cdot \frac{1}{2} \cdot \rho \cdot V_{aft}^2 \cdot S_{aft} \cdot (x_H - x_{AC}) \tag{7.44}$$

$$x_{np} = \frac{\left(1 - \frac{d\epsilon}{d\alpha}\right) \cdot \left(\frac{V_{aft}}{V_{front}}\right)^2 \cdot x_H + x_{AC}}{1 + \left(1 - \frac{d\epsilon}{d\alpha}\right) \cdot \left(\frac{V_{aft}}{V_{front}}\right)^2} \tag{7.45}$$

Using the same values presented in Table 7.19, the neutral point location x_{np} was calculated to be 12.20 m from the nose of the aircraft. This is well behind the most aft c.g. determined from the loading diagrams in Figure 7.37 so the aircraft is expected to be stable in horizontal flight for all c.g. locations.

7.8.10. Control Forces

Contributors / Authors: Hanna, Sven

To ensure that the aircraft can be controlled by the pilot and comply with the regulations, there is a limit on the control forces that are needed in the flight. At this point in the design, the exact elevator deflection and hinge moments remain unknown and further work is needed to estimate them, utilising for instance experimental in-flight measurements. By including the stability margin of 0.05 $\frac{x_{cg}}{MAC}$ and designing the stability for stick-fixed conditions, the control forces requirement imposed by the certifications and pilot convenience can be indirectly accounted for. As the expected c.g. margin is beneficial for the controllability, meaning a slight shift to the left, it is further assumed that the aircraft will remain controllable within its service.

Moreover, the aircraft will be equipped with a fly-by-wire system which means that the flight computer manipulates the control surfaces according to the inputs from the pilots or the autopilot. This implies that the pilot will not necessarily feel the exact forces needed to manipulate the control surfaces on the stick which is beneficial in case further analysis shows that a large stick force is needed to control the aircraft. The fly-by-wire system can be used to make these forces similar to the ones needed to control an S-70 Firehawk which will make the stability and control system compliant with the QTR-STA-04 subsystem requirement.

7.8.11. Engine Tilt Control

Contributor / Author: Ishan

For transitioning from hover to horizontal flight mode, the engines must be tilted using a specific tilt mechanism. There are two main options when designing such a system: using hydraulic or electric motors/actuators. The advantage of using hydraulic motors is the fact that these can produce extremely high torques.

However, they are heavy, require constant maintenance [13] and have a low control resolution. On the other hand, electric motors are much lighter, require little maintenance, but more importantly, have a high resolution for precise control. Therefore, the decision to use electric motors is advantageous.

The biggest challenge when sizing such an electric motor is finding one which has a suitable torque rating. The torque required to tilt the engines is 14 600 N m. Unfortunately, this

Firstly, it is important to understand how the required torque to rotate the engine is found. A simplified model of the engine and rotor assembly must be created. It is important to note that a single resultant force comprising of the engine weight and propeller weight can be modelled as a rectangle, as shown in Figure 7.43.

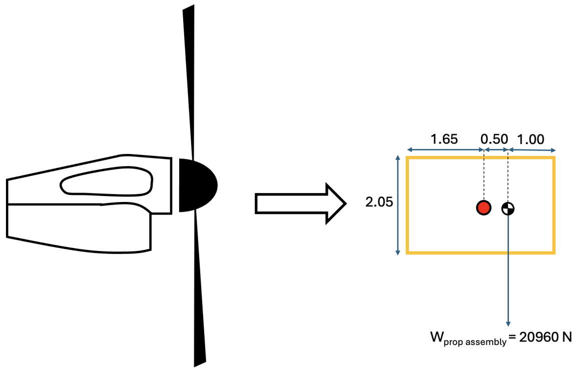

Figure 7.43: *Model of engine and rotor assembly (all dimensions in m) where the red dot indicates the axis of rotation.*

In order to size the required torque, two torque components are required: the load torque and the acceleration torque. The sum of these two components makes the total required torque to be produced. The definitions of these components are given by Equation 7.46 and Equation 7.47:

$$T_a = \frac{J \cdot V}{9.55 \cdot t} \quad (7.46) \qquad T_L = W_{\text{prop assembly}} \cdot r \quad (7.47) \qquad T_{req} = (T_a + T_L) \cdot SF \quad (7.48)$$

J denotes the load inertia of the engine in kg m^2, V denotes the rotational speed of the engine in rpm, t represents the time to accelerate to the prescribed V and r represents the offset between the centre of gravity of the engine assembly and the axis of rotation. Lastly, SF represents the factor of safety which accounts for mechanical efficiency losses and other aerodynamic load constraints on the rotor when tilting the engine assembly. To find the load inertia, Equation 7.49 must be used where A represents the engine assembly length and B represents the engine assembly height:

$$J = \frac{m}{12} \cdot (A^2 + B^2 + 12 \cdot r^2) \quad (7.49)$$

Table 7.22 displays the torque parameters to compute the total required torque to rotate the engine assembly. As one can see from Table 7.22, the required torque is 14 600 N m. There exists no feasible electric motor which

Table 7.22: *Required torque parameters.*

Parameter	Value	Parameter	Value
J [kg m^2]	3045	T_L [Nm]	1197
V [rpm]	7.5	T_a [Nm]	10482
t [s]	2	SF [-]	1.25
r [m]	0.5	T_{req} [Nm]	14600

Table 7.23: *Gear box characteristics.*

Parameter	Value	Parameter	Value
r_1 [m]	0.04	r_3 [m]	0.05
T_1 [-]	7	T_3 [-]	10
r_2 [m]	0.18	r_4 [m]	0.20
T_2 [-]	32	T_4 [-]	41

can produce such a torque. This is why a reduction gearbox is implemented as a design choice. To properly size the reduction gearbox, an initial electric motor torque must be determined which is why an electric

[13] Link [cited on 18-06-2024]

motor must be selected. It was decided to use the YASA 750 ER [14] electric motor due to its low weight and small dimensions which delivers 790 N m of torque and denoted by $T_{elecmotor}$. A reduction gearbox system must be designed. Figure 7.44 shows the design of such a gearbox.

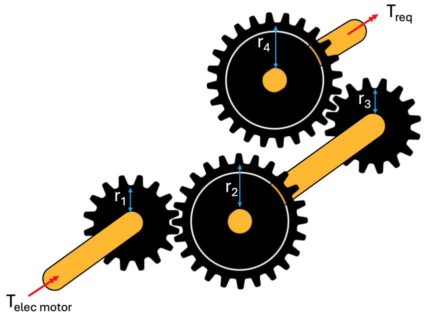

Figure 7.44: *Reduction gearbox design for engine assembly tilt motors.*

Equation 7.50 can be used to size the gears for the output shaft to meet the required torque T_{req}. Furthermore, the gearbox design characteristics can be found in Table 7.23. T refers to the number of teeth on the gear, r refers to the radius of the gear in m and finally n refers to the gear speed in RPM.

$$\frac{T_2}{T_1} = \frac{r_2}{r_1} = \frac{n_1}{n_2} \tag{7.50}$$

The required torque T_{req} is achieved using such a gearbox design. The footprint of this whole system is also relatively small and does fit in its designated wingtip area next to the fuel tanks. However, future iterations of the gearbox can include implementing a planetary gearbox design. Such a design has two advantages: an even smaller footprint and the fact that the input and output shafts are aligned.

A last consideration which must be examined is the locking mechanism of these motors for the horizontal flight mode. Indeed, when the aircraft is in horizontal flight mode, engines must be locked at an angle of 0 degrees. A simple locking mechanism can be added to the gearbox to fulfil this purpose. The exact design of such a mechanism is not shown in this report however must be investigated for a more detailed design of the aircraft.

[14] Link[cited on 18-06-2024]

8 | Aircraft Configuration & System Characteristics

In this chapter, the aircraft configuration and layout are presented along with the fuel, hydraulic, environmental, avionics and electrical systems. The landing gear is determined and the water tank design is explained. Lastly, the interactions between subsystem hardware, software and the data handling flow are addressed.

8.1. Configuration & Layout

This section addresses the configuration and layout for the subsystems of the FireFly.

Fuel System Layout

Contributor / Author: Ishan

Table 8.1: *Fuel subsystem requirements.*

Identifier	Parent	Subsystem Requirements
QTR-FUL-01	FTF-SYS-FDS-06.5	The fuel tanks shall be able to hold 9700 kg of fuel.
QTR-FUL-02	FTF-SYS-FDS-05.15	Fuel shall be able to be supplied to the engine during loads of -1 to 3.25 g.
QTR-FUL-03	FTF-SYS-FDS-06.5	The fuel tanks shall have an inlet with a standard maximum diameter of 2.6 inches for refuelling.
QTR-FUL-04	FTF-SYS-PIL-04.4	The fuel tanks shall be equipped with a bladder sealant bag.
QTR-FUL-05	FTF-SYS-PIL-04.4	The fuel tanks shall not puncture when exposed to loads of -1 to 3.25 g.
QTR-FUL-06	FTF-SYS-FDS-06.4	The fuel tanks shall be equipped with access points for easy inspection and maintenance.
QTR-FUL-07	FTF-SYS-SUP-01.2	The fuel tanks shall be able to hold jet fuel A and jet fuel B.

Since the aircraft is powered by kerosene, it requires a complete fuel system. Similarly to conventional aircraft, most of the fuel is carried in the front and rear wings. However, the volume available in the wings is not sufficient to host all of the required fuel. Therefore, extra fuel tanks are required in the sponsons. A detailed overview of the fuel system layout is displayed in Figure 8.1.

There are some interesting points worth discussing which arise from the design of the fuel subsystem linking to operational activities. Concerns which arise from this fuel system design are related to two major factors: safety during refuelling as well as practicality and short turnaround times. One simple design characteristic of the fuel system addresses both these concerns: the single refuelling points on either side of the aircraft's sponsons. The first advantage of this configuration is that there cannot be any confusion as to which fuel tanks are filled or empty, as fuel is automatically pumped into all fuel tanks evenly. Many fuel starvation accidents or incidents occur due to confusion and miscommunication regarding the quantity of fuel onboard. The second advantage of such a configuration is the practicality of having a single refuelling port on either side of the aircraft. During turnaround periods, the ground handling crew can simply plug the fuel hose into the port and continuously fill the aircraft, instead of having to switch refuelling ports to fill multiple tanks. Furthermore, turnaround times are greatly reduced as the fuel truck can remain in one single position during the refuelling process. This is a major advantage, especially during firefighting operations where turnaround times are the major drivers for fast response times, which itself is a major driver for fire suppression efficiency.

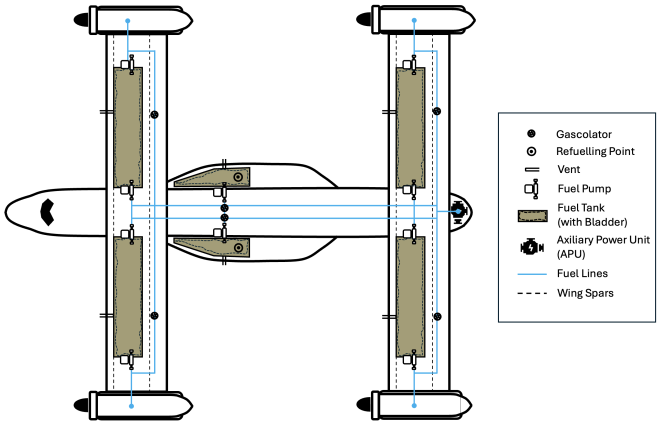

Figure 8.1: *Fuel system design and layout in aircraft.*

In order to size the fuel tanks, the constraining factor is the total fuel mass to be hosted on-board. From the class I and II weight estimations, the total fuel required to be carried onboard the aircraft is 9700 kg. Since the wing box geometry is known thanks to Section 7.3, a decision must be made on the fuel tank cross-section area to use. In the wing box, space must be accommodated for the drive shaft connecting the left and right engines of each wing. Figure 8.2 shows the cross-section and constraint in the geometry of the fuel tank. To mitigate any risks of leaking and puncturing, a bladder tank is present inside a traditional integral tank, adhering to requirements **QT-FUL-04** and **QT-FUL-05**.

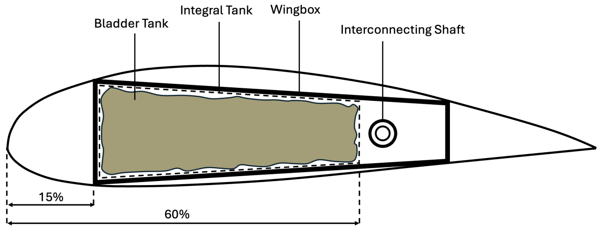

Figure 8.2: *Cross-section of fuel tank design and geometry as a percentage of the chord.*

In terms of how far the fuel tanks expand in the span of the wings, some design constraints were present. At the wing tips, space was required to fit the tilting motors which control the tilt of the engines. Therefore, the wing fuel tanks span to 6 m from the centreline of the fuselage. This geometry generates an available volume equivalent to 35% of the fuel mass in each wing. Therefore, the remaining 30% of the fuel is fitted in the fuselage's sponsons. Table 8.2 gives detailed geometry of the capacity of the aircraft's fuel tanks. The wing tanks consider both left and right tanks as a total.

Table 8.2: *Fuel tank capacities and masses.*

Parameter	**Fuselage Tank**	**Front Wing Tank**	**Rear Wing Tank**	**Total**
Mass Fraction [-]	0.3	0.35	0.35	1
Mass [kg]	2910	3395	3395	9700
Volume [m^3]	3.63	4.23	4.23	12.09

Regarding the fuel pumps themselves, Roskam [33] suggests having 1.5 times the maximum fuel flow rate required. Therefore, the maximum power required must be identified to understand the most constraining flight regime. Section 7.4 shows the most constraining point to be in hover with one engine inoperative. This regime yields a maximum fuel flow of 1.11 kg s^{-1}. Multiplying this by 1.5 yields a required fuel flow of 1.67 kg s^{-1} for the fuel pumps. Placing the fuel pumps at the exit and intake of each fuel tank enables constant fuel pressure across the whole system.

As previously mentioned, concerns which arise from this fuel system design are related to the operational aspects. Having a single refuelling point also impacts other parts of the design, especially the landing gear design. No matter how the aircraft is filled, the landing gear must be able to support the loads as well as prevent tip back. The landing gear design is further elaborated on in Table 8.1.

Hydraulic System Layout

Contributor / Author: Ishan

The aircraft uses multiple hydraulic actuators to move various components. As a result, a hydraulic system is required. To create such a hydraulic system, the following approach is taken: list all the components which require hydraulic actuation and place them in the aircraft. Once this is done, the sizing of the pumps can be achieved. These components are listed below:

- Ailerons
- Elevons
- Rudder
- Nose gear retraction and brakes
- Main gear retraction and brakes
- Water tank drop doors
- Rotor governors
- Rear cargo ramp

The biggest challenge in making such a layout is ensuring that all actuators have sufficient hydraulic pressure and adding redundancy to the system. A constant hydraulic pressure of 20.6 MPa is required at all times [33]. Therefore, hydraulic pumps must constantly pressurise all the hydraulic lines. The number of hydraulic pumps is determined based on this pressure requirement. The flow rate of the hydraulic fluid required is assumed to be the same as the V-22 Osprey, namely 20 L/min [36].

Table 8.3: *Hydraulic design characteristics.*

Parameter	Value
Total Number of Lines [-]	3
Required Pressure per System [MPa]	20.6
Total Required Flow per System [L/min]	20
Hydraulic Fluid Tank Capacity [L]	12
Total Number of Actuators [-]	16
Total Number of Pumps [-]	5
Total Number of Valves [-]	6

Another aspect of designing such a system is to have redundancy. As previously mentioned, for the hydraulic system to function properly, it must be constantly pressurised. Therefore, 3 main hydraulic systems are present: line A, line B and line C. Line A and line B are considered to be primary lines, meaning they are devoted solely to the flight control system. To be more precise, line A is linked to all actuators which control the flight control surfaces: the elevons, ailerons and rudder. Line B controls exclusively the actuation of the rotor governors. The governors are used to change the pitch angles of the rotor blades which mostly allow control in hover mode. Line C is considered secondary, as it powers all secondary functions such as gear retraction, ramp deployment and retardant tank drop doors. There are two pumps for each line, allowing redundancy. These pumps are sized such that if one fails, the remaining one can still pressurise the line. These 3 lines are themselves independent, meaning that in the rare case that one primary line completely fails, line A or B, enough control is still present to safely land the aircraft.

Environmental System

Contributor / Author: Hanna

Table 8.4: *Environmental subsystem requirements.*

Identifier	Parent	Subsystem Requirement
QTR-ENV-01	FTF-SYS-REG-01.8	The cargo compartment shall be equipped with a smoke sensor.
QTR-ENV-02	FTF-SYS-REG-01.8	The cargo compartment shall be equipped with a carbon monoxide sensor.
QTR-ENV-03	FTF-SYS-REG-01.8	The cockpit shall be equipped with a smoke sensor.
QTR-ENV-04	FTF-SYS-REG-01.8	The cockpit shall be equipped with a carbon monoxide sensor.
QTR-ENV-05	FTF-SYS-PIL-05.1	The cockpit shall be equipped with a heat, ventilation, air conditioning (HVAC) controller.
QTR-INV-01	FTF-SYS-PIL-04.1	The aircraft shall have an air-filtering system to filter smoke during flight over fire.
QTR-INV-02	FTF-SYS-PIL-04.1	The internal temperature of the aircraft shall not exceed 30 degrees Celsius during a flight over fire.

The Environmental Control System is mainly used to regulate the cabin air quality and temperature as dictated by **QTR-INV-01** and **QTR-INV-02**. The pressurisation system would not be implemented, as it was decided that cruising altitude does not require that and it would overcomplicate structural design. [1]

As dictated by **QTR-ENV-05**, an emergency oxygen system will be installed, which was dictated by regulations [37]. The choice of the oxygen system was between liquid, gaseous and chemical. The gaseous and liquid systems were discarded as these types of oxygen systems present increased fire hazards. The chemical oxygen was chosen as it is a reliable source of oxygen for the passengers and the associated increase in weight would be acceptable [37]. According to regulations, in unpressurised aircraft cruising at an altitude of 14 000 ft and above, oxygen is mandatory at all times. For safety, it was decided to include oxygen in the aircraft for the whole duration of the respective flight. The pneumatic system will be included and used for air conditioning, and ice protection. The pneumatic system will use an engine compressor bleed air from the engines themselves and the APU. The bleed air system will also be used for cabin heating. It uses an air intake which goes through an air filter and feeds to an air quality controller. This assesses the air quality and regulates the selected air temperature. The air from the air conditioning system will be distributed via a network of ducts. The aircraft is supposed to accommodate 11 passengers. This means that the air conditioning system will need to supply 220 ft^3 of air per minute. When designing the layout, care needs to be taken from the fact that the heating systems, while crucial for crew comfort, pose fire and carbon monoxide poisoning risks. That is why the smoke and carbon monoxide sensors were placed both in cargo compartment and cockpit as dictated by **QTR-ENV-01**, **QTR-ENV-02**, **QTR-ENV-03**, and **QTR-ENV-04**.

Landing Gear

Contributor / Author: Johannes

[1] Link [cited on 05-06-2024]

Table 8.5: *Landing Gear subsystem requirements.*

Identifier	Parent	Subsystem Requirement
QTR-LDG-01	FTF-SYS-FDS-05.8	The landing gear should be stable on uneven surfaces.
QTR-LDG-02	FTF-SYS-FDS-03.3	The landing gear shall be retractable.
QTR-LDG-03	FTF-SYS-REG-01.14	The landing gear shall be able to support the MTOW during ground operations.
QTR-LDG-04	FTF-SYS-AIR-02.2	The landing gear shall be able to support the maximum landing weight.
QTR-LDG-05	FTF-SYS-REG-01.14	The landing gear shall absorb shocks from landing.
QTR-LDG-06	FTF-SYS-REG-01.14	The landing gear shall withstand loads throughout the centre of gravity range.
QTR-LDG-07	FTF-SYS-FDS-06.4	The landing gear design shall allow for easy maintenance.

To design the landing gear subsystem, the loads that the aircraft exerts on the ground must be analysed. From requirement **QTR-LDG-01**, **QTR-LDG-03** and **QTR-LDG-04** in Table 8.5 it is clear that the landing gear should be sized for MTOW on soft uneven surfaces. The landing gear sizing and wheel selection are based on the procedures presented in ADSEE[29] as well as Boeing recommendations for tyre contact area [2].

To fulfil **QTR-LDG-01**, **QTR-LDG-03** and **QTR-LDG-04** it has been determined that the static ground pressure should not exceed 350 kPa and the tyre pressure should be 60 psi [29]. These values are based on operation on hard sand and grass surfaces.

During the design, three main challenges were encountered. Firstly low tyre pressure required combined with the MTOW of 35.000 kg means that the tyre options are very limited. For a configuration of 2 nose wheels and 4 main wheels, it was found that the best options would be 29 in and 48 in tyres respectively as listed in Table 8.6.

Table 8.6: *tyre dimensions*

Tyre dimensions	Outer diameter [in]	Inner diameter [in]	width [in]
Main gear	48	18	18
Nose gear	29	13	9.75

In addition, it must be verified that the static ground pressure doesn't exceed 350 kPa at MTOW. This has been checked by estimating the contact surface area of the tyres as described by Boeing[3] and compared with the minimum surface area needed which is found by dividing the MTOW with the static ground pressure. the required and actual contact area of the tyres at MTOW is presented in Table 8.7.

Table 8.7: *Estimated dimensions of elliptical landing gear footprint.*

wheel contact area footprint	Required area [m^2]	Actual area [m^2]	Major axis [m]	Minor axis [m]
Main gear	0.1935	0.1916	0.63	0.40
Nose gear	0.0841	0.0833	0.42	0.26

From Table 8.7 it can be seen that the actual area of the tyres is marginally smaller than the required area. This is not seen as a problem as the tyres selected for the aircraft are able to operate at an inflation pressure of 59 psi which is low enough that the contact area is above the required contact area.

The second challenge was the longitudinal positioning of the landing gear. Due to the large shift in the centre of gravity during operations such as refuelling the loads on the landing gears change a lot. To combat this,

[2] Link [cited on 13-06-2024]
[3] Link [cited on 13-06-2024]

a configuration with the main wheels being positioned longitudinally next to each other instead of laterally next to each other inspired by the C-130 has been adapted. This allows the main gear to carry more of the load of the aircraft for a wider range of the centre of gravity, thus relieving the load on the nose gear. The main gear is positioned based on both the position of the OEW centre of gravity and a requirement of minimum 8% and maximum 20% of the load to be carried by the nose wheel. Because of the long wheelbase of the main gear the aircraft is not in danger of tipping over even when the centre of gravity is most aft.

Finally, due to the high wings and engines, the centre of gravity of the aircraft is located high above the ground at roughly 2.1 m above the belly of the fuselage. Because of this, the wheelbase needs to be very wide to prevent tipping over laterally during taxiing and operation on sloped surfaces. To maintain a lateral tip-over angle of 30 deg, it has been calculated that the main wheels must be located at 2 m from the centreline of the fuselage. Many exotic concepts of landing gear retraction/deployment mechanisms have been considered to minimise the size of the landing gear fairings. In the end, it has been decided to keep the design simple and use a conventional vertical deployment of the main gear and a folding deployment of the nose gear as done on the C-130. This decision came partly from the realisation that the fairings for the landing gear will also need to contain the fuel stored in the fuselage. It therefore doesn't make sense to make a complex retraction system to make the fairings smaller.

The final landing gear layout dimensions can be seen in Table 8.1 figure and the deployment and retraction mechanism is shown in Figure 8.4a.

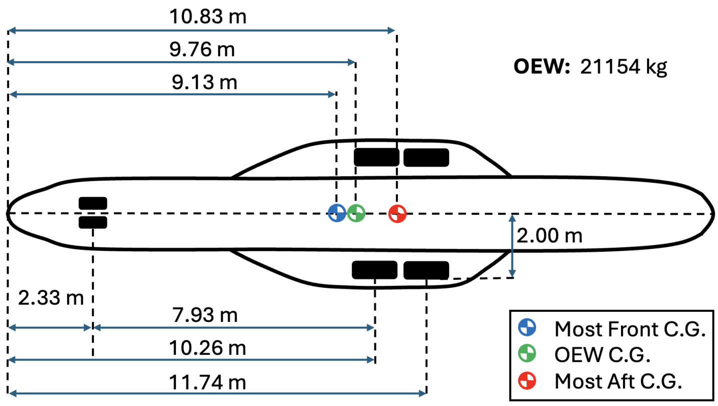

Figure 8.3: *Landing gear layout dimensions.*

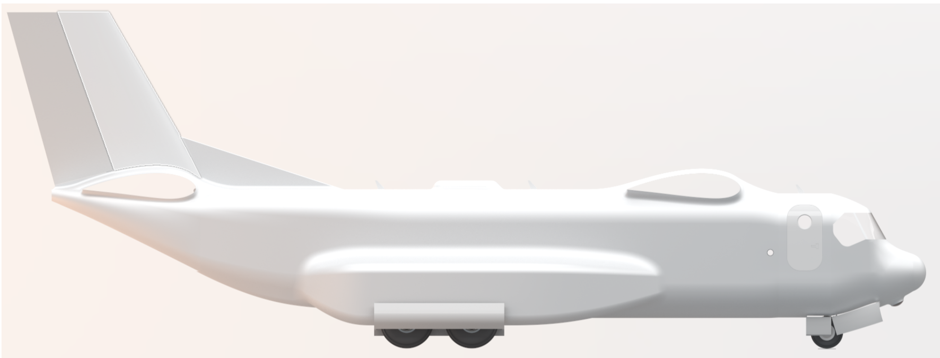

(a) *Side view.*

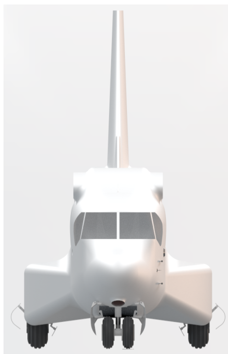

(b) *Front View*

Figure 8.4: *Landing gear deployed.*

In the case of a hydraulic failure, the landing gear should still be able to be deployed. To ensure this a manual backup system is implemented which allows the pilots to extend the landing gear. Due to the simple design of the landing gear deployment mechanism, a manual deployment would be heavily aided by gravity and thus doesn't require much physical strain on the pilots.

Retardant/Water Tank Design

Contributor / Author: Thijs

One of the most important systems for an aerial firefighting aircraft is the retardant/water tank. In order to be an effective firefighter, the tank should have ample capacity, variable drop rates and it must be integrated properly. The full list of requirements is shown in Table 8.8.

Table 8.8: *Retardant tank and dropping mechanism subsystem requirements.*

Identifier	Parent	Subsystem Requirements
Retardant tank subsystem requirements		
QTR-TNK-01	FTF-SYS-FDS-02.1	The tank shall have a capacity of 10.000 L.
QTR-TNK-02	Mission Analysis	The tank shall include a foam injection system with a capacity of 500 L.
QTR-TNK-03	FTF-SYS-FDS-05.2	The tank shall have an inlet for the refilling from the snorkel.
QTR-TNK-04	FTF-SYS-FDS-05.5	The tank shall have an inlet for the refilling from ground equipment.
QTR-TNK-05	FTF-SYS-FDS-05.5	The tank shall have an overflow channel.
QTR-TNK-06	FTF-SYS-FDS-07.3	The structure shall be able to withstand thermal loading in conditions up to 180 °C without critical or catastrophic failure.
QTR-TNK-07	FTF-SYS-FDS-05.2	The inside surface of the retardant tank shall be highly corrosion-resistant to salt water.
QTR-TNK-08	FTF-SYS-FDS-05.2	The inside surface of the retardant tank shall be highly corrosion-resistant to foams.
QTR-TNK-09	FTF-SYS-LOC-01.1	The inside surface of the retardant tank shall be highly corrosion-resistant to long-term retardants.
QTR-TNK-10	FTF-SYS-FDS-06.4	The retardant tank shall include access points for easy inspection and maintenance.
Drop subsystem requirements		
QTR-DRP-01	FTF-SYS-FDS-01.1 / FTF-SYS-FDS-05.3 / FTF-SYS-FDS-05.4 / FTF-SYS-FDS-05.13	Drop doors shall be able to be individually opened.
QTR-DRP-02	FTF-SYS-FDS-01.1 / FTF-SYS-FDS-05.3 / FTF-SYS-FDS-05.4 / FTF-SYS-FDS-05.13	Drop doors shall be able to be partially opened to control retardant exit rate.
QTR-DRP-03	FTF-SYS-FDS-01.1	The retardant tank shall have sensors to monitor the retardant left in the tank.
QTR-DRP-04	FTF-SYS-FDS-01.2	The tank shall be equipped with internal baffles to reduce the effects of sloshing.
QTR-DRP-05	FTF-SYS-FDS-01.2	The tank shall be able to withstand dynamic forces acting from the inside.

External Tank Dimensions

The retardant tank is designed to fit underneath the floor of the aircraft. Due to this design choice, a trade-off must be made between the length of the tank and the height of the tank. If the tank is too high, there is insufficient internal space in the fuselage to transport people or goods effectively. If the tank is too long, however, sloshing during manoeuvres will lead to more drastic changes in the longitudinal location of the centre of gravity leading to controllability issues. The tank was therefore limited to a maximum height of 1 m which leaves an internal height fuselage height of 1.8 m. To achieve the required internal volume as specified by **QTR-TNK-01** the tank length ended up being 7 m which was deemed acceptable.

The tank dimensions and shape are shown in Figure 8.5. The tank narrows towards the bottom which helps in depositing all water/retardant in the tank and ensures a snug fit in the rounded bottom of the fuselage. The tank consists of a straight, rectangular section on the top which holds the majority of the volume and a bottom section which funnels the retardant towards the release doors. The tank consists of two identical sections which are separated along the centreline. This allows the pilot to empty both sections simultaneously, individually or sequentially adhering to requirement **QTR-DRP-01**. The drop doors shall be hydraulically opened and closed allowing for an adjustable mass flow of retardant based on the position of the doors (**QTR-DRP-02**). Either one of the two sections has a volume of approximately 5100 L meaning that the tank can carry around 10 200 L of water/retardant.

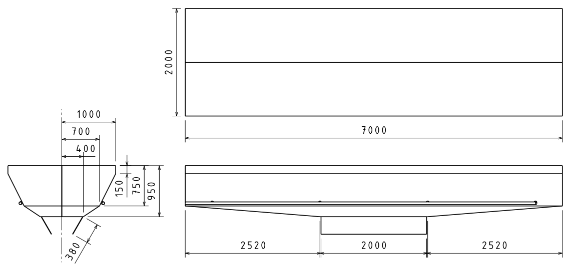

Figure 8.5: *Three-view drawing of the external dimensions of the water tank.*

In order to reduce the effect of a shift in the centre of gravity during manoeuvres due to sloshing, a series of baffles is installed. In each of the sections, seven baffles (**QTR-DRP-04**) are placed with a spacing of one metre. The baffles connect to the centre and outer walls of the sections thus creating seven separate sections which shall reduce the freedom of movement of the tank contents. Almost none of the baffles reach either the bottom or the top of the tank since at the bottom, water must be able to flow to the doors and should thus allow for fast, and free flow. At the top, a small gap is left to allow for the installation of a single overflow/vent channel. If this gap is not present, an area of high-pressure air would build up in the different compartments thus preventing the tank from filling up completely. The centre baffles do constrain the water at the bottom fully. This is done so that while flying with less than a full tank, not all the water is shifted back during pull-up manoeuvres. The exact shift in the centre of gravity for differing tank contents and pitch angles is too complicated to model and analyse within the time frame of this project.

The internal baffle configuration is shown in Figure 8.6.

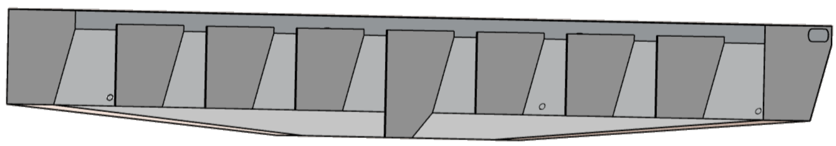

Figure 8.6: *Internal view of one of the tank sections showing internal baffles.*

Refilling, Foam injection and Dropping
Each of the two sections shall contain two filling ports that connect to the snorkel. These ports shall be located on the sides of the tank so that the two semi-separated parts of each of the tanks receive water flow. These ports shall also be connected to an external refilling port for on-the-ground refilling satisfying thus requirements **QTR-TNK-03** and **QTR-TNK-04**. On the rearward-facing panel of each section, an overflow/vent channel is present to purge the overflow of water and to allow air in the tank to vent during filling (**QTR-

TNK-05). The sides of the tanks shall be installed with sensors to monitor the water level. On the sides of each section, tubing is present to inject foam concentrate into the tank which can be injected by the pilot(s) prior to a drop. These tubes are connected to a 500 L concentrate tank placed in front of the main water tank satisfying requirement **QTR-TNK-02**.

The maximum drop rate of the tank can be estimated by making use of Torricelli's law as stated by Equation 8.1 where v is the water flow velocity, g is the gravitational acceleration, h is the height differential between the surface of the water and the exit. and A_d/A_t is the area ratio between the opening and the surface area of the water surface in the tank. Since the volume exiting the tank (dV) is equal to the reduction in the tank, Equation 8.2 can be set up which relates a change in tank water height (dh) to a change in time (dt). Rewriting Equation 8.2 for dh, this equation can be used to discretely model the system to find out how long it will take for the tank to drain.

$$v = \sqrt{\frac{2gh}{1 - A_d^2/A_t^2}} \tag{8.1}$$

$$dV = \dot{m}dt = A_t v dt = A_t\sqrt{\frac{2gh}{1 - A_d^2/A_t^2}} = A_t dh \tag{8.2}$$

Modelling this system where the tank area changes over the height of the tank which is assumed to vary linearly with the three different gradient zones: 0 m<=h<=0.2 m, 0.2 m<h<=0.8 m and 0.8 m<h<=0.95 m. After running this simulation, the water tank height of 0 m (empty) is reached after t_e 2.5 s. In order to establish the average water coverage per distance covered per second, Equation 8.3 can be set up by dividing the total mass of water dropped by the distance covered in that time and by applying a conservative drop loss factor of 0.7 [38].

$$\frac{V}{d \cdot t} = \frac{\dot{m}/\rho t_e}{v_{\text{flight}} t_e t_e} 0.7 = \frac{A_d \overline{v}_{fl}}{v_{\text{flight}} t_e} 0.7 \tag{8.3}$$

Averaging the water exit velocity over the modelled data points and inputting this into Equation 8.3 along with the (maximum) exit area: $A_d = 0.7448\,\text{m}^2$ and converting to litres, yields the dropped water volume per second at different flight speeds and door deploymenys as displayed in Figure 8.7. For intense fires, a water volume of $0.10\,\text{Ls}^{-1}\text{m}^{-2}$ is required to effectively fight it [39]. From the figure, it can be seen that even at speeds far exceeding the drop speed regime of 85-150 kph as specified in Section 5.1, the volume per second per meter is far more sufficient than required. This means that by varying the door deployment, a large range of effective water lines can be produced.

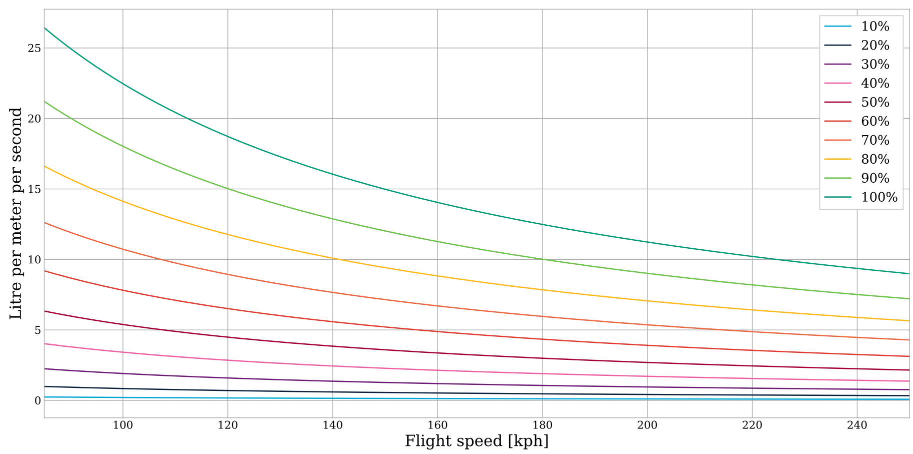

Figure 8.7: *The volume of water (L) dropped per meter travelled over a range of speeds.*

Material and Coating
The water tank will be made of AL-2195 which -of itself- is the most corrosion-resistant aluminium considered. The inside surfaces will then be coated to provide the water tank with excellent corrosion resistance even to salt water and foam concentrate. The surfaces shall receive the same treatment as the Canadair CL-415[4]; Firstly, sulphuric acid anodising leaves a thin layer of aluminium oxides which protects the surface from corrosion. Next, an epoxy primer is applied which prevents the retardant from reacting with the metal. Finally, an additional layer of Polyurethane topcoat is applied which adds an additional and final protective layer which also increases visibility for inspections. This treatment of the tank ultimately provides the water tank with excellent corrosion protection adhering to requirements **QTR-TNK-07**, **QTR-TNK-08** and **QTR-TNK-09**. Finally, the tank shall contain access hatches on top which shall allow for maintenance and inspection from within the aircraft (**QTR-TNK-10**). The choice of aluminium, also means that while operating in hot conditions, the heat is transferred quite effectively to the water carried inside. This means that during the short durations that the aircraft will operate in this regime, the water will heat up before allowing the material to fail (**QTR-TNK-06**). A full heat convection analysis was not possible within the time frame of the project.

Tank Structure and Mass
The water tank must be able to carry a large amount of water which induces hydrostatic loads in the tank. It is therefore important to ensure that the water tank will be able to carry those loads without failure. The hydrostatic load of a liquid is determined by Equation 8.4 where ρ, h and g are the liquid density, height and gravitational acceleration respectively. Since the aircraft must be able to operate in a loading regime between -1 and +3.25 g (**FTF-SYS-FDS-05.15**), an analysis must be performed of the most critical cases for different parts of the tank. The sizing for plate thickness is split into four parts: the central partition plate, the dropping door plate, the top plate and finally the rest of the assembly. The choice was made to have the complex geometry of the side and bottom walls made from the same thickness sheets to reduce manufacturing complexity. The partition and the plate are mounted perpendicular to all other plates and thus do not suffer from these problems.

$$P = \rho h g \tag{8.4}$$

First, an analysis was performed using Equation 8.4 where g was multiplied with the load factor to determine the maximum pressure load over the height of the tank. The resulting plot is shown in Figure 8.8 where 0 is at the very top of the tank. This shows that for all plates except for the top plate, the extreme case is during +3.25 g manoeuvres while the top plate must be designed for -1 g manoeuvres. The plate thickness of the complex geometry is therefore governed by the bottom plates.

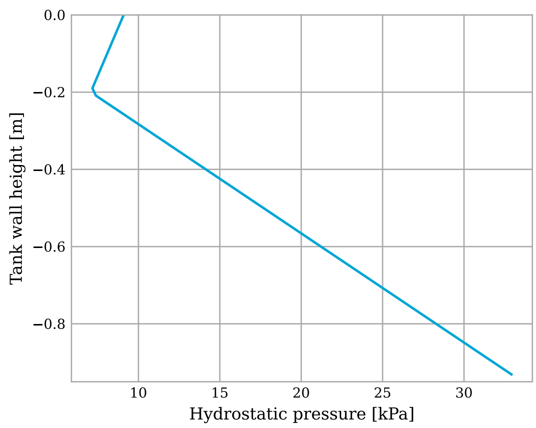

Figure 8.8: *Maximum hydrostatic pressure during aircraft operation over the tank height.*

For the determination of the thickness, standard solutions from Roark's Formulas for Stress and Strain [40] are used. All plates are assumed to be rectangles which fully fit the actual plates, fixed at all edges. The assumption of larger plates yields an overestimation of the ultimate stresses thus adding a margin of safety. The

[4] Link [cited on 06-06-2024]

central partition experiences a linearly decreasing distributed load while the top and bottom plates experience a constant distributed load. The bottom plate of the complex section, although slightly slanted, is also assumed to experience an unvarying load with a magnitude equal to the maximum pressure. The equation for determining the maximum stresses is given by Equation 8.5, where σ_{max} is the maximum stress experienced by the plate, β_1 is a constant which is reliant on the width-height ratio of the plate, q is the (maximum) magnitude of the load, b is the height of the plate and t is the plate thickness. Substituting σ_{max} with the yield stress of the material (σ_y), rewriting the equation for t, substituting Equation 8.4 for q and multiplying the load factor n by a safety factor of 1.5 yields Equation 8.6

$$\sigma_{max} = \frac{\beta_1 q b^2}{t^2} \quad (8.5) \qquad\qquad t = \sqrt{\frac{\beta_1 1.5 n g h_{\text{tank}} \rho b^2}{\sigma_y}} \quad (8.6)$$

The value for β_1 is given for the different loading cases and for the density, the average density of seawater is taken[5] as 1030 kg/m^3. The case-specific input parameters and the resulting thickness for each of the four sizings are tabulated in Table 8.9. The thicknesses were computed using an average yield stress (σ_y) of 549 MPa and a tank height of 0.95 m.

Table 8.9: *Input parameters and the calculated thickness of the panel thickness for each tank section.*

Parameter	partition	door	top	complex
β_1 [-]	0.3068	0.5	0.5	0.5
n [-]	+3.5	+3.5	-1	+3.5
b [m]	0.95	0.38	1	0.36
Thickness [mm]	5.0	2.5	3.6	2.4

With these values for the plate thicknesses, the total mass of the water tank comes down to 735 kg. This mass does not include any of the integrated systems such as the hosing, vent port, hydraulics or the foam concentrate tank.

Avionics

Contributor / Author: Ishan

Table 8.10: *Avionic subsystem requirements.*

Identifier	Parent	Subsystem Requirements
QTR-AVI-01	FTF-SYS-FDS-01.2	The avionics shall include monitoring of retardant level.
QTR-AVI-02	FTF-SYS-FDS-05.9/FTF-SYS-FDS-05.10	The avionics shall include a targeting system for resource drops.
QTR-AVI-03	FTF-SYS-FDS-05.9 / FTF-SYS-FDS-05.10	The avionics shall include a targeting system for retardant drops.
QTR-AVI-04	FTF-SYS-FDS-07.1	The avionics shall include an ice warning system.
QTR-AVI-05	FTF-SYS-FDS-07.1	The avionics shall include a temperature monitoring system.
QTR-AVI-06	FTF-SYS-REG-01.10	The avionics system shall inform the crew about any systems not functioning properly.
QTR-AVI-07	FTF-SYS-FDS-08.1	The avionics shall include a night vision system for the pilots.
QTR-AVI-08	FTF-SYS-FDS-09.1	The avionics shall be able to display LiDAR information.
QTR-AVI-09	FTF-SYS-FDS-09.1	The avionics shall display ADS-B in capabilities to give pilots better situational awareness of the airspace.
QTR-AVI-10	FTF-SYS-SUP-01.3	The avionics shall be off-the-shelf solutions.

Continued on next page

[5] Link [cited on 04-06-2024]

Table 8.10 – continued from previous page

Identifier	Parent	Subsystem Requirements
QTR-AVI-11	FTF-SYS-PIL-03.2	The avionics shall use standard well-known display methods.
QTR-AVI-12	FTF-SYS-PIL-04.2	Shall include Flight Data Recorder (FDR).
QTR-AVI-13	FTF-SYS-PIL-04.2	Shall include Cockpit Voice Recorder (CVR).
QTR-AVI-14	FTF-SYS-PIL-01.3	The aircraft shall be equipped with an ILS system.
QTR-AVI-15	FTF-SYS-PIL-01.2	The avionics shall include an airspeed indicator.
QTR-AVI-16	FTF-SYS-PIL-01.2	The avionics shall include an altimeter.
QTR-AVI-17	FTF-SYS-PIL-01.2	The avionics shall include a magnetic direction indicator.
QTR-AVI-18	FTF-SYS-PIL-01.2	The avionics shall include an Internal Turbine temperature (ITT) gauge for each engine.
QTR-AVI-19	FTF-SYS-PIL-01.2	The avionics shall include a landing gear position indicator.
QTR-AVI-20	FTF-SYS-PIL-01.2	The avionics shall include an Angle of Attack indicator.
QTR-AVI-21	FTF-SYS-PIL-01.2	The avionics shall include turn coordinator.
QTR-AVI-22	FTF-SYS-PIL-01.2	The avionics shall include a clock displaying hours, minutes and seconds.
QTR-AVI-23	FTF-SYS-PIL-01.2	The avionics shall include an attitude indicator.
QTR-AVI-24	FTF-SYS-PIL-01.2	The avionics shall include a heading indicator.
QTR-AVI-25	FTF-SYS-PIL-01.2	The avionics shall include a vertical speed indicator.
QTR-AVI-26	FTF-SYS-PIL-01.2	The avionics shall include GPS navigation.
QTR-AVI-27	FTF-SYS-PIL-01.2	The avoinics shall include a VHF system.
QTR-AVI-28	FTF-SYS-PIL-01.2	The avionics shall include an oil pressure gauge for each engine.
QTR-AVI-29	FTF-SYS-PIL-01.2	The avionics shall include gas generator speed for each engine.
QTR-AVI-30	FTF-SYS-PIL-01.2	The avionics shall include an oil temperature gauge for each engine (air cooled).
QTR-AVI-31	FTF-SYS-PIL-01.2	The avionics shall include an RPM gauge for each engine.
QTR-AVI-32	FTF-SYS-PIL-01.2	The avionics shall include a fuel gauge indicator for the quantity of fuel in each fuel tank.
QTR-AVI-33	FTF-SYS-PIL-01.2	The avionics shall include a torque percentage indicator for each engine.
QTR-AVI-34	FTF-SYS-PIL-01.2	The aircraft shall contain a set of circuit breakers for each electrical system.
QTR-AVI-35	FTF-SYS-PIL-01.2	The aircraft shall be equipped with a navigation display (ND).
QTR-AVI-36	FTF-SYS-PIL-01.2	The avionics shall be able to load a flight plan.
QTR-AVI-37	FTF-SYS-PIL-01.2	The autopilot shall be able to follow a flight plan.
QTR-AVI-38	FTF-SYS-FDS-06.4	Avionics shall be modular for easy maintenance.
QTR-AVI-39	FTF-SYS-REG-02.10	The avionics systems shall be installed according to the installation manual.

The cockpit layout is a vital part of the design, shown in Figure 8.9, as it relates to pilot comfort. It was decided to implement an off-the-shelf avionics display as stated in requirement **QTR-AVI-10**, namely the Garmin G1000 system [6]. This system consists in 3 digital displays: two Primary Flight Displays (PFD), located in front of both pilots' fields of view and one Multi-functional Flight Display (MFD) located between the two PFDs. Additionally, two Flight Management (FMS) interfaces are present for each pilot. These serve as the main input point for pilots to enter performance data, flight plans, navigation, radio communication frequencies and approach procedures.

[6] Link [cited on 18-06-2024]

Figure 8.9: *Cockpit design and layout including flight controls.*

There are some novel functions which have been added to the MFD display mode which are mission-specific. Firstly, the MFD can display LiDAR data and information as well as night vision, which are specified in requirements **QTR-AVI-08** and **QTR-AVI-07** respectively. Secondly, the MFD also displays a targeting system for resources and water/retardant, as specified by requirements **QTR-AVI-02** and **QTR-AVI-03** respectively. Lastly, the MFD also constantly displays the water tank level as well as the selected drop door position in order for the pilot to control the water drop rate. Another addition which has not yet been implemented in the cockpit but certainly can be done in future iterations is display pilot health monitoring. Monitoring of oxygen concentration levels in blood, heart rate, sweat rate and other metrics could certainly help with regard to safety. Lastly, a pilots from the Croatian firefighting squadron provided feedback on this cockpit layout. His main points were regarding the engine parameter display. During firefighting operations, monitoring engine performance is vital and therefore creating a separate display only for engine parameters is an option which can be explored for future design iterations.

Communications System

Contributor / Author: Johannes

Table 8.11: *Communication subsystem requirements.*

Identifier	Parent	Subsystem Requirement
QTR-COM-01	FTF-SYS-FDS-05.8	The aircraft shall have a PA/intercom system to enable communication between pilots and cargo bay.
QTR-COM-02	FTF-SYS-FDS-07.1	Antennas shall be equipped with anti-ice systems to prevent signal disruption during icy conditions.
QTR-COM-03	FTF-SYS-FDS-07.1	The aircraft shall include an Emergency Locator Transmitter (ELT).
QTR-COM-04	FTF-SYS-INV-02.2	The aircraft shall have an ELT detection system.
QTR-COM-05	FTF-SYS-GFC-01.1	The aircraft shall be equipped with VHF (8.33/25 HZ) radio communication.
QTR-COM-06	FTF-SYS-GFC-01.1	The aircraft shall be equipped with UHF radio communication.
QTR-COM-07	FTF-SYS-GFC-01.1 / FTF-SYS-ATC-01.2	The aircraft shall be equipped with ACARS.
QTR-COM-08	FTF-SYS-GFC-01.1 / FTF-SYS-ATC-01.2	The aircraft shall be equipped with CPDLC.
QTR-COM-09	FTF-SYS-ATC-01.2	The aircraft shall be equipped with SATCOM.
QTR-COM-10	FTF-SYS-ATC-02.2	The aircraft shall be equipped with ADS-B out transponder.
QTR-COM-11	FTF-SYS-ATC-02.2	The aircraft shall be equipped with ADS-B in the receiver.
QTR-COM-12	FTF-SYS-PIL-01.2	The aircraft shall be equipped with position lights.
QTR-COM-13	FTF-SYS-PIL-01.2	The aircraft shall be equipped with anticollision lights.
QTR-COM-14	FTF-SYS-PIL-01.2	The aircraft shall have at least one landing light.

Due to regulations from aviation authorities regarding the communication system, some communications systems are required to be on the aircraft. The determination of these systems is based on requirements from EASA's Easy Access Rules for Airborne Communications, Navigation and Surveillance manual (CS-ACNS)[41] and FAA's General Operating and Flight Rules (CFR part 91)[42]. These two documents specifically detail operating requirements for aircraft to be airworthy, including the communication requirements. It has been decided that the following communication systems are necessary to adhere to aviation regulations:

- **Dual VHF (Very High Frequency) Radio – Voice (8.33KHz/25KHz)**
  The standard voice communication system in aviation. Used for communication with ATC.
- **Emergency Locator Transmitter 406MHz**
- **ADS-B out**
  "ADS-B out" works by transmitting flight information through the transponder such as GPS location, speed, vertical speed, altitude, sqwak code and other data to other aircraft and ATC.
- **SATCOM (Satellite Communication) datalink and voice: Inmarsat(FSS) or Iridium(MSS)**
  SATCOM is used when the aircraft is in an area with no radio coverage. Inmarsat works on FSS and uses geostationary satellites to communicate. Iridium works on MSS and uses LEO satellites to communicate. Inmarsat is the most commonly used SATCOM in aviation, however, it does not have cover in the extreme polar regions. For this reason, Iridium is recommended for operations in polar regions.

In addition to the required communication systems it is necessary to look at the mission requirements to realise if additional communication systems are necessary. It has been decided that the following communication systems will be needed during missions:

- **ADS-B in**
  "ADS-B in" allows for the aircraft to receive ADS-B signals transmitted by other aircraft. This gives improved situational awareness to the pilots which is beneficial during missions. Additionally, ADS-B is essential for the traffic collision avoidance system (TCAS) to work.
- **UHF radio**
  UHF (Ultra High Frequency) radio has a shorter range than VHF radio but works better in terrain with a lot of obstacles. This can be a benefit when having to communicate with ground crew in mountainous

terrain or forests.

- **Trunked radio system**
  A trunked radio system is an efficient radio communication system that among other things allows for group communication. This form of communication is already being used in aerial firefighting in Europe to communicate with the ground crew using the system called TETRA[43]
- **ACARS**
  ACARS is a datalink system that allows for short bursts of data to be sent and received. This is limited to a few lines of text. It operates on both VHF radio and satellite.
- **CPDLC**
  CPDLC allows for the aircraft to receive flight instructions that only need to be accepted by the pilot. Thus no voice communication is needed for ATC instructions during the cruise. This is useful as it allows the pilots to spend valuable time on other tasks while travelling to the operation site.
- **Intercom**
  An intercom allows the pilot to communicate with the rest of the crew inside the aircraft. This can be useful in many scenarios such as search and rescue, deployment of ground firefighters etc.

8.1.1. Final Layout of the FireFly

Contributor / Author: Johannes

Upon completion of the subsystem design the final configuration of the FireFly can be modelled. This is done using the 3DEXPERIENCE platform. This section describes the main challenges and design choices made when integrating the individual subsystems in the final configuration.

In Figure 8.10 a front view of the FireFly in hover mode can be seen. It contains dimensions already presented in the previous chapter mainly related to the width of different parts of the aircraft, such as wingspan and fuselage width. It also contains dimensions not yet discussed, specifically the nacelle width and total width of the aircraft measured from the propeller tips. The nacelle has been sized based on an estimate of the total engine size derived from the size of the AE1107F turboshaft and a gearbox of similar size. The engine nacelles have dimensions of roughly: 3.15 x 2.1 x 1.3 m. They are designed such that the turboshaft is positioned at the bottom and the gearbox at the top. This allows for the propeller to be in line with the chord of the wing and the air inlet to be below the wing.

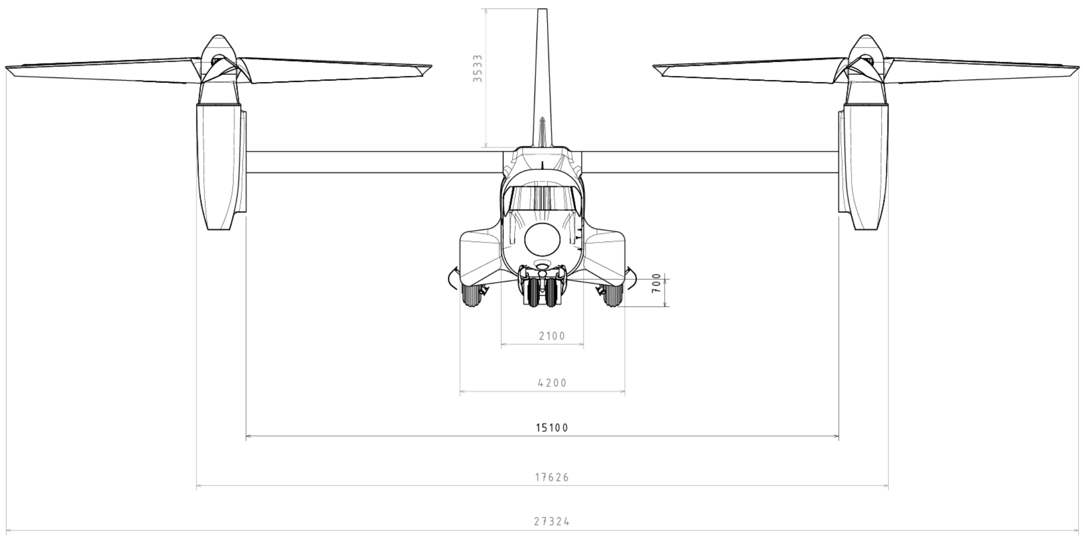

Figure 8.10: *Drawing Front View - Vertical Flight.*

In Figure 8.11 a side view of the FireFly in a typical ground configuration can be seen. From this view it is very clear that due to the high floor level of the aircraft, the loading ramp at the rear of the aircraft needs to be long to not be too steep. The ramp itself is approximately two times as long as the cargo door. For this reason, a telescopic design was adopted in which the ramp first rotates to open and then extrudes 3 m to reach the ground.

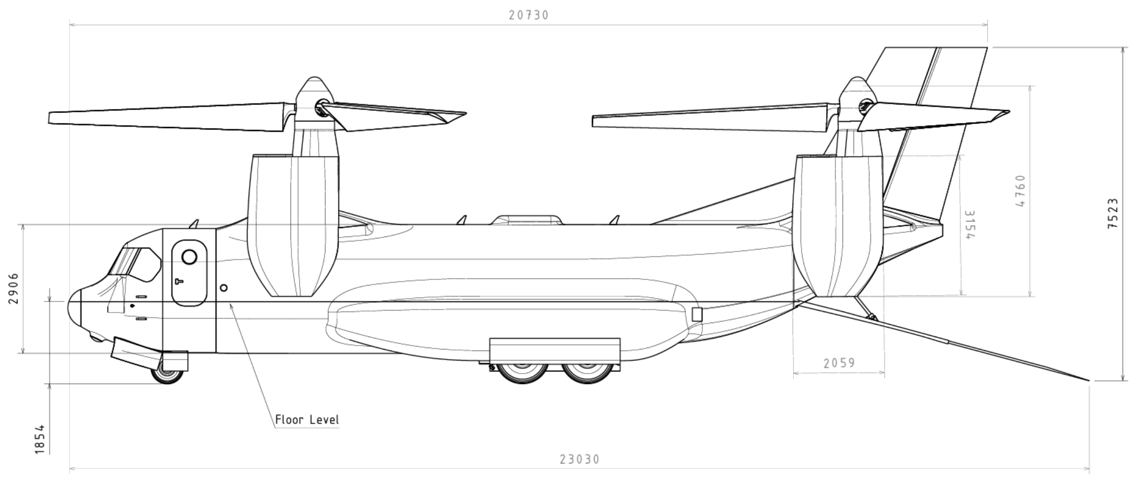

Figure 8.11: *Drawing Side View - Vertical Flight (Dimensions in mm).*

Figure 8.12 shows the top view of the FireFly during hover mode. The most interesting aspect of this drawing is the spacing between the rotors and the fuselage. It can be seen that the rotor distance from the fuselage is 1.2 m. The distance from the front rotor to the rear rotor is only 26 cm which was decided as this is similar to the distance between the V22 osprey rotors and fuselage. It has not been explored exactly what the implications of having the propellers this close is.

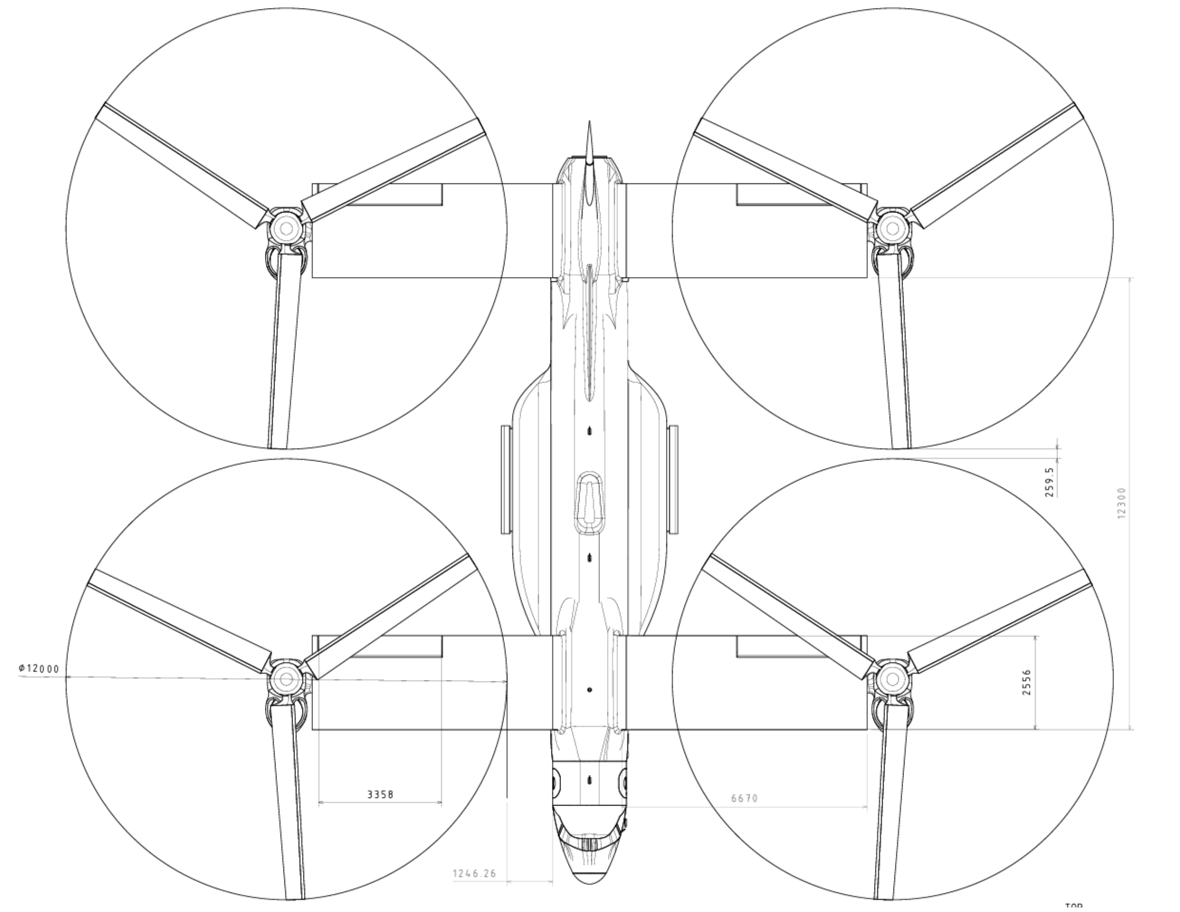

Figure 8.12: *Drawing Top View - Vertical Flight (Dimensions in mm).*

A front view of the FireFly in forward flight mode can be seen in Figure 8.13. This drawing serves mainly to show the distance between the rotors and the fuselage.

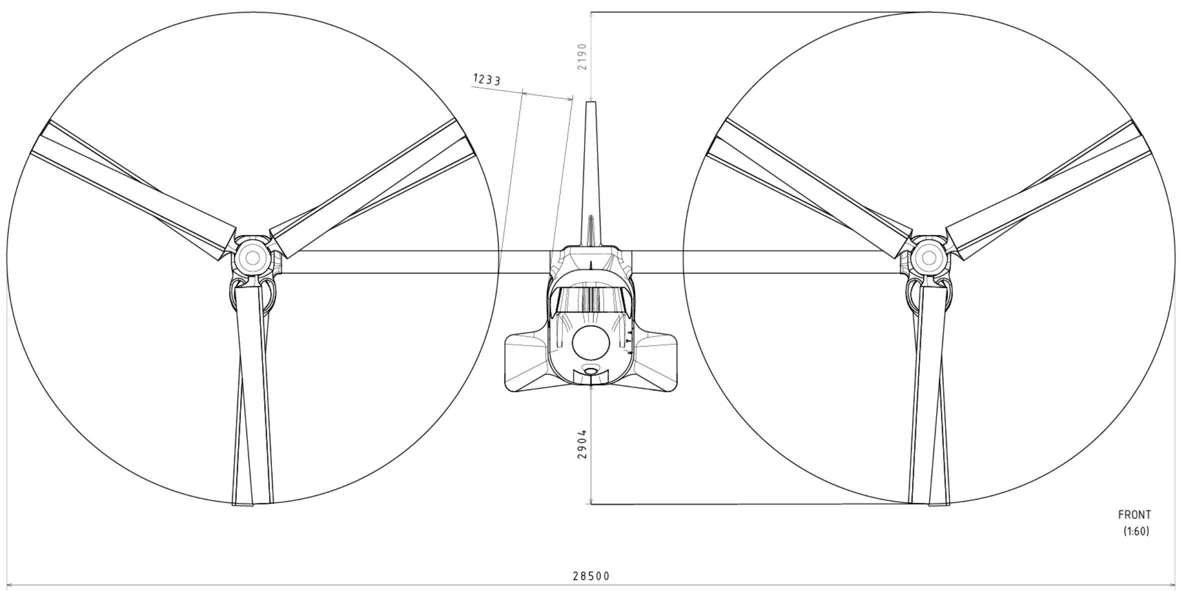

Figure 8.13: *Drawing Top View - Forward Flight (Dimensions in mm).*

based on the previous drawings it can be concluded that the subsystems designed can all be integrated in a realistic way to form a sensible aircraft configuration.

Finally, a render has been made, presented in Figure 8.14, to show the FireFly in a typical ground configuration with landing gear deployed, landing lights on, ramp extended and engines in vertical position.

Figure 8.14: *Render of FireFly in Ground Configuration.*

8.2. Interactions Between Subsystem Hardware

Contributors: Ishan, Hanna, Caitlin, Sven. Authors: Ishan

The hardware (H/W) of the system is visualised in a block diagram in order to get an overview of the components in the aircraft. The purpose of this diagram is to gain an understanding of all high-level hardware components required for each subsystem and how they interrelate with each other. This diagram is somewhat linked to the N2 chart which displays dependencies between subsystems.

The most important conclusion that can be extracted from this diagram is the fact that FMC and DMC are central computers and manage almost all incoming data. Therefore, there should be redundancies in the number of them as well as the location to mitigate the risks of such a failure.

There are many hardware components for each subsystem, however, only the ones which are deemed most important are displayed in Figure 8.15. All subsystems are colour-coded as indicated in the legend. The figure displays 11 subsystems:

Avionics Subsystem

The FMS is the central piece of hardware for the avionics to function properly. Its primary function is to receive, manage and manipulate data from one subsystem and re-direct it to another once it is in its correct form. For example, it manages all the data incoming from the Air Data Inertial Reference Unit (ADIRU) such as pressure, temperature and angle of attack. It then transfers the relevant data to the Display Management Computer (DMC) for cockpit display. All navigation data is transferred to the FMC via the Very High-Frequency Omnidirectional Range (VOR) and GPS antennas. The Instrument Landing System (ILS) also relays its data to the FMC which is later used in the flight control subsystem's autopilot (AP). Lastly, the FMC is also connected to the Electronic Engine Controller (EEC) from the propulsion subsystem.

Flight Controls Subsystem

The Primary Flight Computer (PFC) is also connected to the FMC. The PFC takes its relevant data from the FMC and calculates the required flight control deflections based either on pilot control input or AP input. If the input comes from the pilot, the PFC shares the intended action to the Power Control Unit, which itself

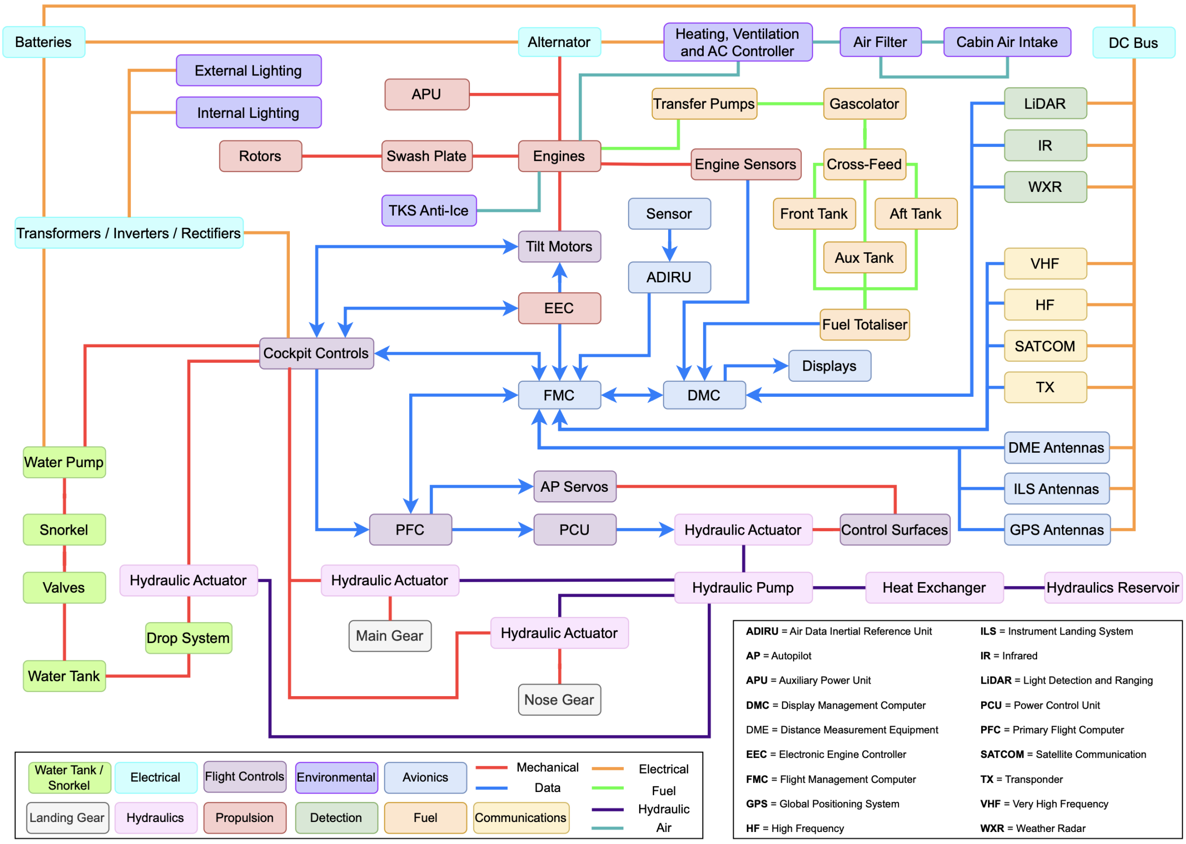

Figure 8.15: *Hardware block diagram showing the interrelation between high-level components of subsystems.*

calculates the power to be delivered to the hydraulic actuator to ensure the proper deflection of the control surface. However, if the input comes from the AP system, the PFC shares the intended action with the AP servos which itself deflects the required control surface by the correct amount.

Propulsion Subsystem

The EEC interacts with the FMC and is the central part of the propulsion system. All control inputs going to the engines go through this controller. This controller also dictates the amount of fuel required for each engine. It also manages all data originating from the engine sensors, ITT, Gas Generator Speed, Exhaust Gas Temperature, oil temperature and fuel pressure. The engines themselves are connected to a swash plate, which is used to control the pitch angle of the rotor blades. The Auxiliary Power Unit (APU) is a separate turbine used to start the engines and potentially power other subsystems through the alternator.

Electrical Subsystem

The alternator is a component which converts mechanical energy from the engines or APU to electrical energy to power all electronic systems. It is directly connected to the batteries which store this electrical energy. The batteries are connected to the transformers/inverters/rectifier which manipulate the current and voltage to power all on-board electronics. Furthermore, the water pump is electrically powered and therefore also requires electrical energy. The detection system, communication system and avionic antennas are all connected to the Direct Current (DC) bus.

Communication Subsystem

The communication subsystem uses 3 main receivers: VHF, HF and SATCOM. These all receive and transmit data and are managed by the FMC. HF is used for long-range communication. VHF is the system which is used most often for communication with ATC and ground fire fighting crew. SATCOM is used to transfer information using for example the Controller Pilot Data Link Communication (CPDLC) protocol.

Water Tank and Snorkel Subsystem

The water tank (which can also accommodate retardant) and snorkel subsystem is connected directly to electric power in order for the electric water pump to be functional. The snorkel is connected to a valve system which opens and closes to regulate the refill rate. The tank itself contains a drop system which is operated by a hydraulic actuator through cockpit controls.

Hydraulics Subsystem

The hydraulic subsystem contains mainly a hydraulic fluid reservoir with lines dispersing to actuators for other relevant subsystems. The hydraulic pressure is achieved using a hydraulic pump. A heat exchanger is also required to keep the hydraulic fluid at the optimum temperature given that the aircraft is going to be exposed to extreme heat (from flying close to fires) and cold (from cruising at high altitude).

Fuel Subsystem

The fuel system contains 3 main fuel tanks: the front wing tank, the aft wing tank and an auxiliary tank placed in the fuselage. Fuel lines directly feed this fuel into the engines. In order for the tanks to maintain pressure, transfer pumps are connected to the fuel lines. Their purpose is also to transfer fuel between different tanks using the cross-feed system. Lastly, a fuel tank level sensor is present in each tank, and a fuel totaliser sums the amount of fuel remaining in each tank. It directly sends the quantity to the DMC.

Detection Subsystem

The detection subsystem is used to keep the pilots situationally aware. LiDAR helps map the terrain, providing useful information for when the pilots are flying at low altitudes during fire suppressant drops. IR cameras read heat signatures and display them to pilots to indicate where the hottest part of the wildfires are. Lastly, the weather radar displays information about precipitation, lightning and general storm activity and intensity. All of the detection subsystem components send data to the DMC, which itself manipulates it and displays it on cockpit displays.

Environmental Subsystem

The Environmental Control System is mainly used to regulate the cabin air quality and temperature. It was decided that the pressurisation system would not be implemented. Firstly ,the cruise altitude will remain below 10000 ft and for commercial aircraft it is still considered as an altitude not requiring pressurisation for the crew's safety and comfort. Secondly, implementing the pressurisation system would significantly complicate the design from a structure standpoint. [7]. For crew safety, an emergency oxygen system will be installed. According to regulations, in unpressurised aircraft cruising at an altitude of 14000 ft and above, oxygen is mandatory at all times. The anti-icing system is going to use the TKS anti-icing system. The system uses the bleed air from the engines and sprays a de-icing fluid to break the bonds between the ice and structure on the ice-sensitive areas.

Landing Gear Subsystem

The landing gear subsystem is actuated solely using the hydraulics subsystem. Two separate actuators are used to deploy the main landing gear and the nose landing gear. Obviously, this is controlled by the pilots which is why the actuator interacts mechanically with the cockpit controls.

8.3. Interactions Between Subsystem Software

Contributor / Author: Ishan

A software (S/W) diagram is needed to provide instructions to the hardware components. There are some major takeaways from this diagram. Firstly, one can identify how central the FMS is. This system's software manages almost all incoming data, manipulates it, and sends it to the relevant subsystem software or component. A failure of this would be catastrophic, meaning redundancy is absolutely key for this part of the software. Secondly, it is interesting to note the interactions between each system. Some systems require constant feedback (such as the autopilot software), meaning data constantly flows to and from this software, while others only require input (such as the tank deployment software).

After having created such a diagram, it is imperative to adapt the design. As previously stated, a key conclu-

[7] Link [cited on 05-06-2024]

sion is that the FMS is central and therefore needs redundancy. To address this, the cockpit will be outfitted with two independent (yet linked in terms of the input data) FMS and displays. Each pilot will have its own FMS and therefore FMC. Such a design ensures the aircraft can still perfectly operate on one FMS and carry out its mission. Additionally, software constantly cross-checking the two FMSs for discrepancies will be present to avoid displaying false information and raise a master caution if this is the case. This diagram also helps to identify risks (as the one stated above) and therefore can be appended to the risk analysis table. The approach to the software diagram is as follows: assign software that manages each subsystem or

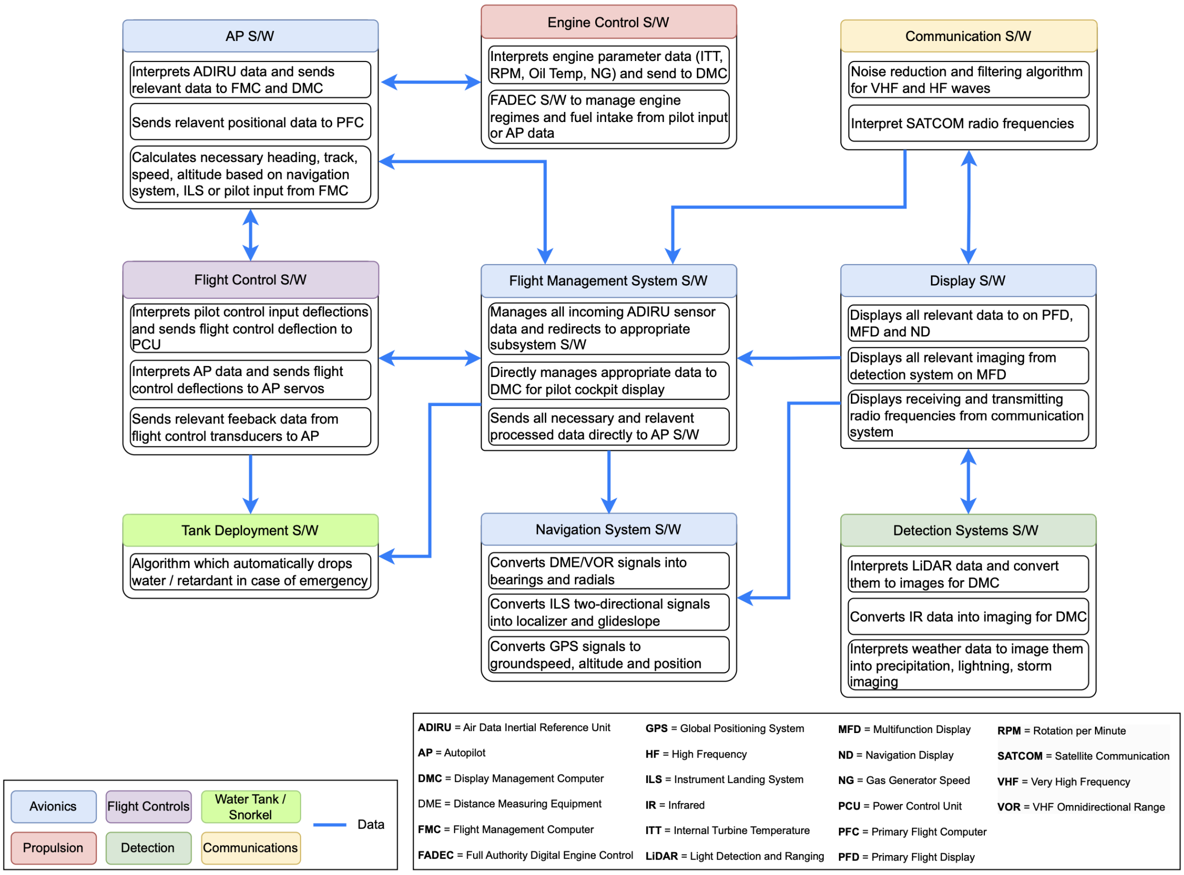

Figure 8.16: *Software block diagram showing the interrelation between different software managing subsystems.*

major component and interlink each software based on the relevant input/output data required. Generally, the software for each subsystem manipulates, interprets and converts the necessary data from its respective inputs (sensors or feedback data). A simple example of this would be interpreting pitot tube data. This sensor measures the dynamic pressure and the total pressure. However, this data is not displayed to pilots. Instead, the FMS interprets this data and calculates an indicated airspeed. Therefore, software is required to perform this calculation. Figure 8.16 shows how this software interacts with each other and the major functions that they perform.

8.4. Data Handling and Flow Between Subsystems and Components

Contributor/Author: Ishan

The data handling block diagram shows how and where the data flows through the aircraft system.The purpose of Figure 8.17 is to understand the various types of data and where they are being processed. There is one interesting conclusion which can be drawn from this diagram: the data flow between the FMC and DMC is crucial. The pilots are able to monitor and make decisions based on data flowing back and forth between the FMC and DMC. If this link breaks, the pilots will simply have manual control of the aircraft but nothing else. All information which is displayed to the pilots would be nonexistent. To remedy this, a design choice is made. The FMC-DMC link will be redundant in the sense that multiple independent data lines will be present. The following approach to Figure 8.17 is used; Each sensor is investigated to understand what type

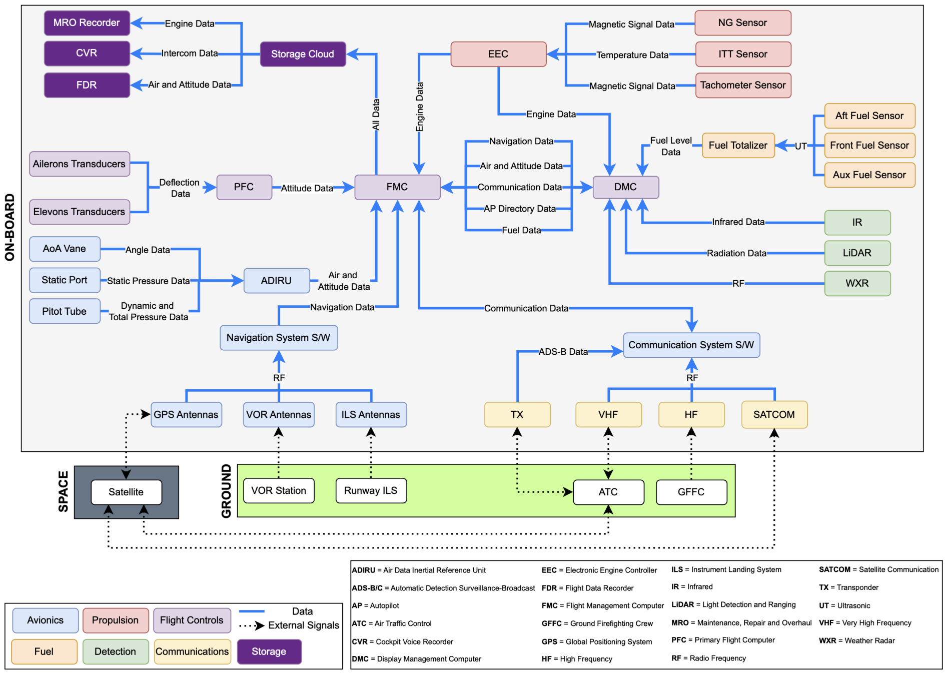

Figure 8.17: *Data handling diagram showing the interrelations and data types between all subsystems.*

of signal or data it receives and transmits. Then, data packages are created from the relevant subsystem before merging mainly into the DMC and FMC. A data package is, for example, the "communication data" or the "navigation data".

In terms of data handling, a storage unit in the form of a storage cloud is present and connected to the FMC. From the storage cloud, engine data is stored in the Maintenance, Repair and Overhaul (MRO) recorder. This helps the maintenance crew on the airbase to perform targeted maintenance, and make adjustments to aircraft to prevent failures or long-term grounding.

8.5. Electrical Block Diagram

Contributors: Nino, Thijs. Authors: Thijs

In order to have reliable electrical power availability on the aircraft, power will be generated by multiple generators. Each of the turboshaft engines mounted on the aircraft will be connected to an alternating current (AC) generator. An additional AC generator shall be connected to the auxiliary power unit for startup power. An external power port shall be present to supply the aircraft with AC ground power when on the ground. The AC current from the generator and ground power feeds into a Transformer Rectifier Unit (TRU) and an AC Power Distribution Unit (PDU).

The TRU converts AC to DC power which is used to supply charge to the batteries which will be able to power the essential electrical systems in case of total power system failure. The TRU and the batteries feed into the DC PDU which supplies current to DC busses 1 and 2. These buses control the energy supply to their respective systems. The AC current from the generators that feed directly into the AC PDU is similarly fed to DC busses 1 and 2 which feed into their respective systems.

In case of a complete power system failure, the batteries will supply DC power directly through the DC PDU and will convert DC to AC through an inverter ensuring that a full range of power is available. The relations of each system are displayed schematically in Figure 8.18.

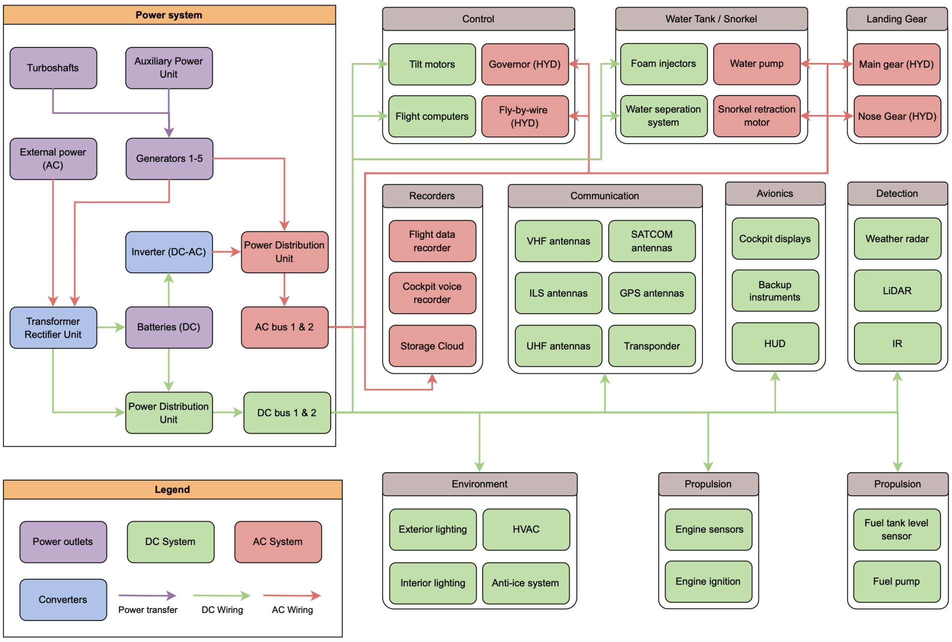

Figure 8.18: *Electronics block diagram.*

The specifics of each system are not yet known and will be elaborated upon in a later design stage. The electrical architecture, however, is constructed so that once the voltage and power requirements of the systems are known, specific generator, inverter, TFU and PDU design can be performed.

Power System

The power system consists of the power outlets, converters and wiring.

- **Power sources** are the sources of the power running the aircraft. This includes the power tap, which is the main source of power in both configurations. It will tap power from the engines and feed power into the rest of the aircraft. Through a transformer, it can power the batteries and the DC systems of the aircraft. The batteries will be a power source if the engines are not running. The power will flow into the DC systems and through an inverter to go to the AC systems. The ram air turbine will be an emergency power source that can be extended out of the fuselage when necessary. It will produce an AC that can power the batteries and other systems in the same way the power tap can.
- **The converters** will convert AC into DC and vice-versa. This is important when power has to go directly from the power tap or ram air turbine into the DC systems or from the battery directly into the AC systems.
- **Wiring** will take the power from the sources to the systems that need it. The aircraft will have separate wiring for AC and DC currents. A further subdivision into high-voltage and low-voltage wiring will also be necessary when designing the electrical systems, however, this is beyond the scope of this report.

Additionally, an APU must be present, especially to provide initial power for engine start up. Since the aircraft uses almost the same engines as the V-22 Osprey (same model but more modern variant), a similar APU can be used. The V-22 uses a 300 HP APU, however, fewer hydraulic and electric systems are on-board of it compared to the FireFly. Therefore, a slightly higher power rating is required from the APU. This is why the Honeywell RE220 [8] APU is chosen. This specific APU also provides bleed air which is required for the internal cabin environment.

DC Systems

The DC system usually operates on low voltages and is therefore mostly used in smaller components. Furthermore, components that require high reliability are usually connected to the aircraft's DC system. A more detailed description of the subsystems using DC power can be found below:

[8] Link [cited on 18-06-2024]

- **Monitoring Systems** is responsible for all detection and monitoring of the aircraft fluid levels. This includes oil pressure, oil level, fuel level etc. In the case of a firefighting aircraft, the monitoring system will also be responsible for the measurement of water/retardant in the tank.
- **External sensors** refers to all probes that are mounted externally on the aircraft. This includes the pitot tube, static ports, temperature sensor and angle of attack sensor.
- **Communication** subsystems are very large and include many components, the major ones being: HF/VHF/UHF radio, SATCOM and transponders such as ADS-B. Furthermore, all transmitters and receivers are also powered by DC.
- **Navigation** shares some components with communication such as transponders, VHF radio signals, ADS-B, transmitters and receivers. They all operate on the DC electrical system because of the high need for reliability.
- **Cockpit instruments** refers to all instruments in the cockpit not covered by the communication and navigation category.
- **Interior Lighting** does not require as high power as the exterior lighting and is therefore on the DC system. This category includes Cockpit lighting, instrument lighting, cabin lighting and emergency lighting.
- **Controllers** All controllers in the aircraft will operate on DC because they don't require a high voltage. It is important to distinguish between the controller and the operation itself. The controller only sends a signal to a system to perform a task but does not perform the task itself.
- **Engine ignition** is the process of starting up the engines. This must be done with either a ground power unit or with the DC electric system since the AC system is not active when the engines are not running.
- **The anti-ice system** is in charge of the anti-icing of the plane. This was found to run on DC power according to [44].

AC Systems

The AC subsystem is capable of higher voltages and will therefore generally be used for larger components and components on the outside of the plane.

- **HUD** is the heads-up-display. It will show all important information for the pilot on the window of the aircraft. This includes a synthetic vision system that will aid the pilots in navigation when visibility is bad.
- **Pumps** are all pumps included in the aircraft. The fuel pumps for the engine and the water pumps in the snorkel are the main examples. These will require a large amount of power, meaning an AC voltage supply will be the most appropriate.
- **The fly-by-wire system** is the system required for fly-by-wire. All power for this was found to be AC from [44].
- **Hydraulics** includes all hydraulic systems that are present in the plane. For example the ailerons, elevators and rudder, but also the doors for the dropping system.
- **The collision avoidance system** was found to run on AC current according to [44].
- **Flight Recorder** was found to run on AC current according to [44].
- **Exterior Lighting** refers to all light on the exterior of the aircraft. This includes landing lights, taxi lights, navigation Lights and anti-collision lights. These require a high power output and are therefore run on AC instead of DC.
- **The HVAC system** will run on AC power as found in [44].

9 | Feasibility of FireFly

Contributor / Author: Sven

To assess whether further development of FireFly is recommended, it is important to analyse the project's feasibility. The basis of this analysis will be an evaluation of compliance with the initial user requirement which can be found in Section 9.1 together with a compliance matrix which summarises and evaluates all user requirements. The results of the compliance evaluation are used to generate recommendations for future development of the project and for steps that are required to ensure compliance with all requirements if compliance with some of them is not proven at this point of the project, this is discussed in Section 9.2.

9.1. User Requirement Compliance

The compliance matrix is made to show an overview of all user requirements agreed upon in the project plan report [45]. The user requirements were developed into the mission, stakeholder and system requirements as presented in the baseline report [14]. The system requirements were further expanded into the subsystem requirements. All subsystem requirements relevant to each subsystem can be found in the respective subsystem section of this report. Compliance with the user requirements is summarised in the compliance matrix present in Table 9.1. Further compliance with specific subsystem requirements can be found in Appendix B, where a responsible person was set to conduct the verification test posed and thus, confirm the compliance of the requirements, where applicable. The initials of the responsible person can be found in the C.C. columns, which stand for 'Compliance Check'. The initials of all group members are displayed on the cover page of this report.

Furthermore, for the user requirements, the tick- (✓) and cross (×) symbol signify compliance or inability to meet the requirement at this stage respectively. If both symbols are present, the requirement was partially met or further analysis has to be performed to assess the compliance.

Table 9.1: *User requirements compliance matrix.*

Identifier	Requirement	Compliance
FF-US-01	The aircraft shall suppress wildfires effectively using water and/or retardant.	✓
FF-US-02	The aircraft shall have VTOL capability.	✓
FF-US-03	The aircraft shall have the ability to refill water tanks in a hover.	✓
FF-US-04	The aircraft shall have a water/retardant tank capacity of at least 10,000 L.	✓
FF-US-05	The aircraft shall have a maximum cruise speed of at least 400 km/h.	✓
FF-US-06	Make the aircraft reliability and operational availability equal to or better than that of comparable aircraft.	✓ / ×
FF-US-07	Provide systems and avionics architecture that will enable autonomous operations in cruise.	✓
FF-US-08	The aircraft shall be capable of Visual Flight Rules (VFR) landing with an autopilot.	✓
FF-US-09	The aircraft shall be capable of Instrument Flight Rules (IFR) landing with an autopilot.	✓
FF-US-10	The aircraft shall be capable of flight in known icing conditions.	✓
FF-US-11	The aircraft shall meet applicable certification rules in CS Part 25/29 depending on applicability.	✓ / ×

A brief discussion on compliance with each user requirement will be presented in the form of a list:

- **FF-US-01:** The aircraft is capable of dropping both water and fire retardant. Additionally, the aircraft is equipped with a snorkel which allows it to refill the water tanks inflight without a need to return to base before the next drop. Variable water dropping speed is possible as well as a wide range of ground speeds during dropping manoeuvre due to its tilting rotors. All mentioned characteristics allow the aircraft to effectively suppress wildfires. More detailed analysis of aircraft characteristics can be found in Chapter 7.

- **FF-US-02:** The aircraft has VTOL capability due to its four tilting rotors.
- **FF-US-03:** The aircraft is able to refill the water tanks in hover using the snorkel device.
- **FF-US-04:** The aircraft is equipped with a water/retardant tank with the capacity to carry 10,200 L of liquid. Additional information on the water/retardant tank can be found in Figure 8.1.
- **FF-US-05:** The aircraft is designed to sustain a cruise speed of 400 km/h but is also capable of achieving higher airspeeds due to excess power generated in horizontal cruise flight.
- **FF-US-06:** The aircraft has high operational availability since it is capable of operating from a high variety of airfields due to its VTOL capability. The capabilities of aerial firefighting helicopters and water scoopers are combined due to the VTOL characteristics of the FireFly combined with high cruise speeds in horizontal flight mode. Additional description of the mission capabilities can be found in Chapter 5. The reliability of the FireFly aircraft is expected to be similar to the competitive aircraft such as the Canadair Cl-415 or the Firehawk since it mostly makes use of critical components available on the market such as the engines, avionics and the snorkel system. Nevertheless, comprehensive reliability analysis and testing have to be performed to get a proper estimation. The reliability of some components is discussed in Section 11.2.
- **FF-US-07:** Autonomous flight in cruise is performed through autopilot via Navigation mode (using a flight plan entered in the computer) or by manually selecting altitude, heading and speed. Additional information on the avionics can be found in Chapter 8.
- **FF-US-08** and **FF-US-09:** The aircraft is equipped with an ILS Cat II system which allows it to land using autopilot in both VFR and IFR flight. Additional information on the avionics is found in Chapter 8.
- **FF-US-10:** The aircraft is equipped with anti-icing equipment. Additional information on anti-icing system is found in Section 8.2.
- **FF-US-11:** The aircraft is expected to meet most of the applicable certification rules but further analysis is needed to prove compliance with some aspects of CS Part 25 and 29 such as the requirements on flights with gust and in turbulent airflow.

9.2. Feasibility Analysis

As can be seen in the compliance matrix Table 9.1, the FireFly aircraft fully complies with all but two initial user requirements. Two requirements, namely FF-US-06 and FF-US-11, require additional analysis to determine whether the FireFly aircraft is fully compliant with them. Unfortunately, the two requirements in question are critical for the aircraft's operations since they concern the certification and its reliability. If the aircraft cannot fulfil certification requirements it will not be cleared to fly by the regulatory agencies which would ultimately make the aircraft unusable. Additionally, if the reliability and certification requirements are not met, the safety of the aircraft might not be at an adequate level. As mentioned earlier, at the current stage of design, the aircraft is expected to eventually meet these requirements once the more detailed design and analyses are performed. This claim is made based on the fact that the aircraft does not make use of completely new technologies. The biggest challenge is expected in terms of stability and control because an unconventional quad tilt rotor with tandem wings configuration is used but preliminary findings from Section 7.8 are promising. Additionally, the aerodynamic aspects of the configuration have to be analysed further along with their implications on the aircraft's performance. Compliance with some of the requirements, especially from the safety aspect, will have to be demonstrated through a series of tests on the prototype aircraft and components.

To provide full compliance with all requirements a compliance matrix has to be made for stakeholder, system and subsystem requirements similar to the one made in Table 9.1. All subsystems were designed to comply with their respective requirements so the final product is expected to meet them. Analysis of compliance with all remaining requirements will also help prove compliance with the highest level, user requirements since most stakeholder and system requirements were derived from the initial user requirements. Furthermore, additional system and stakeholder requirements were created to include advanced features such as (medical) evacuation or a detection system to provide data about the fire in order to make the aircraft multifunctional and make a higher impact on the aerial firefighting fleet. Compliance with these additional requirements is also going to strengthen FireFly's market attractiveness making the project more financially viable. Motivated by the compliance with all but two user requirements at this stage of the design as well as additional features discussed in this report, the FireFly aircraft is deemed feasible and further development is recommended. The aircraft is expected to make a high impact on an aerial firefighting mission due to its high cruise speed, high water/retardant dropping capacity, VTOL capability and multi-functionality.

10 | Verification & Validation

For the final design of the FireFly's subsystem, the subsystem verification & validation (V&V) plan had to be established to verify and validate the requirements used to design the FireFly. This is an extension to the system requirement V&V plan described in the Midterm Report [9][pg. 34]. To ensure that the aircraft was designed to a sufficient degree, this plan was set in place to verify and validate the models used in the design phase and to ensure that all requirements will be met during the V&V and certification process of the FireFly.

10.1. Mission Requirements

Contributor / Author: Lauren

Similarly to the V&V set-up for the requirements in the Midterm Report, a verification and validation test was assigned to each subsystem requirement. Since the subsystem requirements stem from the system requirements, the new V&V is used to replace the system requirement V&V plan. The aim of the plan is to obtain a Means of Compliance from the verification engineer to move further with the certification process of the FireFly. Each test was derived from the EASA's standardised Means of Compliance for verification and validation [46]. These standard V&V procedures can be seen in the list below:

- Ground test - test on the entire aircraft.
- Calculation/Analysis - a few simple equations.
- Simulation - extensive computational model.
- Laboratory test - testing a single component.
- Flight test
- Design review - drawings and design reports.
- Compliance statement - pre-existing reports.
- Safety assessment
- Inspection - visual, by listening, etc.
- Equipment qualifications - previously certified by the supplier.

The final verification & validation tests for the subsystem requirements can be seen in Appendix B. As mentioned in the Section 9.1, each verification or validation test has been checked by a responsible person which is represented by their initials in order to check the compliance of the requirements. Furthermore, if the verification or validation test cannot be conducted at this moment due to not having a prototype aircraft, components etc., it is marked by F.A. meaning for Future Analysis.

As mentioned in the previous report, a partnership with the German Aerospace Centre (DLR) and Delft University of Technology will be established to carry out a variety of V&V procedures. These include inspection, laboratory, ground and flight testing. Furthermore, it was estimated the total V&V process will cost approximately €405 million. This cost estimate was derived from financial statements of Boeing and Airbus and analyses from corporations like the RAND corporation [47] [48]. The cost breakdown and reasoning can be found in the Midterm Report [9].

10.2. Model Requirements

Contributor / Author: Lauren

To verify and validate the models that were used, a standard was put in place for the coding models developed in Python Versions 3.10-3.12. The following system tests were carried out per programme:

- Integration testing - Check if a definition correctly receives data and passes the processed data as an output (Such as in a class).
- Functional testing - Test the inputs and outputs of chunks of code.
- End-to-end testing - Test the end result of the entire programme.

Class II V&V

The Class II model was used to perform Class II weight estimation as described in Section 7.2. The different weight categories were calculated and the iterative process was performed. For the V&V, the definitions referred to in the plan if not followed by its name/function refers to the components of the different categories mentioned in Section 7.2. For example, the engine system weight estimation has a separate definition to calculate the estimated mass of following components: nacelle, propeller, engine controls, engine starting system, propeller controls and the oil system & cooler.

Table 10.1: *Verification & Validation for the Class II model.*

Test Performed	Result	Performed by
Input class/initialise definition: Ensure TOML file variables are read and assigned to their respective variable correctly using print statements.	All inputs are read and assigned correctly.	LJ
Class - Inputclass/definition - init: Visually inspect that imperial units are applied correctly.	All inputs are correctly converted to imperial units.	LJ
Class - Class II/definition - init: Inputs from Inputclass are correctly assigned to self	All inputs are correctly assigned to self.	LJ
Class - Class II/Definitions: Self variables are well defined and outputs are correct.	All self variables are well defined and outputs are correct against hand calculations for each definition.	LJ
Class - Class II/Definition - total weight: Subsystem component masses have been calculated correctly.	Correct summation of component masses as per previous mass calculations.	LJ
Class - Class II/Defining nonetype variables in init definition: All nonetype variables are replaced with correct figures.	All nonetype variables are correctly replaced with their respective values after all calculations have been performed.	LJ
Class - Class II/Definition - names: All requests for component mass is processed correctly.	Each component mass is called correctly from the names definition.	LJ
File - ClassII.py: Iteration for MTOW is within 5%	Iteration loop works as expected as per hand calculations.	LJ
File - ClassII.py: When the 'groups' boolean is true, component masses print correctly as per total weight definition.	Iteration loop works as expected as per hand calculations.	LJ

Fatigue V&V

The fatigue model was used to carry out the fatigue analysis as described in Table 6.1. It was used to analyse the fatigue of AL7068, AL2195 T8 and AL2024 for different load cases throughout the mission.

Table 10.2: *Verification & Validation for the fatigue model.*

Test Performed	Result	Performed by
Definition - Fatigue: Input & output data correctly processed using print statements and hand calculations.	Inputs were as expected and the outputs matched hand calculations.	LJ
Definition - Fatigue: Compare stress calculations to hand calculations for N=20000.	Results matched exactly.	LJ
Definition - Fatigue & plotting: Running fatigue function and plotting results correctly.	Produces plots with correct fatigue stress for correct cycle number.	LJ
Definition - Cyclic: Ensure that the inputs are correctly processed and plotted using print statements.	Inputs were correct and the resulting plot was as expected.	LJ

Inverse Power Loading vs Wing Loading V&V

The inverse power loading vs wing loading model was used to analyse the performance of the FireFly and to produce Figure 7.35. In Table 10.3, the definitions without name or functionality defined refer to definitions regarding the performance parameters mentioned in Subsection 7.7.1.

Table 10.3: *Inverse Power Loading vs Wing Loading V&V.*

Test Performed	Result	Performed by
Input class/initialise definition: Ensure inputs are processed and assigned correctly using print statements.	All inputs are read and assigned correctly.	LJ
Class - Power wing loading/Definitions: Ensure that the input data is correct, the formula is correct and the output matches hand calculations.	All definitions' input data is correct, formulas are correctly inputted and outputs match hand calculations.	LJ
Class - Power wing loading/graph - definition: Ensure that the plot has correct labels and corresponding data plotted.	The plot prints the correct performance data and are labelled correctly.	LJ
File - Power-wing-loading-diagram.py: Ensure that 'graph' boolean prints the graph when set to true.	Graph prints when boolean is set to true.	LJ

Structural Algorithm V&V

The structural analysis algorithm is a modular framework consisting of four key modules: assembly.py, element.py, internal_loads.py and materials.py. The assembly is built from elements, which take material properties from materials.py. The internal loads and their distributions are calculated in internal_loads.py and are passed to the assembly to calculate the deflections and the stresses.

Table 10.4: *Verification & Validation for the Structural Model.*

Test performed	Result	Performed by
Class - Materials, materials.py: Ensure that all the material properties in materials.py have been correctly entered from Granta.	All material properties have been correctly assigned to the correct materials.	JC
Class - MaterialChoice2, materials.py: Ensure that the correct material class is instantiated.	The correct material class is instantiated when the choice for that specific material is made.	JC
Definition - centroid, internal_loads.py: Compare the computed centroid of a distributed load to hand calculations for the distributed wing weight.	The results matched.	JC
Class - Hover, internal_loads.py: Compare the computed reaction loads to hand calculations for the hover case.	The results matched.	JC
Class - NVMT/Initialisation, internal_loads.py: Ensure that an NVMT instance correctly extracts the reaction loads from the correct load case	When hover is specified, the NVMT class indeed takes the reaction loads from the Hover class	JC
Class - NVMT/Definition - V_variation, M_variation and T_variation, internal_loads.py: Compare the internal shear force, bending moment and torque variation with hand calculations for hover.	The results match.	JC
Class - WingCell/Initialisation, element.py: Ensure that a WingCell instance assigns the correct geometrical properties to self when the setting is specified as 'rectangular' or 'trapezoidal'.	The WingCell class correctly assumes the specified cell geometry.	JC
Class - WingSection/Initialisation, element.py: Ensure that a WingSection instance assigns the correct geometrical properties and internal loads to self.	The WingSection class correctly assumes the specified geometry and subjects itself to the specified internal loads.	JC

Continued on next page

Table 10.4 – continued from previous page

Test performed	Result	Performed by
Class - Element/Initialisation, element.py: Ensure that an Element instance assigns the correct element type, geometrical properties and internal loads to self.	The Element class correctly assumes the specified structural type and geometry and subjects itself to the specified internal loads.	JC
Class - Assembly/Initialisation, assembly.py: Ensure that an Assembly instance assembles the structure correctly and correctly assigns the internal loads to self.	The Assembly class assembles the structure from the correct elements and correctly applies the internal loads along its length.	JC

10.3. Sensitivity Analysis

Contributor / Author: Jimmy

Due to the iterative nature of design, there are many parameters which are subject to change. These changes include changes in aspect ratio, MTOW and the centre of gravity location. The aspect ratio may change depending on the aims for the aerodynamic performance and the centre of gravity location shifts all the time throughout the process of determining the weight and balance of the aircraft. Finally, the MTOW may increase in later design stages as is often the case in the design of aircraft. These changes can affect the design of the aircraft in various ways, be it through the structural design, the aerodynamics or propulsion.

Materials and Structures

The effects of these changes on the structural design framework are investigated by analysing the sensitivity of the material choice and by analysing the sensitivity of the wing box structure to the aforementioned changes.

The structural aspect of the material selection is mainly based on the structural efficiency, i.e. the structural mass. The materials sensitivity analysis therefore looked at the increase in structural mass for each material caused by an increase in aspect ratio and MTOW. The results are shown in Figure 10.1 and Figure 10.2 respectively. Varying the maximum load factor and the centre of gravity location has also been investigated, but increases in aspect ratio and MTOW yielded more extreme changes. Calculating the structural mass for each material is based on the same model used in Section 6.1.

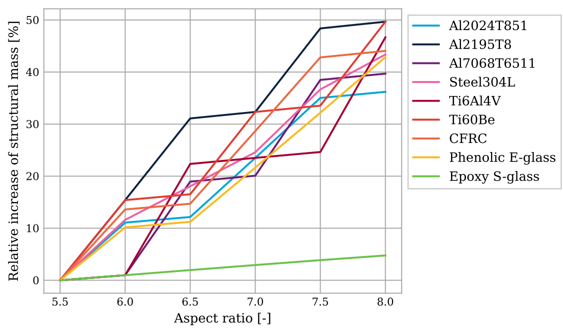

Figure 10.1: *Relative increase in structural mass per material by varying the aspect ratio in increments of 0.5.*

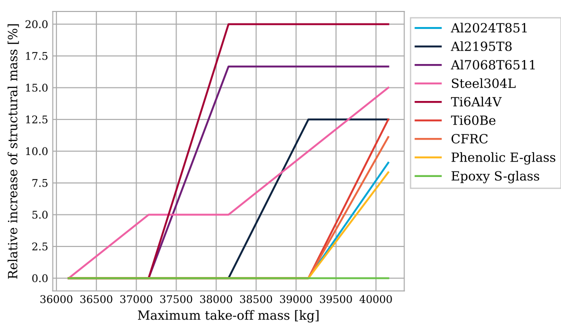

Figure 10.2: *Relative increase in structural mass per material by varying the MTOW in increments of* 1000 kg.

The relative changes in structural mass were plotted because the absolute structural mass would result in plots which were too unclear because Steel304 has a much higher mass compared to the other materials, which compressed the curves of the other materials. Looking at Figure 10.1, increasing the aspect ratio causes Al2195T8 to experience the largest relative increase in structural mass. Figure 10.2 shows that the structural mass of Al7068 is more sensitive to MTOW compared to Al2195 and Al2024. The sensitivity of Al2195 to aspect ratio is an argument against choosing Al2195 over Al7068, however, the sensitivity of Al7068 to MTOW is an argument against choosing Al7068. Because an increase in MTOW is more likely than an increase in aspect ratio, it stands to reason that Al2195 remains the material of choice for the wing box.

Although the material trade-off for the wing resulted in Al2195T8 being chosen, it is still worthwhile to investigate the effects on the structural mass and cost of the wing box for the three aluminium alloys considered: Al2024T851, Al2195T8 and Al7068T6511 when the aspect ratio or the MTOW are increased. The results are shown in Figure 10.3, Figure 10.5, Figure 10.4 and Figure 10.6.

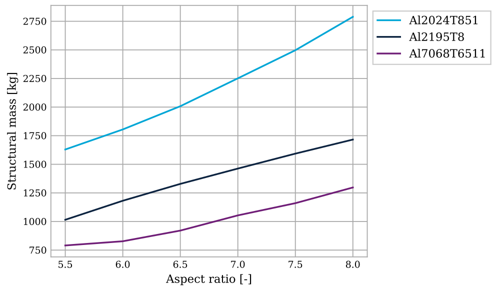

Figure 10.3: *Masses of the three wing box designs by varying the aspect ratio in increments of 0.5.*

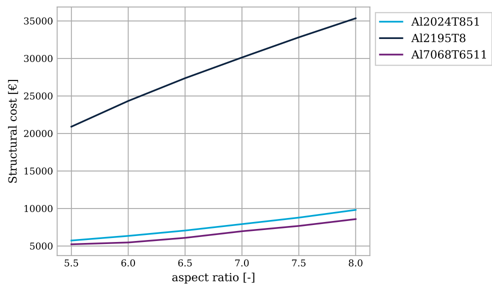

Figure 10.4: *Costs of the three wing box designs by varying the aspect ratio in increments of 0.5.*

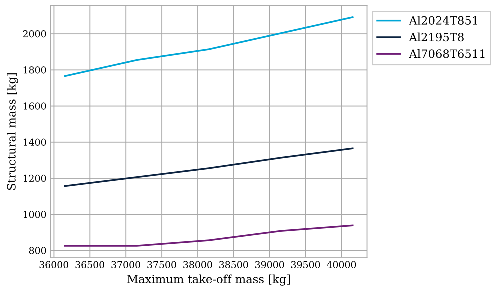

Figure 10.5: *Masses of the three wing box designs by varying the MTOW in increments of* 1000 kg.

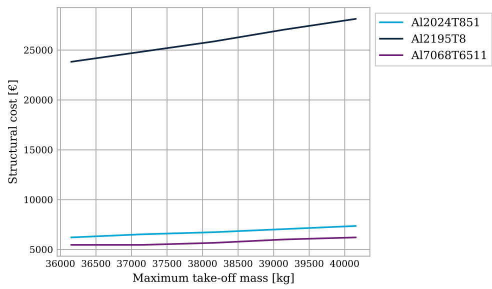

Figure 10.6: *Costs of the three wing box designs by varying the MTOW in increments of* 1000 kg.

Figure 10.3 and Figure 10.5 show that the baseline design made from Al2024T851 is more sensitive to changes in aspect ratio or MTOW, which means it contributes more to a snowball effect of increasing mass compared to designs made from Al2195T8 and Al7068T6511. Between Al2195 and Al7068, the structural mass is about equally sensitive to changes in aspect ratio and MTOW. Although Al7068 is inherently lighter because it is stronger, Al2195 is vastly superior when it comes to fatigue, so this alone will not be enough to reconsider the use of Al2195T8 as the wing box material. However, looking at Figure 10.4 and Figure 10.6, it is clear the cost of an Al2195T8 wing box is much more sensitive compared to Al2024T851 and Al7068T6511. The combination of a very high cost and a high sensitivity to increases in aspect ratio and MTOW give Al7068T6511 a small edge in case the aspect ratio or the MTOW is much higher, which can happen in a later design stage. This then has implications for the fatigue performance of the structure, because Al7068 has the worst crack propagation performance of the three. A more detailed study and trade-off is recommended for the next design phase.

Aerodynamics

Any changes in the inputs will also impact the aerodynamic performance of the aircraft. This can be seen in how the drag coefficient reacts to changes in aspect ratio and MTOW. These two parameters are thought to be the two most likely subject to change. The results have been plotted in Figure 10.7.

Figure 10.7 indicates that increasing the aspect ratio whilst keeping the wing surface area constant decreases the drag coefficient, which is exactly as expected. Increasing the aspect ratio makes an aircraft more aerodynamically efficient. However, this is not a reason to massively increase the aspect ratio due to structural considerations. As already shown in Figure 10.3, increasing the aspect ratio also leads to an increase in structural mass. This means that the aspect ratio must not grow too large. Furthermore, Figure 10.7 shows that increasing the MTOW while setting the aspect ratio to constant leads to a decrease in the drag coefficient. Assuming the wing loading W/S is kept constant, increasing the MTOW leads to an increase in wing surface

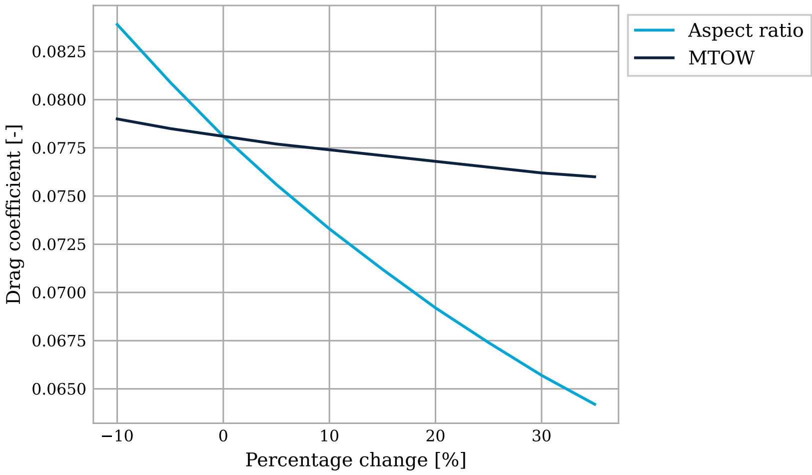

Figure 10.7: *Drag coefficient of the FireFly when varying the aspect ratio and MTOW by increments of 5%.*

area. By increasing the wing surface area, the required lift coefficient becomes lower, which also leads to a lower induced drag. This causes the total drag coefficient to be lower too. However, increasing MTOW will also increase the structural weight as should already have become apparent from Figure 10.5. Therefore, one should take care not to let the MTOW grow too much.

Propulsion

Possibly the most crucial subsystem to the mission performance is the propulsion system. To hover, the propulsion system must provide enough power, and to climb in hover mode, it must provide even more. It must therefore be investigated how the aspect ratio and the MTOW would affect the propulsion system by analysing how a change in aspect ratio or MTOW changes the power required to climb in hover mode. As mentioned before, the aspect ratio and MTOW are most likely to change, so it makes sense to look at the effects of these changes on the propulsion system. The results of this have been shown in Figure 10.8.

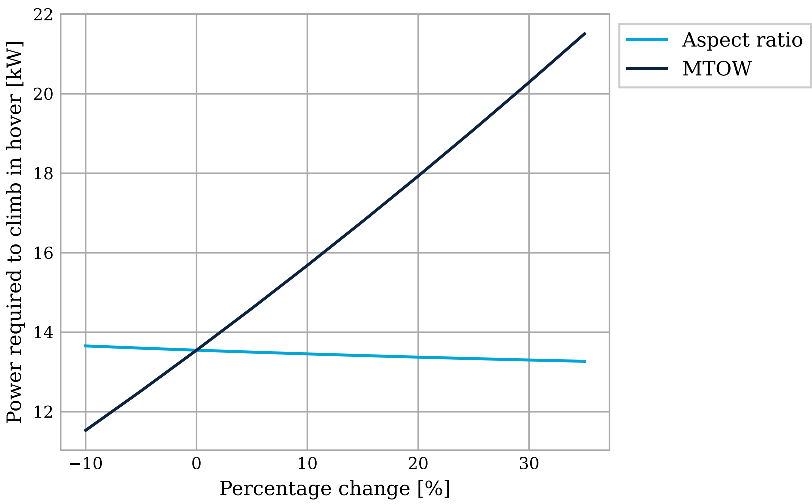

Figure 10.8: *Power required to climb in hover mode of the FireFly when varying the aspect ratio and MTOW by increments of 5%.*

Figure 10.8 shows that changing the MTOW has a profound effect on the required power. This makes sense as the required power is constrained by the required rate of climb, which means there is a required amount of excess power. Increasing the MTOW increases this required excess power. This is another reason to not let the MTOW grow too large, because it may result in completely different engines which must be used. On the flip side, Figure 10.8 implies that changes in the aspect ratio barely change the required power. The biggest effect the aspect ratio has on the required power is through downloading, however, this downloading is small in comparison to the total required power.

11 | Technical Risk Assessment & RAMS

Risk management is a central part of creating a safe aircraft. AFF aircraft fly through remote and hostile environments including smoke and high heat exposure, creating more risks than for conventional aircraft. In order to asses as many risks as possible, the risk analysis (Section 11.1) has been split up into two sections: general risks and FireFly-specific risks. After the risks have been identified, mitigation strategies are implemented to reduce the likelihood and/or consequence of the risk. From the risk analysis, it was concluded that the main risks arise from the nature of the rotor configuration.

11.1. Technical Risk Analysis

Contributors/Authors: Hanna, Ishan

In the analysis, the first step is to identify the risk and define possible scenarios. Secondly, the frequency of those scenarios can be evaluated and their consequences can also be determined. Finally, the risks need to be quantified in order to conduct an appropriate analysis in sufficient detail.

The risks will be scored based on two different aspects. First, the risk will be quantified based on likelihood, for which 5 levels were taken into account: very high (P>70%, "Feasible In Theory"), high (50% < P < 70%, "Working Laboratory Model"), moderate (30% < P < 50%, "Based on Non-Flight Engineering"), low (1% < P < 30%, "Extrapolated from Existing Flight Design") and very low (P < 1%, "Proven Flight Design"). More detail on the categories can be found in the Baseline Report [14]. The likelihood of the risk is taken over the lifetime of the aircraft operations. Secondly, the probability of occurrence is evaluated using literature research occasionally using the help of engineering judgement. To quantify the impact, four different levels were defined: Negligible (small inconvenience or non-operational impact), Marginal (secondary mission cannot be fulfilled), Critical (mission success is questionable) and Catastrophic (full loss of aircraft). Further explanations are included in the Baseline Report [14].

First, the general technical risks are considered, which are identified during the conceptual design phase, when the two firefighter concepts are developed simultaneously. These risks can be seen in Table 11.1.

Table 11.1: *List of general technical risks.*

Risk Code	Requirement	Risk	Likelihood	Impact	Consequence
TR1	FTF-STK-PIL-01	The aircraft is uncontrollable in autonomous operations	Low	Catastrophic	Losing control of the aircraft and mission failure
TR2	FTF-SYS-FDS-05.1	The engines do not supply enough power for the aircraft to perform VTOL at MTOW	Low	Critical	Loss of VTOL capabilities during take-off/tanking/landing as planned
TR3	FTF-SYS-FDS-04.1	The aircraft has too much drag	Low	Critical	The aircraft is too slow and cannot reach the required cruise speed at MTOW
TR4	FTF-SYS-FDS-05.2	Failure of the pumping system when refilling the water/retardant tank	Low	Critical	The tank cannot be refilled and there is not enough water for the extinguishing of fires
TR5	FTF-STK-PIL-01	Malfunction of sensors while performing the autonomous operations	Moderate	Critical	The aircraft loses control and the pilot has to take over

Continued on next page

Table 11.1 – continued from previous page

Risk Code	Requirement	Risk	Likelihood	Impact	Consequence
TR6	FTF-STK-FDS-09	Malfunction of the night vision system	Low	Catastrophic	The aircraft cannot fly at night and perform night-time operations
TR7	FTF-SYS-FDS-01.3	Failure of the water dispersion system	Low	Critical	Inefficient fire prevention strategy
TR8	FTF-STK-CRW-02	Communication system interference/malfunction	Moderate	Critical	Lack of communication with the ground crew
TR9	FTF-STK-ATC-01	Malfunction of the transponder	Very low	Catastrophic	Critical data not being sent to the dispatcher, TCAS inactive
TR10	FTF-SYS-REG-01.1	The caution/master caution information system is defective	Low	Catastrophic	The flight crew is not alerted when the anti-ice or de-ice system is not functioning normally
TR11	FTF-SYS-REG-01.1	The ice protection system fails to activate due to a technical malfunction	Low	Catastrophic	Ice build-up can't be combated in flight
TR12	FTF-SYS-REG-01.3	Lower engine power than expected due to different atmospheric conditions during operations	Very High	Catastrophic	Aircraft will not be compliant with engine power ratings as stated in CS-E 40
TR13	FTF-STK-PIL-04	Emergency door not opening	Very low	Catastrophic	The safety of the crew is jeopardised
TR14	FTF-SYS-FDS-07.3	The heat resistance of the aircraft structure is lower than accounted for	High	Catastrophic	The structural integrity of the aircraft is compromised
TR15	FTF-SYS-PIL-04.3	Inability to maintain rotor RPM after abrupt engine loss	Moderate	Critical	Unpredictable loss of altitude
TR16	FTF-SYS-PIL-04.3	Failure of shared drive shaft causing asymmetric thrust	Low	Catastrophic	Insufficient controllability
TR17	FTF-SYS-PIL-04.3	Autorotation capability not sufficient	High	Catastrophic	Powerless glide impossible
TR18	FTF-SYS-PIL-04.3	Hard clutch engagement occurs	Low	Catastrophic	Key components are damaged and the aircraft starts moving erratically
TR19	FTF-STK-OWN-02	Cost inflation of the aircraft components	High	Marginal	Total aircraft cost is higher than expected
TR20	FTF-STK-INV-01	Unexpected technical costs arise during development	Very high	Marginal	Development costs exceed the budget
TR21	FTF-STK-OWN-01	Aircraft is rendered inoperable	Low	Critical	Aircraft must be retired earlier than planned, unexpectedly reducing fleet capabilities
TR22	FTF-SYS-INV-02.1	Unexpected maintenance required	Moderate	Critical	Maintenance cost per flight hour exceeds the requirement

Continued on next page

Table 11.1 – continued from previous page

Risk Code	Requirement	Risk	Likelihood	Impact	Consequence
TR23	FTF-SYS-FDS-02.1	The tank meter incorrectly displays the water/retardant level.	Low	Critical	The tank isn't fully filled and the aircraft cannot effectively extinguish fire
TR24	FTF-STK-PIL-03	The new design poses challenges for pilots unfamiliar with it	Very high	Critical	The pilots experience an extra workload due to training and unfamiliarity with the design
TR25	FTF-STK-OWN-01	Design flaws leave the aircraft inoperable before its minimum lifespan has been reached	Low	Catastrophic	The aircraft will have to be discarded within the planned lifespan resulting in a bad reputation for the company
TR26	FTF-SYS-FDS-01.1	The dropping mechanism is defective	Low	Critical	No effective drops can be performed during the mission
TR27	FTF-STK-FDS-01	The tank erodes because of the composition of retardant	Low	Marginal	Unexpected maintenance on the tank, resulting in extra expenses
TR28	FTF-STK-FDS-11	Malfunction of the Helicopter Flight Rescue System	Very low	Marginal	Evacuations and drop-offs cannot be performed in-flight anymore, the aircraft will have to land before cargo and/or passengers can enter or leave the vehicle
TR29	FTF-STK-SUP-01	The supplier delivers flawed parts that cannot handle the loads/conditions necessary as communicated by the design department	Low	Catastrophic	Either the flawed parts have to be replaced or worst case the aircraft will be left inoperable due to safety concerns
TR30	FTF-SYS-FDS-01.3	Due to system malfunction the aircraft cannot remain stable during the water/retardant release phase	Low	Critical	The dispersion of the water/retardant will not be optimal, hindering the fire fighting operation
TR31	FTF-SYS-FDS-05.7	Malfunction of the heat monitoring system	Low	Marginal	When the heat caused by the fire cannot be monitored anymore it is hard to determine whether the aircraft is being exposed to more heat than it is designed for, resulting in system overheating or component damage

Continued on next page

Table 11.1 – continued from previous page

Risk Code	Requirement	Risk	Likelihood	Impact	Consequence
TR32	FTF-SYS-FDS-07.2	The aircraft will experience corrosion after being exposed to an environment with salty water for a longer period of time	High	Critical	Unscheduled maintenance has to be performed on the aircraft, and some parts might need replacing sooner than anticipated, costs will be higher than expected

After identifying the risks, mitigation can be performed. The mitigation strategies are divided into four categories: Reduction, Avoidance, Transfer and Acceptance. The detailed description of each category can be found in the Baseline Report [14]. Below in Table 11.2 the mitigation strategies are described.

Table 11.2: *Risk mitigation plan for general technical risks.*

Risk Code	Category	Mitigation Strategy	Verification	Likelihood	Impact
TR1	Reduction	Perform tests of the autonomous flight system in operational conditions	Tests are supervised by certified independent staff	Very low	Catastrophic
TR2	Reduction	Thorough testing of the engines, monitoring different circumstances such as wind to ensure VTOL capability	Tests are supervised by certified independent staff	Very low	Critical
TR3	Reduction	Detailed analysis of the surfaces in the aircraft	Wind tunnel testing of the aircraft to see if the results agree with calculations	Very low	Critical
TR4	Reduction	Perform tests of the pumping system in operational conditions	Tests are supervised by certified independent staff	Very low	Critical
TR5	Reduction	Implement a fail-safe sensor system	Test the fail-safe sensor system in operational conditions	Moderate	Negligible
TR6	Reduction [49]	Use of battery powered night vision system independent of aircraft electrical power	Check the battery percentage	Very low	Marginal
TR7	Reduction	Implement a fail-safe release mechanism	Test the fail-safe release mechanism in operational conditions	Low	Marginal
TR8	Reduction [50]	Implement anti-cyber attack measures such as in-system warnings and ensuring high safety of network	Perform communication system tests	Low	Critical
TR9	Reduction	Implement a fail-safe transponder system	Test the fail-safe transponder system in operational conditions	Very low	Negligible
TR10	Transfer	Establish routine check-up procedures of the caution information system in the operations manual	Log every check-up and any findings	Very low	Critical

Continued on next page

Table 11.2 – continued from previous page

Risk Code	Category	Mitigation Strategy	Verification	Likelihood	Impact
TR11	Transfer	Establish routine check-up procedures for the ice protection systems in the maintenance manual	Log every check-up and any findings	Very low	Critical
TR12	Reduction	Test engine power with atmospheric conditions encountered during operations	Tests are supervised by certified independent staff	Moderate	Critical
TR13	Reduction	Introduce requirements on the safety equipment with redundant systems	Test the emergency equipment in various conditions	Very low	Critical
TR14	Reduction	Implement sufficient safety factors and choose materials typical for the firefighting industry	Heat laboratory testing	Low	Catastrophic
TR15	Reduction	Introduce requirements for a stable autorotation	Test the autorotation capabilities in the desired condition	Low	Critical
TR16	Reduction	Introduce requirements for maintaining controllability after engine loss, such as sufficient margin and control surfaces	Conduct a simulation of aircraft parameters after engine loss	Very low	Critical
TR17	Reduction	Introduce requirements for minimum rotor size to allow autorotation	Test the autorotation capability of the aircraft under operational conditions in case of sudden power loss of all engines	Low	Catastrophic
TR18	Reduction	Design the drive shaft to be able to handle the shock load of a sudden engine loss	Test the drive shaft in case of a sudden engine failure under operational conditions	Very low	Catastrophic
TR19	Reduction	Include an expected inflation margin in the costs	Inspect the budget continuously	Moderate	Marginal
TR20	Reduction	Include contingencies in the development budget	Continuously check the difference between actual costs and target cost	Moderate	Marginal
TR21	Transfer	Establish a fleet operations standard to always have reserve aircraft	Perform fleet inspections by certified independent staff	Low	Marginal
TR22	Transfer	Establish regular maintenance procedures	Ensure the planning of the relevant maintenance procedures and analyse the schedule	Low	Critical
TR23	Reduction	Implement a tank volume measurement system with redundancies	Test the detection levels in the laboratory in various scenarios	Very low	Critical
TR24	Acceptance	Ensure that the aircraft is easily controllable, the pilots will get used to flying using the new system over time	Test the new system on (experienced) pilots to see how fast they get used to it	Moderate	Critical

Continued on next page

Table 11.2 – continued from previous page

Risk Code	Category	Mitigation Strategy	Verification	Likelihood	Impact
TR25	Reduction	Take suitable safety factors into account and ensure that the design is checked by several engineers before production	Continuously evaluate the safety factor and other design choices	Very low	Catastrophic
TR26	Reduction	Elaborate testing of the dropping system and regular inspection during maintenance operations	Testing by certified professionals	Low	Marginal
TR27	Reduction	Creating a manual that highlights which retardants are allowed to be used and a warning system in case a wrong retardant is placed in the tank	Extensive material analysis using several different types of retardants	Very low	Negligible
TR28	Reduction	Using an already proven design and having a qualified maintenance crew performing regular maintenance on the aircraft	Researching available options extensively	Very low	Negligible
TR29	Reduction	Only working together with reliable suppliers that are known within the aircraft industry as well as ensuring clear communication about expectations between the suppliers and the design team	Ensuring communication between suppliers and design team at all times and researching available suppliers and their reputation well	Very low	Critical
TR30	Reduction	Design the aircraft to remain stable even when big load-changes occur	Testing of the system in extreme situations such as gusts of wind	Very low	Marginal
TR31	Transfer	Look into special coatings that can withstand this as well as selecting and designing components that can handle this heat	Heat laboratory testing	Very low	Marginal
TR32	Reduction	Choose coatings or materials that can resist this for the parts of the aircraft that can come into contact with salty water	Testing in a laboratory by exposing materials to salty water solutions and seeing how they react	Very low	Marginal

After the mitigation strategies are compiled, the pre- and post-mitigation risk maps can be produced as seen in Figure 11.1a and Figure 11.1b.

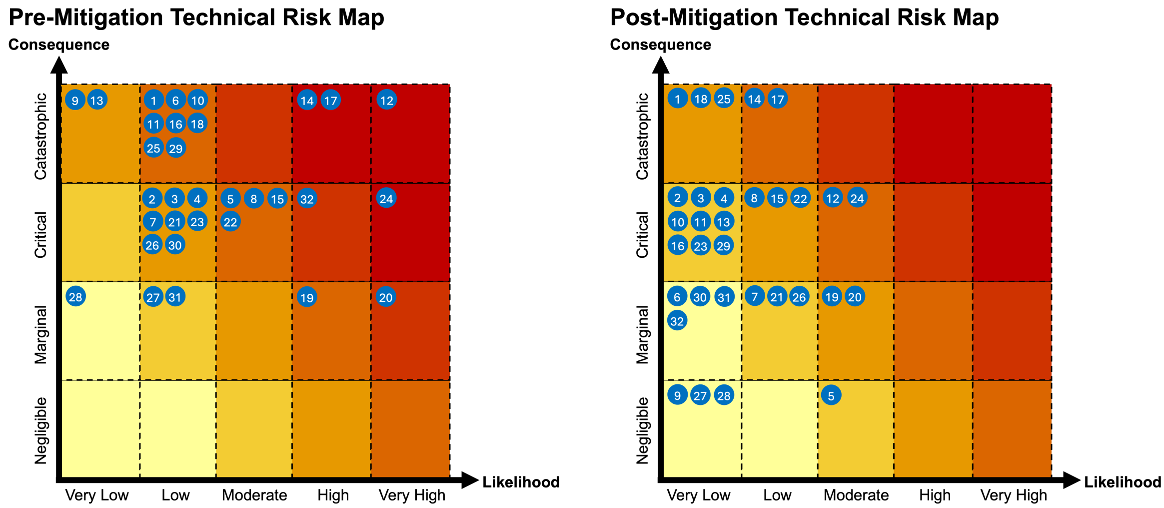

(a) *Technical risk map pre-mitigation.*

(b) *Technical risk map post-mitigation.*

Figure 11.1: *Technical risk maps for general risks.*

The main takeaway from the risk maps is that the number of catastrophic risks is reduced by eight risks, showing the effectiveness of the FireFly team's global approach to risk.
Apart from the general risks, the tilt-rotor concept-specific risks had to be taken into account as well. They were developed during the span of the final design analysis. The likelihood and impact are assigned using analogical philosophy to the general risks in Table 11.1. The FireFly concept-specific risks are defined in Table 11.3.

Table 11.3: *List of technical risks for the FireFly.*

Risk Code	Requirement	Risk	Likelihood	Impact	Consequence
QTRR1	FTF-SYS-FDS-04.1	Failure of the tilting-system on 1 rotor	Low	Critical	The rotor will not be able to be tilted anymore resulting in reduction of either speed or VTOL capabilities
QTRR2	FTF-SYS-FDS-04.1	Failure of one rotor	Low	Critical	The aircraft will still be operable, however, the required speed cannot be obtained anymore
QTRR3	FTF-SYS-FDS-05.1	Failure of several rotors on one wing	Very low	Catastrophic	The aircraft will not be able to produce enough lift anymore, loss of height and aircraft becomes unstable
QTRR4	FTF-SYS-FDS-05.1	Failure of several rotors on different wings	Very low	Critical	The aircraft will not be able to produce enough lift anymore, loss of height, dangerous if above fire

Continued on next page

Table 11.3 – continued from previous page

Risk Code	Requirement	Risk	Likelihood	Impact	Consequence
QTRR5	FTF-SYS-FDS-04.1	Failure of the tilting-system on 2 rotors or more	Low	Catastrophic	The rotors will not be able to be tilted anymore resulting in catastrophic loss of either speed or VTOL capabilities, the aircraft is no longer operative, when tilt-system failure occurs on adjacent rotors, the aircraft will become unstable
QTRR6	FTF-SYS-REG-02.5	Structural failure of the integrated water tank	Low	Critical	A crack in the tank can lead to water leaking all over in the aircraft structure, causing major weight and balance issues thus resulting in instability. Additionally, corrosion can arise on the inner structure which is difficult to detect and can lead to structural failures
QTRR7	FTF-SYS-REG-01.8	Electric system placed behind cockpit catches on fire	Low	Catastrophic	Could cause an cabin fire and potentially a cockpit fire which could inhibit pilot actions
QTRR8	QTR-FUL-04	Puncture of fuel tanks	Low	Catastrophic	Fuel leakage in could cause mass and balance issues, but more importantly is a massive fire hazard
QTRR9	QTR-FUL-02	Failure of the fuel pump	Moderate	Critical	Could potentially lead to engine failure due to fuel starvation if fuel flow is not maintained
QTRR10	QTR-FUL-06	Fuel contamination	Moderate	Critical	Could lead to engine roughness at potentially engine failure
QTRR11	QTR-FUL-06	Fuel line blockage	Low	Critical	A complete blockage could lead to the engine being inoperative due to lack of fuel
QTRR12	QTR-FUL-04	Leakage in a hydraulic line	Low	Catastrophic	A leakage of primary control hydraulics can lead to the complete loss of control of the aircraft
QTRR13	QTR-LDG-02	Failure of landing gear deployment	Low	Critical	Can cause structural fuselage damage if a belly landing is required
QTRR14	QTR-AVI-15, QTR-AVI-16	Failure of the PFD	Low	Catastrophic	Loss of all primary instruments such as speed, altitude and heading

Continued on next page

Table 11.3 – continued from previous page

Risk Code	Requirement	Risk	Likelihood	Impact	Consequence
QTRR15	QTR-AVI-35	Failure of the MFD	Low	Marginal	Loss of display of maps, navigation, engine parameters, detection systems and other non-critical instruments
QTRR16	QTR-AVI-36	Failure of the FMS	Low	Critical	Loss of landing approaches and procedure charts, communications means, navigation and flight planning capabilities
QTRR17	QTR-ENV-05	Failure of the HVAC system	Low	Critical	The environment in the aircraft could impact crew's health and vigilance, restricting the aircraft's further operations, as well as cause damage to the avionics
QTRR18	QTR-DRP-01	Failure of drop tank door	Low	Marginal	Ineffectiveness in firefighting operations, load imbalance as well as possible mechanical damage to door
QTRR19	QTR-REF-02	Failure of snorkel deployment	Low	Negligible	Increase in the turnaround time and inefficiency in firefighting operations
QTRR20	QTR-REF-03	Failure of water pump	Low	Negligible	Reduced capability to extinguish fires
QTRR21	QTR-ELE-04	Failure of the AC or DC bus	Low	Catastrophic	Potential loss of communication and navigation system, along with making the aircraft uncontrollable due to potential loss of electric tilt motors
QTRR22	QTR-PYL-11	Winch fails	Low	Marginal	Delayed logistics and operations, along with safety hazard for the ground crew
QTRR23	QTR-TNK-05	Water tank overflows	Moderate	Critical	Inefficiency in firefighting operations, as well as controllability issues due to balance shift
QTRR24	QTR-STA-04	Control surfaces require too much force	Low	Critical	The aircraft will not be controllable and further operations could be deemed infeasible
QTRR25	QTR-LDG-04	Aircraft sinks in soft ground surface	Moderate	Marginal	Structural damage to the undercarriage and delays in operations as work will be needed to extricate it

Continued on next page

Table 11.3 – continued from previous page

Risk Code	Requirement	Risk	Likelihood	Impact	Consequence
QTRR26	QTR-LDG-06	Aircraft tips back while parked	Low	Critical	Exposing the aircraft to higher structural loads, possibly causing a safety hazard to the ground crew
QTRR27	QTR-STR-07	Detailed structural analysis reveals the structure buckles under compressive load	Moderate	Catastrophic	Loss of load bearing capability leading to structural failure
QTRR28	QTR-STR-01	Detailed dynamic analysis reveals the structure is particularly susceptible to aeroelastic flutter	Moderate	Critical	Useful life of the structure is rapidly used up due to the oscillating loads, necessitating more frequent maintenance
QTRR29	QTR-STR-08	Detailed heat analysis of the structure reveals that the structure heats up considerably due to the heat above the wildfire	Moderate	Critical	The thermal expansion of parts of the structure causes thermal stresses in the structure, which results in additional stress

After identifying the concept-specific risks, mitigation strategies are proposed. The category for each mitigation strategy is assigned using the same philosophy as the general risk mitigation strategy.

Table 11.4: *Technical risk mitigation FireFly specific concept*

Risk Code	Category	Mitigation Strategy	Verification	Likelihood	Impact
QTRR1	Avoidance	Implement redundant tilting system. Install sensors detecting tilting system malfunctions.	Research of proven tilting concepts	Very low	Critical
QTRR2	Reduction	Train the pilots how to react in case of engine failure. Implement maintenance procedures	Regularly test the pilots and the procedures	Very low	Marginal
QTRR3	Acceptance	Train the firefighting crew with the emergency procedures. Avoid unsafe loads during the flight	Check the safety requirements during each step of the design phase	Very low	Catastrophic
QTRR4	Acceptance	Ensure there are enough safety measures allowing to adjust the rotor setting	Check the safety requirements during each step of the design phase	Very low	Critical
QTRR5	Acceptance	Ensure there that rotor settings can be adjusted in all phases, look into concepts of tilting systems that have been proven to be reliable in the past in for example military operations	Check the safety requirements during each step of the mission	Very low	Catastrophic
QTRR6	Reduction	Maintenance crew will perform regular tank inspections, every 15 engine flight hours	Implement instructions in maintenance manuals	Very Low	Critical

Continued on next page

Table 11.4 – continued from previous page

Risk Code	Category	Mitigation Strategy	Verification	Likelihood	Impact
QTRR7	Reduction	All electrical components should be properly insulated with fire resistant material to avoid short circuits	Inspect electrical components for slashes in wires	Low	Critical
QTRR8	Reduction	Use of bladder tank within integral tank to protect the fuel from puncturing.	Inspect state of fuel tanks	Very Low	Critical
QTRR9	Transfer	Use a safety factor when sizing fuel pumps in order for remaining working pumps to still provide fuel pressure and flow.	Check fuel pump specifications	Low	Marginal
QTRR10	Reduction	Make use of gascolators which filter foreign material and separate contaminants.	Ensure proper installation of gascolator in aircraft	Very Low	Critical
QTRR11	Reduction	Use of redundant fuel lines to deliver fuel from tanks to engines.	Ensure enough fuel can be delivered to engine via redundant lines	Low	Marginal
QTRR12	Avoidance	Use independent hydraulic lines (A, B and C) to isolate hydraulic leaks.	Ensure 3 separate hydraulic systems are installed in the aircraft.	Low	Critical
QTRR13	Reduction	Install a manual gear deployment handle which can be used by one of the pilots in emergency situations.	Ensure manual handle is installed and functional by regularly checking on it during maintenance.	Low	Marginal
QTRR14	Reduce	Presence of backup primary instruments which display primary flight information such as airspeed, altitude and heading.	Ensure all backup instruments are working before all flights.	Low	Marginal
QTRR15	Acceptance	Since the MFD doesn't display critical flight information, the risk is simply accepted.	-	Low	Marginal
QTRR16	Reduce	Have an independent FMS for each pilot with redundancy.	Cross check FMS information and functioning before every flight	Low	Marginal
QTRR17	Reduce	Use of emergency oxygen masks for the pilot and crew.	Check oxygen tank levels before each flight	Low	Marginal
QTRR18	Reduction	The drop doors can be opened using a manual pump operated in case of emergency by the pilots.	Ensure the manual pump is correctly installed and functional before every flight	Low	Negligible
QTRR19	Acceptance	The failure of the deployment of the snorkel system does not pose risks to the safety of the flight.	-	Low	Negligible
QTRR20	Reduction	Regular maintenance between missions to check working condition of water pump.	Check the proper function of water pump during aircraft pre-flight checks	Very Low	Negligible
QTRR21	Reduction	Use multiple AC and DC buses for redundancy.	Check the design implementation of having two separate buses.	Low	Critical

Continued on next page

Table 11.4 – continued from previous page

Risk Code	Category	Mitigation Strategy	Verification	Likelihood	Impact
QTRR22	Reduction	Ensure regular maintenance and proper working condition of winch.	Check the proper functioning of winch during pre-flight checks for missions where winch might be necessary	Very Low	Marginal
QTRR23	Reduction	Overflow channels are present in the tank to disperse overflow water.	Ensure this design choice is implemented in water tank	Moderate	Marginal
QTRR24	Reduction	A fly-by-wire system is used to mimic the control forces of a Sikorsky S-70.	Simulate control forces from the fly-by-wire system to ensure they properly replicate those of the Sikorsky S-70	Very Low	Critical
QTRR25	Reduction	Low air pressure tyres are chosen which have a large contact surface and therefore exert less static pressure on soft surfaces.	Check the tyre pressure before each mission which potentially requires unimproved surface landings	Very Low	Marginal
QTRR26	Reduction	The aircraft's landing gear is properly positioned to ensure that no matter the loading condition it will not tip back.	Ensure c.g. range complies with landing gear placement.	Very Low	Critical
QTRR27	Reduction	Increase the structural stability by adding more stiffeners to increase the area moment of inertia and by partitioning the structure into bays	Finite element analysis of the structure subjected to compressive bending loads	Very low	Catastrophic
QTRR28	Reduction	Increase the structural stiffness by adding more material to increase the area moment of inertia and mass moment of inertia	Analysis of the aeroelastic response of a structure in a CFD model combined with a structural model	Very low	Critical
QTRR29	Reduction	Use a more heat resistant material or design a heat sink system	Analyse the temperature field with a heat transfer model of the structure	Very low	Critical

After identifying the mitigation strategies the pre- and post-mitigation risk maps were compiled as seen below in Figure 11.2a and Figure 11.2b.

The main takeaway from the risk maps is that the number of catastrophic risks is reduced by five risks, showing the effectiveness of the FireFly team's approach to concept-specific risk.

11.2. RAMS

Contributor/Author: Caitlin

Reliability, Availability, Maintainability and Safety (RAMS) are analysed for the aircraft to have a clear indication of when the aircraft becomes inoperable.

11.2.1. Reliability

Reliability of the aircraft is defined as the probability that it will function in a satisfactory manner for a specific period of time and operating conditions. A redundancy philosophy is applied to the aircraft to increase the reliability.

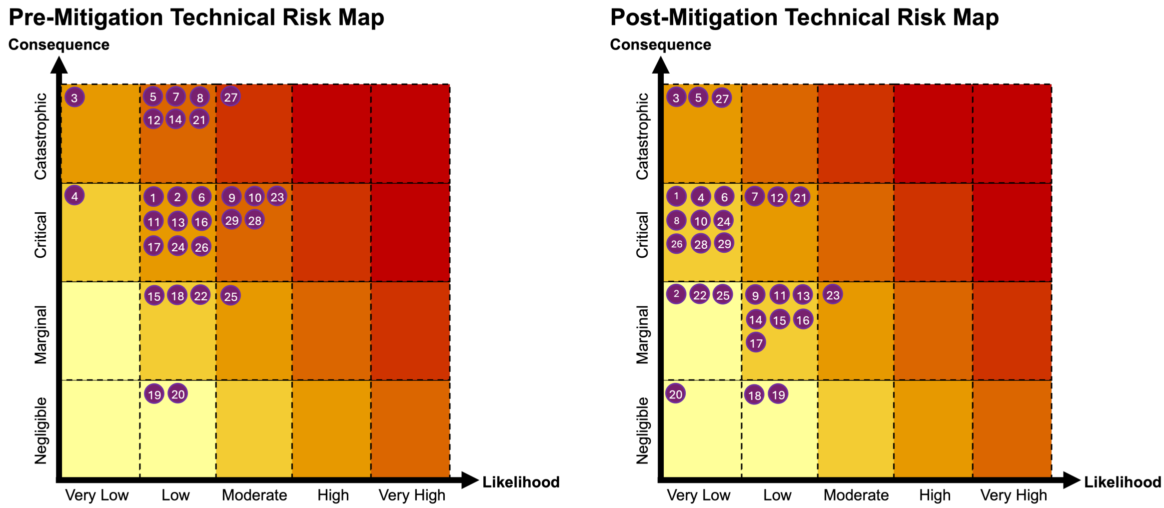

(a) *Technical risk map pre-mitigation.*

(b) *Technical risk map post-mitigation.*

Figure 11.2: *Technical risk maps for QTR risks.*

According to Roskam III [34], there are two scenarios to consider in terms of engine reliability:

- Engine Failure during take-off and/or go-around.
- Engine failure during overwater flight.

Both these scenarios are considered with the one-engine inoperative requirement. This requirement ensures flight is still possible with one engine out of order by having the rotor run with the opposing engine. A rate of reliability is estimated for individual components of the FireFly. The reliability of the engines should be at least 97%. This rate makes it very improbable that two engines are inoperative at the same time and thus reduces the risk of failure. The reliability can be further investigated once detailed design has been completed and is recommended to be done for the next design phase.

A redundancy philosophy is applied in order to stay operational should a component fail. An overview of redundant systems can be found in Table 11.5.

Table 11.5: *Redundancy in aircraft systems.*

System	Redundancy
Fuel system	The fuel system has two fuel lines connected to all tanks. This ensures fuel flow through at least one line at all times, if one of them were to fail. A visual of the fuel lines is found in Figure 8.1.
Hydraulic system	The hydraulic system has three main lines running through the aircraft which connect to different subsystems. Line A connects to the control surfaces in the wings, line B connects to the engines, or more specifically the rotor governors and line C connects to the landing gear and rear cargo ramp. Should one of the lines fail, then the other two will continue working as intended. This redundancy is also discussed in Table 8.1.
Engines	The engines are all connected by means of a shaft connection. This means that an engine can power a rotor blade that it is not directly attached to. This ensures that the aircraft stays operational should one of the engines be inoperative.
Electrical system	A transformer rectifier unit converts power used to supply charge to the batteries. These batteries will be able to power essential electrical systems in case of complete power failure. This was elaborated upon in Section 8.5.

11.2.2. Availabilty

The availability of the aircraft is important to know beforehand as firefighting missions can occur on a moment's notice. The aircraft should be able to take off at all times in an ideal case so that the time taken to get to a fire is minimal and damage can be minimised. Availability is measured in 'readiness', which is defined as the probability that the aircraft is ready when required.

A factor that reduces the availability of the aircraft is the downtime needed for maintenance; This time would preferably be minimised. To ensure this, regular inspections will be performed on the aircraft and any issues will be addressed immediately. Following this, the maintenance should take place during periods of time when wildfires have a lower chance of occurring.

Another factor is the turnaround time during a mission. Preferably, this should also be minimised since response time is an important variable that could make a large difference in the spread of a wild fire. The turnaround time will be needed to refill fuel and/or retardant foam, as well as the time it takes to get from the fire to the airport.

11.2.3. Maintenance

Maintenance is required for the aircraft to remain safe and operational. In the material analysis, it was determined that the aircraft should be safe to operate for ten years without maintenance. This was determined based on the fatigue analysis on the wing. However, as it is desirable to have the aircraft operational for a more extensive period, maintenance will be performed in set intervals.

In addition to the fatigue analysis, a crack propagation analysis was conducted, investigating the rate of crack growth of the chosen materials of the fuselage and wing starting from 1 mm. In ten years, the crack growth without maintenance will not exceed its critical crack length. However, it is recommended that

Other components that require regular maintenance are the water tank and pump system to ensure that the pumps retain their effectiveness. Also, the landing gear and control surfaces will need regular maintenance to ensure a smooth mission operation.

In external communications with an experienced firefighting pilot, it was found that aircraft undergo maintenance on a daily basis. This includes pre-flight, mid-flight and post-flight inspection. Additionally, the aircraft undergoes a weekly four-hour inspection and, annually, an inspection that can last several months. The annual inspection leaves plenty of room for repair should it be needed.

Last but not least, aircraft undergo an inspection after every 50 flight hours, accompanied by a test flight to ensure the proper functioning of all systems. It was decided to have the same maintenance schedule for the FireFly as many systems are on board for which optimal performance is required. This information is taken into account in Table 11.6 where the safety-critical functions are described.

11.2.4. Safety

Safety is a high priority during the design of an aircraft. The danger posed to humans or equipment and structures is kept to a minimum whenever possible and safety-critical functions are applied to the aircraft.

Since the aircraft is an aerial firefighter, the environment in which it operates, brings a lot of risk.

If a failure of components of the aircraft causes catastrophic failure to people, the aircraft or the environment, they are called safety critical functions or systems. The severity of the malfunctions is classified in the same way as was done in Section 11.1, using 'negligible', 'marginal', 'critical' and 'catastrophic'. In Table 11.6 safety critical functions and their mitigation strategy are shown.

Table 11.6: *Safety critical functions and mitigation strategy.*

System	Malfunction	Severity and Effect	Mitigation
Snorkel	Leakage	Negligible, if the snorkel leaks, it does not bring any risk to people, structures or the environment. However, it could influence the firefighting mission negatively by having a potentially longer response time.	The snorkel should be inspected per the manufacturer's specification to avoid leakage from occurring.
Snorkel	Clogged snorkel	Moderate, the snorkel will not be able to gather water as intended and will severely impact the response time, therefore endangering the environment in case of a wildfire.	The snorkel should be inspected before, during and after every mission to clear any debris.
Pump	Pump malfunction	Negligible, the FireFly will not be able to refill if the pump malfunctions and as a result will have to fly back to the airport whenever the payload is dropped.	The pump will need to have maintenance per the manufacturer's specification, in addition to inspection before, during and after a mission.
Landing gear	Nose strut fails	Critical, both vertical and conventional landing is no longer possible. Belly landing is still possible, however.	Maintenance will be done every firefighting week during the weekly maintenance to avoid cracks and fatigue from occurring.
Landing gear	Main strut fails	Negligible, there are four struts in total on the main landing gear such that should one fail, the other struts could still carry the weight.	Inspection should be done every week during the weekly maintenance such that cracks can be detected and maintained if necessary.
Landing gear	Wheel falls off	Moderate, the FireFly will have to land vertically and carefully such that no other systems are damaged.	Maintenance should be performed every week to ensure failure will not occur.
Landing gear	Landing gear doesn't deploy	Moderate, the FireFly is not able to land safely without landing gear as the structure might get damaged.	The aircraft will drop any payload on board and have a reinforced fuselage belly. The aircraft will then land on its belly, where it is important to descend at the minimum descent rate. This is done to avoid any structural damage to the aircraft.
Water Tank	Leakage	Negligible, there will be less payload to drop on or nearby wildfires.	Inspection should be done every week. Additionally, maintenance will be done annually.
Wing structure	Buckling	Catastrophic, the FireFly will no longer be able to keep itself in the air due to the lack of lift being generated.	Regular inspection should be done to avoid structural failure. Maintenance will be performed every 180 flight hours.
Fuselage Structure	Buckling	Critical-catastrophic, the Firefly would be generating less or no lift depending on the severity of the structural failure.	The payload should be dropped immediately in order to alleviate the stresses acting on the fuselage. To avoid buckling, maintenance should be done every 50 flight hours, in addition to the weekly maintenance performed.

Continued on next page

Table 11.6 – continued from previous page

System	Malfunction	Severity and Effect	Mitigation
Propeller blade	Structural failure one blade	Critical, the blades could damage other systems within the aircraft.	Blades are not positioned next to critical systems and people in the aircraft. If one blade breaks, the payload should immediately be dropped. Of the remaining three rotor blades, the two opposing blades should carry the main load and the third one will act as a stabiliser. The aircraft should be able to stay in the air as it is generating just enough lift. The blades should undergo inspection before every mission.
Propeller blade	Two-blade failure	Catastrophic, the aircraft would become unstable and unable to stay in the air.	If two blades fail, the aircraft is unable to produce enough lift to continue hovering and will not produce enough forward thrust in horizontal flight. Regular maintenance will be performed to reduce the risk of failure. There is a very small chance of regaining control if the fuselage or other structures are not damaged and the operational blades are of opposing engines.
Engines	One engine failure	Moderate, the propeller blade attached to the engine could stop spinning and generating lift or thrust.	The propeller on the engine will be able to operate on the power of the opposing engine.
Engines	Two engine failure	Critical, the two accompanying propeller blades will stop spinning and additionally, less power will be generated.	The two inoperative propeller blades can still be utilised by employing the shaft connection to the other engines. As a consequence of less power being available, the FireFly will need to make a controlled descent.
Engines	Three engine failure	Catastrophic, there is not enough power to keep the aircraft in the air in addition to not being able to generate enough power for the electrical systems.	Inspection on the engines is done before, during and after every mission as well as weekly maintenance. This should avoid any engine failure.
Engines	Engine overheating	Critical, there is a risk of fire.	A firewall will be placed in between the engines and the rest of the structure such that a potential fire has no chance of spreading to the rest of the structure.

Continued on next page

Table 11.6 – continued from previous page

System	Malfunction	Severity and Effect	Mitigation
Fuel tank	Leakage	Moderate, the fuel will leak out of the tank and potentially shorten a mission.	A bladder tank is used as well as an aluminium tank. Should one of them be leaking, the other would still contain the fuel. Regular inspection should be done in order to assess when maintenance is required. Full maintenance should be done every 360 flight hours
Hydraulic system	Pump failure	Moderate, the hydraulic system is designed to be able to operate with one pump inoperative.	The pumps will undergo maintenance per the manufacturer's specifications to avoid failure.
Hydraulic system	Tank failure	Moderate, no extra fluid can be added or subtracted from the lines, but the system still works	The hydraulic system should be able to operate until the pressure in the lines has decreased below a certain threshold. The aircraft should land immediately to avoid potential accidents.
Hydraulic system	Fire	Moderate, the hydraulic fluid could burn and damage the system.	The hydraulic system will use fire-resistant fluid such as MIL-PRF-83282 which is a synthetic hydrocarbon[1].

[1] Link [cited on 13-06-2024]

12 | Market Analysis and Return on Investment

For the FireFly to be a success, it not only needs to be designed well, but it also needs to be financially viable. This market analysis is an iteration of the earlier market analysis in the Baseline report [14]. However, this analysis focuses on the financial viability of the FireFly project. This section analyses the growing AFF aircraft market and defines the relevant market segments and competitors for FireFly, which aids in understanding and predicting possible risks and opportunities. Using this analysis, a market gap for the FireFly is identified in the mid- to high-capacity aircraft and helicopter range. Within this range the market volume is estimated at 77 units per year and a market share of 19% is found to be achievable for the FireFly. With this market share and a selling price of $60 million, a Return on Investment of 7% can be reached after 10 years and a break-even is reached at a hundred units sold.

12.1. Market Analysis

This market analysis first identifies the relevant stakeholders and market segment of FireFly, it then assesses the competitiveness of the market and identifies competitors. It looks at the future market and then estimates the market volume and the achievable market share for FireFly.

Stakeholder analysis

Contributors/Authors: Bob

In the baseline report [14], stakeholders were identified, in this report these are iterated from a business standpoint. In Figure 12.1 they are ranked based on interest and power. Below the most relevant stakeholders are defined as key with regard to their influence on sales of the aircraft:

- **Fire Departments** - **Key**, these are potential customers and it is important that they recognise the added value of FireFly to their fleet.
- **Aircraft Owner** - **Key**, these are also potential customers, as a lot of AFF aircraft are privately operated by providing service when and where necessary.
- **Manufacturer** - **Key**, if the manufacturer has problems production will halt meaning delivery of new aircraft and spare parts is threatened.
- **Pilots** - **Key**, pilots will be the end user of the FireFly, if FireFly is uncontrollable or unsafe the pilots will inform their superiors which can be detrimental to sales.
- **Ground Firefighter Crew** - **Non-Key**, they are affected by the operations of FireFly but have little power over acquiring the aircraft.
- **Maintenance Instance** - **Non-Key**, the FireFly needs to be maintainable to guarantee operational readiness. Maintenance service must be accessible to the owner of the aircraft.
- **Local population** - **Non-Key**, the local population can have political influence on the government if wildfires threaten their homes.
- **Fuel/Retardant Suppliers** - **Non-Key**, critical to operations, they have little influence on acquiring the FireFly aircraft however.
- **Airbases** - **Non-Key**, they affect deployment facilitation and need to be informed so that they account for AFF operations.
- **Air Traffic Control** - **Key**, they regulate the flight paths and ensure safety in the airspace. Their cooperation is essential for operational efficiency.
- **Regulatory Agencies** - **Key**, if FireFly does not comply with regulations, regulatory agencies have the power to ground it.
- **Investors** - **Key**, these will provide a big part of the development cost, their satisfaction is crucial to the project's success.
- **Government** - **Key**, the government often provides the funding for the purchase of new AFF aircraft. So not only the fire departments but also the government need to recognise the added value FireFly will bring.

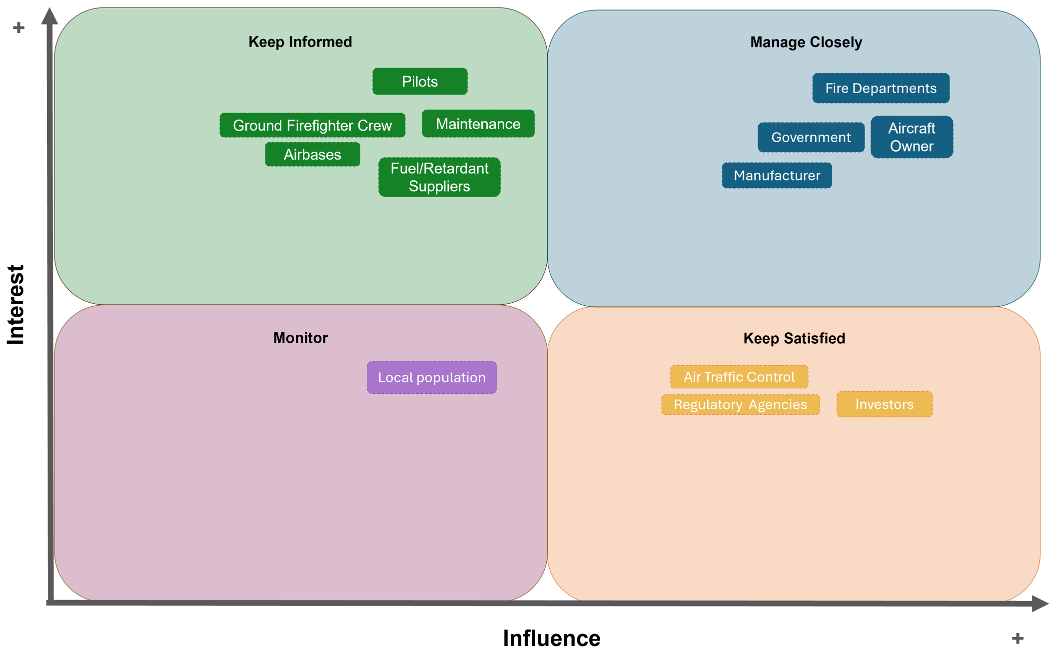

Figure 12.1: *Stakeholder map*

Market Segmentation

Contributors/Authors: Hanna, Bob

To specifically analyse the possible solutions and current market trends, the relevant market for FireFly has to be defined by considering 3 factors: AFF type, service and region. This way, the relevant competitors come to light, and sales possibilities are investigated globally. Below, the factors and their categories are listed and explained:

- **Aircraft types**
  - **Air tankers**, aircraft that have their retardant tanks filled at base.
    - (Single Engine) Air Tankers (SEAT), aircraft with a capacity of 400 to 6000 litres.
    - Large Air tankers (LAT), aircraft with a capacity of 6000 to 19000 litres.
    - Very Large Air Tankers (VLAT), aircraft with a capacity of over 19000 litres.
  - **Scoopers**, aircraft with the ability to land on water to refill their tanks.
    - Single Engine Scoopers (SES).
    - Multi Engine Scoopers (MES).
  - **Rotorcraft**, helicopters with the ability to carry retardant either in (external) tanks or buckets.
    - Type 1, rotorcraft with a capacity of over 10000 litres.
    - Type 2, rotorcraft with a capacity between 1200 and 10000 litres.
    - Type 3, rotorcraft with a capacity between 450 and 1200 litres.
- **Service**
  - **Fire Supression**, (preventively) laying down retardant to suppress wildfires and keep them under control.
  - **Air tactical support**, providing visual support and guidance to other aircraft and ground personnel.
  - **Personnel and Equipment transport**.
  - **Search, rescue and evacuation operations**.
- **Region**
  - North America
  - Europe
  - Australia
  - Latin America
  - Asia Pacific

- Middle East and Africa

Market Gap

Contributors/Authors: Hanna, Bob

As of now, the market is dominated by either large fixed-wing air tankers or smaller rotorcraft which can be characterised by scooping and VTOL capabilities. This opens the possibility of filling that gap with a new aircraft combining the capabilities of both of those aircraft types - a fixed-wing aircraft with VTOL capability. Additionally, no special-built aerial firefighter is being designed right now except for a new iteration of the Canadair CL-415. The majority of aerial firefighters on the market are retrofitted from outdated aircraft, meaning that they do not possess the best technology, as this was not their purpose. What's more, this has led to an increased number of accidents in aerial firefighting as compared to other aircraft operations. Designing an aerial firefighter specifically for AFF, using the newest technology would be an innovative solution bringing technologically modern design to the aerial firefighting industry.

Target Market

Contributors/Authors: Hanna, Bob

From the market segmentation, it was determined that the target market segment for the FireFly will be:
Aircraft type: Fixed-Wing, SEAT/LAT and MES & Rotorcraft, Types 1 and 2
As FireFly combines both functionalities, it will be competing in the market along with these types.
Service: Fire Suppression.
FireFly having a relatively large water tank would make it a fire-extinguishing aircraft.
Region: North America/Europe/Australia.
As the aerial firefighter is usually considered to be military equipment, it is expected that it will be operated in NATO countries and will not be sold into regions with geopolitical conflicts. What's more the chosen regions have a large number of wildfires, meaning that there is a market need for new equipment in those regions.

SWOT Analysis

Contributor/Author: Hanna

The Strengths, Weaknesses, Opportunities and Threats (SWOT) Analysis was performed to identify the risks associated with the Market. In the analysis both internal, design specific risks and strengths are highlighted along with external risks and opportunities associated with how the product would interact with the market. This is presented in Figure 12.2.

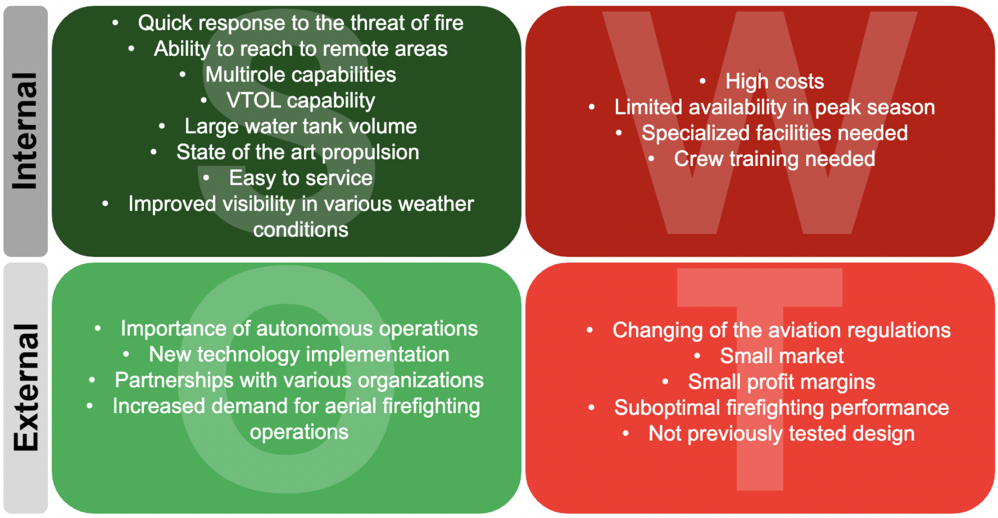

Figure 12.2: *SWOT Analysis.*

From the SWOT Analysis, the main barriers to entry were identified as:

- Expensive acquisition and maintenance.
- All pilots and crew will need to go through specialised, lengthy training, which will likely cause additional costs.
- The compensation for the highly specialised crew is expected to be on a high level, while they are working only several days per month.
- Aerial firefighting aircraft are usually classified as military equipment and therefore there could be political restrictions while trying to sell the aircraft to another country [1].

Marketing Strategy

Contributors/Authors: Hanna, Bob

To come up with a marketing strategy, first, the customers have to be identified. From the stakeholder analysis, it is established that for aerial firefighting, the typical customers are national/regional AFF organisations, governmental departments and private operators that offer their services to (local) governments. Their decisions regarding the purchase of AFFA will be primarily driven by the increasing number of wildfires in the region and the state of the currently owned fleet. The key decision maker was identified to be the Head of the Environmental/Security department of each region.

Entering the market with a novel design like the FireFly can be difficult. This can be mitigated by initially focusing on economically prosperous areas like California which will have more funding to purchase the first units. This way the capabilities and effectiveness of FireFly can be proven and show to other potential customers that it is worth the investment. The channels that will be used to reach stakeholders and customers have been identified as majorly regional fairs for firefighting, aviation conferences and fairs, air shows and security summit meetings. Through these channels, the marketing message will mainly focus on the versatility of the design both in AFF operation and in other applications.
The pricing strategy resulting from those market factors would have to ensure that the aircraft remains affordable, with a sufficiently low profit margin while ensuring a good return on investment. Typically, for an aerial firefighter of a similar size to FireFly, the selling price ranges between 40 and 70 million dollars depending on size and the age of the design.[2] [3] The delivery of aircraft would be prioritised based on the price offered by the customer, meaning that if the profit is larger, the aircraft would be delivered faster to the customer.

Competitors

Contributors/Authors: Hanna, Bob

To assess the competitiveness of the market, a broad analysis called Porter's five forces is used. This type of analysis is useful for getting a general idea of what the market is like as a whole. From these 5 forces, it is

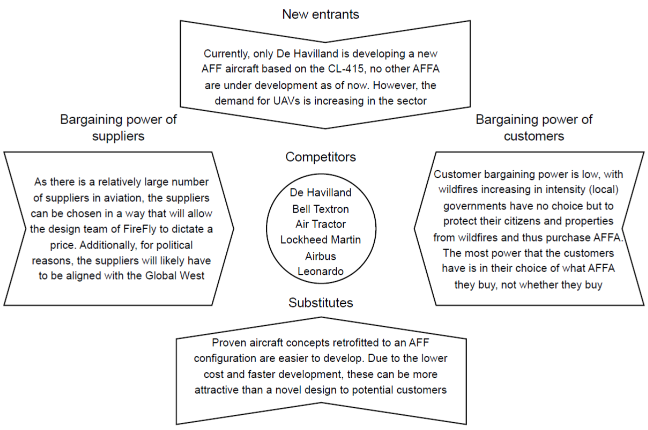

Figure 12.3: *Porter's 5 forces analysis.*

determined that the main competitors for FireFly will be Boeing, De Havilland and Sikorsky. These three companies have modern AFF aircraft in development or production with comparable capacity and capabilities as

[1] Link [cited on 19-06-2024]
[2] Link [cited on 18-06-2024]
[3] Link [cited on 18-06-2024]

FireFly;

- Boeing Vertol CH-47 Chinook, price: $65 million, capacity: 11000 L, max. velocity: 302 km/h, MTOW: 24500 kg [4]
- De Havilland DHC-515, price: $56 million, capacity: 7000 L, max. velocity: 360 km/h, MTOW: 20000 kg [5]
- Sikorsky S-70 FIREHAWK, price: $25 million, capacity: 3800 L, max. velocity: 268 km/h, MTOW: 10000 kg [6]

Market Forecast

Contributors/Authors: Thijs

With climate change becoming more and more apparent, an increase in wildfire frequency and intensity can be observed around the world. It is estimated that by 2030, global wildfire frequency will increase by 14% and up to 50% by 2100. This means that the aerial firefighting market is likely to increase due to the increased demand. The market increase is difficult to estimate but most market research reports point to an estimated global Compound Annual Growth Rate (CAGR) of 5.5-7%. The resulting market size is therefore estimated at 2-4.5 Billion USD in 2032.[7]

The largest growth is estimated to occur in the Asia-Pacific region with an estimated CAGR of 7.8% due to strong economic growth in the area and an increasing pattern of wildfires. Europe and North America show lesser growth but are still projected to increase their ownership and operation of aerial firefighting aircraft. The market share of rotorcraft is increasing relative to fixed-wing aircraft[8]. This is due to the increased versatility of rotorcraft at the cost of fast response times.

Market Volume of the Product

Contributors/Authors: Hanna, Bob

To estimate the market volume of the FireFly, the market growth rate, aircraft lifetime and global AFF fleet are necessary. In FireFly's case, it will only be competing with a segment of the total AFF market as mentioned in Figure 12.1. So for this estimate, only this segment is considered.

It is estimated that the US has about 500 operational aerial firefighters the US federal government has 300 aircraft in service and CAL FIRE just by itself already has 80 aircraft in its future fleet. Australia has a fleet of about 500 aerial firefighters in total, while in the EU an estimated total of 400 AFF aircraft are operational. This means the total comes down to 1400 aircraft. Through empirical analysis of the CAL FIRE, Australian and EU AFF fleets it is estimated that 42% of these aircraft are of the types that the FireFly is competitive with. Leading to a relevant fleet of 588 aircraft.
Regarding aircraft lifespan, owing to difficult conditions the typical lifetime of an aerial firefighter is between 10 and 15 years, meaning that the fleet of aircraft will need to be replaced or serviced.
As for the annual growth rate, as mentioned in Figure 12.1, the number of wildfires is increasing globally. Therefore the number of aircraft on the market will increase with time as can be seen from the CAGRs in Figure 12.1. In this estimation, the annual growth rate will be equal to 6.5%, derived from the CAGR of the market. [9]
Finally, the following driver tree shows the estimate of the total number of aerial firefighters sold each year; the market volume.

[4] Link 1 Link 2 Link 3 [cited on 18-06-2024]
[5] Data based on CL-415 Link 1 Link 2 [cited on 18-06-2024]
[6] Link 1 Link 2 [cited on 18-06-2024]
[7] Link 1 Link 2 Link 3 Link 4 Link 5 [cited on 11-06-2024]
[8] Link [cited on 11-06-2024]
[9] Link 1 Link 2 Link 3 Link 4 Link 5 [cited on 18-06-2024]

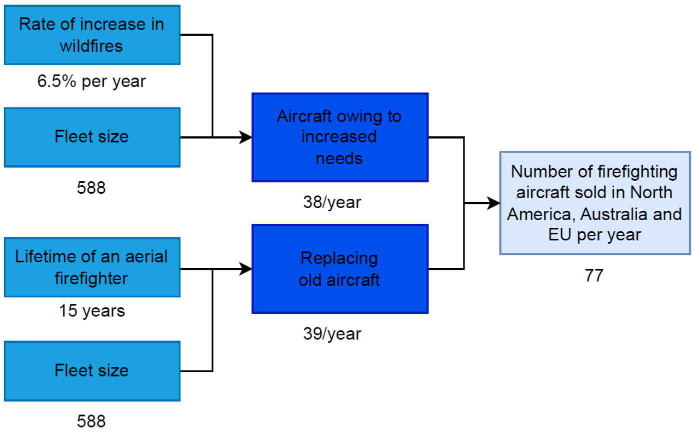

Figure 12.4: *Driver tree for market volume.*

Expected Share of the Market

Contributors/Authors: Bob

Using the market volume of 77 units per year together with the 12 units per year production rate of the FireFly found in Subsection 12.2.1, the achievable market share can be estimated, assuming that every FireFly produced is sold. With an average selling price of $50 million per unit, the total accessible market is worth $3.9 billion. This means that at a selling price of $60 million, the achievable market share is 19%. In units, the achievable market share is 15%.

12.2. Return On Investment (ROI)

In this section, first, the development and production costs for the FireFly project are calculated after which the direct operational cost is estimated. Finally, a projection is made on the Return on Investment.

12.2.1. Development and Production Cost

Contributors/Authors: Thijs, Sven

The cost of designing, testing and operating a new aircraft can be split up into two main phases; Research, development, test & evaluation cost (RDTE) and the actual production of the aircraft. For determining the Firefly's programme cost, the method Roskam proposed is used [37]. This method is a long, detailed process with statistical relations thus providing a good preliminary ballpark of the aircraft costs.

The inputs for the estimation are the MTOM in lbs, the maximum speed in kts along with some other parameters that had to be assumed. For the maximum speed, Roskam states that for commercial aircraft, the cruise design speed must be taken; for military aircraft, the level speed at full power must be taken. Due to the nature and mission of the aircraft, for past estimations, it was assumed to be a military aircraft but due to its VTOL capabilities (and thus grand excess power during cruise), the choice was made to assume the dash speed of 400 km/h.

RDTE cost

First, the RDTE cost was computed. This cost is broken down into five separate costs in Table 12.1. In this analysis, no RDTE profit is assumed. At this stage, the number of prototype aircraft was assumed to be eight. According to Roskam, this is at the high end for commercial aircraft and the low end for military aircraft and therefore seemed appropriate for the FireFly. Additionally, a cost factor of 1.5 was applied to account for the complexity and novelty of the design which is likely to increase the development cost. The cost of the aircraft avionics could not be determined exactly since no specific systems were chosen, so the cost of the avionics was set at 15% of the aircraft cost which in the first iteration was set at 35 million USD. Finally, The test and simulation facilities cost must be scaled according to the level of specialized testing facilities required for the aircraft development. This factor ranges between 0 and 0.2 where 0.2 represents an intense level of specialized facilities (as for the B-2 bomber and X-29). This level was set at 0.05 for the FireFly as some new facilities must likely be set up, but a lot of testing facilities already exist and can therefore be used.

The individual costs and total RDTE costs (rounded up to the nearest million) are compiled in Table 12.1

Table 12.1: *The estimated individual costs and total RDTE cost of the FireFly.*

Cost	Description	Amount [Million USD2024]
C_{aed_r}	Airframe engineering and design cost	134.6
C_{dst_r}	Development support and testing cost	33.7
C_{fta_r}	Flight test airplanes cost	678.5
C_{fto_r}	Flight test operations cost	22.0
C_{tsf_r}	Test and simulation facilities	43.4
C_{RDTE}	**Total cost**	913

Manufacturing cost and unit cost
Once the concept has been designed, tested and certified, the manufacturing process starts. Here, the different costs of each aircraft are estimated. This cost is split up into:

- Airframe engineering and design cost (C_{aed_m})
- Airplane programme production cost (C_{apc_m})

The airframe engineering cost consists of the funds required to amend/append the design after production of the initial design has started. The airplane programme production cost contains the material, tooling, personnel and subsystem costs that are required to produce a certain number of aircraft. The inputs for these costs are the same as the RDTE costs and flow down from them. The total manufacturing cost depends on the number of aircraft to be made. Since the RDTE cost is also included in the cost of each individual aircraft, a higher production size leads to a cheaper aircraft. In Figure 12.5, the individual aircraft production cost is plotted against the total number of aircraft produced. It can be observed that at the low production numbers (10-50), the aircraft price is quite high but reaches an asymptotic value of around 35 million USD quite quickly. The manufacturing cost is a function of the aircraft production rate. For this analysis, a production rate of one aircraft per month was assumed. A sensitivity analysis was performed into the impact of this number which showed that the aircraft price would change less than 0.5% when the aircraft production rate was increased. The rate of one aircraft per month was thus kept and assumed (for now) to be correct and realistic.

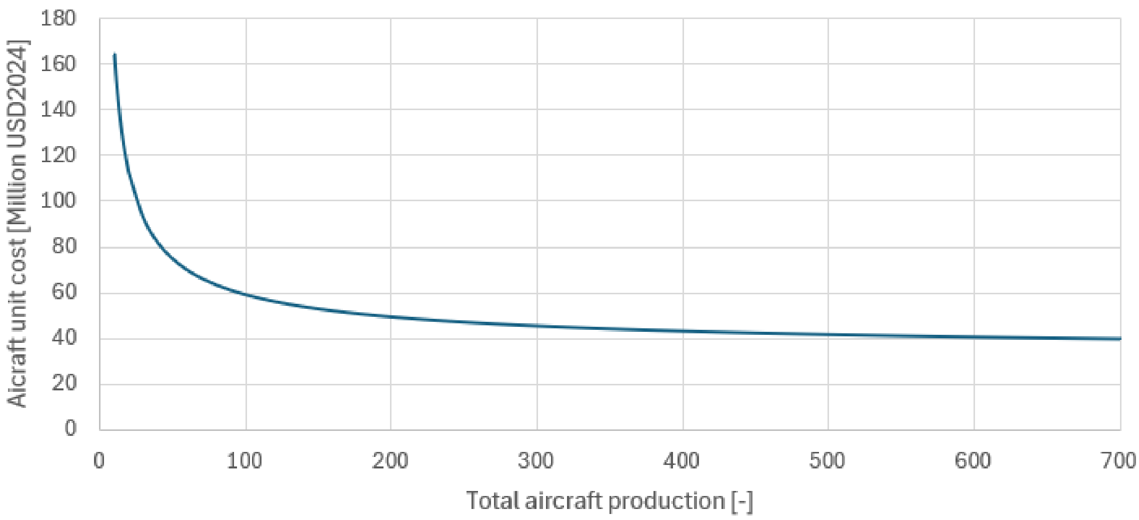

Figure 12.5: *The estimated unit cost of the FireFly at different production sizes.*

The final cost of the aircraft is therefore between 50 and 60 million USD2024 based on the likely production size of FireFly: 80-150 aircraft. This number does not include the profit that is to be made by selling the aircraft. Input factors that had to be estimated based on the aircraft design were all taken on the high end as an overestimation of the design and production costs are preferable over an underestimation.

To determine the market price of the FireFly aircraft, a profit margin has to be added to the estimated unit cost of the aircraft. The first estimate of the profit margin will be set at 10% of the unit production cost according to Roskam[37]. This margin was chosen because the methodology developed by Roskam was also used to determine the RDTE cost and production unit cost. For the estimated production size of 80 to 150 aircraft, the market unit price of the product is in the range of 50 to 70 million USD2024 when the profit margin is added.

Direct Operational Cost

Contributor/Author: Hanna

To calculate the direct operational costs, the following components were decided to be taken into account. If not mentioned otherwise the values and methodology in Table 12.2 were taken from [51].

Table 12.2: *Capital and insurance costs summary.*

Item	Explanation	Min	Max
	Capital and insurance cost		
Aircraft flight hours [h per year]	Estimated number of hours the aircraft will be used for missions per year	160	200
Finance and insurance cost [%]	Estimated costs regarding financial reporting and insurance as a percentage of flight hours	5	10
Net flight hours[h per year]	Estimated number of hours taking into account insurance and financial costs	168	220
	Fuel costs		
Jet A-1 fuel cost [$ per L]	The fuel will be bought in bulk in order to hedge fuel costs and avoid market fluctuations. The price chosen is accurate for the year 2023.[10]	-	1.4
Fuel use [l per hour]	Based on the chosen engine configurations, the following fuel flow was calculated.	-	4000
Fuel cost [$ per flight hour]	Calculated based on fuel flow and fuel cost	-	5600
Fuel cost [$ per year]	Calculated based on the net flight hours per year	940000	1230000
	Crew costs		
Pilot salary [$ per year]	The salary was increased to account for the high specialisation of the pilot. There are 2 pilots.	70000	110000
Crew salary [$ per year]	The standard salary of a firefighting crew member was included. The number of crew members could range from 0 to 5	30000	40000
Total crew cost [$ per year]	The lower value was obtained for the case when there is no crew on board and the higher value was obtained for a full capacity with 5 crew members	140000	420000
	Infrastructure cost		
Hangar costs [$ per year]	The infrastructure yearly fee for storing the aircraft in a hangar [11]	25000	35000
	Maintenance costs		
Mechanic wrap rate [$ per hour]	The mechanical costs containing both direct and indirect costs associated with a mechanic contract	60	100
Maintenance rate [- per flight hour]	The maintenance rate expressed as a fraction of the total flight hours	0.25	1

Continued on next page

[10] Link [cited on 12-06-2024]
[11] Link [cited on 13-06-2024]

Table 12.2 – continued from previous page

Item	Explanation	Min	Max
Total maintenance cost [$ per year]	Maintenance cost taking into account the fraction of time that the aircraft will need servicing	2500	22000
	Total costs summation		
Direct operational cost [$ per year]	The sum of minimum and maximum expected total costs	**1100000**	**1700000**
Direct operational cost [$ per flight hour]	The hourly cost	**5000**	**10000**

12.2.2. Projected Return on Investment

Contributor/Author: Bob

After defining the market for the FireFly, analysing the achievable market share and establishing its RDTE and Production costs, an estimate of the ROI can be made. The ROI is established by dividing the positive balance between the total cost of development and production and the number of aircraft by the total cost. This ROI is analysed to see how many aircraft need to be sold to turn a profit and if this is achievable with the current and future AFF market. For this analysis, any lifetime engineering costs have not been taken into account. These are costs that come up due to, amongst others, technical defects, warranties and updates. However, this is compensated for as the RDTE and manufacturing costs have been estimated conservatively. In further iteration and more in-depth analysis of the ROI, lifetime engineering will need to be accounted for.

By first analysing the return on investment for various prices per unit, a reasonable selling price of $60 million is found. As can be seen in Figure 12.6, this price results in a break-even at about a hundred units sold while being competitive compared to the Boeing CH-47 Chinook. Resulting in a return on investment of 7% after ten years if the market share from Figure 12.1 is achieved. Selling a hundred units is realistic in the AFF market; of the CL-215 and CL-415, 125 and 95 units have been sold respectively.

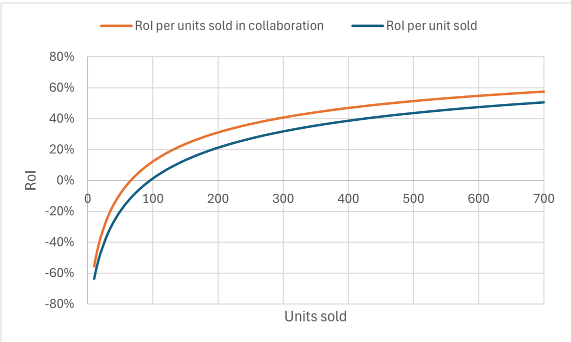

Figure 12.6: *Projected Return on Investment against the number of units sold.*

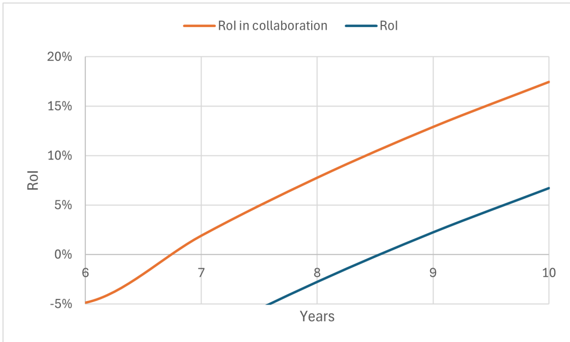

Figure 12.7: *Projected Return on Investment after a decade of achieving target market share.*

To further increase this return on investment while keeping the price of the FireFly competitive, partnerships with established industry names should be investigated. Such a proposal can take on multiple forms and significantly lower RDTE costs. An established industry partner has decades of experience in developing (tilt)rotorcraft and has access to advanced testing facilities and production plants. Taking these advantages into account in the RDTE and production cost calculations from section Subsection 12.2.1 results in the RDTE cost decreasing by 20% and production cost decreasing by 4% per unit at 100 units produced. The blue curves in the figures above reflect the effects of this. The break-even point is reached at 65 units and, after a decade, the ROI is 17%.

Some suggestions for possible partners would be Bell Textron and Boeing as these have decades of experience in successfully developing tiltrotor aircraft and even did a concept study on a tandem wing configuration like the FireFly.[52]

13 | Further Development

After having completed the preliminary design phase the next step for the FireFly project is to move on to further detailed design and operational design. This chapter gives an outline of the activities that should follow for the project to move forward after the DSE. The project design & development logic diagram is presented as well as the Gantt chart showing the timeline for the tasks to be completed. Finally, a cost breakdown structure is presented, showing the total cost of project assuming production of 100 FireFly aircrafts.

13.1. Project Design & Development Logic

Contributor / Author: Hanna

The Development Logic diagram shows what should be done after the Final Report submission to complete the design of the FireFly. It incorporates all the necessary steps from the further Detail Design Phase, until the End-Of-Life while explaining the operations. It should be mentioned that it starts at phase 3 as phase 1 (conceptual design) and phase 2 (preliminary design) have already been completed.

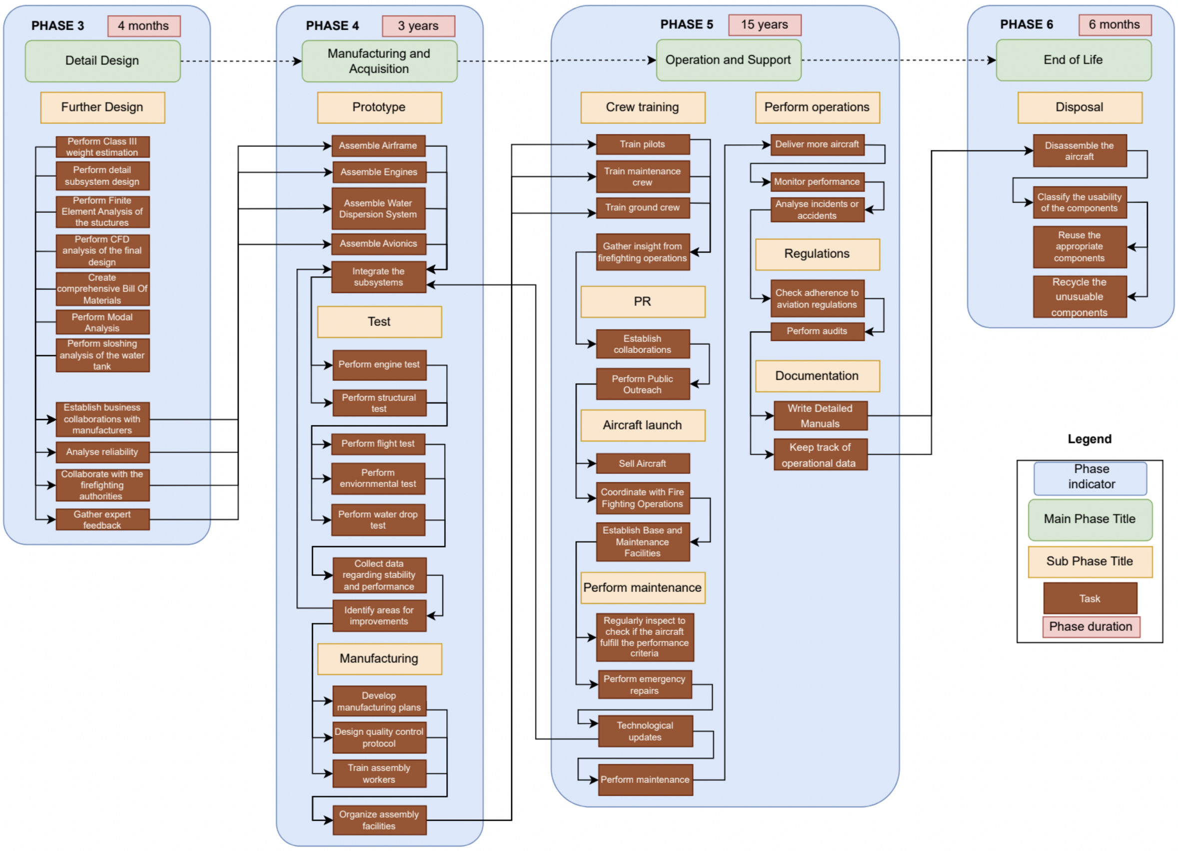

Figure 13.1: *Project Design & Development logic diagram.*

13.2. Gantt Chart

Contributor / Author: Caitlin

The project Gantt chart was made for activities after the end of the current project. It outlines the design steps that still need to be taken. As was done for the current design phase, the Gantt chart includes the end and start date for tasks, as well as a rough estimate of the days needed. The chart outlines further design processes up until the point where the aircraft is to be sold. Further activities shall be done during the operational period such as maintenance and inspection. The tasks are the same as in Figure 13.1 but are cut off in the Gantt chart. This is due to the limitations of the programme.

Figure 13.2: *Caption for image 1*

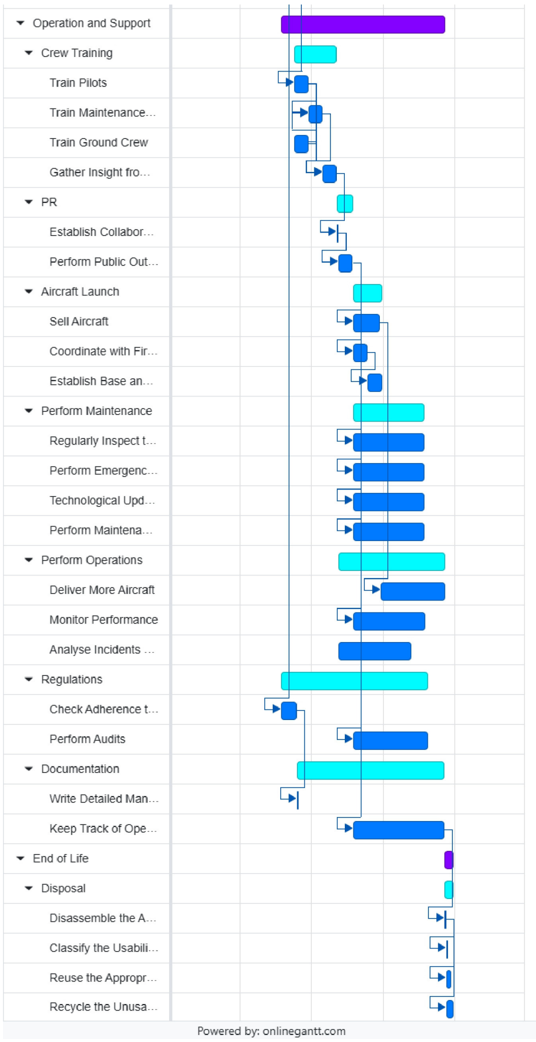

Figure 13.3: *Caption for image 2*

Figure 13.4: *Overall caption for both images*

13.3. Cost break-down structure

Contributor / Author: Johannes

A detailed cost breakdown structure in the case of the development of 100 FireFly aircraft can be found in Section A.1. This diagram is based on the development and manufacturing cost discussed in Subsection 12.2.1 as well as an additional breakdown of these costs following from the PD&D diagram. Tasks that are present in the PD&D diagram, but do not contribute to the cost of the project are not included in the cost breakdown structure. It is assumed that during manufacturing the total cost is split into: 50% structure and integration, 25% engine assembly 15% avionics assembly and 10% final assembly.

14 | Conclusion

Author: Caitlin

The aircraft that was chosen in a trade-off in a previous phase was designed in this report. It is a quad tilt-rotor firefighting aircraft that was named the FireFly for its bright colours and double-wing configuration. Many systems and subsystems have been designed throughout the project. The most notable conclusions are presented here.

After using a functional flow diagram to determine what function and performance was required from the FireFly, the necessary system and subsystem requirements were iterated and created. The most important function to fulfil was to be able to carry a payload of 10000L of water that was to be used to extinguish a fire. Additionally, the speed of the aircraft should be above 400km/h.

Sustainability was an important consideration in the design of this aircraft. Many sustainable options were not viable for firefighting, so instead the focus was put on how many emissions would be evaded by putting out wildfires. In areas such as material selection, an emphasis was put on using as many recyclable materials as possible.

The material selection was done for the fuselage, wings, water tank, rotor blades and fuel tank. It was found that one of the stronger and more durable aluminium (AL2195 T8) was the most suitable choice for the fuselage, water tank and wings. A fatigue analysis and crack propagation analysis were done on the material and structures to ensure a lifetime of at least ten years. Additionally, a production plan was created for the production phase of the project. From the material characteristics and the geometry obtained from the class II weight estimation, it was possible to determine the structural elements of the aircraft. A stress analysis was done to determine the thickness of the fuselage and the wing boxes.

The propulsion system consisted of four AE1107F tilt rotors with 12 m diametre propeller blades. This was determined in the aerodynamics analysis. The aerodynamics system also helped to determine the wing sizing which was primarily sized for horizontal cruise. The rotors were primarily sized for hover flight and then assessed to see what their performance was in horizontal flight.

The aircraft was determined to be stable in horizontal flight, however, it is recommended to implement a closed-loop control system for hover mode to ensure stability and control. The FireFLy is expected to be controllable and stable in horizontal flight, however, the methods used were not completely adjusted to tandem configuration. Therefore it will need to be iterated but the results look promising.

The configuration of the aircraft was determined for the external layout and for the internal layout. It was found that positioning of the centre of gravity required the landing gear to be placed outside of the fuselage and as such additional sponsons were added. These were then also utilised as fuel storage in the fuselage. The internal layout consisted of the hydraulics system, the fuel system, the cockpit layout and the water tank system.

After creating a compliance matrix on the user requirements, it was possible to do a feasibility analysis. This analysis showed that it is necessary to perform further assessments on certification and reliability as the FireFly does not comply with these requirements.

Furthermore, the risk analysis investigated any risks associated with the project of designing the aircraft. It was used as a tool to integrate safety into the design. The Reliability, availability, maintenance and safety analysis showed that the biggest risk during the mission is if one of the rotor blades fails. The aircraft would lose lift and power such that it would become much more unstable.

Last but not least, the Return on Investment estimated that there would be a profit margin of around 17% after a decade. This is a promising figure which indicates that the product is financially viable.

Future development of the aircraft would consist of more detailed design, production and testing of the aircraft. Recommendations for future development include further analysis of the aerodynamics and the propulsion to determine the feasibility of the design. Additionally, further analysis should be conducted on the effect of heat transfer through the structure and how to slow it down.

Bibliography

[1] Brundtland, G., and Khalid, M., "Our Common Future," *Brundtland Commission*, March 1987, p. 41.

[2] Lindsay, K., and Pelai, R., "Canada needs to get ready for a future fraught with fire: How can the forest sector respond?" *Canadian Climate Institute*, January 2024.

[3] Ritchie, H., "What share of global CO2 emissions come from aviation?" *Our World in Data*, 2024.

[4] Álvarez, S., Planelles, R., and Rubio, A., "Carbon footprint from helitankers: sustainable decision making in aerial wildfire fighting," *International Journal of Wildland Fire*, Vol. 24, 2015, pp. 983–988.

[5] Copernicus, "Highest wildfire emissions for March in Spain since at least 2003, according to CAMS data," , 2023.

[6] NIFC, *Interagency Air Tactical Group Supervisor's Guide*, 2nd ed., December 2008. Interagency Publish.

[7] NWCG, *Interagency Aerial Supervision Guide*, 3rd ed., April 2016.

[8] NWCG, *NWCG Standards for Aerial Supervision*, January 2022.

[9] DSE Groups 13 and 14, "Midterm Report for the Design of a VTOL Firefighter Aircraft," , 2024.

[10] Pugno, N., Ciavarella, M., Cornetti, P., and Carpinteri, A., "A generalized Paris' law for fatigue crack growth," *Journal of the Mechanics and Physics of Solids*, Vol. 54, No. 7, 2006, pp. 1333–1349.

[11] Roskam, J., *Airplane Design Part I: Preliminary sizing of airplanes*, DARcorporation, 1989.

[12] TUDelft DSE group 13, "Midterm Report for the Design of a VTOL Firefighter Aircraft," , 2024.

[13] Roskam, J., *Airplane Design Part V: Component Weight Estimation*, Vol. 5, DARorporation, 1989.

[14] DSE Groups 13 and 14, "Baseline Report for the Design of a VTOL Firefighter Aircraft," , 2024.

[15] Ashby, M. F., Shercliff, H., and Cebon, D., *Materials: Engineering, Science, Processing and Design*, 4th ed., Butterworth-Heinemann, 2019.

[16] Soprunenko, E., Valeriy, P., Vladimir, R., and Egor, L., "Simulation of impact assesment of crown forest fires on boudary layer of atmosphere using software PHOENICS," Tech. rep., XXI International Symposium Atmospheric and Ocean Optics. Atmospheric Physics, 2015.

[17] Megson, T., *Aircraft structures for engineering students*, Butterworth-Heinemann Inc, 2017.

[18] Hibbeler, R., *Mechanics of Materials*, 8th ed., Prentice Hall, 2011.

[19] Inman, D. J., *Engineering Vibration*, 4th ed., Pearson, 2014.

[20] "Jane's All the World's Aircraft," Online, April 2021.

[21] ICAO, "Annex 16 Environmental Protection Volume I Aircraft Noise," , 2017.

[22] Marte, J., and Kurtz, D., "A Review of Aerodynamic Noise From Propellers, Rofors, and Liff Fans," , 1970.

[23] Rosenstein, H., and Clark, R., "Aerodynamic design v-22 1986-14," , 9 1986.

[24] Nederlof, R., "Improved modeling of propeller-wing interactions with a lifting-line approach," , May 2020.

[25] Mcveigh, M. A., Liu, J., O'toole, S., Woods, S., and Formula, C., "V-22 Osprey Aerodynamic Development - A Progress Review," , 1986.

[26] Rwigema, M., "Propeller Blade Element Momentum Theory with Vortex Wake Deflection," *Proceedings of 27th International Congress of Aeronautical Sciences*, 2010, pp. 1–9.

[27] Roskam, J., *Airplane Design Part VI: Preliminary Calculation of Aerodynamic, Thrust and Power Characteristics*, DARorporation, 1987.

[28] Collins, P., and Williams, J., *The Aerodynamics of V/STOL Aircraft*, AGARD, 1968.

[29] R., V., M.F.M., H., and B.T.C., Z., *A/C Preliminary Sizing, Aerospace Design and Systems Engineering Elements I – AE1222-II*, 2022. Lecture 3: Lecture Slides.

[30] "Jane's All the World's Aircraft: Canadair CL-415," Online, May 2024.

[31] Struminska, A., and Filippone, A., "Flight performance analysis of aerial fire fighting," *Aeronautical Journal*, 2024.

[32] Roskam, J., and of Kansas, U., *Airplane Design: Part 2 - preliminary configuration design and integration of the propulsion system*, DARcorporation, 1985.

[33] Roskam, J., *Airplane Design Part II: Preliminary Configuration Design and Integration of the Propulsion System*, DARcorporation, 1985.

[34] Roskam, J., *Airplane Design Part III: Layout Design of Cockpit, Fuselage, Wing and Empennage: Cutaways and Inboard Profiles*, 6th ed., DARcorporation, 2018.

[35] Oliviero, F., *Lecture 7 - design for AC longitudinal stability – AE3211-I*, 2024. Lecture 7: Lecture Slides.
[36] Bell Boeing, "V-22 Pocket Guide," Tech. rep., Bell Boeing V-22 Program Office, 2007.
[37] Roskam, J., *Airplane Design Part VIII: Airplane Cost Estimation: Design, Development, Manufacturing and Operating*, 5th ed., DARcorporation, 2018.
[38] Penney, G., Habibi, D., Cattani, M., and Carter, M., "Calculation of Critical Water Flow Rates for Wildfire Suppression," , January 2019.
[39] Hansen, R., "Estimating the amount of water required to extinguish wildfires under different conditions and in various fuel types," , June 2012.
[40] Young, W., and Budynas, R., *Roark's Formulas for Stress and Strain*, 7th ed., McGraw-Hill, 2002.
[41] EASA, *Easy Access Rules for Airborne Communications, Navigation and Surveillance (CS-ACNS)*, October 2021.
[42] FAA, *14 CFR Part 91: General Operating and Flight Rules*, May 2024.
[43] "Interview: Rafael Selma Beltrán, Titan Aerial Firefighting," , 2022.
[44] Bombardier, "Canadair Regional Jet 100/200 - Electrical," , 2012.
[45] DSE Groups 13 and 14, "Project Plan for the Design of a VTOL Firefighter Aircraft," , 2024.
[46] Hamann, R., and van Tooren, M., *Systems Engineering & Technical Management Techniques - Part 2*, 1st ed., January 2006. Lecture Notes.
[47] The Boeing Company, "The Boeing Company 2009 Annual Report," , 2010.
[48] Embraer, "2001 Annual Report," , 2002.
[49] "Night Vision Imaging System (NVIS) | SKYbrary Aviation Safety — skybrary.aero," , 2023.
[50] Future Communications Study Operational Concepts and Requirements Team, "A COMMUNICATIONS OPERATING CONCEPT AND REQUIREMENTS FOR THE FUTURE RADIO SYSTEM VERSION 2.0," , 2005.
[51] Hamilton, B. A., "Urban Air Mobility (UAM) Market Study," Tech. Rep. 20190001472, National Aeronautics and Space Administration, 2018.
[52] Daily, D., "Bell-Boeing Quad tiltrotor Completes First WindTunnel Testing," , 10 2006.

A | Appendix A

A.1. Functional- Flow Diagram and Breakdown Structure

Functional Breakdown Structure

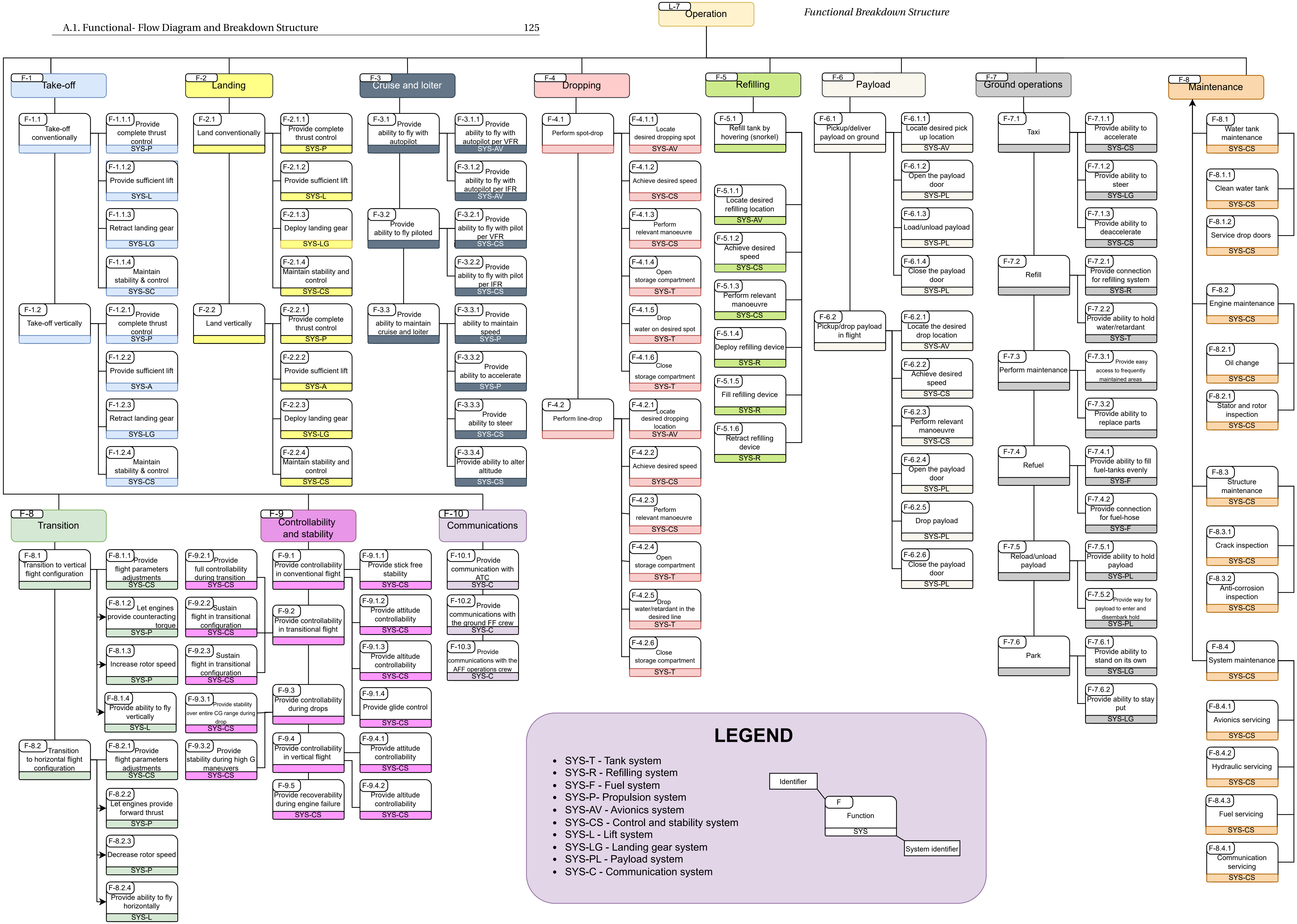

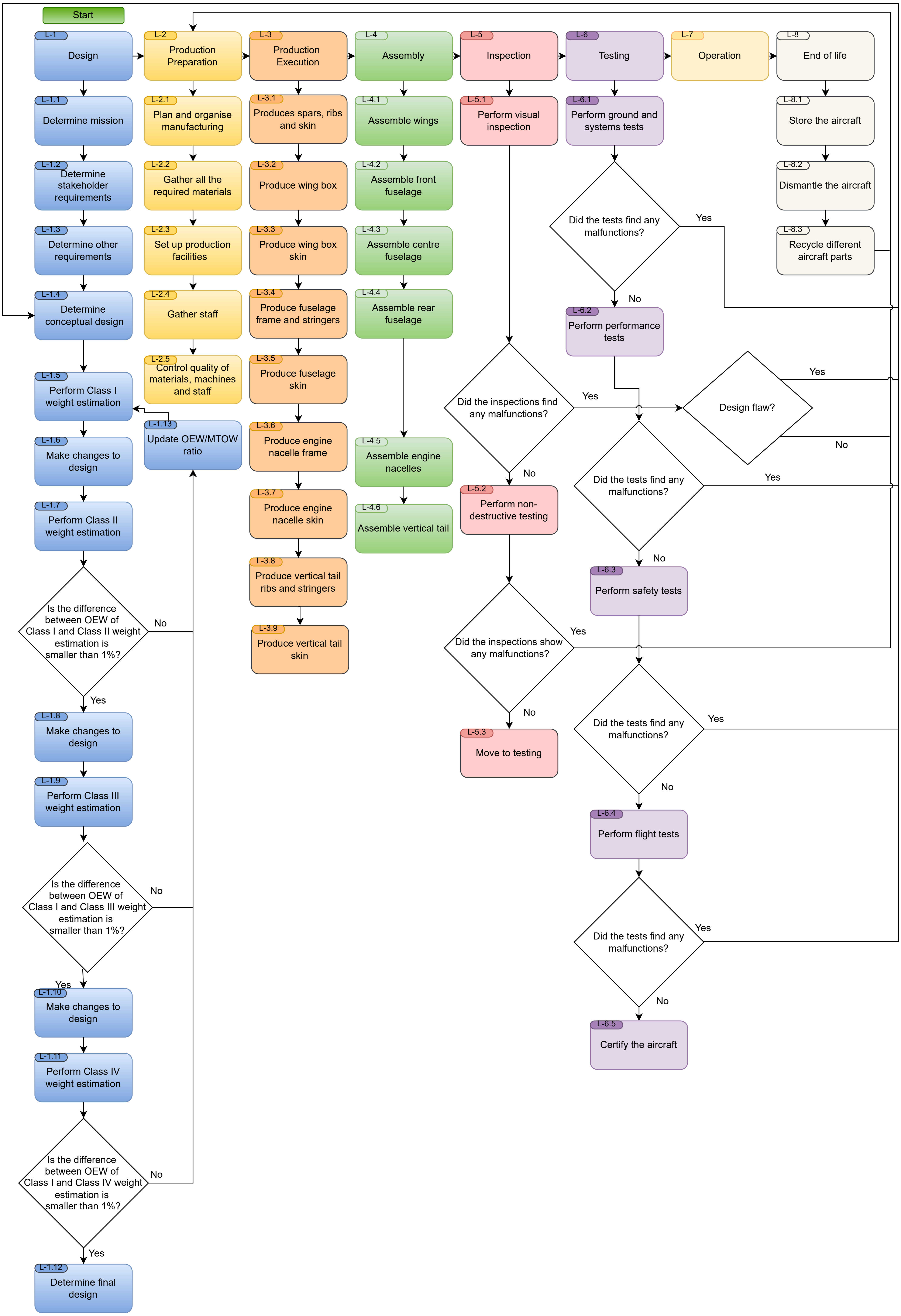
Start
L-1 Design
L-1.1 Determine mission
L-1.2 Determine stakeholder requirements
L-1.3 Determine other requirements
L-1.4 Determine conceptual design
L-1.5 Perform Class I weight estimation
L-1.6 Make changes to design
L-1.7 Perform Class II weight estimation
Is the difference between OEW of Class I and Class II weight estimation is smaller than 1%?
No
Yes
L-1.8 Make changes to design
L-1.9 Perform Class III weight estimation
Is the difference between OEW of Class I and Class III weight estimation is smaller than 1%?
No
Yes
L-1.10 Make changes to design
L-1.11 Perform Class IV weight estimation
Is the difference between OEW of Class I and Class IV weight estimation is smaller than 1%?
No
Yes
L-1.12 Determine final design
L-1.13 Update OEW/MTOW ratio
L-2 Production Preparation
L-2.1 Plan and organise manufacturing
L-2.2 Gather all the required materials
L-2.3 Set up production facilities
L-2.4 Gather staff
L-2.5 Control quality of materials, machines and staff
L-3 Production Execution
L-3.1 Produces spars, ribs and skin
L-3.2 Produce wing box
L-3.3 Produce wing box skin
L-3.4 Produce fuselage frame and stringers
L-3.5 Produce fuselage skin
L-3.6 Produce engine nacelle frame
L-3.7 Produce engine nacelle skin
L-3.8 Produce vertical tail ribs and stringers
L-3.9 Produce vertical tail skin
L-4 Assembly
L-4.1 Assemble wings
L-4.2 Assemble front fuselage
L-4.3 Assemble centre fuselage
L-4.4 Assemble rear fuselage
L-4.5 Assemble engine nacelles
L-4.6 Assemble vertical tail
L-5 Inspection
L-5.1 Perform visual inspection
Did the inspections find any malfunctions?
Yes
No
L-5.2 Perform non-destructive testing
Did the inspections show any malfunctions?
Yes
No
L-5.3 Move to testing
L-6 Testing
L-6.1 Perform ground and systems tests
Did the tests find any malfunctions?
Yes
No
L-6.2 Perform performance tests
Design flaw?
Yes
No
Did the tests find any malfunctions?
Yes
No
L-6.3 Perform safety tests
Did the tests find any malfunctions?
Yes
No
L-6.4 Perform flight tests
Did the tests find any malfunctions?
Yes
No
L-6.5 Certify the aircraft
L-7 Operation
L-8 End of life
L-8.1 Store the aircraft
L-8.2 Dismantle the aircraft
L-8.3 Recycle different aircraft parts

Functional Flow Diagram (Operations)

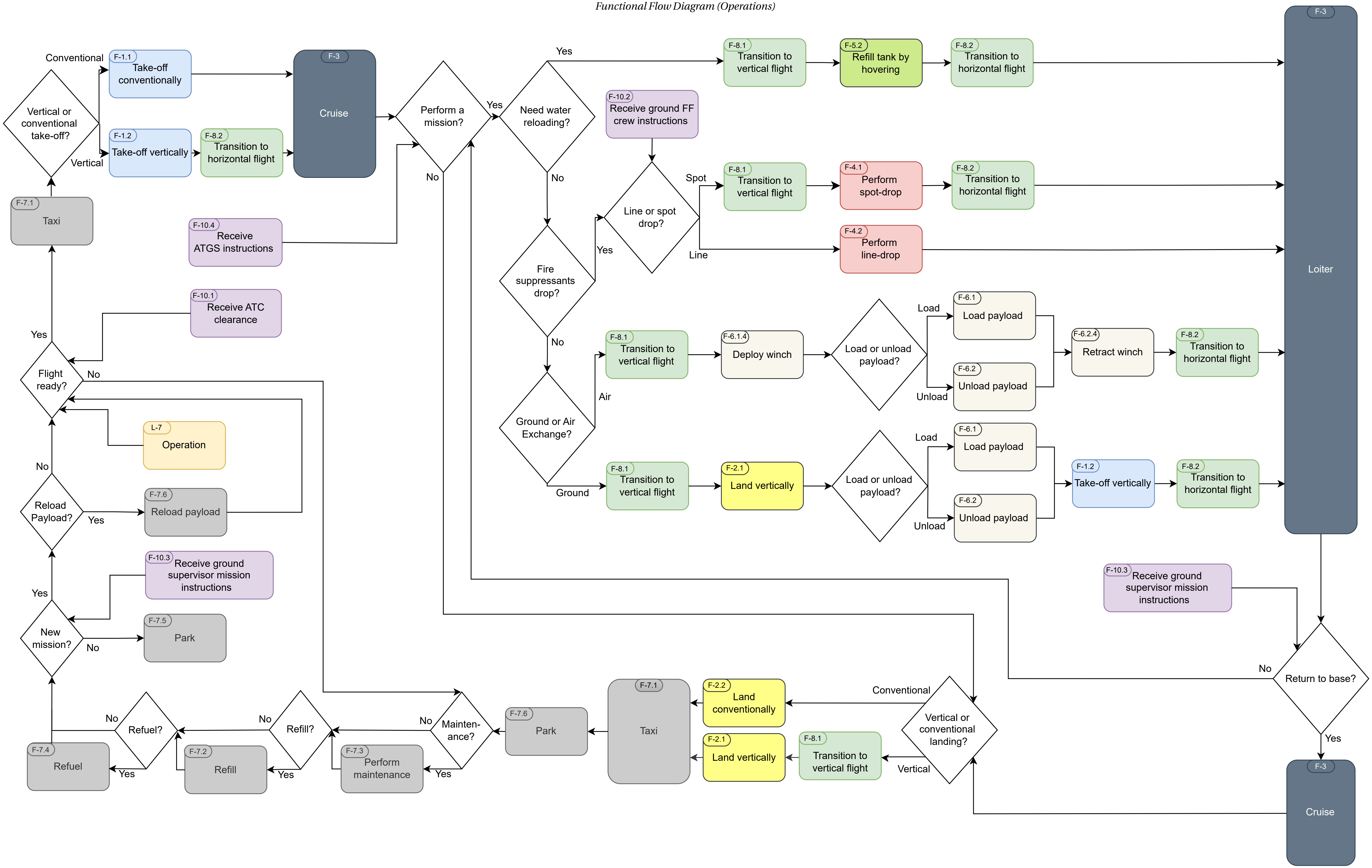

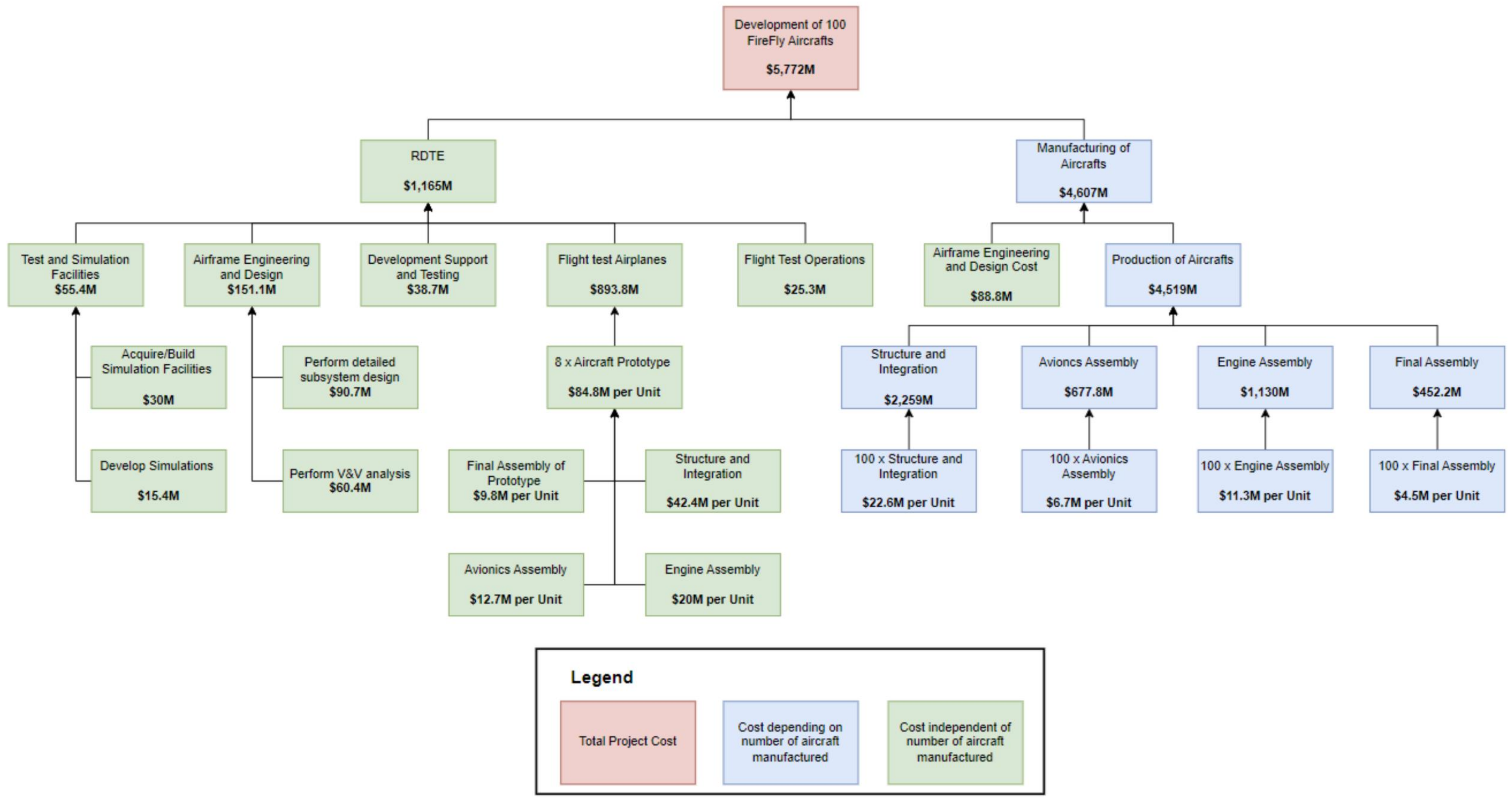
Development of 100 FireFly Aircrafts
$5,772M
RDTE
$1,165M
Manufacturing of Aircrafts
$4,607M
Test and Simulation Facilities
$55.4M
Airframe Engineering and Design
$151.1M
Development Support and Testing
$38.7M
Flight test Airplanes
$893.8M
Flight Test Operations
$25.3M
Airframe Engineering and Design Cost
$88.8M
Production of Aircrafts
$4,519M
Acquire/Build Simulation Facilities
$30M
Develop Simulations
$15.4M
Perform detailed subsystem design
$90.7M
Perform V&V analysis
$60.4M
8 x Aircraft Prototype
$84.8M per Unit
Final Assembly of Prototype
$9.8M per Unit
Structure and Integration
$42.4M per Unit
Avionics Assembly
$12.7M per Unit
Engine Assembly
$20M per Unit
Structure and Integration
$2,259M
Avioncs Assembly
$677.8M
Engine Assembly
$1,130M
Final Assembly
$452.2M
100 x Structure and Integration
$22.6M per Unit
100 x Avionics Assembly
$6.7M per Unit
100 x Engine Assembly
$11.3M per Unit
100 x Final Assembly
$4.5M per Unit
Legend
Total Project Cost
Cost depending on number of aircraft manufactured
Cost independent of number of aircraft manufactured

B | V&V Plan

B.1. Subsystem Requirements V&V Plan

Table B.1: *List of V&V Procedures for the Drop System.*

Identifier	Verification method	C.C.	Validation method	C.C.
QTR-DRP-01	Design review - Ensure that the drop doors have been designed to open individually.	TS	Ground test & Flight test - Open the drop doors individually on the ground and during a mission.	F.A.
QTR-DRP-02	Design review - Ensure that the doors have been designed to be opened partially.	TS	Ground test & Flight test - Open the drop doors partially on the ground and during a mission.	F.A.
QTR-DRP-03	Design review - Ensure that the sensors have been incorporated into the design.	TS	Inspection - Visually inspect that the sensors are on the retardant tank.	F.A.
QTR-DRP-04	Design review - Ensure that the tank has been designed with internal baffles.	TS	Inspection - Visually inspect that the tank has baffles	F.A.
QTR-DRP-05	Laboratory test - Test that the tank is able to withstand the dynamic forces experienced during flight.	F.A.	Flight test - Test that the tank withstands the dynamic loads during flight.	F.A.

Table B.2: *List of V&V Procedures for the Communication System.*

Identifier	Verification method	C.C.	Validation method	C.C.
QTR-COM-01	Design review - Ensure that the PA/intercom system is in the design.	IK	Inspection - Visually inspect that there is a PA/intercom system onboard.	F.A.
QTR-COM-02	Equipment qualifications - Check that the antennas are equipped with anti-icing systems.	F.A.	Ground test - Test that antennas anti-ice system works.	F.A.
QTR-COM-03	Design review - Ensure that an ELT is incorporated in the design.	IK	Inspection - Visually inspect that there is an ELT onboard.	F.A.
QTR-COM-04	Design review - Ensure that an ELT detection system is incorporated in the design.	IK	Inspection - Visually inspect that there is an ELT detection system onboard.	F.A.
QTR-COM-05	Design review - Ensure that a VHF radio communication system is incorporated in the design.	IK	Inspection - Visually inspect that there is a VHF system onboard.	F.A.
QTR-COM-06	Design review - Ensure that a UHF radio communication system is incorporated in the design.	IK	Inspection - Visually inspect that there is a UHF system onboard.	F.A.
QTR-COM-07	Design review - Ensure that a ACARS system is incorporated in the design.	IK	Inspection - Visually inspect that there is a ACARS system onboard.	F.A.
QTR-COM-08	Design review - Ensure that a CPDLC system is incorporated in the design.	IK	Inspection - Visually inspect that there is a CPDLC system onboard.	F.A.
QTR-COM-09	Design review - Ensure that a SATCOM communication system is incorporated in the design.	IK	Inspection - Visually inspect that there is a SATCOM system onboard.	F.A.
QTR-COM-10	Design review - Ensure that a ADS-B out transponder system is incorporated in the design.	IK	Inspection - Visually inspect that there is a ADS-B out transponder onboard.	F.A.

Continued on next page

Table B.2 – continued from previous page

Identifier	Verification method	C.C.	Validation method	C.C.
QTR-COM-11	Design review - Ensure that an ADS-B in receiver is incorporated in the design.	IK	Inspection - Visually inspect that there is an ADS-B in receiver onboard.	F.A.
QTR-COM-12	Design review - Ensure that the position lights have been incorporated in the design.	IK	Inspection - Visually inspect that the aircraft is equipped with position lights.	F.A.
QTR-COM-13	Design review - Ensure that the anticollision lights have been incorporated in the design.	IK	Inspection - Visually inspect that the aircraft is equipped with anticollision lights	F.A.
QTR-COM-14	Design review - Ensure that there is at least one landing light has been incorporated in the design.	IK	Inspection - Visually inspect that the aircraft is equipped with at least one landing light.	F.A.

Table B.3: *List of V&V Procedures for the internal environment.*

Identifier	Verification method	C.C.	Validation method	C.C.
QTR-INV-01	Design review - Ensure that an airfiltering system has been incorporated into the design.	TS	Inspection - Visually inspect that there is an airfiltering system.	F.A.
QTR-INV-02	Simulation - Simulate the conditions over a fire and investigate how the heat propogates through the structure.	F.A.	Ground test - Simulate a mission conditions and investigate the internal temperature.	F.A.

Table B.4: *List of V&V Procedures for the lift system.*

Identifier	Verification Method	C.C.	Validation Method	C.C.
QTR-LFT-01	Calculation/Analysis & simulation - Design the wing to withstand these loads.	LJ	Ground test - Test the airframe with these loads.	F.A.
QTR-LFT-02	Design review - Ensure that an anti-icing system has been incorporated into the design.	NB	Inspection - Visually inspect that there is an anti-icing system within the lift system.	F.A.
QTR-LFT-03	Design review - Ensure that a de-icing system has been incorporated into the design.	NB	Inspection - Visually inspect that there is a de-icing system within the lift system.	F.A.
QTR-LFT-04	Calculation/Analysis - Design the wing to be able to cruise at 3000m	NB	Flight test - Fly the prototype at 3000m.	F.A.
QTR-LFT-05	Design review - Ensure that an anti-icing system has been incorporated into the wing.	NB	Inspection - Visually inspect that there is an anti-icing system within the wing.	F.A.
QTR-LFT-06	Calculation/Analysis & simulation - Investigate this case through calculations and simulation.	NB	Flight test - Fly the prototype with these conditions.	F.A.

Table B.5: *List of V&V Procedures for the avionics system.*

Identifier	Verification method	C.C.	Validation method	C.C.
QTR-AVI-01	Design review - Ensure that the avionics design includes a retardant level monitor.	IK	Inspection - Visually inspect that the cockpit is equipped with a retardant level monitor	F.A.
QTR-AVI-02	Design review - Ensure that the avionics design includes a targeting system for retardant drops.	IK	Inspection - Visually inspect that the cockpit is equipped with a targeting system for retardant drops.	F.A.

Continued on next page

Table B.5 – continued from previous page

Identifier	Verification method	C.C.	Validation method	C.C.
QTR-AVI-03	Design review - Ensure that the avionics design includes a targeting system for resource drops.	IK	Inspection - Visually inspect that the cockpit is equipped with a targeting system for resource drops.	F.A.
QTR-AVI-04	Design review - Ensure that the avionics design includes an ice warning system.	IK	Inspection - Visually inspect that the cockpit is equipped with an ice warning system.	F.A.
QTR-AVI-05	Design review - Ensure that the avionics design includes a temperature monitoring system.	IK	Inspection - Visually inspect that the cockpit is equipped with a temperature monitoring system.	F.A.
QTR-AVI-06	Design review - Ensure that the avionics design includes a crew information system.	IK	Inspection - Visually inspect that the cockpit is equipped with a crew information system.	F.A.
QTR-AVI-07	Design review - Ensure that the avionics design includes a night vision system.	IK	Inspection - Visually inspect that the cockpit is equipped with a night vision system.	F.A.
QTR-AVI-08	Design review - Ensure that the avionics design can display LiDAR information.	IK	Inspection - Visually inspect that the cockpit can display LiDAR information.	F.A.
QTR-AVI-09	Design review - Ensure that the avionics design includes a display for ADS-B capabilities.	IK	Inspection - Visually inspect that the cockpit is equipped with a display for ADS-B capabilities.	F.A.
QTR-AVI-10	Design review - Ensure that the avionics design includes off the shelf solutions only.	IK	Compliance statements - Ensure that the different components are off the shelf certified.	F.A.
QTR-AVI-11	Design review - Ensure that the avionics design includes well known display methods only.	IK	Compliance statements - Ensure that the avionics display methods are certified and known.	F.A.
QTR-AVI-12	Design review - Ensure that the avionics design includes an FDR.	IK	Inspection - Visually inspect that the cockpit is equipped with an FDR.	F.A.
QTR-AVI-13	Design review - Ensure that the avionics design includes a CVR.	IK	Inspection - Visually inspect that the cockpit is equipped with a CVR.	F.A.
QTR-AVI-14	Design review - Ensure that the avionics design is equipped with an ILS system.	IK	Inspection - Visually inspect that the cockpit is equipped with an ILS system.	F.A.
QTR-AVI-15	Design review - Ensure that the avionics design includes an airspeed indicator.	IK	Inspection - Visually inspect that the cockpit is equipped with an airspeed indicator.	F.A.
QTR-AVI-16	Design review - Ensure that the avionics design includes an altimeter.	IK	Inspection - Visually inspect that the cockpit is equipped with an altimeter.	F.A.
QTR-AVI-17	Design review - Ensure that the avionics design includes a magnetic direction indicator.	IK	Inspection - Visually inspect that the cockpit is equipped with a magnetic direction indicator.	F.A.
QTR-AVI-18	Design review - Ensure that the avionics design includes ITT gauge for each engine.	IK	Inspection - Visually inspect that the cockpit is equipped with an ITT gauge for each engine.	F.A.
QTR-AVI-19	Design review - Ensure that the avionics design includes a landing gear position indicator.	IK	Inspection - Visually inspect that the cockpit is equipped with a landing gear position indicator.	F.A.
QTR-AVI-20	Design review - Ensure that the avionics design includes an AoA indicator.	IK	Inspection - Visually inspect that the cockpit is equipped with an AoA indicator.	F.A.
QTR-AVI-21	Design review - Ensure that the avionics design includes a turn coordinator.	IK	Inspection - Visually inspect that the cockpit is equipped with a turn coordinator.	F.A.

Continued on next page

Table B.5 – continued from previous page

Identifier	Verification method	C.C.	Validation method	C.C.
QTR-AVI-22	Design review - Ensure that the avionics design includes a clock displaying hours, minutes and seconds.	IK	Inspection - Visually inspect that the cockpit is equipped with a clock displaying hours, minutes and seconds.	F.A.
QTR-AVI-23	Design review - Ensure that the avionics design includes an attitude indicator.	IK	Inspection - Visually inspect that the cockpit is equipped with an attitude indicator.	F.A.
QTR-AVI-24	Design review - Ensure that the avionics design includes a heading indicator.	IK	Inspection - Visually inspect that the cockpit is equipped with a heading indicator.	F.A.
QTR-AVI-25	Design review - Ensure that the avionics design includes a vertical speed indicator.	IK	Inspection - Visually inspect that the cockpit is equipped with a vertical speed indicator.	F.A.
QTR-AVI-26	Design review - Ensure that the avionics design includes GPS navigation.	IK	Inspection - Visually inspect that the cockpit is equipped with GPS navigation.	F.A.
QTR-AVI-27	Design review - Ensure that the avionics design includes a VHF system.	IK	Inspection - Visually inspect that the cockpit is equipped with a VHF system.	F.A.
QTR-AVI-28	Design review - Ensure that the avionics design includes an oil pressure gauge for each engine.	IK	Inspection - Visually inspect that the cockpit is equipped with an oil pressure gauge for each engine.	F.A.
QTR-AVI-29	Design review - Ensure that the avionics design includes an NG for each engine.	IK	Inspection - Visually inspect that the cockpit is equipped with an NG for each engine.	F.A.
QTR-AVI-30	Design review - Ensure that the avionics design includes an oil temperature gauge for each engine.	IK	Inspection - Visually inspect that the cockpit is equipped with an oil temperature gauge for each engine.	F.A.
QTR-AVI-31	Design review - Ensure that the avionics design includes an RPM gauge for each engine.	IK	Inspection - Visually inspect that the cockpit is equipped with an RPM gauge for each engine.	F.A.
QTR-AVI-32	Design review - Ensure that the avionics design includes a fuel gauge indicator for fuel in each fuel tank.	IK	Inspection - Visually inspect that the cockpit is equipped with a fuel gauge indicator for fuel in each fuel tank.	F.A.
QTR-AVI-33	Design review - Ensure that the avionics design includes a torque percentage indicator for each engine.	IK	Inspection - Visually inspect that the cockpit is equipped with a torque percentage indicator for each engine.	F.A.
QTR-AVI-34	Design review - Ensure that the avionics design includes a set of circuit breakers for each electrical system.	IK	Inspection - Visually inspect that the cockpit is equipped with a set of circuit breakers for each electrical system.	F.A.
QTR-AVI-35	Design review - Ensure that the avionics design includes an ND.	IK	Inspection - Visually inspect that the cockpit is equipped with an ND.	F.A.
QTR-AVI-36	Simulation - Test that the avionics can load a flight plan.	IK	Flight test - Test that the avionics can load a flight plan.	F.A.
QTR-AVI-37	Simulation - Test that the avionics can follow a flight plan.	IK	Flight test - Test that the avionics can follow a flight plan.	F.A.
QTR-AVI-38	Design review - Ensure that the avionics are designed in a modular way.	IK	Inspection - Visually inspect that the avionics are designed in a modular way.	F.A.
QTR-AVI-39	Equipment qualifications - Ensure that the avionics system is installed according to the installation manual.	IK	Compliance statements - Ensure that the avionics system has been correctly installed according to the installation manual.	F.A.

Table B.6: *List of V&V Procedures for the fuel system.*

Identifier	Verification method	C.C.	Validation method	C.C.
QTR-FUL-01	Design Review - Ensure that the tank was designed to carry 9700kg of fuel.	IK	Ground test - Fill the tank.	F.A.
QTR-FUL-02	Calculation/Analysis - Analyse if the fuel system can pump fuel to the engines under these loads.	IK	Ground test - Test the fuel system under these loads.	F.A.
QTR-FUL-03	Design Review - Ensure that the fuel tank has a sufficient inlet.	IK	Inspection - Visually inspect that the fuel tank has a sufficient inlet.	F.A.
QTR-FUL-04	Design Review - Ensure that the fuel tank design incorporates a bladder sealant bag.	CC	Inspection - Visually inspect that the fuel tank design incorporates a bladder sealant bag.	F.A.
QTR-FUL-05	Calculation/Analysis - Analyse if the fuel tank will puncture under these loads.	IK	Laboratory test - Test the bladder sealant bag under these loads.	F.A.
QTR-FUL-06	Design Review - Ensure that the fuel tanks are equipped with easy access points.	IK	Inspection - Visually inspect that the fuel tank has easy access points.	F.A.
QTR-FUL-07	Calculation/Analysis - Analyse if the material chosen will not degrade when carrying these fuels.	CC	Laboratory test - Test the presence of jet fuel A and jet fuel B.	F.A.

Table B.7: *List of V&V Procedures for the propulsion system.*

Identifier	Verification method	C.C.	Validation method	C.C.
QTR-PRP-01	Calculation/Analysis - Analyse if the fuel flow is indeed this during ferry flight.	JD	Flight test - Monitor the mass flow rate during drop and refilling conditions.	F.A.
QTR-PRP-02	Calculation/Analysis - Analyse if the fuel flow is indeed this during refilling and dropping phases.	JD	Flight test - Monitor the mass flow rate during ferry flight conditions.	F.A.
QTR-PRP-03	Calculation/Analysis - Analyse if the fuel flow is indeed this with a full retardant tank at a minimum dash speed of 400 km/hr.	JD	Flight test - Monitor the mass flow rate with a full retardant tank at a minimum dash speed of 400 km/hr.	F.A.
QTR-PRP-04	Design Review - Ensure that a tilting mechanism has been incorporated into the design.	JD	Inspection - Visually inspect that the tilting mechanism has been incorporated into the design.	F.A.
QTR-PRP-05	Design Review - Ensure that the tilting mechanism has been to designed to rotate the engine's thrust vector 135° from its horizontal flight mode position.	JD	Ground test - Test the tilting mechanism with the prototype aircraft.	F.A.
QTR-PRP-06	Design Review - Ensure that controls have been designed to tilt the rotors independently.	JD	Ground test - Test the independent tilting functionality of the prototype aircraft.	F.A.
QTR-PRP-07	Equipment qualifications - Ensure that engines can provide this thrust.	BB	Ground test - Test if the engines produce 35kN of thrust at sea level.	F.A.
QTR-PRP-08	Design Review - Ensure that controls have been designed to provide dynamic thrust changes during refilling.	F.A.	Flight test - Test that the controls provide dynamic thrust changes during refilling.	F.A.
QTR-PRP-09	Calculation/Analysis - Analyse the deformation of the rotor blades under these loads.	F.A.	Laboratory test - Analyse the deformation of the rotors under these loads.	F.A.

Continued on next page

Table B.7 – continued from previous page

Identifier	Verification method	C.C.	Validation method	C.C.
QTR-PRP-10	Calculation/Analysis - Analyse if the engines can provide 27kN of thrust at 3000m in ISA conditions.	BB	Flight test - Test that the engines can provide this thrust at 3000m.	F.A.
QTR-PRP-11	Design review - Ensure that the engine inlet has an anti-icing system incorporated into the design.	BB	Inspection - Visually inspect that the engine inlet has an anti-icing system.	F.A.
QTR-PRP-12	Design review - Ensure that the individual propeller blades are equipped with an anti-icing system.	F.A.	Inspection - Visually inspect that the individual propeller blades are equipped with an anti-icing system.	F.A.
QTR-PRP-13	Design review - Ensure that the powerplant is easily accessible.	JD	Inspection - Inspect that the power plant is easily accessible.	F.A.
QTR-PRP-14	Design review - Ensure that a protective coating has been incorporated into the design.	CC	Inspection - Inspect that the coating has been applied to the propeller blades.	F.A.
QTR-PRP-15	Design review - Ensure that the coupling of the engines does not affect the operation of all engines if one were to fail.	F.A.	Flight test - Test the operation of the engines when one is inoperative.	F.A.
QTR-PRP-16	Design review - Ensure the control system allows individual stopping of the engines.	F.A.	Ground test - Test that the controls successfully stop the engines individually.	F.A.
QTR-PRP-17	Design review - Ensure the control system allows individual restarting of the engines in cruise.	F.A.	Flight test - Test that the engines can be individually restarted in cruise.	F.A.
QTR-PRP-18	Equipment qualifications - Determine the power rating of each engine.	BB	Ground test - Confirm the power rating of the engines.	F.A.
QTR-PRP-19	Compliance statement - Ensure that the engines are CS-E certified.	BB	Ground test - Confirm the CS-E certification.	F.A.
QTR-PRP-20	Design review - Ensure that the engines are easily accessible in the design.	JD	Inspection - Visually inspect that the engines are easily accessible.	F.A.
QTR-PRP-21	Equipment qualifications - Determine if the parts are industry standard.	F.A.	Compliance statement - Confirm that the parts comply with industry standard.	F.A.
QTR-PRP-22	Laboratory test - Test the propellers on a set up in impact resistance.	F.A.	Ground test - Test the propellers of the prototype on impact resistance.	F.A.
QTR-PRP-23	Equipment qualifications - Ensure that the engines can run of Jet A-1 and Jet B fuels.	BB	Laboratory test - Test that the engines can run on Jet A-1 and Jet B fuels.	F.A.

Table B.8: *List of V&V Procedures for the electric system.*

Identifier	Verification method	C.C.	Validation method	C.C.
QTR-ELE-01	Design review - Ensure that infrared cameras have been incorporated into the design.	IK	Inspection - Visually inspect that the FireFly is equipped with infrared cameras.	F.A.
QTR-ELE-02	Design review - Ensure that high resolution cameras have been incorporated into the design.	IK	Inspection - Visually inspect that the FireFly is equipped with high resolution cameras.	F.A.
QTR-ELE-03	Design review - Ensure that LiDAR has been incorporated into the design.	IK	Inspection - Visually inspect that the FireFly is equipped with LiDAR.	F.A.
QTR-ELE-04	Design review - Ensure that the corrosion resistant sealed housing has been incorporated into the design.	IK	Inspection - Visually inspect that the electronics are in a corrosion resistant sealed housing.	F.A.

Continued on next page

Table B.8 – continued from previous page

Identifier	Verification method	C.C.	Validation method	C.C.
QTR-ELE-05	Equipment qualifications - Confirm that the parts are standard components.	IK	Compliance statement - Confirm that the parts comply with what is expected.	F.A.

Table B.9: *List of V&V Procedures for the payload.*

Identifier	Verification method	C.C.	Validation method	C.C.
QTR-PYL-01	Design review - Ensure that the internal cabin can fit six evacuees with two stretchers.	LJ	Ground test - Test that six evacuees and two stretchers can fit into the internal cabin.	F.A.
QTR-PYL-02	Calculation/Analysis & Design review - Calculate the placement of the hoist to allow boarding while hovering and ensure that it is incorporated into the design.	IK	Inspection & Flight test - Inspect that the hoist in the correct position and test the hoisting capabilities during hover.	F.A.
QTR-PYL-03	Design review - Ensure that the cargo bay is equipped with seating in the internal cabin design.	IK	Inspection - Visually inspect that there are seats in the internal cabin.	F.A.
QTR-PYL-04	Calculation/Analysis - Determine if the half pallet can fit into the internal cabin.	LJ	Ground test - Load a half pallet into the internal cabin.	F.A.
QTR-PYL-05	Design review - Ensure that a roller system in the floor has been incorporated into the design.	IK	Inspection - Visually inspect the roller system in the floor.	F.A.
QTR-PYL-06	Design review - Ensure that the cargo bay design has a static line incorporated in it.	IK	Inspection - Visually inspect the static line in the cargo bay.	F.A.
QTR-PYL-07	Calculation/Analysis - Analyse if the door can be opened in horizontal flight conditions.	IK	Flight test - Open the door during horizontal flight.	F.A.
QTR-PYL-08	Calculation/Analysis - Analyse if the door can be opened in hover.	IK	Flight test - Open the door during hover.	F.A.
QTR-PYL-09	Equipment qualifications - Ensure that the heating system can heat the space to 20 degrees or below.	IK	Ground test - Measure the temperature in the cargo bay.	F.A.
QTR-PYL-10	Design review - Ensure that an emergency exist accessible from the cargohold has been incorporated into the design.	JD	Safety assessment.	F.A.
QTR-PYL-11	Equipment qualifications & Design review - Ensure that winch can carry 275kg and can extend 76 metres. Ensure that the winch has been incorporated into the design.	IK	Inspection & Flight test - Visually inspect that there is a winch and test that the winch can carry 275kg and can extend 76 metres.	F.A.
QTR-PYL-12	Equipment qualifications - Ensure the stretcher is compatible with the winch.	IK	Inspection - Inspect if the stretcher is compatible with the winch.	F.A.

Table B.10: *List of V&V Procedures for the retardant tank system.*

Identifier	Verification method	C.C.	Validation method	C.C.
QTR-TNK-01	Design review - Ensure that the tank is designed for 10,000 Litres.	TS	Ground test - Fill the tank up with 10,000L of water.	F.A.

Continued on next page

Table B.10 – continued from previous page

Identifier	Verification method	C.C.	Validation method	C.C.
QTR-TNK-02	Design review - Ensure that a foam injection with a capacity of 500 Litres has been incorporated into the design.	TS	Inspection & Ground test - Inspect that the foam injection in the tank system and fill the injection system with 500 Litres of water.	F.A.
QTR-TNK-03	Design review - Ensure that the inlet for refilling from ground equipment is present in the design.	TS	Inspection - Visually inspect that the inlet is in the tank.	F.A.
QTR-TNK-04	Design review - Ensure that the inlet for refilling from the snorkel is present in the design.	TS	Inspection - Visually inspect that the inlet is in the tank.	F.A.
QTR-TNK-05	Design review - Ensure an overflow channel is present in the design.	TS	Inspection - Visually inspect that an overflow channel is present.	F.A.
QTR-TNK-06	Calculation/Analysis - Analyse the thermal loading on the tank up to 180 degrees.	TS	Laboratory test - Test the structure under thermal loading of up to 180 degrees.	F.A.
QTR-TNK-07	Design review - Ensure that the tank has a corrosion resistant coating to salt water or is made out of a corrosion resistant material.	CC	Laboratory test - Test the corrosion resistant capabilities of the tank under salt water.	F.A.
QTR-TNK-08	Design review - Ensure that the tank has a corrosion resistant coating to foams or is made out of a corrosion resistant material.	CC	Laboratory test - Test the corrosion resistant capabilities of the tank under foam.	F.A.
QTR-TNK-09	Design review - Ensure that the tank has a corrosion resistant coating to long term retardents or is made out of a corrosion resistant material.	CC	Laboratory test - Test the corrosion resistant capabilities of the tank under long term retardent.	F.A.
QTR-TNK-10	Design review - Ensure easy access points are present in the design.	TS	Inspection - Visually inspect if there are easy access points in the tank.	F.A.

Table B.11: *List of V&V Procedures for the refilling system.*

Identifier	Verification method	C.C.	Validation method	C.C.
QTR-REF-01	Equipment qualifications - Ensure that the snorkel can refill the 10,000 L tank.	TS	Ground test - Test that the snorkel can refill the 10,000 L tank.	F.A.
QTR-REF-02	Equipment qualifications - Ensure that the snorkel can extend to 7 metres.	TS	Ground test - Extend the snorkel 7 metres.	F.A.
QTR-REF-03	Equipment qualifications - Ensure that the pump is used for aerial firefighting.	TS	Compliance statements - Ensure that the pump is used for aerial firefighting.	F.A.

Table B.12: *List of V&V procedures for the control & stability system.*

Identifier	Verification method	C.C.	Validation method	C.C.
QTR-STA-01	Design review - Ensure the control system can compensate for changes in the cg location during flight.	F.A.	Flight test - Ensure the control system can compensate for changes in the cg location during flight.	F.A.
QTR-STA-02	Design review - Ensure the control system includes predictive algorithms for effects on stability due to retardant drop.	F.A.	Flight test - Ensure the control system includes predictive algorithms for effects on stability due to retardant drop.	F.A.

Continued on next page

Table B.12 – continued from previous page

Identifier	Verification method	C.C.	Validation method	C.C.
QTR-STA-03	Design review - Ensure that a salt water protective coating has been chosen for the control surfaces.	F.A.	Inspection - Inspect that the coating has been applied to the control surfaces.	F.A.
QTR-STA-04	Simulation - Ensure that the fly-by-wire imitates the stick forces of an S-70.	F.A.	Flight test - Confirm that the fly-by-wire imitates the stick forces of an S-70.	F.A.
QTR-STA-05	Calculation/Analysis - Analyse if the empennage allows for longitudinal stability.	SP	Flight test - Test the longitudinal stability of the empennage.	F.A.

Table B.13: *List of V&V Procedures for the environmental system.*

Identifier	Verification method	C.C.	Validation method	C.C.
QTR-ENV-01	Design review - Ensure that the cargo compartment design has a smoke sensor.	IK	Inspection - Visually inspect that a smoke sensor is present in the cargo compartment.	F.A.
QTR-ENV-02	Design review - Ensure that the cargo compartment design has a carbon monoxide sensor.	IK	Inspection - Visually inspect that a carbon monoxide sensor is present in the cargo compartment.	F.A.
QTR-ENV-03	Design review - Ensure that the cockpit design has a smoke sensor.	IK	Inspection - Visually inspect that a smoke sensor is present in the cockpit.	F.A.
QTR-ENV-04	Design review - Ensure that the cockpit design has a carbon monoxide sensor.	IK	Inspection - Visually inspect that a carbon monoxide sensor is present in the cockpit.	F.A.
QTR-ENV-05	Design review - Ensure that the cockpit design has a HVAC.	IK	Inspection - Visually inspect that a HVAC is present in the cockpit.	F.A.

Table B.14: *List of V&V Procedures for the landing gear.*

Identifier	Verification method	C.C.	Validation method	C.C.
QTR-LDG-01	Equipment qualifications - Ensure that the tyres are large enough and have a low enough pressure to be stable on uneven surfaces.	JD	Ground test - Test the landing gears on uneven surfaces.	F.A.
QTR-LDG-02	Design review - Ensure that the landing gear design is retractable.	JD	Ground test - Test if the landing gear is retractable.	F.A.
QTR-LDG-03	Calculation/Analysis - Analyse if the aircraft can move with MTOW.	JD	Ground test - Test that the aircraft can perform ground operations with MTOW.	F.A.
QTR-LDG-04	Calculation/Analysis - Analyse if the aircraft can land with MTOW.	IK	Flight test - Land with MTOW.	F.A.
QTR-LDG-05	Laboratory test - Test the landing gear for shocks using a lab test set-up.	F.A.	Flight test - Test the landing gear for the expected shocks.	F.A.
QTR-LDG-06	Calculation/Analysis - Analyse the loads acting on the landing gear for the expected centre of gravity loads.	IK	Flight test - Test the landing gear for different centre of gravity positions.	F.A.
QTR-LDG-07	Design review - Ensure that the landing gear design is easily maintainable.	JD	Compliance statement - Check compliance for maintenance.	F.A.

Table B.15: *List of V&V Procedures for the structural system.*

Identifier	Verification method	C.C.	Validation method	C.C.
QTR-STR-01	Calculation/Analysis - Determine the required thickness to withstand these loads.	JC	Flight test - Expose the structure to these loads during a mission scenario.	F.A.
QTR-STR-02	Design review - Ensure that the fuselage is equipped with the required emergency exit doors.	JD	Safety assessment.	F.A.
QTR-STR-03	Design review - Ensure the windshield is equipped with an anti-icing system.	IK	Inspection - Visually inspect that the windshield is equipped with an anti-icing system.	F.A.
QTR-STR-04	Design review - Ensure the material chosen is salt water corrosion resistant.	CC	Laboratory test - Test the material in the presence of salt water.	F.A.
QTR-STR-05	Design review - Ensure protective coating for all exposed metallic surfaces is present in the design.	CC	Inspection - Visually inspect that all exposed metallic surfaces have a protective coating.	F.A.
QTR-STR-06	Calculation/Analysis - Analyse the fatigue loading of the chosen material.	JC	Laboratory test - Perform a fatigue loading test on the chosen material.	F.A.
QTR-STR-07	Laboratory test - Expose the structure to ultimate loads.	F.A.	Flight test - Expose the structure to the ultimate loads for 3 seconds.	F.A.
QTR-STR-08	Simulation - Simulate the heat propagation through the material for 30 seconds.	F.A.	Laboratory test - Expose the material to 30 seconds of 180 degrees.	F.A.
QTR-STR-09	Design review - Ensure that there is a sufficient field of view to both pilots.	JD	Inspection - Visually inspect that there is sufficient field of view to both pilots in accordance to CS regulations.	F.A.
QTR-STR-10	Design review - Ensure that there are reinforced structural elements in the cockpit.	IK	Inspection - Inspect that there are reinforced structural elements in the cockpit.	F.A.
QTR-STR-11	Design review - Ensure that there is an emergency exit accessible from the cargo compartment.	JD	Safety assessment.	F.A.
QTR-STR-12	Design review - Ensure that there is an emergency exit accessible from the cockpit.	JD	Safety assessment.	F.A.
QTR-STR-13	Design review - Ensure that the pilots have sufficient visibility in the design.	JD	Simulation - Simulate reduced visibility for the cockpit design.	F.A.
QTR-STR-14	Design review - Ensure that a person of height 1.88 cm can fit in the internal cabin.	TS	Inspection - Measure the internal height of the cabin.	F.A.

Continued on next page

Table B.15 – continued from previous page

Identifier	Verification method	C.C.	Validation method	C.C.
QTR-STR-15	Design review - Ensure crucial structural components are equipped with strain sensors.	JC	Inspection - Ensure that crucial structural components are equipped with strain sensors.	F.A.
QTR-STR-16	Calculation/Analysis - Analyse the chosen material in different thermal loading cycles.	F.A.	Laboratory test - Test the material with the expected thermal loading cycles.	F.A.